



# Self-assemblies of azacitidine prodrugs: a promising strategy of treatment for myelodysplastic syndromes and acute myeloid leukemia

Milad Baroud

## ► To cite this version:

Milad Baroud. Self-assemblies of azacitidine prodrugs: a promising strategy of treatment for myelodysplastic syndromes and acute myeloid leukemia. Human health and pathology. Université d'Angers; Université libanaise de Beyrouth (Liban), 2021. English. NNT : 2021ANGE0062 . tel-03712959

**HAL Id: tel-03712959**

**<https://theses.hal.science/tel-03712959>**

Submitted on 4 Jul 2022

**HAL** is a multi-disciplinary open access archive for the deposit and dissemination of scientific research documents, whether they are published or not. The documents may come from teaching and research institutions in France or abroad, or from public or private research centers.

L'archive ouverte pluridisciplinaire **HAL**, est destinée au dépôt et à la diffusion de documents scientifiques de niveau recherche, publiés ou non, émanant des établissements d'enseignement et de recherche français ou étrangers, des laboratoires publics ou privés.

# THESE DE DOCTORAT DE

L'UNIVERSITE D'ANGERS

ECOLE DOCTORALE N° 605

*Biologie Santé*

Spécialité: CANCÉROLOGIE SANTE

Par

**Milad BAROUD**

## **Self-assemblies of azacitidine prodrugs: a promising strategy of treatment for myelodysplastic syndromes and acute myeloid leukemia**

Thèse présentée et soutenue à Angers, le 9 décembre 2021

Unité de recherche: Micro et Nanomédecines Translationnelles, INSERM 1066 - CNRS 6021

### **Rapporteurs avant soutenance:**

Dr. Yohann Corvis  
Dr. Lucie Sancey

MCU-Associate Professor, Université Paris Descartes, CNRS UMR 8258 – Inserm U 1267  
Director of research CNRS, Université Grenoble Alpes, CNRS UMR 5309 – Inserm U1209

### **Composition du Jury:**

Pr. Patrick Dallemagne  
Dr. Yohann Corvis  
Dr. Lucie Sancey  
Dr. Sylvain Thepot

PU, University of Caen Normandy, CERMN, FR CNRS 3038 INC3M **Président**  
MCU- Associate Professor, Université Paris Descartes, CNRS UMR 8258 – Inserm U 1267  
Director of research CNRS, Université Grenoble Alpes, CNRS UMR 5309 – Inserm U1209  
PH, CHU d'Angers, Maladies du sang

### **Directeur de thèse**

Pr. Olivier Duval

PU-PH, Université d'Angers, CNRS UMR 6021 – Inserm U1066

### **Co-directeur de thèse**

Dr. Elise Lepeltier

MCU- Associate Professor, Université d'Angers, CNRS 6021 – Inserm 1066

### **Co-encadrant**

Pr. Yolla El-Makhour

PU, Université Libanaise, EHRL

**L'auteur du présent document vous autorise à le partager, reproduire, distribuer et communiquer selon les conditions suivantes :**



- Vous devez le citer en l'attribuant de la manière indiquée par l'auteur (mais pas d'une manière qui suggérerait qu'il approuve votre utilisation de l'œuvre).
- Vous n'avez pas le droit d'utiliser ce document à des fins commerciales.
- Vous n'avez pas le droit de le modifier, de le transformer ou de l'adapter.

**Consulter la licence creative commons complète en français :**  
**<http://creativecommons.org/licences/by-nc-nd/2.0/fr/>**

Ces conditions d'utilisation (attribution, pas d'utilisation commerciale, pas de modification) sont symbolisées par les icônes positionnées en pied de page.



## ACKNOWLEDGEMENTS

First of all, I would like to thank Prof. Patrick Saulnier, director of MINT, for welcoming me to his laboratory during this thesis.

I would like to express my deep gratitude to Prof. Olivier DUVAL, Dr. Elise Lepeltier and Prof. Yolla El-Makhour my research supervisors, for the opportunity to work on this project. But most importantly, for their guidance, encouragement and patience in teaching me the skills needed to become a researcher. An additional thanks must go to you Elise, during these 3 years you have been everything a student needs in a director and MORE, a great source of knowledge and motivation, that made me love research even more. You are a marvelous mentor but more importantly a genuinely great human, your strength, kindness, support, and understanding are the reason I could reach the finish line, am grateful to have met such an inspiring person. I'll never be able to thank you enough.

To Dr. Sylvain THEPOT, I'd like to accord a thanks for your constant counsel during my thesis.

I would also like to thank Prof. Catherine PASSIRANI, your guidance during this time was indispensable. Thank you for showing me that nothing suites success more than humbleness and modesty.

I can't forget to thank Nolwenn LAUTRAM for helping me with chromatography and mass spectrometry. For answering my endless questions, teaching me greatly in a field that was foreign to me.

Many thanks must go to "Ligue contre le cancer" for financing this work.

I must also thank my colleagues Lena, Vincent. I wish you a bright future.

I would like to thank the members of my dissertation committee for generously offering their time, expertise and guidance in review of my thesis.

To Pierre, thank you for being an inquisitive researcher. It drives us both harder, I wish you a great future.

Norraseth, a great office mate, I wish you the best in your endeavours.

To my friends here in France, no words can describe the gratitude I feel towards you, you made a foreigner feel at home amongst his family, which alone means the world to me (#99). Claire, my sister you were there for me in the hardest of times and in the happiest moments as well, your kindness shines so brightly. Abdallah, well no words can truly describe you, in you I found a friend and a brother that can simply finish my sentences, surely you aided me tremendously in the lab and all my queries, but more importantly you were a great support to me during this time, we shared a lot of tough times but even so much more laughter, you are unfailingly always there, shokran. Kevin, nobody gets my weird humor like you do, thanks for the many laughs we shared together.



## ACKNOWLEDGEMENTS

Valentin, thank you for being such an accepting, caring and open person, the many many talks we had together mean so much to me. Helene, you're a very compassionate person that cares deeply for her friends thank you for that and more. I have been blessed to meet such a great group of friends who embraced my weirdness and craziness with their own, the crazy nights and moments we shared together will always be the best memories I have of these three years.

It is rare to meet a friend that you click with so well, truly a person that knows you to the core of your soul, a friend that can understand you without the need to speak, and can be counted on to be there no matter happens, Flavien, thank you for being that and being a beacon of happiness, smiles (and cheese). I will cherish the moments we shared, knowing I found in you a lifelong friend.

Majda, don't be suspicious. Every moment we spent together was jam packed with fun and memories, may that never end.

To Heba, a gentle soul beyond all. Your smile brightness up the whole place☺. Keep smiling and stay the caring person that you are, but pleaseeeee stop force feeding us.

Marrie-anne, HELLO MAJ. You suddenly and swiftly became a dear friend, you taught me what strength is, what kindness is and DEFINETLY what craziness is. Thank you.

Cecile, you're a very open person (that hates people :O), your company is always delightful. I expect great craziness from you and MAJ XD.

To Mostafa, Adham, Abbas, Rayan and Mojtaba, our friendship has spanned many years now and I know it will span many more years to come, thank you for hearing me out, for your advice and unwavering support through these years, for the tears of laughter, and your hearts of gold. No words of thanks can ever rightfully repay you.

Bashar, thank you for being a big brother to me here, with you I feel am still in Lebanon, in the midst of my family.

Finally, and most importantly, to my family, no words, no acts, nothing can come close to describe my gratitude. First to my mother Hala, no words are needed nor are able to describe a mother, you sacrificed EVERYTHING for me to reach this point, words fail to convey my feelings and gratitude, and simply put I hope I made you proud. To my father Ibrahim, this is as much your dream as it is mine and thank you for your strength and the lessons you taught me, for the person you raised me to be. Lastly, to my sister Sara, my debt to you can never be repaid, the burdens you shouldered just to see me chase and achieve my dreams are monumental, you are truly the embodiment of strength and my inspiration, thank you for your support, thank you for being you.

"I am just a child who has never grown up. I still keep asking these 'how' and 'why' questions. Occasionally, I find an answer."

**Stephen Hawking**

## Table of Contents

List of figures .....	1
List of tables .....	2
List of Abbreviations .....	3
Chapter 1: State of the art.....	6
1. In the pursue of a cure for MDS and AML: where do we stand?.....	7
1.1. The modern approach in the treatment of MDS and AML .....	7
1.2. Azacitidine: Out of favor chemotherapeutic drug that may still be ripe with opportunities.....	20
2. Fatty acid metabolism: a novel vulnerable target in MDS .....	22
2.1. Fatty acid-mediated ferroptotic cell death in cancers.....	23
2.2. Other methods by which fatty acids act as anti-cancer agents.....	26
3. The evolution of nucleosidic analogues: self-assembly of prodrugs into nanoparticles for cancer drug delivery .....	29
4. Nanomedicines: a developing prospective for MDS and AML .....	53
5. The nanoparticle enhanced: self-assembling prodrugs .....	54
5.1. Self-assembly and PUFAylation .....	56
5.2. Cell membrane interactions and nanoparticle entry into cells .....	57
6. Aims of this project .....	61
Chapter 2: Prodrug synthesis and self-assembly .....	63
1. The three-step approach for prodrug synthesis.....	64
1.1. Overview of the 3-step synthesis process.....	65
1.2. Protection of azacitidine.....	66
1.3. Conjugation of protected azacitidine to the fatty acid .....	70
1.4. Removal of the silyl protecting group.....	75
2. Azacitidine Omega-3 self-assemblies: synthesis, characterization, and potent applications for myelodysplastic syndromes. ....	77
Supplementary data.....	93
3. Nanoparticle tracking analysis.....	96

4. Conclusion .....	98
Chapter 3: Viability assay and internalization study .....	99
1. Materials and methods.....	99
1.1. Materials .....	99
1.2. Cell culture .....	99
1.3. Self-assembly formulation .....	100
1.4. Self-assembly based FRET formulation .....	100
1.5. MTT.....	101
1.6. Cell internalization of FRET self-assemblies .....	101
2. Results and discussion .....	102
2.1. Cytotoxicity studies .....	102
2.2. Cell internalization study of the self-assemblies .....	105
3. Conclusion .....	109
Discussion and perspectives .....	110
1. Prodrug synthesis .....	111
2. Self-assembly formulation.....	113
3. Evaluation of the biological effects.....	116
References .....	119

## List of figures

Figure 1: Key hematopathological features that are observed in MDS..	9
Figure 2: Quantitative stem and progenitor alterations in MDS subgroups.	11
Figure 3: MDS treatment algorithm..	13
Figure 4: Chemical structure of azacitidine and decitabine.	16
Figure 5: Chemical structure of guadecitabine.	17
Figure 6: Hydrolysis of azacitidine..	21
Figure 7: Mechanisms of ferroptosis..	24
Figure 8: Chemical structure of EPA and DHA.	25
Figure 9: Several mechanisms by which omega-3 can affect cancers.	26
Figure 10: The decennary progress of anti-cancer unsaturated fatty acid prodrugs..	55
Figure 11: Cell internalization pathways of nanoparticles <sup>209</sup> .	59
Figure 12: Synthesis and formulation approaches for the development of an inventive platform for azacitidine administration.	61
Figure 13: Synthesis of the squalenoyl adenosine conjugate.	64
Figure 14: The 3-step synthesis pathway for the synthesis of azacitidine-fatty acid conjugates.	65
Figure 15: Experimental setup under inert conditions.	66
Figure 16: UPLC chromatogram of protected azacitidine.	67
Figure 17: <sup>1</sup> H NMR spectra of protected azacitidine.	68
Figure 18: Mass spectra of the protected azacitidine.	68
Figure 19: Chemical structure of DMAPA.	70
Figure 20: <sup>1</sup> H NMR of the DMAPA-OA conjugate.	72
Figure 21: <sup>1</sup> H NMR of the protected azacitidine-OA conjugate.	73
Figure 22: Mass spectra of protected the azacitidine-OA conjugate.	73
Figure 23: Mass spectra of the protected azacitidine-EPA conjugate.	74
Figure 24: Mass spectra of the protected azacitidine-DHA conjugate.	74
Figure 25: Mass spectra of the azacitidine-EPA conjugate.	75
Figure 26: Mass spectra of the azacitidine-DHA conjugate.	76
Figure 27: Population distribution graphs of the AzaDHA and AzaEPA self-assemblies obtained by NTA.	97
Figure 28: Chemical structure of CholEsteryl BODIPY <sup>TM</sup> FL C12 and CholEsteryl <sup>TM</sup> BODIPY C11.	100

<b>Figure 29: Cytotoxicity studies of the self-assemblies compared to the free azacitidine and fatty acids at different time points. (A) 6 hours, (B) 24 hours, (C) 48 hours....</b>	<b>104</b>
<b>Figure 30: Fluorescence spectra of the different BODIPY self-assemblies at 0.5% and 1% in concentration of dyes. ....</b>	<b>106</b>
<b>Figure 31: Internalization of FRET AzaEPA and AzaDHA self-assemblies. ....</b>	<b>108</b>
<b>Figure 32: Chemical structure of omega-3 fatty acids. ....</b>	<b>114</b>
<b>Figure 33: Cryo-TEM images of AzaDHA (A) and AzaEPA (B) self-assemblies showing the presence micelles. ....</b>	<b>115</b>
<b>Figure S 1: Mass spectra of the azacitidine-EPA conjugate. ....</b>	<b>93</b>
<b>Figure S 2: Mass spectra of the azacitidine-DHA conjugate. ....</b>	<b>93</b>
<b>Figure S 3: Chromatogram of the azacitidine-EPA conjugate to determine its purity. ....</b>	<b>94</b>
<b>Figure S 4: Chromatogram of the azacitidine-EPA conjugate to determine its purity. ....</b>	<b>95</b>
<b>Figure S 5: Chromatogram of the azacitidine-DHA conjugate to determine its purity ....</b>	<b>95</b>

## List of tables

<b>Table 1: World Health Organization classification of myelodysplastic syndrome. ....</b>	<b>8</b>
<b>Table 2: Recurrent mutations in myelodysplastic syndromes. ....</b>	<b>10</b>
<b>Table 3: Novel treatment approaches for MDS. ....</b>	<b>18</b>
<b>Table 4: Initial conditions used in the protection reaction of azacitidine. ....</b>	<b>69</b>
<b>Table 5: The half maximal inhibitory concentration determined by a MTT assay on HL-60 cells, after treatment by azacitidine, fatty acids and self-assemblies at different time points. ....</b>	<b>104</b>
<b>Table 6: Physical characteristics of the fluorescent self-assemblies. ....</b>	<b>107</b>

## List of Abbreviations

MDS	myelodysplastic syndromes
AML	acute myelodysplastic leukemia
FAB	French-American-British group
CMP	common myeloid progenitors
MEP	megakaryocyte-erythrocyte progenitor
GMP	granulocyte-monocyte progenitor
FACS	Analysis of fluorescence-activated cell sorting
WHO	World Health Organization
NCCN	National Comprehensive Cancer Network
MDS-RS	MDS with ring sideroblasts
MDS-EB	MDS with excess blasts
MDS-U	MDS unidentifiable
WPSS	World Health Organization Prognostic Scoring System
MDA-LR	M.D. Anderson Lower-Risk MDS Prognostic Scoring System
MDAS	Global M.D. Anderson Risk Model Score for MDS
IPSS-R	Revised International Prognostic Scoring System (IPSS-R)
HCT	allogenic hematopoietic stem cell transplant
ESA	erythropoiesis-stimulating agent
EMA	erythropoiesis- maturing agent
FDA	US Food and Drug Administration
EMA	European Medicines Agency
RBC	Red blood cell
ATG	antithymocyte globulin
HLA	human leukocyte antigen
FATP	fatty acid transport protein
LDLR	low density lipoprotein receptor
FABP	fatty acid binding proteins
LPO	lethal lipid peroxide
HMA	hypomethylating agent
ROS	reactive oxygen species
EPA	eicosapentaenoic acid
DHA	docosahexaenoic acid
GPX4	glutathione peroxidase 4

MUFA	mono-unsaturated fatty acid
PUFA	poly-unsaturated fatty acid
NEDD8	neural precursor cell expressed developmentally downregulated
IDH	isocitrate dehydrogenase
BCL2	B-cell lymphoma
PD1	programmed death 1
PDL1	programmed death ligand 1
CTLA4	cytotoxic T-lymphocyte antigen 4
TIM3	T cell immunoglobulin and mucin domain-containing protein 3
TP53	Tumor protein 53
hENT1	Human Equilibrative Nucleoside Transporter 1
DNMT1	DNA methyl transferase 1
PEG	polyethylene glycol
RP-HPLC	semi-preparative reversed phase high-performance liquid chromatography
TBDMSCI	tert-Butyldimethylsilyl chloride
ET <sub>3</sub> N	triethylamine
HATU	Hexafluorophosphate Azabenzotriazole Tetramethyl Uronium
DMAP	4-dimethylaminopyridine
DIPEA	N, N-Diisopropylethylamine
TBAF	tetra-n-butylammonium fluoride
DMF	Dimethylformamide
THF	Tetrahydrofuran
NMR	Nuclear magnetic resonance
UPLC	Ultra Performance Liquid Chromatography
DMSO	dimethyl sulfoxide
HBTU	Hexafluorophosphate Benzotriazole Tetramethyl Uronium
EDC	1-Ethyl-3-(3-dimethylaminopropyl) carbodiimide
DMAPA	dimethylaminopropylamine
EtCOCl	ethyl chloroformate
MgSO <sub>4</sub>	magnesium sulfate
FTIR	Fourier-transform infrared spectroscopy
Cryo-TEM	Transmission electron cryomicroscopy
CAC	critical aggregation concentration
DLS	Dynamic light scattering
NTA	Nanoparticle Tracking Analysis



NaH <sub>2</sub> PO <sub>4</sub>	Monosodium phosphate
PDI	Polydispersity Index
DOSY	Diffusion ordered spectroscopy
FRET	Förster Resonance Energy Transfer
FACS	Fluorescence-Activated Cell Sorting
PBS	Phosphate-buffered saline
FBS	Fetal bovine serum
MTT	3-(4,5-dimethylthiazol-2-yl)-2,5-diphenyltetrazolium bromide
MFI	mean fluorescence intensity
MALS	Multiangle light scattering
SAXS	Small-angle X-ray scattering

## Chapter 1: State of the art

This section aims to introduce the general aspect of the project, describing at first the disease that was selected and the thought process behind choosing the suitable strategy to a novel treatment approach.

First, the myelodysplastic syndrome is introduced in its biological and clinical aspects. Then, the current treatments for this disease with the limitations these treatments carry, showing a need of a new treatment approach, are discussed. The possible upcoming treatments by inspecting the most promising clinical trials are then presented. The choice of azacitidine as the most promising drug for the treatment of MDS is then explained in showcasing the undergoing clinical trials.

Following that, we focus on Omega-3 fatty acids and their promise in the field of cancer treatment, while describing the biological aspects of their anti-cancer effects and the possibility of having a synergistic effect with the azacitidine.

Then, the importance of the nucleosidic analogues, as azacitidine and others, while proposing to develop them into prodrugs to enhance their biological effect, is discussed through a published review paper. We even go a step further in introducing the possible self-association of these prodrugs, thus gaining a further advantage meanwhile battling all the limitation of the parent molecule.

Lastly, the mechanisms by which these obtained azacitidine self-assemblies are able to enter the cells are discussed.

# **1. In the pursue of a cure for MDS and AML: where do we stand?**

Despite the fact that the German physician Wilhelm Olivier Leube in the early 20<sup>th</sup> century started to observe and document several cases of severe megaloblastic anemia, the first classification of the myelodysplastic syndromes (MDS) was established in 1982 by the French-American-British group (FAB)<sup>1,2</sup>. From that point forwards, even though extensive advances have been made in the classification and diagnosis of this disease, the treatment options remain limited and a grim prognosis awaits patients that are resistant to one of the few options of available treatment, as this disease may evolve into acute myelodysplastic leukemia (AML). The huge variation in types of this disorder coupled to a poor understanding of its origin consequently makes this hematologic cancer one of the biggest challenges currently being tackled by hemato-oncology. The Incidence of MDS is higher in elderly patients and bone marrow allogenic transplantation is the only curative treatment<sup>3</sup>. However, due to age, most of MDS patients are not eligible to such aggressive therapy. Additionally, challenges in drug delivery and resistance to treatment are the main hurdles that MDS and AML present. Present-day treatments are still non-satisfactory, with the focus being on symptom management instead of curative options<sup>4</sup>. Nonetheless, advances in medical research and development of novel treatment options are showing promising strides in combating this ailment. In this chapter, we focus on the current treatments of MDS and AML, and the drugs being developed to counter the various hurdles presented by this disease and investigating treatment prospects that might pave the path to a cure.

## **1.1. The modern approach in the treatment of MDS and AML**

The myelodysplastic syndromes are a clonal disorder of the hematopoietic stem cell characterized by evident morphological dysplasia (abnormal cells that may develop into a cancerous component), showing variable degrees of cytopenias (decreased blood cell count) with a possibility of progressing into acute myeloid leukemia.

To reach the point of discussing the treatment approach for this disease, several key points about the disease that impact the treatment plan must be first introduced.

MDS occurs in the general population at a rate of 4.5 per 100,000 people per year, with males being more prone to developing MDS when compared to females (6.2 vs. 3.3 per 100,000 people, per year), not to mention that the risk increases with age. People younger than 40 exhibit a rather low prevalence ~0.1 per 100,000 people per year, escalating to 26.9 per 100,000 people

per year for people aged 70 to 79 and additionally rises to 55.4 per 100,000 people per year in elderly above 80<sup>5,6</sup>.

Since the first classification of MDS that occurred in 1982 by FAB<sup>1</sup>, several updated classifications were presented over the years, culminating in 2001<sup>7</sup> when the World Health Organization (WHO) proposed a novel classification that was then updated in 2008<sup>8</sup> and 2016<sup>9</sup>. Previously, cytopenias was a "*sine qua non*" in diagnosis and classification, whereas currently the new WHO classification relies solely on the blast percentages and the grade of the dysplasia and the cytogenetic clonal abnormality with few definite cytopenias slightly influencing the classification<sup>9</sup>. Presently there are six MDS categories that are based upon cytogenetics and bone marrow morphology, presented in **Table 1**, the key hematopathological features are presented in **Figure 1**<sup>10-12</sup>. Aside the six agreed upon categories, "refractory cytopenia of childhood" isn't considered as a solid category, rather it is termed a provisional entity that can be later modified or removed.

Name	Dysplastic lineages	Cytopenias	BM and PB blasts
MDS with single lineage dysplasia	1	1-2	BM <5%, PB <1%, no Auer rods
MDS with multilineage dysplasia	2-3	1-3	BM <5%, PB <1%, no Auer rods
MDS with ring sideroblasts (MDS-RS)			
MDS-RS with single lineage dysplasia	1	1-2	BM <5%, PB <1%, no Auer rods
MDS-RS with multilineage dysplasia	2- 3	1-3	BM <5%, PB <1%, no Auer rods
MDS with isolated del(5q)	1-3	1-2	BM <5%, PB <1%, no Auer rods
MDS with excess blasts (MDS-EB)			
MDS-EB-1	0-3	1-3	BM 5%-9% or PB 2%-4%, no Auer rods
MDS-EB-2	0-3	1-3	BM 10%-19% or PB 5%-19% or Auer rods
MDS, unclassifiable (MDS-U)			
MDS-U with 1% blood blasts	1-3	1-3	BM <5%, PB <1%, no Auer rods
MDS-U with single lineage dysplasia and pancytopenia	1	3	BM <5%, PB <1%, no Auer rods
MDS-U based on defining cytogenetic abnormality	0	1-3	BM <5%, PB <1%, no Auer rods
Refractory cytopenia of childhood	1-3	1-3	BM <5%, PB <2%

**Table 1: World Health Organization classification of myelodysplastic syndrome.** BM: bone marrow; PB: peripheral blood. Auer rods (**Figure 1**) are pink or red-stained needle-shaped structures seen in the cytoplasm of myeloid cells that are of clinical diagnostic significance in MDS and AML<sup>13</sup>. (Adapted from Arber *et al.*, Blood, 2016<sup>9</sup>)

Analysis by fluorescence-activated cell sorting (FACS) coupled with high throughput sequencing studies on primary samples and studies on mouse models, are the chief means by which we are expanding our understanding of the clonal evolution whether as MDS or in its progressed form of AML<sup>14-17</sup>.

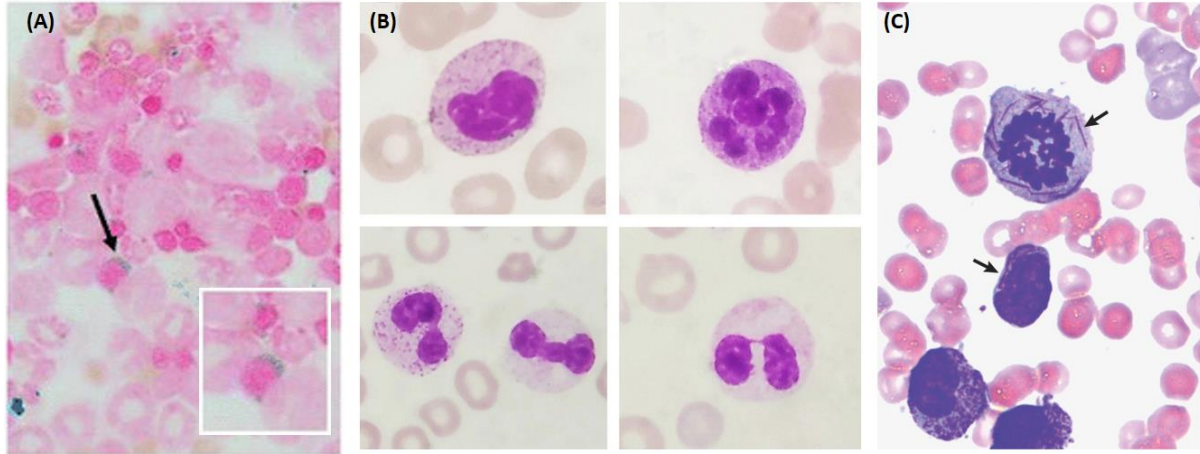


**Figure 1: Key hematopathological features that are observed in MDS.** (a) Ring sideroblasts, (b) dysplasia observed in neutrophil's nucleus, (c) Auer rods. Adapted from Visconte *et al.* 2014, Shekhar *et al.* 2021, and Gordon *et al.* 2017, respectively.

Medullary blast quantification for classification changed during the past 20 years with AML diagnostic considered above 30% blast in the FAB classification whereas it is above 20% in the WHO classification<sup>18,19</sup>.

A dispute is still ongoing on the division between MDS and AML: in comparison to *de novo* AML, the clinical outcomes of MDS cases rely upon specific molecular and biological features that impact the speed of the disease in tandem with the amount of blasts<sup>9,20</sup>. In several cases, the distinction is more challenging, as the WHO alongside the National Comprehensive Cancer Network (NCCN) consider patients with a blast numbers between 20% to 29%, while showing clinical stability to have either high-risk MDS or AML<sup>20,21</sup>. In patients showing either *NMP1* or *FLT3* mutations, AML is the usual suspect rather than MDS<sup>22</sup>. Therefore, it is of utmost importance to combine the genetic features of the abnormal cells, the recurrent genetic mutations being presented in **Table 2** (50 different<sup>14,23</sup>), and the morphology of these anomalous cells with their

Functional group	Included genes
DNA methylation	<i>DNMT3A, TET2, IDH1, IDH2</i>
Chromatin modification	<i>EZH2, SUZ12, EED, JARID2, ASXL1, KMT2, KDM6A, ARID2, PHF6, ATRX</i>
Cohesin complex formation	<i>STAG2, RAD21, SMC3, SMC1A</i>
RNA splicing	<i>SF3B1, SRSF2, U2AF1, U2AF2, ZRSR2, SF1, PRPF8, LUC7L2</i>
Transcription	<i>RUNX1, ETV6, GATA2, IRF1, CEBPA, BCOR, BCORL1, NCOR2, CUX1</i>
Cytokine receptor/tyrosine kinase	<i>FLT3, KIT, JAK2, MPL, CALR, CSF3R</i>
Other signaling	<i>GNAS, GNB1, FBWX7, PTEN</i>
DNA repair	<i>ATM, BRCC3, FANCL</i>
Checkpoint/cell cycle	<i>TP53, CDKN2A</i>
Other	<i>NPM1, SETBP1, DDX41</i>

**Table 2: Recurrent mutations in myelodysplastic syndromes.** (Adapted from Arber *et al.*, 2016<sup>4</sup>)

quantity to reach a more precise distinction between the two diseases and their subtypes. It will insure a better choice of clinical action that can be personalized to suit the patient's unique condition.

MDS cannot be justly discussed without regarding its clinical impact particularly in prognosis, as it plays a key role in the choice of treatment. Though the WHO's classification methodology is a staple in diagnosis. Taken alone, it is insufficient to decide the course of action when it comes to treatment options, as MDS will vary between patients and the approach must rely on the diagnosis combined with another prognostic-dependent classification to finally arrive to the precise treatment route needed. Then again, as observed in the old classifications (previous WHO and FAB classifications) leading up to this new WHO classification, due to the large variables of this disease including the various cell types that can be affected, the different genetic mutations that can occur singly or simultaneously (**Table 2**), and the age of the patient among other variables, there exists various prognostic classification approaches, of which the most prevalent are<sup>24</sup>: World Health Organization Prognostic Scoring System (WPSS)<sup>25</sup>, M.D. Anderson Lower-Risk MDS Prognostic Scoring System (MDA-LR)<sup>26</sup>, Global M.D. Anderson Risk Model Score for MDS (MDAS)<sup>27</sup>, and Revised International Prognostic Scoring System (IPSS-R)<sup>25</sup>. These classification models rely upon different combinations of certified prognostic features including:

- blast percentage in bone marrow
- type and number of chromosome abnormalities in the cells
- red blood cell levels
- platelet levels in the blood
- neutrophil levels in the blood
- patient's age
- severity of low blood cell counts
- serum ferritin levels

Though they differ in the methodology of prognosis, all the systems aim to produce a weighted scoring system that splits patients into different risk categories (**Figure 2**), which play a crucial role in determining (i) the risk of each patient to develop AML, (ii) the best suited therapy for each case and (iii) the eligibility of the patient to undergo a stem cell transplant<sup>24,28-31</sup>.

**Figure 2** presents a simplified general model of the different progenitor populations in healthy and MDS cells, focusing on the alternative pathways of differentiation occurring at the progenitor and hematopoietic stem cell stage. A low risk MDS presents an increased common myeloid progenitors growth coupled to a decrease in the megakaryocyte-erythrocyte progenitor populations, while high risk MDS is mainly characterized by granulocyte-monocyte progenitor expansion<sup>32,33</sup>.

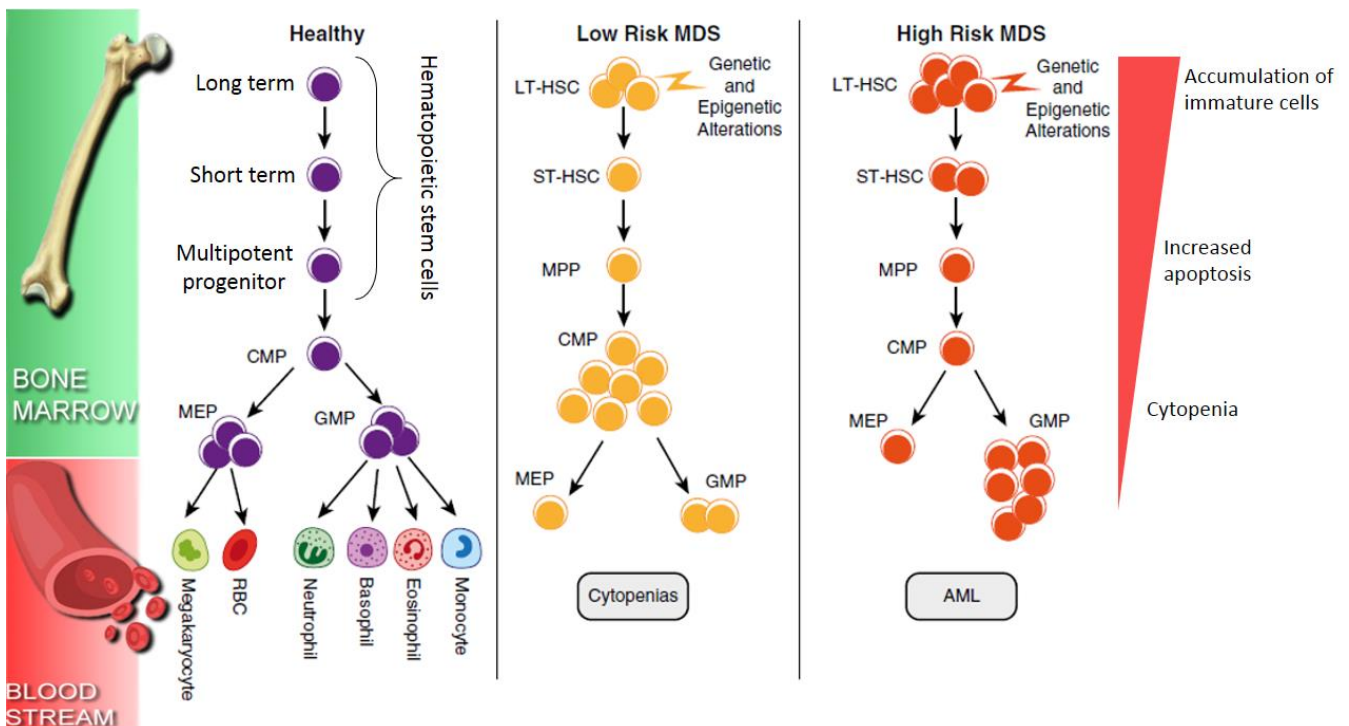


**Figure 2: Quantitative stem and progenitor alterations in MDS subgroups.** CMP: common myeloid progenitors; GMP: granulocyte-monocyte progenitor; MEP: megakaryocyte-erythrocyte progenitor; MkP: megakaryocyte progenitor; EPP: early erythroid progenitor (Adapted from Shastri *et al.*, 2017<sup>34</sup>).

### 1.1.1. Therapeutic approaches for MDS

When approaching the treatment for MDS that are two end points to be sought: in low risk patient the aims is to increase quality of life with first to enhance the peripheral blood numbers including the reduction of bleeding and improving the hemoglobin. In higher risk MDS the aims is to increase life expectancy and to modify and impede the disease advancement<sup>35</sup>. Therefore, selecting the adequate therapy for the patient will rely upon the risk group the patient fits in/

the degree of MDS development, the physical state of the patient, aim of the treatment and suitability of the patient for allogeneic hematopoietic stem cell transplant (HCT). Thus, in some cases, an immediate treatment might not be necessary and regular follow up and observation is sufficient. As such both the NCCN and WHO recommend separating patients into either low or high risk groups, depending on their prognostic scores, as discussed previously<sup>21,36</sup>.

The treatments for low-risk MDS patient are focused on hematological improvement, in order to avert the rise of any complications such as infections or bleeding while increasing their quality of life and diminishing the taxing blood transfusions. Whereas, in the case of high-risk patients, the main concern shifts towards slowing the course of the disease and increasing the survival rate, and if permitted, to advance to a cure via HCT<sup>21,37,38</sup>.

Nevertheless, all patients in both risk groups receive supportive care, a fundamental step in their MDS therapy. It is comprised of clinical monitoring, psychological support and quality of life evaluation, followed when needed by red blood cell and platelet transfusion in cases of symptomatic anemia and bleeding cases respectively. In instances, when bacterial infections occur, antibiotics are given. For iron overload, it is directly treated with iron chelation therapy for low-risk patients, whereas high-risk patients receive iron chelation only if they respond to hypomethylating agent therapy or are planned to undergo HCT. A more comprehensive algorithm for choosing the treatment for MDS is presented in **Figure 3**.

As MDS is a widely heterogeneous disease with varying types, symptoms and varies between different cases, the choice of treatment must be then personalized. Owing to the lack of a specified and well characterized molecular target, a biologically driven method is unachievable in most cases, and the treatments must rely on the treatment algorithms reflected by the prognostic results of each patient as discussed below.

### **a) Supportive care**

Considering that 80% of MDS patients suffer from anemia, erythropoiesis-stimulating and maturing agents (ESAs and EMAs) are a regularly used treatment option. ESAs, for instance recombinant erythropoietin or darbepoetin, are considered as the vanguard treatment for anemia in patients with low-risk MDS, as recommended by NCCN. In spite of that, ESAs in most circumstances show a feeble effect with a short-term activity. Serum erythropoietin levels appear to be a valid indicator to predict the response to ESA treatments with lower serum levels (<100 - <500 U/L), showing a better response than higher ones (>500 U/L)<sup>39-41</sup>.

Luspatercept, an activin receptor ligand-blocking agent that is undergoing phases 2 and 3 clinical trials, has shown promising results in trials via neutralizing the negative regulation of late-stage erythropoiesis. Lately, luspatercept, upon the results of stage 3 clinical study, has been approved



by the US Food and Drug Administration (FDA) for the treatment of MDS upon the failure of ESA treatment in patients needing more than 2 RBC unit transfusion over 8 weeks in low-risk MDS patients presenting ring sideroblasts or myelodysplastic neoplasm with ring sideroblasts and thrombocytosis. The European Medicines Agency (EMA) also approved luspatercept in anemia cases necessitating consistent RBC transfusions in adult patients with MDS<sup>42-44</sup>.

The sensible use of platelet transfusion should always be maintained in MDS since it carries the risk of an auto-immune reaction (alloimmunization). Patients displaying mucosal bleeding and refractory thrombocytopenia can be treated with antifibrinolytic agents such as aminocaproic acid<sup>45</sup>. In low risk MDS patients with thrombocytopenia, thrombopoietin receptor agonists can be used and are approved as they decrease bleeding complications<sup>46</sup>.

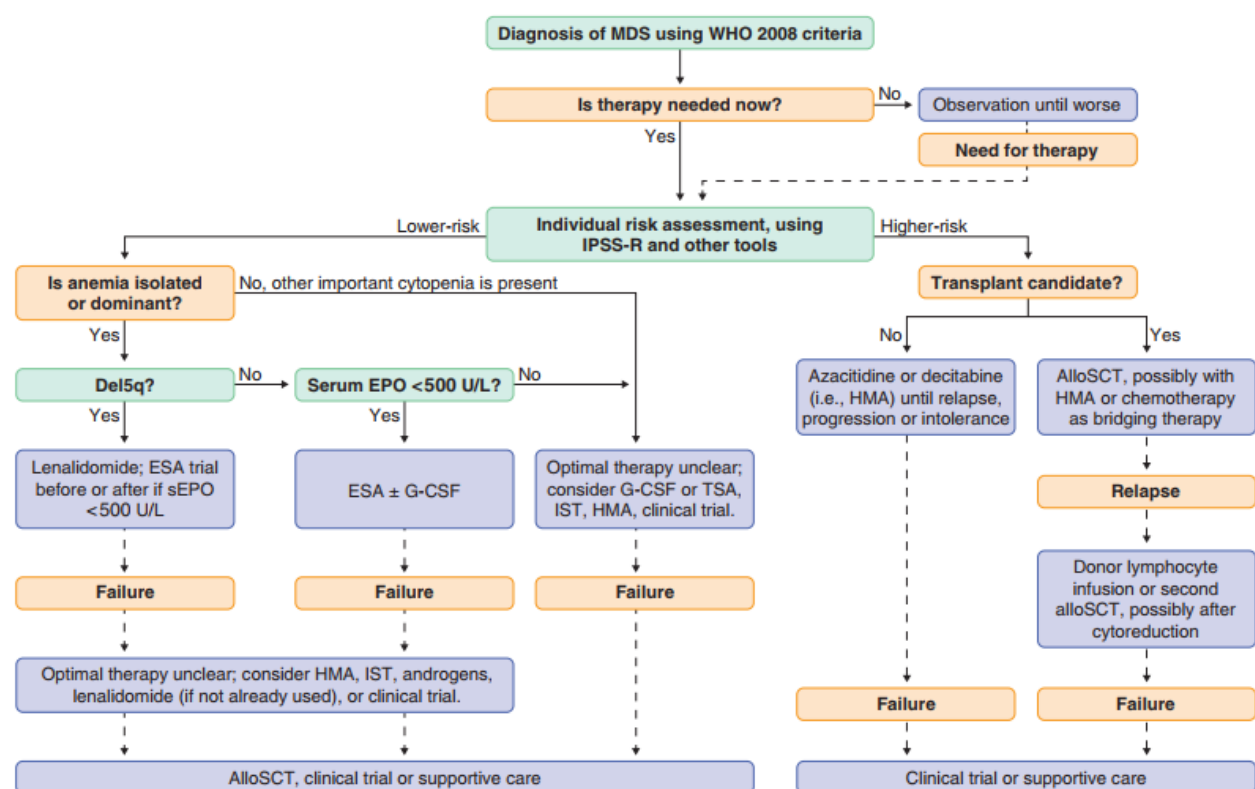


**Figure 3: MDS treatment algorithm.** G-CSF: granulocyte colony stimulating factor; sEPO: serum EPO level; TSA: thrombopoietin receptor agonist (thrombopoiesis stimulating agent). (Adapted from goldman-cecil medicine<sup>47</sup>)

## b) Iron chelation therapy

Iron overload followed by tissue injury is observed in some MDS patients, mainly due to receiving multiple RBC transfusions. There is a correlation between the number of transfusions received and the level of iron. It is still unclear how this iron overload is affecting the patients, as patients with lower serum ferritin levels show better outcomes than higher ones, whether because iron

deposits in crucial tissues and organs or simply being a marker of inflammation. Owing the discussed uncertainty and a lack in evidence of death in MDS patients secondary to iron overload, coupled to the toxicity of existing chelators such as deferasirox and deferoxamine, makes the use of this approach a well calculated and considered option to be mainly used for low-risk cases having a high transfusion need<sup>47</sup>. Iron overload seems to be involved in leukemic transformation and Iron chelation is associated with higher life expectancy<sup>48</sup>.

### **c) Immunosuppressive therapy**

A fair number of MDS patients might display an auto-immune attack by T-lymphocytes against hematopoietic cells owing to a mutation in T-cell STAT-3. In such cases, the NCCN recommends immunosuppressive therapy with antithymocyte globulin (ATG) with or without calcineurin inhibitors such as cyclosporine A. A 6 month-regimen of ATG and cyclosporine A is recommended for patients younger than 60 years old displaying normal cytogenetics, <5% bone marrow blasts and needing transfusion but that cannot have hematopoietic growth factors. ATG is also advised in the cases of hypoplastic bone marrow (depleted bone marrow cells mainly due to auto-immune attacks). ATG appears to give a better response in MDS patients displaying single lineage dysplasia with absence of ring sideroblasts, hypoplastic marrow, younger than 60, female sex, trisomy 8 and a limited reliance on transfusions<sup>21,36,37,39</sup>.

### **d) Immunomodulatory agents**

Lenalidomide is the chief immunomodulatory agent used for MDS patients. Initial reports of MDS patients displaying improvement after thalidomide therapy led to the first clinical trials of lenalidomide that eventually led to the approval of this drug by the FDA, EMA and recommendation by the NCCN. The three organizations agree on the treatment with lenalidomide for low-risk patients presenting del(5q) (a subtype of MDS presenting with the deletion of the long arm "q" of chromosome 5) with or without cytogenetic abnormalities excluding the ones that affect chromosome 7. The NCCN also recommends it in patients with symptomatic anemia and in patients with symptomatic anemia without del(5q) MDS that did not respond to initial therapy.

In a phase 3 clinical study of patients with low-risk non-del(5q) MDS, and upon lenalidomide treatment, 27% of the patients treated with lenalidomide showed an increase in RBC transfusion independence compared to 2.5% in the placebo group. Additionally, a retrospective cohort study

submits that the presence of TP53 mutations can play a predictive role for the disease progression in MDS patients with low-risk del(5q) also treated with lenalidomide<sup>49-52</sup>.

#### e) DNA hypomethylating agents

Initially antimetabolite agents were first used in 1980 as a treatment via low doses of cytarabine, or also called Ara-c, a nucleosidic analogue: it was considered as a cytoreductive therapy for MDS patients. Since then, the use of low doses of Ara-c has been substituted by two other DNA hypomethylating nucleosidic analogues: azacitidine and decitabine (**Figure 4**). These analogues act on the DNA methyltransferase causing permanent inhibition of the enzyme, leading to alteration of gene expression by decreasing the methylation levels of the cytosine thus impacting the DNA epigenetic status. Nonetheless, the exact action mechanism of these hypomethylating agents haven't been fully proven, still the use of these agents has become a staple in the treatment of high-risk MDS patients and in low-risk MDS patients following the failure of the conventional approaches, and in the cases of delays for patients eligible for HCT procedures. Several studies have shown that the implementation of azacitidine has resulted in slowing the course of the disease and improved patient's quality of life<sup>53,54</sup>. The pivotal study Fenaux and coworkers compared conventional therapies (low Ara-c doses, different chemotherapies and supportive care) to a 7-day azacitidine course: it showed an average survival period increase of 9 months in patients receiving the hypomethylating agent treatment compared to the conventional therapies, leading to the implementation of azacitidine as the customary drug of choice in high-risk MDS patients. Similar results have been obtained with the use of decitabine, though with a slightly decreased success owing to poorly optimized treatment regimen<sup>55</sup>. The presence of epigenetic gene mutations (TET2 and ASXL1) seems to be a good indicator that reflects higher chance of therapy success, as they are likely to demonstrate granulomonocytic hematopoietic skewing (advancement in the differentiation) compared to the early clonal dominance<sup>56</sup>. It is worth mentioning that hypomethylating agents have several adverse effect notably gastrointestinal problems and cytopenias. As a consequence of the limited number of options in the treatment of higher-risk MDS, these two hypomethylating agents are still the go to treatments, though having a low response rate, with only half of the patients showing improvement after treatment. The other major issue is that, upon the failure of these hypomethylating agents, the life expectancy of the patient is around 6 months or less. Currently

there are various new therapies and combination being tested to overcome this hurdle<sup>21,37,38,40,57,58</sup>.

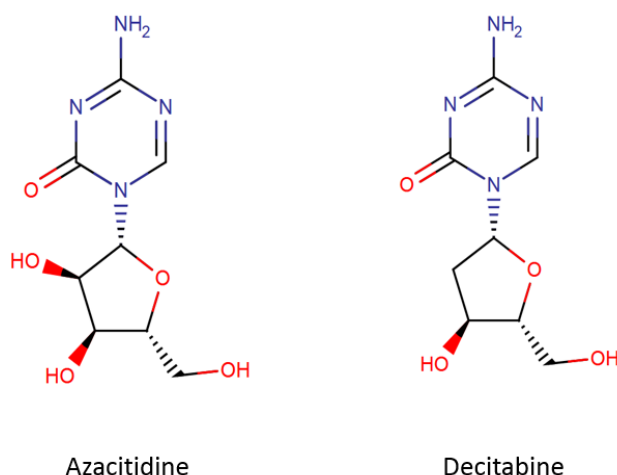


**Figure 4: Chemical structure of azacitidine and decitabine.** Decitabine is a deoxy analogue of azacitidine

#### f) Stem cell transplant

All patients with high-risk MDS that are younger than 70 years old, without other major malady, should be considered for allogeneic hematopoietic stem cell transplant, as it is the only available possible cure for MDS. Even so, several variables have to be deliberated such as the psychological state, the prognostic score, other comorbid conditions and the availability of a suitable donor. Considering that most patients are old, it decreases the chance of finding a suitable donor from their immediate family even if they have a human leukocyte antigen (HLA) match, since the age and possible diseases would impede that. Thus, such patients are treated with a hypomethylating agent to decrease the MDS/leukemic burden until a suitable unrelated donor can be found in the registries. Furthermore, recent studies show that cord blood HCT may be a viable option in these cases<sup>59,60</sup>. Even after transplantation, relapse is still a common possibility, with only one third of the transplant patients having a disease-free survival. The highest chances of success are if the transplant is done as soon as possible after the diagnosis, with opposing ideas on the use of hypomethylating agents during this period as it might lead to the selection of resistant MDS cells<sup>61-64</sup>. Additionally, in order to decrease risk of relapse after transplantation, some trial use azacitidine after transplantation<sup>65,66</sup>.

##### 1.1.2. Novel approaches for MDS treatment

There exist several challenges that are faced by the current medication regimens for MDS be it in low- or high-risk cases. They include chromosomal and molecular defects that lead to changes in the MDS cells on a pathological or physiological scale, impacting the progression of the disease,

often accelerating it. Not to mention that the number of available medications for the different stages of MDS is quite limited, additionally the available treatments are not very effective as less than half MDS patients are eligible for the treatments, meaning that the failure of the main treatment options usually foreshadows a grim prognosis. Even though current treatments may succeed in slowing the course of the disease, they are not curative and can only increase the survival time. Thus, several new approaches are under investigation to counter this limitation: the development of new agents or the use of old agents in combination therapies, especially for the high-risk MDS cases. Guadecitabine (**Figure 5**), a second-generation hypomethylating agent based on decitabine, is showing promising results in phase 2 and 3 clinical studies on patients after the failure of traditional hypomethylating agents (clinical study NCT02907359)<sup>67</sup>. Similar approaches are presented in **Table 3**, while focusing on improvements on the traditional azacitidine molecule, as it is still the most promising hypomethylating agent present.

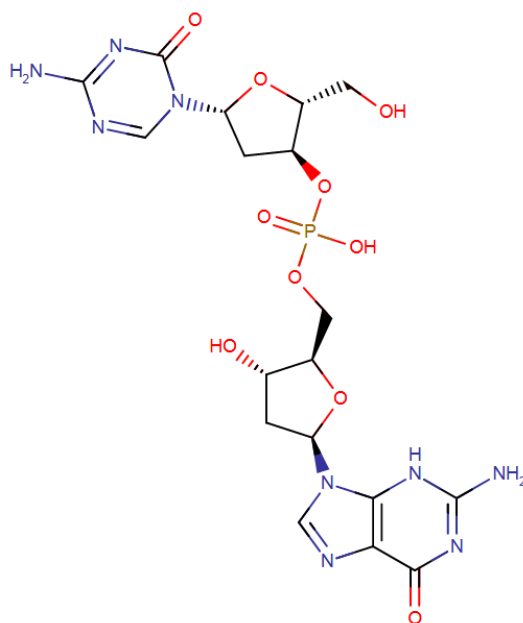


**Figure 5: Chemical structure of guadecitabine.**

Therapeutic agents	Phase	Mode of action	Results	Ref
<b>Low-risk MDS</b>				
Luspatercept	3	Activin receptor fusion protein	Transfusion independence ≥8 weeks: 38% (vs. 13% with placebo, P < 0.001)	44
Sotatercept	2	Activin receptor fusion protein	Hematologic response (erythroid): 49%	68
Roxadustat	3	HIF prolyl hydroxylase inhibitor	Transfusion independence ≥56 days: 38%	69
Imetelstat	2	Telomerase inhibitor	Transfusion independence ≥8 weeks: 42%	70
CC-486	3	Oral azacitidine	Transfusion dependence ≥56 days: 31% (vs. 11% with placebo, P = 0.0002)	71
<b>High-risk MDS</b>				
Guadecitabine	2	Second-generation HMA (decitabine linked to guanosine)	Hematologic response: 14.3%, azacitidine failure, high-risk, and higher demethylation in blood were associated with better OS	72
ASTX727	3	Second-generation HMA (fixed decitabine and cedazuridine)	Response rate: 61%, Complete response rate: 21%	73
Pevonedistat ± azacitidine	2	NEDD8 inhibitor	Response rate: 79% (vs. 57% with azacitidine alone), complete response rate: 52% (vs. 27% with azacitidine alone)	74
Enasidenib ± azacitidine	2	IDH2 inhibitor	Response rate: 67%; 100% in HMA-naïve patients (enasidenib + azacitidine), 50% in HMA-failure patients (enasidenib alone)	75
Enasidenib	2	IDH2 inhibitor	Response rate: 53%, 46% in patients with prior HMA, complete response rate: 0%	76
Olutasidenib ± azacitidine	2	IDH1 inhibitor	Response rate: 59%, 33% with olutasidenib alone, 73% with olutasidenib + azacitidine	77
Venetoclax ± azacitidine	1b	BCL2 inhibitor	Response rate: 7% with venetoclax alone, 50% with venetoclax + azacitidine	78
Venetoclax ± azacitidine	1b	BCL2 inhibitor	Response rate: 70%	79
Durvalumab + azacitidine	2	PD-L1 inhibitor	Response rate: 62% (vs. 48% with azacitidine alone)	80
Atezolizumab ± azacitidine	1b	PD-L1 inhibitor	Response rate: 9% with atezolizumab + azacitidine (HMA failure), 62% with atezolizumab + azacitidine (HMA naïve)	81

**Table 3: Novel treatment approaches for MDS.**

Therapeutic agents	Phase	Mode of action	Results	Ref
Nivolumab or ipilimumab ± azacitidine	2	PD-1/CTLA-4 inhibitor	Response rate: 75% with nivolumab + azacitidine (HMA naïve), 71% with ipilimumab + azacitidine (HMA naïve), 13% with nivolumab monotherapy (HMA failure), 35% with ipilimumab monotherapy (HMA failure)	82
Sabatolimab + azacitidine or decitabine	1b	TIM-3-targeted antibody	Response rate: 63%, including 50% in high-risk MDS and 85% in very high-risk MDS	83
Rigosertib + azacitidine	2	Multikinase inhibitor	Response rate: 90%	84
Glasdegib + cytarabine/daunorubicin	2	Hedgehog pathway inhibitor	Complete response rate: 46% (includes patients with AML)	85
<b>TP53-mutated MDS</b>				
Eprenetapopt + azacitidine	2	Small-molecule inhibitor of apoptosis in TP53-mutated cancer cells	Response rate: 75%	86
Eprenetapopt + azacitidine	2	small-molecule inhibitor of apoptosis in TP53-mutated cancer cells	Response rate: 71%	87
Magrolimab + azacitidine	1b	CD47-targeted antibody	Response rate: 100% (including 2 patients with TP53-mutated MDS)	88

**Table 3: Continued.** AML: acute myeloid leukemia, BCL2: B-cell lymphoma 2, CTLA-4: cytotoxic T-lymphocyte antigen 4, HMA: hypomethylating agent, IDH1/2: isocitrate dehydrogenase 1/2, NEDD8: neural precursor cell expressed developmentally downregulated 8, OS: overall survival, PD-1: programmed death-1, PD-L1: programmed death-ligand 1, TIM3: T cell immunoglobulin and mucin domain-containing protein 3, TP53: Tumor protein 53, RBC: red blood cell. (Adapted from Platzbecker *et al.*, 2021<sup>89</sup>)

## 1.2. Azacitidine: Out of favor chemotherapeutic drug that may still be ripe with opportunities

Azacitidine (**Figure 4**), a HMA that was discussed previously and still being used to treat MDS especially in its high-risk forms, have been showing unsatisfactory results, leaving a lot of patients with terrible prognosis: a mere 6-month survival time after its failure which occurs surprisingly in 38% of the cases with only 44% of patients reaching remission in MDS<sup>90</sup>. All patients after response to azacitidine will relapse and median overall survival after azacitidine relapse is very low (5 months) with no conventional second line therapy<sup>91</sup>.

That being said, azacitidine battle is not yet lost and positive results cannot be denied. In the absence of other treatments, the efforts of the researchers, as demonstrated in **Table 3**, rotate towards solving these shortcomings via conjugating it to other molecules or using it in combination therapies. The most recent FDA/EMA sanctioned advancement is the approval of oral formulations of azacitidine in 2020/2021 respectively. Although, its use is only validated in maintenance treatment after intensive chemotherapy for AML<sup>92</sup>.

Azacitidine is the first hypomethylating agent approved by the US Food and Drug Administration (FDA) in 2004 and later by the European Medicines Agency (EMA) in 2008 for the treatment of MDS. Its introduction as a treatment option was a breakthrough in the field of treatment of MDS especially of high-risk one as it is the first drug that was able to alter the course of the disease and delay the leukemic transformation. At low concentrations, the current concentration that is used as a treatment, it acts as a hypomethylating agent, but at higher concentrations it displays cytotoxic effects.

Diving into its chemistry, the 4-amino-1- $\beta$ -D-ribofuranosyl-S-triazin-2(1H)-one molecule (**Figure 4**) was first synthesized in 1964 by Sworm *et al*<sup>93</sup>. It is a pyrimidine nucleoside analog of cytosine with the carbon 5 of the nucleobase ring substituted by a nitrogen: the hypomethylating activity owes to this substitution.

When it comes to its mode of action, its first crucial to note that hypermethylation of the DNA, more accurately of the CpG island in the promotor region of several genes, is a characteristic of MDS cells as well as several other diseases mainly of the cancer family. For MDS, the hypermethylation of one of the tumor suppressor genes P15 causes its silencing and the loss of regulation in the cells, leading to MDS, a process that occurs more frequently in high-risk MDS. The ability of azacitidine to inhibit the methylation process, which leads to hypomethylation and thus the reactivation of the silenced tumor suppressor genes, is what lead this molecule to become the go-to treatment of MDS.



Upon its entry to the cell by the action of human Equilibrative Nucleoside Transporter 1 (hENT1), azacitidine will undergo successive phosphorylation steps by the regular nucleic acid kinases to reach its final tri-phosphorylated forms, allowing its integration into the DNA and RNA. At that point, azacitidine being a ribonucleoside, it has a greater affinity for RNA, even if its effects are still largely vague and needing modern studies to verify them. Few older studies show that incorporation into the RNA inhibits transfer RNAs methylation and processing via decreasing the transfer RNA methyl transferase levels, additionally it can disrupt ribosomal RNA processing causing the inhibition of messenger RNA and protein synthesis, finally resulting in apoptotic cell death<sup>94-96</sup>. Indeed, though as it incorporates into the DNA, binds and inhibits the enzyme that methylates DNA, called DNA methyl transferase 1(DNMT1), DNMT1 inhibition by azacitidine is not observed in resting cells (as hENT1 levels increase MDS<sup>97</sup>) and occurs at azacitidine concentrations that do not cause major suppression of DNA synthesis<sup>98-100</sup>.

Other than the clinical shortcomings of azacitidine discussed previously, there are several other weaknesses in the drug, on a biochemical level. As **Figure 6** shows azacitidine is sensitive to water: a rapid and reversible hydrolysis that produces N-formylribosylguanyllurea followed by its irreversible hydrolysis to ribosylguanyllurea<sup>101,102</sup>, thus it has a rather short half-life after administration. Additionally, because of its hydrophilic nature, it is clear that it has a rather hindered entry into the cell, a problem common to most hydrophilic drugs. Finally, the presence of nucleoside deaminase in the blood further decreases the half-life of this molecule and allows its rapid degradation and elimination<sup>102-106</sup>.

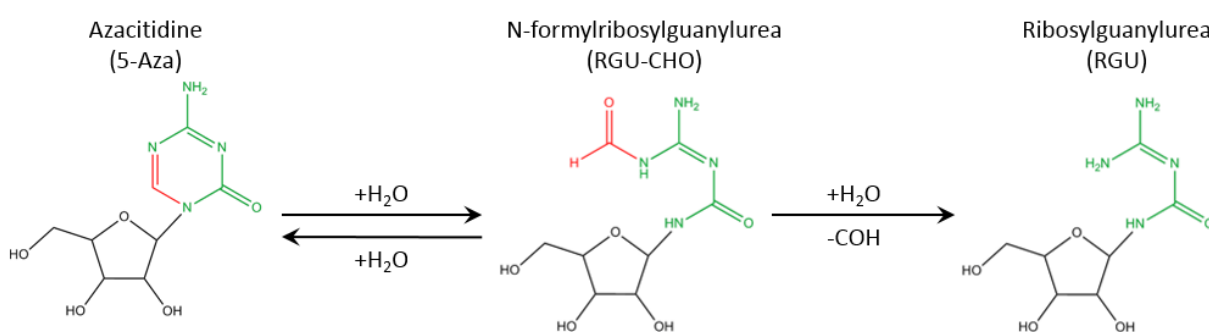


**Figure 6: Hydrolysis of azacitidine.** Adapted from Balouzet *et al.*, 2017<sup>98</sup>.

Several clinical studies are aiming to improve azacitidine via combination of synergistic treatments. Recent studies have proposed that azacitidine may function by inducing proapoptotic proteins upon combining it with venetoclax, giving rise to a new clinical study. This combination enhanced the overall survival by 1.5 times in AML, with longer lasting response to treatment and reduced transfusion dependency. Additionally, this response was also observed in more complicated cases as MDS with TP53 mutation and AML<sup>107-109</sup>.

Another study using co-treatments used azacitidine with etoposide and cytarabine. It was administered in patients' ineligible for intensive chemotherapy: this combination therapy had considerably improved the overall response rates ( $P = 0.002$ ). Additionally, it succeeded to prolong survival for these initially poor prognosed patients (8 months,  $P < 0.001$ )<sup>110</sup>.

Therefore, azacitidine, though being a valid treatment, has still several limitations. To allow this molecule to reach its full potential, these restrictions must be dealt with not only on a clinical level (by using a co-treatment that will synergize with it) but also on a biochemical level to further enhance its activity. Fatty acids implications in fighting cancers and similar maladies have been researched recently and have shown interesting results, making them a potential strategy to be used.

## **2. Fatty acid metabolism: a novel vulnerable target in MDS**

The study of the lipidome in cancers in general, and more specifically in AML, has a long history, which can reflect its role and impact in MDS. Most of the studies on MDS, occurring *in vitro* and *in vivo*, are applied on AML models, due to a lack in actual MDS models, which can accurately reflect the impact of the tested treatments. Not to mention again that these close diseases share similarities in their profile and MDS may develop into AML.

Starting from the 1960s, the lipid profiles and metabolism has been studied in AML, the lipid contents of normal and abnormal leukocytes was described, for instance in the case of cholesterol, it was observed that its levels were significantly lower when compared to normal leukocytes<sup>111,112</sup>.

The assembly of lipids into new biological membranes is a crucial step in cell proliferation, a process that is further accelerated for cancer cells. Fatty acids, the building blocks of lipids, can either be acquired from exogenous sources (through diet) or via endogenous synthesis. Cells preferentially utilize the exogenous fatty acids especially in well-nourished individuals, while the endogenous synthesis pathway is minimally utilized. Protein-mediated transport is responsible for the uptake of these exogenous fatty acids, the main transporters that facilitate this process include fatty acid translocase (FAT)/CD36, fatty acid transport proteins (FATPs)/SLC27A, low density lipoprotein receptor (LDLR), and fatty acid binding proteins (FABPs).

Due to the enormous need of cancer cells for fatty acids, the endogenous synthesis is more active when compared to normal cells, emphasizing the vital role of fatty acids in tumorigenesis<sup>113-115</sup>.

Therefore, this dire requirement of cancer cells to fatty acids creates a potential loop hole that can be exploited as a novel target to attack the cancer cells. Indeed, research is being conducted to find and understand novel mechanisms to achieve this aim: two out of the dozen omega-3 fatty acids present in nature, docosahexaenoic acid (DHA) and eicosapentaenoic acid (EPA), receive a lot of scientific curiosity due to promising results they are showing on different levels.

## **2.1. Fatty acid-mediated ferroptotic cell death in cancers**

Overtime, scientific research identified different types of cell death compromised of autophagy, apoptosis, pyroptosis, necroptosis and ferroptosis<sup>116</sup>.

In short, ferroptosis occurs upon the buildup of iron-dependent lethal lipid peroxides (LPOs). Cancer cells are protected from reactive oxygen species (ROS) mediated damage by their saturated membrane lipids that are less vulnerable to peroxidation, though unsaturated ones are more susceptible to ROS attacks: it enforces the importance of lipids and lipid metabolism for different cancer functions as tumorigenesis and metastasis. Lipid peroxidation is the driving force behind ferroptosis, additionally LPOs are implicated in several cell signaling pathways and events, such as the production of eicosanoids, signaling molecules involved in various cell mechanisms including cellular survival and proliferation, invasion and migration. The ability to regulate the lipid metabolism and consequently ferroptosis creates an innovative means by which we can treat cancer<sup>117-119</sup>.

Cells undergoing ferroptosis exhibit reduced mitochondria with several abnormalities as the shrinking of the mitochondrial folds and membrane. Furthermore, another feature that allows to differentiate between ferroptosis and other forms of cell death is that the nucleus and its components are not affected or changed morphologically<sup>120</sup>.

$\text{Fe}^{3+}$  is converted to  $\text{Fe}^{2+}$  after it is imported by transferrin receptor 1 (TFR1) and placed in endosomes. Following that, the obtained  $\text{Fe}^{2+}$  is then released from the endosomes into a labile iron pool (LIP) in the cytoplasm, via the action of divalent metal transporter 1 (DMT1) in case it is not transported back outside the cell. After accumulation of large quantities of iron, it is stored in ferritin (iron storage protein complex). Some studies indicate that heat shock protein beta-1 (HSPB1) can impact ferroptosis regulation negatively, since it inhibits the accumulation and absorption of intracellular iron by inhibiting TFR1 expression. Iron-responsive element binding protein 2 (IREB2), a transcription factor implemented in iron metabolism, will as well reduce ferroptosis upon its silencing. Nonetheless, the exact role of iron in ferroptosis is still unclear. Still, the over-production and reduced elimination of  $\text{Fe}^{2+}$  will eventually lead to a buildup of LPOs that will then usher ferroptosis<sup>117,121-123</sup>.

Other than the iron pathway, glutathione peroxidase 4 (GPX4) is another molecule that can affect ferroptosis (**Figure 7**). The GPX4-glutathione-cysteine pathway and the GPX4 peroxidation play a role in initiating ferroptosis. As GPX4 can decrease the quantity of ROS which will inhibit ferroptosis, thus genetic mutations that affect GPX4 and molecules that can block its action will lead to ferroptosis. Indeed, several studies have shown molecules that inactivate GPX4 such as ML162, ML210 and RSL3 caused an increase in ROS production, thus triggering ferroptosis<sup>124-126</sup>.

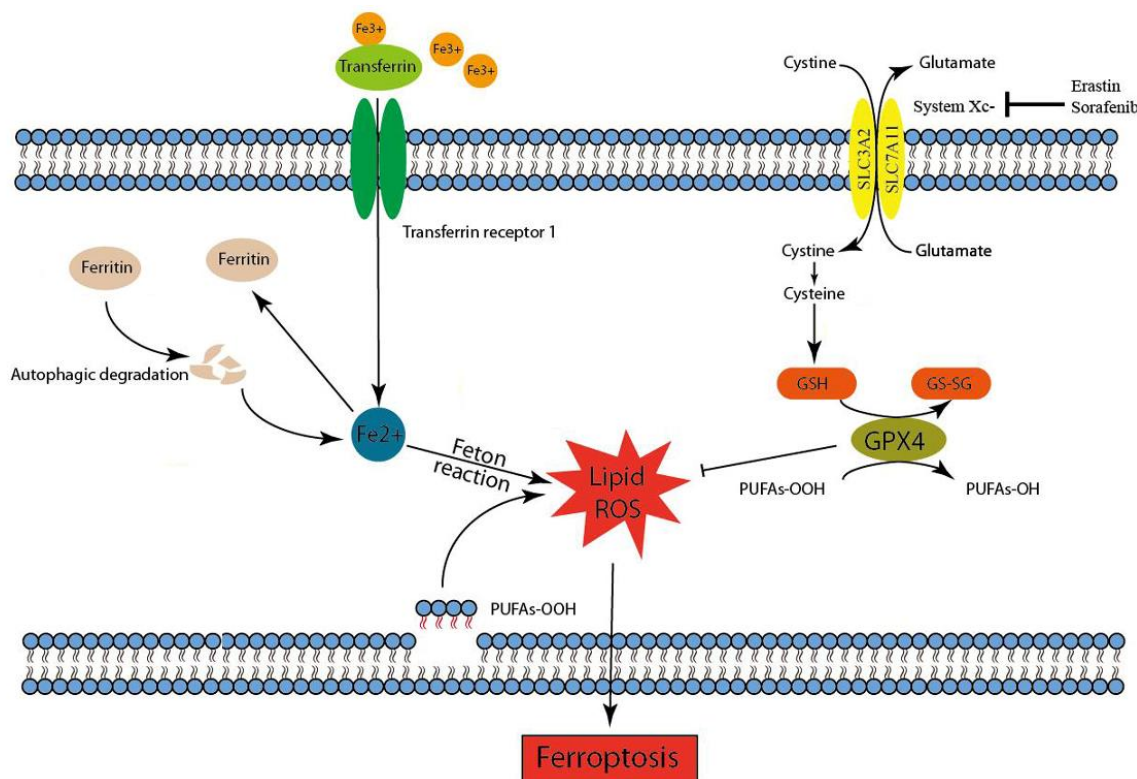


**Figure 7: Mechanisms of ferroptosis.** GSH depletion and the ensuing inactivation of GPX4 starts upon the inhibition of system Xc- (system Xc- is an amino acid antiporter that typically mediates the exchange of extracellular cystine and intracellular glutamate across the cellular plasma membrane), resulting in the accumulation of lethal lipid peroxides and initiation of ferroptosis in the presence of iron. High amounts of Fe<sup>2+</sup> accumulate lipid ROS via the Fenton reaction, causing ferroptosis. (GSH: glutathione; GS-SG: oxidized glutathione; GPX4: glutathione peroxidase 4; ROS: reactive oxygen species; PUFA: polyunsaturated fatty acids). Adapted from Lu *et al.*, 2018<sup>127</sup>.

Bearing in mind that MDS cells, similar to cancer cells, accumulate a high level of iron compared to normal cells, and both abnormal cell types additionally display a high metabolic rate in order to maintain their prompt proliferation, accompanied by an increase in ROS production. Then, targeting the antioxidant defense mechanism of cancer cells may be an effective potential treatment strategy by pushing them towards oxidative stress-mediated cell death, such as ferroptosis.

Several studies were successful in displaying the impact of targeting ferroptosis to counter different blood maladies. Indeed, a study showed that a ferroptosis inducer called erastin was able to increase the sensitivity of acute myeloid leukemia cells to chemotherapeutic agents, as low doses of erastin were able to synergize with Ara-c and doxorubicin in AML HL60 cell line<sup>128</sup>. In other studies, they aimed to utilize the iron overload that occurs in MDS/AML as a loop hole against these maladies rather than performing iron chelation therapy to relive this overload<sup>129,130</sup>. Both omega-3 fatty acids DHA and EPA (**Figure 8**<sup>131</sup>) have been shown to aid in achieving ferroptosis in different cancers.

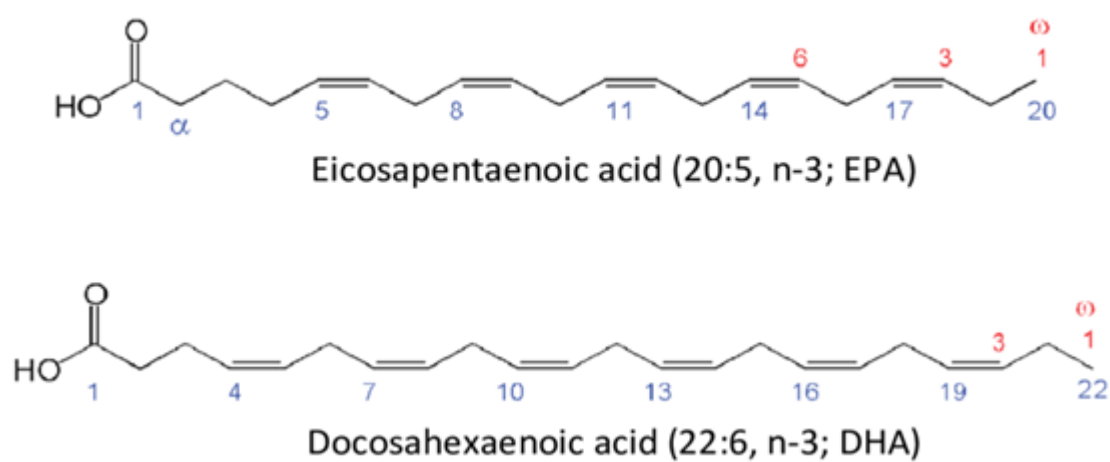


**Figure 8: Chemical structure of EPA and DHA.**

A study showed that DHA enhanced the cytotoxicity of doxorubicin in breast cancer cell line by increasing cellular levels of lipid peroxidation. Additionally, this outcome could be ended by the use of a lipid peroxidation inhibitor<sup>132</sup>. Another study proved that DHA sensitized rat breast cancers to radio treatment, and the administration of vitamin E repressed the beneficial effect of DHA, signifying that this effect can be mediated through oxidative damage to the peroxidizable lipids<sup>133</sup>. Yet a different study also revealed that DHA sensitized breast cancer cells to anthracyclines, and showed an increase in the ROS level, the sensitization was credited to a reduction of GPX1 induced by DHA, as vitamin E eliminated the effect of DHA both during sensitization to chemotherapy and GPX1 inhibition<sup>134</sup>. Additionally, another research establish that DHA induced cell death via ROS generation and caspase 8 activation in some breast cancer cell lines, claiming that fish oil diet increased the levels of EPA and DHA inside the tumors in nude mice and inhibited the *in vivo* breast cancer growth<sup>135</sup>. As well, a second study reported a synergistic effect of n-3 PUFAs and rapamycin, leading to cell cycle arrest in breast cancer cell lines. An additional inhibition of glycolysis and glutamine metabolism was also observed<sup>136</sup>.

Finally, a docosahexaenoic acid based nanoparticle managed to prompt ferroptotic cell death in hepatocellular carcinoma via lipid peroxidation and depletion of glutathione and GPX4<sup>137</sup>.

Consequently, considering the substantial need of cancer cells for fatty acids and their importance in various cellular functions, exploiting this point to prompt ferroptotic cell death in these cells using ferroptosis triggering agents can be a promising method to battle the abnormal cells. Additionally, using such agents in combination therapies with traditional MDS drugs is an interesting angle to contemplate. Lastly, the omega-3 fatty acids discussed appear to be interesting candidates out of the many fatty acids available, and have shown enticing results.

## 2.2. Other methods by which fatty acids act as anti-cancer agents

Excluding ferroptosis, various research efforts and studies have demonstrated that fatty acids including omega-3 fatty acids can work against cancers in various different pathways (**Figure 9**), bringing to light to significance of these molecules in the battle against this stubborn foe.

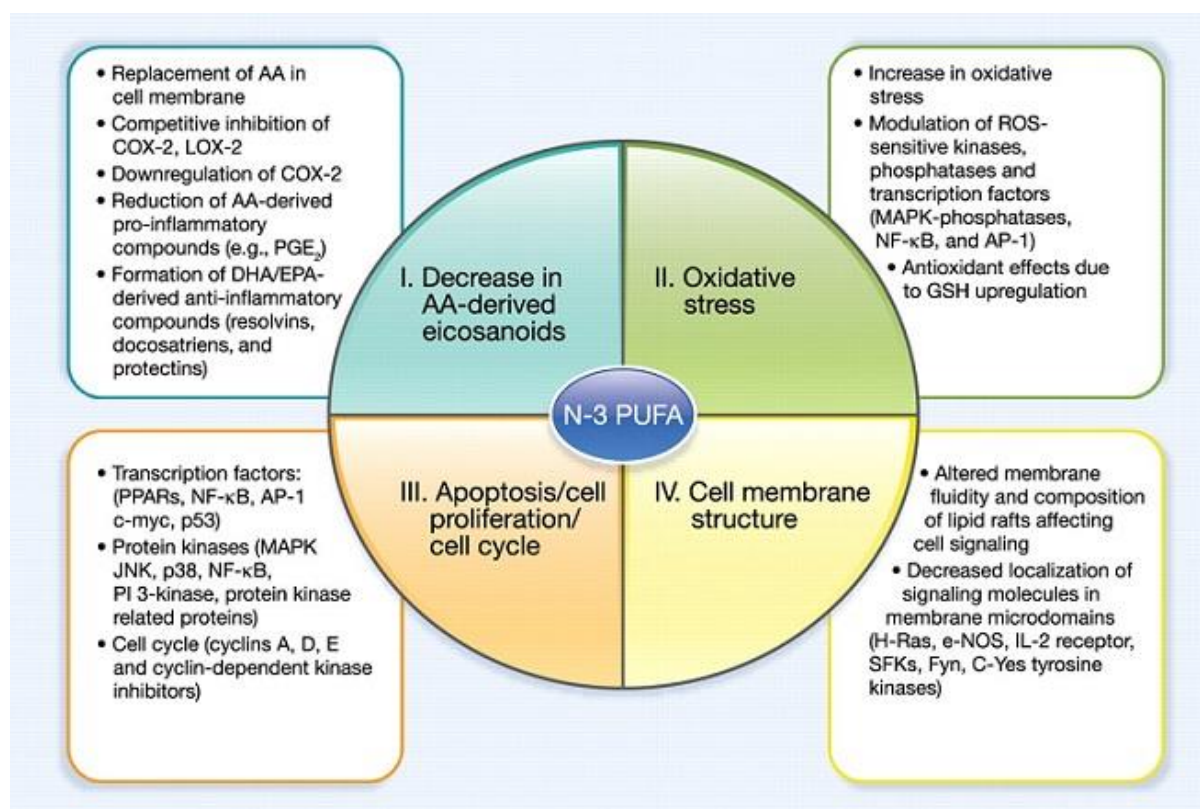


**Figure 9: Several mechanisms by which omega-3 can affect cancers.** (AA: arachidonic acid; COX-2: cyclooxygenase-2; GSH: glutathione; IL-2: interleukin 2; JNK: c-jun NH kinase; LOX: lipooxygenase; SFK: Src-family kinase; MAPK: mitogen-activated protein kinase; PI: phosphatidylinositol; PGE<sub>2</sub>: prostaglandin E<sub>2</sub>; ROS: reactive oxygen species). Signori et al., 2011<sup>138</sup>.



A study done by Frédéric Picou *et al.* has shown that n-3 polyunsaturated fatty acids are able to induce cell death in acute myeloid leukemia, different fatty acids including DHA and EPA lead to inhibit the growth of AML cell lines and to induce cell death via oxidative stress pathways. Furthermore, the study shows a synergistic effect that was obtained after the combination of the fatty acids with Ara-c, a previously used hypomethylating agent<sup>139</sup>. Similar studies on DHA and EPA also showed different pathways that these fatty acids utilize to impede cancer progression<sup>140-143</sup>.

Another *in vivo* study by Varney *et al.* demonstrated that omega 3 fatty acids were able to reduce the number of abnormal progenitor cells and push them towards differentiation. The omega 3 and 6 fatty acids of the mice diet were controlled, the omega 3 ones being in a higher proportion, it leads to a decrease in the number of myeloid progenitor cells, while increasing differentiation without affecting peripheral white blood cell numbers<sup>144</sup>.

Considering that PUFAs alongside other fatty acids and lipids makeup the cell membrane, they are able to hinder the membrane proteins functionality by altering the lipid rafts. A study established that DHA and EPA modified the composition of rafts present on the cell membrane and therefore impact the epidermal growth factor receptor (EGFR) and MAP kinase signaling pathways, leading to the apoptotic cell death in breast cancer cells<sup>145</sup>. Likewise, a study established that omega-3 PUFAs can enhance the cell membrane levels of fatty acid unsaturation, while reducing the activation of EGFR and eventually cause apoptosis of breast cancer cells. A continuation of that study then showed that these PUFAs could further decrease breast cancer cell propagation by modifying the lipid raft biochemical and physical properties<sup>146,147</sup>.

Another mechanism that DHA and EPA have been shown to counter breast cancer by is via the regulation of several receptors and enzymes including Enhancer of Zeste homolog 2 (EZH2), transient receptor potential canonical 3 (TRPC3), p53 and Bcl-2<sup>148-150</sup>.

Starting in the earlier 2000s and for several years of studies, Menendez *et al.* revealed that mono-unsaturated fatty acids (MUFAs) such as oleic acid (OA) and poly-unsaturated fatty acids (PUFAs) like alpha-linolenic acid (ALA), gamma-linolenic (GLA) and DHA are capable of sensitizing breast cancer cells to different chemotherapeutic agents including docetaxel, paclitaxel, vinorelbine and trastuzumab through reducing the expression of HER2<sup>151-156</sup>. Additionally, GLA also enhanced the activity of anticancer drugs such as paclitaxel, vinorelbine and docetaxel in a ROS-independent manner on breast cancer cells<sup>157,158</sup>.

A different study was able to verify results in agreement with Menendez *et al.*'s work, displaying that omega-3 PUFAs battled breast cancer via inhibiting the HER2 pathway as well in mice, in which these fatty acids could be produced from omega-6 PUFAs inside the cells<sup>159</sup>.

A 2005 study demonstrated that EPA managed to suppress cellular proliferation in human breast cancer mouse models owing to a G protein-coupled receptor that is activated by omega-3 PUFAs that triggers its signaling pathway<sup>160</sup>.

Another study similarly showed that omega-3 fatty acids decreased the proliferation of ER+ breast cancer cells. This outcome was achieved via the activation of a G protein-coupled receptor. Additionally, it inhibits other signaling pathways such as EGFR, Erk1/2 and AKT<sup>161</sup>.

Finally, whether through ferroptosis or various other pathways, fatty acids in general and especially DHA and EPA fatty acids of the omega-3 family, have shown an impressive range of functions and possibilities in the battle against different cancers. An indication that is further corroborated by a huge increase of clinical trials that are noticing the great opportunities lying in these molecules, such as DHA-paclitaxel in treating patients with metastatic pancreatic and colorectal cancers (identifiers NCT00024375 and NCT00024401 respectively) or EPA and DHA for non-small cell lung cancer patients (Identifier NCT04175769) among numerous others. Clearly EPA and DHA are two prime candidates to solve the azacitidine issues that have been discussed, probably through conjugating the nucleosidic analogue to the fatty acids to create a prodrug, but is that enough to reach the full potential of this treatment or is there a further step that can be taken to further improve on this idea? Certainly, their self-assembly seem to hold the answer.



### **3. The evolution of nucleosidic analogues: self-assembly of prodrugs into nanoparticles for cancer drug delivery**

In this part, a review published in *Nanoscale Advances* (2021) discusses the present state of nucleosidic analogues, their evolution over time, and sheds a light on their possible future aspects. Knowing that these analogues are a great method to confront cancer, their shortcoming that are restricting from reaching their full medicinal potential are described. Two solutions that can improve the shortcoming of this therapeutic agent are discussed: the prodrug solution and the nanoparticle solution. Lastly, a novel strategy derived from the combination of these solutions is contemplated, a method that can ultimately be the true answer to our problems with its ability to solve the limitations of the nucleosidic analogues, while being devoid of the shortcomings of the prodrug and traditional nanoparticles.

## REVIEW

[View Article Online](#)  
[View Journal](#) | [View Issue](#)Cite this: *Nanoscale Adv.*, 2021, 3, 2157

# The evolution of nucleosidic analogues: self-assembly of prodrugs into nanoparticles for cancer drug delivery

Milad Baroud,<sup>a</sup> Elise Lepeltier,<sup>a\*</sup> Sylvain Thepot,<sup>bcd</sup> Yolla El-Makhour<sup>e</sup> and Olivier Duval<sup>ab</sup>

Nucleoside and nucleotide analogs are essential tools in our limited arsenal in the fight against cancer. However, these structures face severe drawbacks such as rapid plasma degradation or hydrophilicity, limiting their clinical application. Here, different aspects of nucleoside and nucleotide analogs have been exposed, while providing their shortcomings. Aiming to improve their fate in the body and combating their drawbacks, two different approaches have been discussed, the prodrug and nanocarrier technologies. Finally, a novel approach called "PUFylation" based on both the prodrug and nanocarrier technologies has been introduced, promising to be the supreme method to create a novel nucleoside or nucleotide analog based formulation, with enhanced efficacy and highly reduced toxicity.

Received 29th December 2020  
Accepted 20th February 2021

DOI: 10.1039/d0na01084g

[rsc.li/nanoscale-advances](http://rsc.li/nanoscale-advances)

## 1. Introduction

Cancer has proven to be a detrimental disease that has had severe impacts on a global scale. It occurs as cells lose their regulatory ability and start to proliferate and multiply in an unrestrained fashion, followed potentially by the invasion of adjacent organs and tissues, eventually spreading throughout the body and impeding the vital functions of the affected areas. This loss in regulatory ability springs from the cumulative defects occurring at the genetic level with various genes being mutated leading to a loss of normal function and the abnormal cells exhibiting characteristics and functions that differ from their past behavior.<sup>1</sup>

This odd growth of cells will lead to the formation of a tumor, an unnatural mass of cells that can be either benign or malignant. Moles and lipomas are a common example of benign tumors; such tumors are restricted to their original location without spreading to adjacent areas, whereas malignant tumors also identified as cancers have the ability to invade surrounding tissues and spread throughout the body (metastasis) utilizing the lymphatic and circulatory systems.

In 2015, the assessment of the World Health Organization (WHO) showed that cancer is the first or second prominent

cause of death before the age of 70 years in 91 of 172 countries. By 2018, there were an estimated 18.1 million new cancer cases and 9.6 million cancer deaths worldwide, with the prevailing type of cancer observed being lung cancer.<sup>2,3</sup>

Concerning the treatment of cancer, the rise of systemic adjuvant therapy, in combination with local surgery and/or radio therapy, caused a plummet in radical surgery as both had similar results.

Of these adjuvant therapies, nucleosidic anti-cancer agents have become a staple chemotherapeutic treatment for many cancers. Anticancer nucleosides can be divided into two categories: analogs of purine and pyrimidine nucleosides and nucleobases. Concerning purine analogs, cladribine and fludarabine are two of the most prominent drugs being used as a treatment for low-grade malignant blood disorders.<sup>4</sup> With regard to pyrimidine analogs, cytarabine is a principal drug in the treatment of acute leukemia, gemcitabine is used in the treatment of various solid tumors and hematological cancers and diseases, and finally, fluorouracil and its prodrug capecitabine have shown activity in colorectal and breast cancers. The improvements that traditional analogs have undergone, coupled with the ability of using them in the treatment of a wide range of cancers, have solidified the role of nucleoside analogs as a significant chemotherapeutic agent, not to mention a growth in their popularity that occurred with the understanding of their exact mechanism of action.<sup>5-9</sup>

However, traditional chemotherapeutics display a high toxicity profile with a small therapeutic window, leading to different severe side effects and a lowered efficacy due to the cancer cell's ability of drug efflux through active pumps called "multidrug resistance".<sup>10,11</sup> Consequently, several novel approaches are stemming to address and overcome these

<sup>a</sup>Micro et Nanomédecines Translationnelles, MINT, UNIV Angers, UMR INSERM 1066, UMR CNRS 6021, Angers, France. E-mail: [elise.lepeltier@univ-angers.fr](mailto:elise.lepeltier@univ-angers.fr)

<sup>b</sup>University Hospital of Angers, Hematology, 49933 Angers, France

<sup>c</sup>Université d'Angers, Inserm, CRCINA, 49000 Angers, France

<sup>d</sup>Fédération Hospitalo-Universitaire 'Grand Ouest Against Leukemia' (FHU GOAL), France

<sup>e</sup>Environmental Health Research Lab (EHRL), Faculty of Sciences V, Lebanese University, Nabatieh, Lebanon





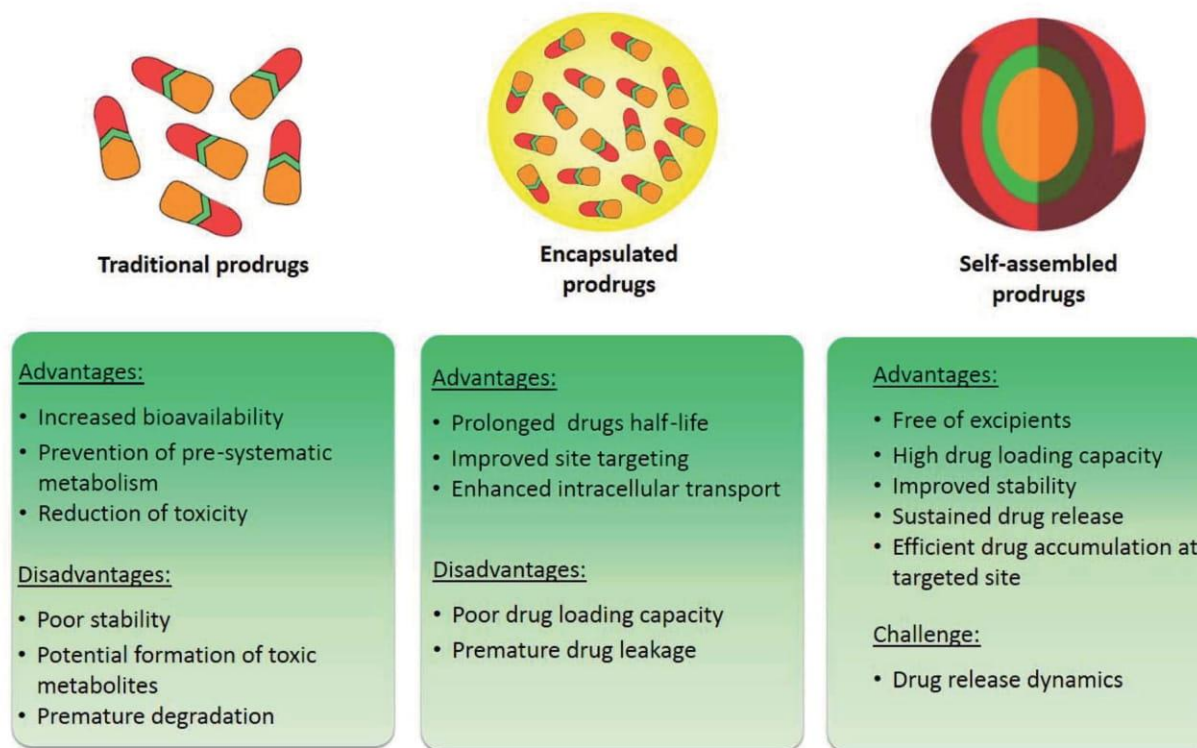


Fig. 1 Strategies applied to improve the delivery efficiency of anticancer drugs: prodrugs, encapsulation and self-assembled prodrug-based nano-DDSs.

shortcomings, namely the prodrug strategy and nanoparticle drug delivery systems (nano-DDSs).<sup>12,13</sup> Prodrugs are pharmacologically inactive molecules that can be metabolized into their active form *in vivo*. The novelty of prodrugs emerges from their ability to overcome the flaws present in the parent drugs, for instance chemical instability, poor water solubility, severe toxicity, and low permeability.<sup>12,14–16</sup> In addition, benefiting from the rapid development of biomaterials and nanotechnology, nano-DDSs have shown distinct advantages in anticancer drug delivery, including improved drug availability, prolonged systemic circulation time, increased tumor accumulation, and spatiotemporally controlled drug release. On top of that, prodrug-based nanoparticles incorporate the advantages gained from both approaches (Fig. 1) allowing for a more stable drug and a further decrease in toxicity as the specificity of the drug increases while offering maximal drug loading capabilities.<sup>17</sup>

## 2. An overview of nucleosides

Nucleosides and nucleotides are organic molecules that play a key role in several bodily functions, as they are included in the signaling pathways inside cells, metabolism, DNA and RNA synthesis, and enzymatic regulation.

Synthetic equivalents of these compounds have been produced; these analogs are capable of mimicking the activity of the original compounds. Thus, they are able to interact with several key enzymes (such as kinases, ribonucleotide reductase,

DNA methyl transferases, purine and pyrimidine nucleoside phosphorylases and thymidylate synthase). Additionally, they gain the ability of “hijacking” the conventional metabolic pathways of the original nucleotides owing to the structural similarity they share, leading to the inhibition of cellular division by assimilating into DNA or RNA. This ability of analogs has given rise to numerous medicinal applications including the capacity to inhibit the growth of cancer cells.<sup>18,19</sup>

To form a nucleoside, a nucleobase, either a purine (adenine or guanine) or a pyrimidine (cytosine, uracil or thymine), is needed to bind to a pentose sugar ring (a ribose or a deoxyribose). A further modification of the primary alcohol from the sugar ring with a phosphoric acid yields a nucleotide (Fig. 2).<sup>20</sup>

### 2.1. Nucleobases

A nucleobase, also called a nitrogen base, is a carbon-based molecule containing a nitrogen atom and reacting with the chemical properties of a Lewis base due to the lone pair of electrons of the mentioned nitrogen atom.

Nucleobases can either be a purine or a pyrimidine, characterized by a weak reactivity to electrophilic aromatic substitution and are thus considered weak bases. Owing to their cyclic nature they are non-polar, and function to bond nucleic acids together.<sup>21,22</sup>

Regarding analogs, the nitrogen bases that are incorporated are rarely the natural ATGC-bases and are frequently modified with 4 major categories being observed ranging between halogenation (with fluorine and chlorine being the most commonly



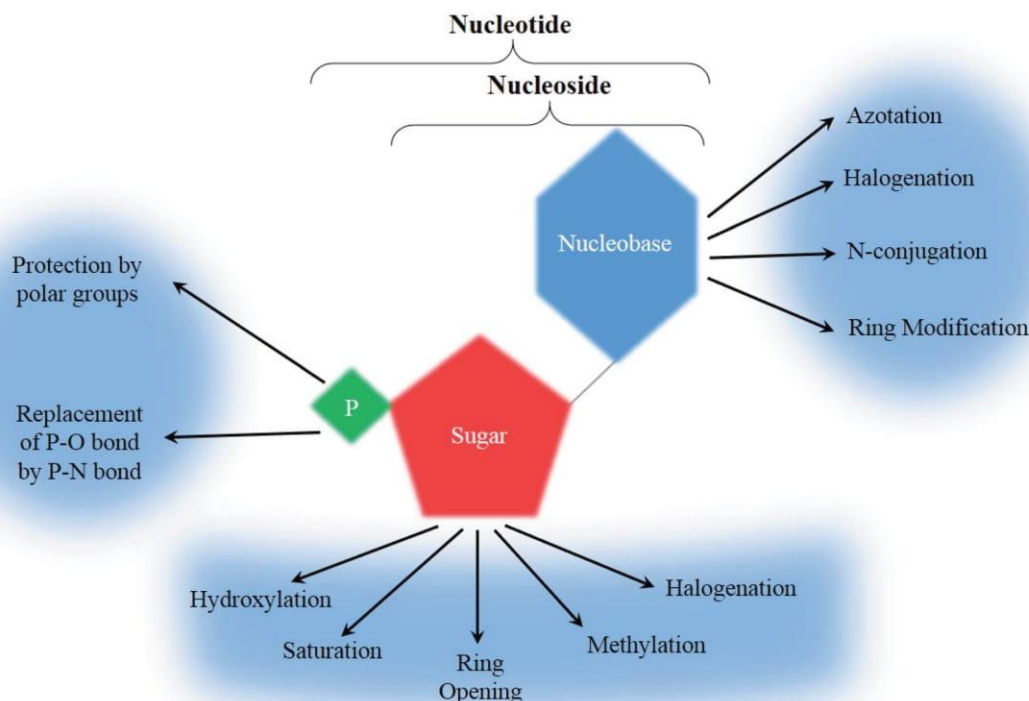


Fig. 2 General structure and chemical modifications of nucleosides and nucleotides to form analogs.

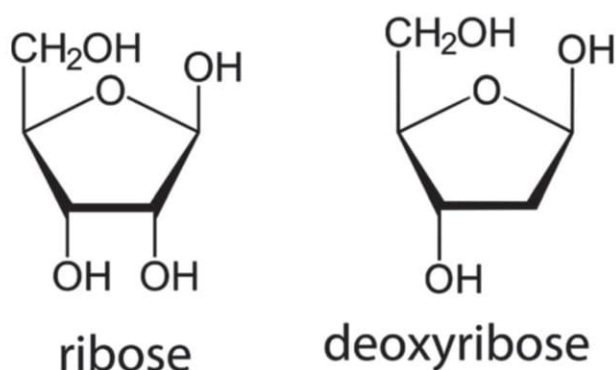


Fig. 3 Structure of sugar rings: ribose and deoxyribose.

used), azotation, N-conjugation, and ring modification (Fig. 2). Few other modifications that don't fit into the main groups have been observed and will be mentioned separately.

## 2.2. Sugar ring

The second building block of a nucleoside, the pentose sugar ring can be either a ribose or 2'-deoxyribose (Fig. 3). The major function of the 2'-deoxyribose is becoming the backbone of the DNA molecule, while the ribose becomes the backbone of the RNA molecule. Similar to the nucleobases, the sugar ring is rarely intact and is often modified with the main changes being halogenation, methylation, saturation, ring opening, and hydroxylation/de-hydroxylation (Fig. 2).

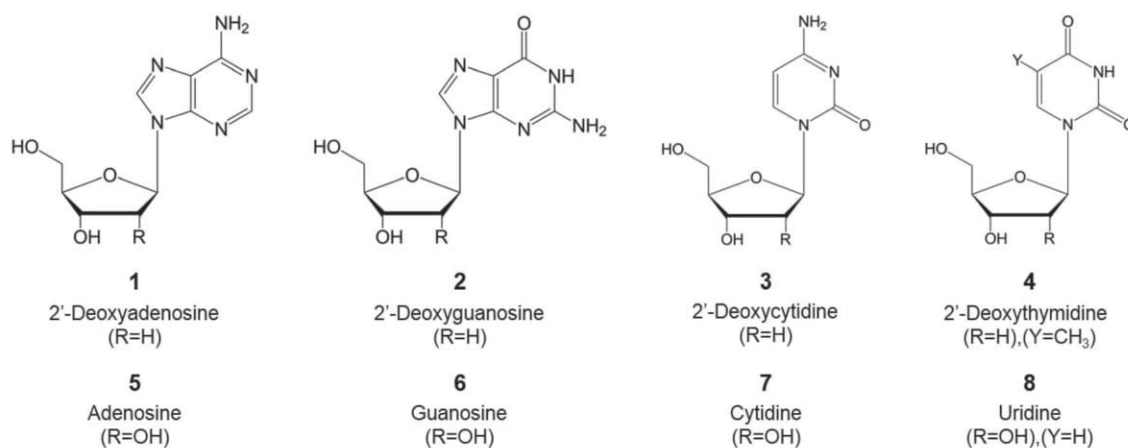


Fig. 4 Different types of natural nucleoside that constitute nucleic acids.



Table 1 A list of FDA and EMA approved chemotherapeutic nucleosidic analogs

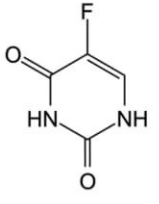
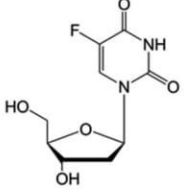
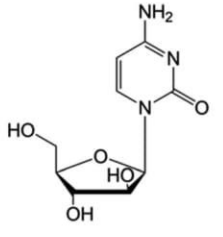
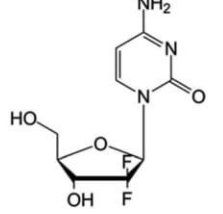
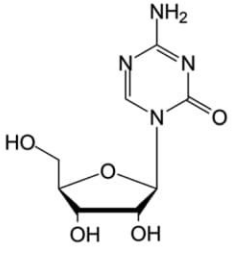
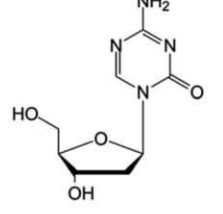
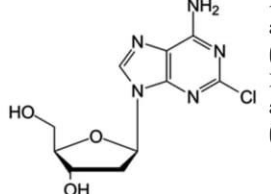
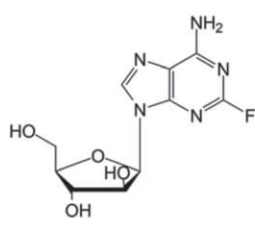
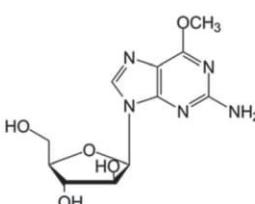
Name	Structure	Status <sup>a</sup>	Chemical modification	Targeted cancer	Mechanism of action	
Fluorouracil		FDA approved (1962) EMA approved (NA)	• Uracil modification by F-halogenation	• Colon, esophageal, stomach, pancreatic, breast, and cervical cancers	• Enzymatic inhibition	37
Floxuridine		FDA approved (1970)	• Cytosine modification by F-halogenation	• Colon cancer	• Enzymatic inhibition • DNA synthesis inhibition	38
Cytarabine		FDA approved (1969) EMA approved (2001)	• Replacement of the ribose sugar ring with an arabinose	• Acute myelogenous leukemia • Lymphoblastic leukemia	• DNA polymerase inhibition	5
Gemcitabine		FDA approved (1996) EMA approved (2008)	• Sugar ring F-halogenation	• Pancreatic, lung, breast, and bladder cancers	• Enzymatic inhibition	7
Azacitidine		FDA approved (2004) EMA approved (2008)	• Cytosine modification by azotation	• Myelodysplastic syndromes (MDS) • Acute myeloid leukemia (AML)	• DNA hypomethylation	39
Decitabine		FDA approved (2006) EMA approved (2006)	• Cytosine modification by azotation	• Myelodysplastic syndromes (MDS) • Acute myeloid leukemia (AML)	• DNA hypomethylation	6
Cladribine		FDA approved (1993) EMA approved (2004)	• Adenine modification by Cl-halogenation	• Hairy-cell leukemia • Non-Hodgkin lymphoma	• Enzymatic depletion • ATP accumulation	40





Table 1 (Contd.)

Name	Structure	Status <sup>a</sup>	Chemical modification	Targeted cancer	Mechanism of action	
Fludarabine		FDA approved (1991) EMA approved (2014)	<ul style="list-style-type: none"> <li>• Adenine modification by F-halogenation</li> <li>• Replacement of the ribose sugar ring with an arabinose</li> </ul>	• Chronic lymphocytic leukemia	<ul style="list-style-type: none"> <li>• Nucleic acid synthesis inhibition</li> <li>• Enzymatic inhibition</li> </ul>	41
Nelarabine		FDA approved (2005)	<ul style="list-style-type: none"> <li>• Guanine by modification of a functional group</li> <li>• Sugar ring is an arabinose instead of ribose</li> </ul>	• T-cell acute lymphoblastic leukemia and lymphoma	• DNA synthesis inhibition	42

<sup>a</sup> Approval status was verified by the European Medicines Agency (<http://www.ema.europa.eu>) and the US Food and Drug Administration (<http://www.fda.gov>).

### 3. Chemotherapeutic nucleoside analogs

Most of the present natural nucleoside analogs that are being used or are under development are derived from one of the following nucleosides presented in Fig. 4. The joining of a purine (either an adenine or guanine) or a pyrimidine (cytosine, thymine or uracil) base with a pentose ring ( $\beta$ -D-deoxy-ribofuranose or  $\beta$ -D-ribofuranose for DNA or RNA, respectively) forms the nucleic acid. These nucleic acids can then be modified variously (*i.e.* azotation of the nucleobase, halogenation of the sugar ring...) as described in Fig. 2 to obtain the nucleosidic analogs utilized in the course of cancer treatment.

#### 3.1. Advancements in therapeutic nucleoside analogs for cancer treatment

Fluorouracil opened the door for advancements in the field of therapeutic nucleoside analogs for cancer treatment as it was the first FDA approved one in 1962, a uracil nucleobase modified by fluorine halogenation; it was widely used in the treatment of different cancers including colon, esophageal, and cervical cancers. Following that, several other nucleoside based drugs emerged: floxuridine, a prime example of these drugs based on fluorouracil and having it as the metabolite, is used for the treatment of colon cancer. The rest of the FDA and EMA approved drugs are presented in Table 1. Despite the limited number of approved nucleoside analogs for the treatment of various cancerous tumors, numerous other ones are being developed and tested in countless clinical trials (Table 2) either separately or in association for their synergistic effects, such as 8-chloroadenosine, a promising new analogue undergoing phase I/II trials on patients with relapse or refractory acute myeloid leukemia.

#### 3.2. Mechanisms of action

In the course of cancer treatment, the analogs function as antimetabolites, *via* mimicking the metabolic pathway of the intrinsic nucleotides. Nucleosidic transporters facilitate the entry of selected nucleoside analogs (NAs),<sup>45</sup> and they are phosphorylated by several kinases: 5NT – 5'-nucleotidase, nucleoside monophosphate kinase (NMPK), nucleoside diphosphate kinase (NDPK), and finally creatine kinase or 3-phosphoglycerate kinase, leading to the building up of di- and tri-phosphorylated nucleoside analogs in cancer cells. These molecules will then act, after obtaining their active forms as mono-, di- and tri-phosphorylated nucleosides, by inhibiting intracellular enzymes, like polymerases or ribonucleotide reductase (RNR), as well as by being assimilated into newly synthesized DNA and RNA. The assimilation of nucleoside or nucleotide analogs into DNA may induce the termination of chain elongation<sup>16</sup> (Fig. 5). An in-depth knowledge of the mechanism of action of currently used compounds is of great value for the development of novel molecules. These data have led to the development of molecules that act independently of membrane transporters or activating kinases and are less susceptible to degradation. A better understanding of the mechanism of action of these compounds will also contribute to the rational development of synergistic combinations of nucleoside or nucleotide analogs with drugs that have different and/or complementary action.

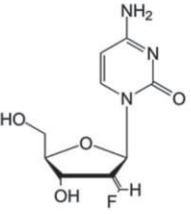
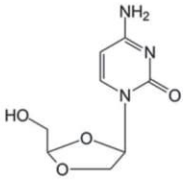
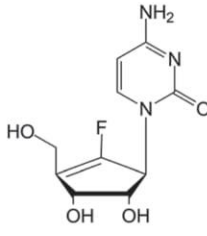
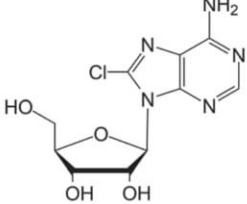
#### 3.3. Mechanism of resistance

It is vital that a deeper understanding of the mechanism of resistance towards nucleoside and nucleotide analogs is reached.

Three broad mechanisms of resistance arise after considering cell line and clinical studies.



Table 2 A list of chemotherapeutic nucleosidic analogs in clinical trials

Name	Structure	Status <sup>a</sup>	Chemical modification	Targeted cancer	Mechanism of action	
Tezacitabine		Phase I/II trials	• Sugar ring modification by fluoromethylene-halogenation	• Refractory solid tumors	• Enzymatic inhibition	43
Troxacitabine		Phase I/II trials	• Sugar ring modification by dihydroxylation • L-Enantiomer	• Acute myelogenous leukemia (AML)	• Inhibitor of DNA polymerases	44 and 45
rx-3117		Phase I/II trials	• Sugar replacement by a cyclopentene ring and F-halogenation	• Metastatic bladder cancer • Metastatic pancreatic cancer	• DNA hypomethylation	46 and 47
8-Chloroadenosine		Phase I/II trials	• Adenine modification by Cl-halogenation	• Recurrent acute myeloid leukemia	• Enzymatic inhibition	48

<sup>a</sup> Trial status was verified by the NIH – U.S. National Library of Medicine clinical trials database (<http://www.clinicaltrials.gov>).

The first resistance mechanism emerges from a lack in the intracellular levels of nucleic acid triphosphates owing to either a decreased level of activating enzymes, insufficient cellular uptake of the therapeutic molecule, or enhanced nucleic acid degradation due to higher levels of 5-nucleotidase or deaminases.<sup>23,24</sup> Such processes have been deeply observed in the case of cancer resistance to cytarabine.<sup>25–27</sup>

The second resistance mechanism arises from an insufficient alteration to the DNA strands, mainly as a result of inadequate ribonucleotide reductase inhibition, as observed by Heinemann *et al.* in the case of gemcitabine resistance.<sup>28,29</sup>

The third resistance mechanism results from a decreased apoptosis induction. It comes as a result of an increase in the levels of pro-apoptotic molecules such as Bax, coupled with a decrease in the levels of anti-apoptotic molecules like Bcl-2: these level alterations occur when DNA damage is detected leading to a surge in the expression of the *p53* gene. Building on this, several studies have uncovered that mutations in the *p53* gene in different cancers have given rise to nucleoside analog resistance, namely showing that the fludarabine resistance gained by chronic lymphocytic leukemia cells was due to mutations in the *p53* gene.<sup>30–33</sup>

Though most causes behind cancer resistance to nucleoside and nucleotide analogs seem to fall under one of these chief mechanisms, different and less frequent mechanisms do occur in several odd cases and have been extensively compiled by Tsesmetzis *et al.*<sup>34</sup>

Several approaches have risen to bypass these resistance mechanisms including restrictions in nucleoside transport and metabolism, such as masking the negative charge of the molecule thus resulting in neutral and membrane-permeable nucleotides. Indeed, nucleotide and nucleoside analog-based prodrugs such as capecitabine<sup>35,36</sup> and other similar molecules have been developed and are undergoing continuous studies and clinical trials.

## 4. The prodrug approach

The term prodrug was introduced 50 years ago in 1958 when Adrien Albert suggested that the prodrug approach could be used to alter certain drug properties or drug toxicity.<sup>49</sup>

A prodrug is a biologically inert, small molecule that is metabolized *in vivo* through a spontaneous process (*e.g.* hydrolytic degradation) or *via* a bio-catalytic mechanism to





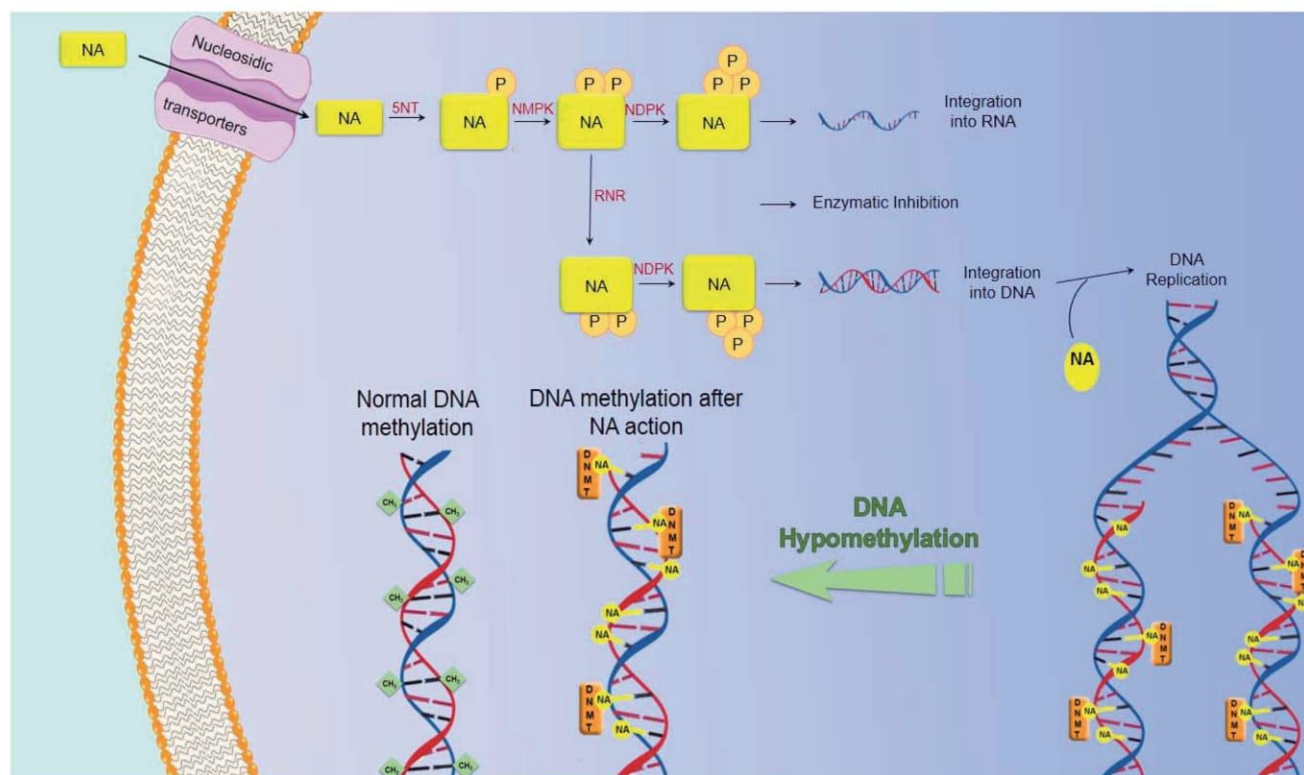


Fig. 5 Mechanism of action of nucleosidic analogs.

release the pharmacologically active molecule near the targeted tissue, consequently allowing a specific release of the active entity at its target site: among different strategies to improve the selectivity of chemotherapy drugs, the targeted prodrug strategy is a particularly favorable approach for highly selective chemotherapy.

The general design of a prodrug is depicted in Fig. 6(a). A chemotherapy prodrug may contain four components: the parent drug or its derivative that exhibits the pharmacological effect; a metabolically labile chemical linker which binds the functional group of the parent drug (hydroxyl, carboxylic, amine, carbonyl, phosphate groups, *etc.*) to the rest of the prodrug designated as the “promoiety”; a polymer spacer, or an enzymatically cleavable spacer that can release the parent drug in the presence of a tumor-specific enzyme; and an optional targeting moiety for specific delivery to tumor cells.<sup>14,15,50</sup> With that in mind, there exist several key points to consider going into the design process:

- Parent drug: what are the functional groups present in this molecule that will allow a chemical prodrug derivatization?
- Promoiety: choosing a molecule that is safe and is readily excreted from the body. The disease state, dose and the duration of therapy should also be taken into account.
- Parent and prodrug: an expansive understanding of the pharmacokinetics is crucial, especially absorption, distribution, metabolism, and excretion.
- Degradation by-products: a thorough consideration of this category is crucial as these by-products and their interactions

can affect chemical and physical stability and lead to the formation of new degradation products.

Given their fundamental characteristic, the inert pre-metabolism form, prodrugs improve the pharmacological properties of their active parent molecule through a simple chemical modification. The objective behind the traditional prodrug approach is to improve solubility in water or diffusion through the lipid membrane, chemical stability, oral or local absorption, brain permeability, and to reduce unacceptable taste, irritation or pain, pre-systemic metabolism, and toxicity.

Prodrugs allow the targeting of specific antigens, peptide transporters, or enzymes that are over-expressed on tumor cells or the microenvironment: it can be achieved by conjugating a tumor-specific ligand or a polymer to the chemotherapy drug *via* a cleavable linker.<sup>51</sup>

#### 4.1. Classification based on linkers

The choice of the functional linking group between the promoiety and the parent drug has an imperative impact on the design of the prodrug. To ensure that the active drug will be released in the desired area and under the desired conditions, this functional group should be enzymatically/chemically cleavable or be self-immolative (pH). This will occur either at the surface of the cancerous cells owing to a specific ligand–receptor combination or upon reaching and interacting with the tumor’s microenvironment, due to a change in the pH or the presence of an overexpressed enzyme. As the linker should stay intact in the course of its circulation until it arrives at the





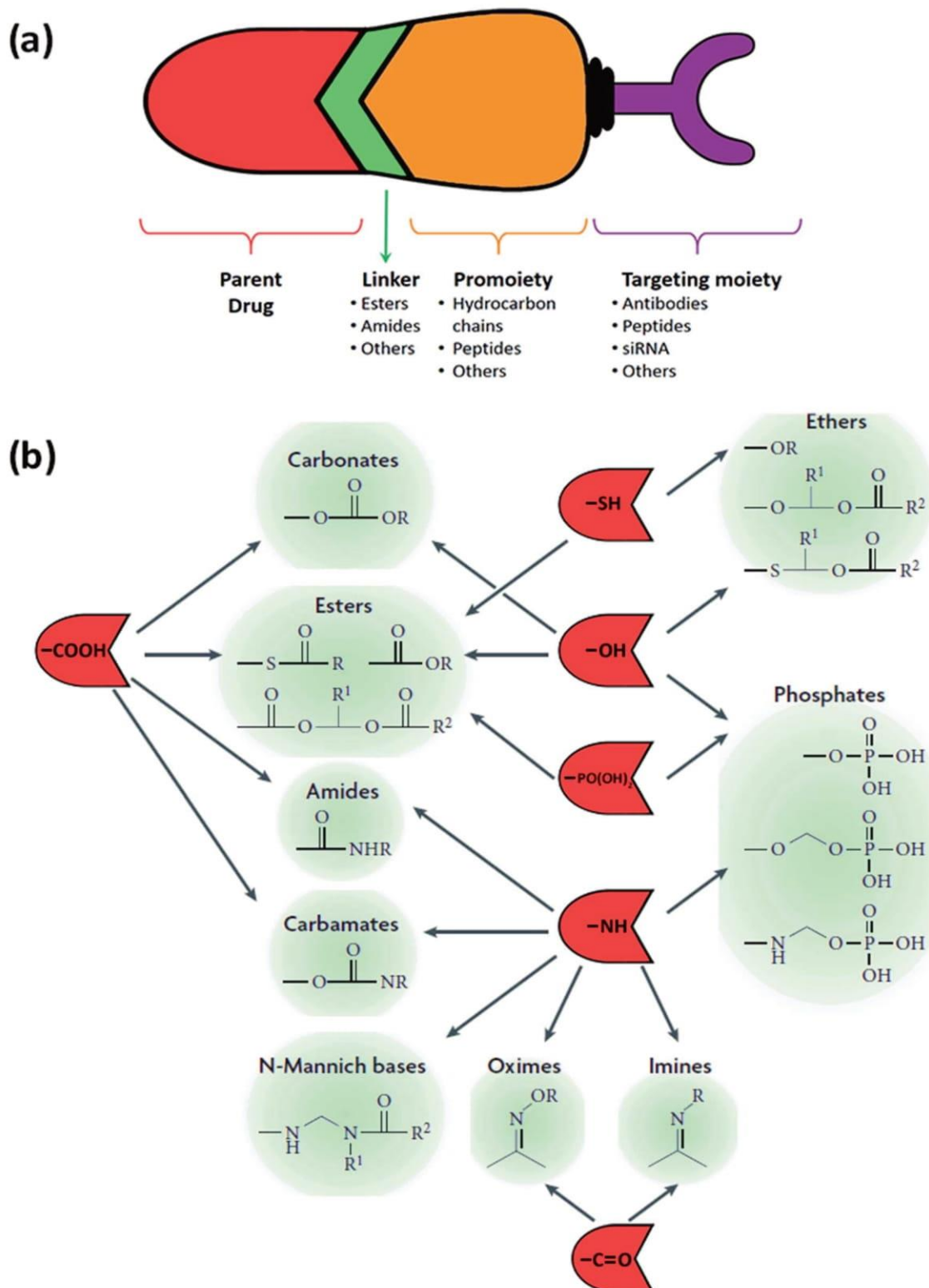


Fig. 6 (a) The general design of a prodrug. (b) Functional groups on parent drugs that are used in prodrug design (shown in red) and conjugated to the desired promoiety using compatible linkers (shown in green). Adapted from ref. <sup>53</sup>.

desired site, its stability is of vital significance. Therefore, a handful of functional groups that present such characteristics are used in the design of prodrugs (Fig. 6(b)), with the two main and heavily utilized families being esters and amides.

**4.1.1. Ester linkers in prodrug design.** Nearly 49% of all the prodrugs found on the market feature esters as the linker between the promoiety and the drug, on account of them being activated by enzymatic hydrolysis, coupled with their ability to



be readily cleaved by a wide array of esterases in biological environments.<sup>52</sup> Moreover, ester prodrugs are able to enhance the lipophilicity of water-soluble molecules *via* masking charged groups such as phosphates and carboxylic acids, consequently achieving passive membrane permeability.<sup>53</sup>

A variety of links can be established, as they are usually introduced *via* conjugation using charged groups such as phosphates or phosphate salts, hemi-esters, and sulfates. These functional groups can be easily hydrolyzed by the action of sulfatases, ubiquitous esterase, and phosphatases usually present in the liver, blood and other tissues and organs, permitting the release of the active parent drugs. The ester bond's half-life can vary from several minutes to several hours depending on the accessibility of this bond determined by the environmental conditions and differences in the structure of the prodrug.<sup>28,29</sup>

In the case of carboxylic acid esters, the precise prediction of pharmacokinetic characteristics in humans is very challenging, due to the variation between humans and other species used in the preclinical studies.<sup>54,55</sup>

Concerning phosphate ester prodrugs, they are mainly employed in the augmentation of the aqueous solubility of the parent molecule, as the presence of the dianionic phosphate moiety increases the aqueous solubility, thus improving the oral or parenteral administration. Namely, drugs with a poor water solubility stemming from their hydroxyl and amine functional groups are the target of such an approach. They exhibit an improved chemical stability and a swift metabolism back to the parent drug by phosphatases present in the liver or the intestinal brush border. Furthermore, as phosphate esters are hydrolyzed by alkaline phosphatases at analogous rates in humans and other species used in the preclinical studies, they gain an advantage over carboxylic acid esters.<sup>53,56,57</sup>

Alternatively, carbamates are derivatives of carboxylic acids and amines, while carbonates are derivatives of carboxylic acids and alcohols, and both have a greater enzymatic stability when compared to other esters, due to the heteroatoms on both sides of the carbonyl group. However, they are more vulnerable to hydrolysis than amides.<sup>33,34</sup>

**4.1.2. Amide linkers in prodrug design.** The limited popularity of amides comes from their high enzymatic stability *in vivo*, where the half-life of this bond ranges from several hours to several days in the plasma, if specific enzymes aren't present.<sup>58</sup> Amide bonds are sought after due to their improved oral absorption stemming from the attachment of specific intestinal uptake transporter substrates.<sup>59,60</sup> The amide bond is usually hydrolyzed by ubiquitous carboxylesterases, peptidases or proteases.<sup>61</sup>

## 4.2. Perks of the prodrug approach

The prodrug approach has proven to be a great aid in overcoming the drawbacks of traditional drugs in the pharmacokinetic and pharmacodynamic domains, for instance poor stability and solubility, insufficient blood-brain barrier permeability, deficient oral absorption and early metabolism.<sup>62</sup>

**4.2.1. Aqueous solubility.** The solubility of the drug is enhanced remarkably by the addition of a phosphate group that

is coupled *via* a formaldehyde spacer group or to a functional group like alcohol or amine, improving solubility by several orders of magnitude. Thus phosphate-based prodrugs tackle the problem of molecules with limited absorption due to low solubility that was traditionally solved by administering high doses, which usually led to irregular and undesirable outcomes in clinical cases.<sup>63</sup>

When it comes to nucleoside analogs, their therapeutic effect relies on successive phosphorylation *via* different kinases until they reach their triphosphate form. But this process is kinetically led at the first phosphorylation step. Thus, nucleoside analogs regularly either have phosphonate present or are delivered as their monophosphorylated form.<sup>64</sup>

However, this approach has been widely applied to pronucleosides and pronucleotides in the anti-viral domain (the work of Hostetler *et al.* is a prime example<sup>65</sup> where traditional anti-viral nucleosides underwent esterification with an alkoxyalkyl group), essentially masking them as lysophospholipids, allowing these molecules to be readily taken up in the gastrointestinal tract and improving their circulation time in plasma. The active metabolite similarly has a longer half-life within cells, allowing intermittent dosing. Limited research in the domain of anti-cancer pronucleosides exists, though the work of Perigaud *et al.* on gemcitabine phosphoester prodrugs offers great insights.<sup>66,67</sup>

**4.2.2. Passive permeability.** Drug molecules that are polar and charged are challenging, with low permeability across biological membranes, leading to a low bioavailability. As a result, improving membrane permeability might be the largest advantage gained by the use of prodrugs.

By masking the polar groups of the parent drugs, the lipophilicity of these molecules is enhanced. Hydrophilic groups like carboxyl, phosphate, hydroxyl, or amine groups have been conjugated to more lipophilic alkyl or aryl esters or *N*-acyl derivatives, which under the action of peptidases or esterases are readily hydrolyzed back to the parent.<sup>16</sup>

**4.2.3. Exploiting the cell carrier-mediated transport.** Cell carrier-mediated transport is another method by which polar and charged drugs can gain entry into the cell. Using drugs or promoieties that have a structural resemblance to endogenous substrates will allow cell carrier-mediated transport to be taken advantage of to aid in the internalization of molecules by the cell.<sup>68</sup>

Vig *et al.* explored this point, where amino acid ester prodrugs of floxuridine were developed to target the oligopeptide transporters that are greatly expressed in the epithelial cells constituting the intestinal brush border membrane and are involved in the transport of ACE inhibitors, di and tri-peptides and an assortment of other drugs across the intestine.<sup>69</sup>

**4.2.4. Prolonged duration of action.** Aiming to control the release rate of the parent drug and its absorption/tissue distribution, prodrugs based on molecules with modified dissolution properties can be developed. To achieve this, the parent drug is conjugated to various molecules such as polymers, fatty acid esters, *etc.* and are then formulated into oil-based vehicles.<sup>70,71</sup>

Zuwala *et al.* worked on the antiretroviral nucleosidic analogue agent azidothymidine, and they showed that the





conjugation of azidothymidine to poly(methacrylic acid) leads to an increased duration of action when compared to the free azidothymidine.<sup>72</sup> Though this work is against viral diseases, the advantages gained can be readily translated to impact the cancer field.

**4.2.5. Targeting site-specific enzymes.** A prodrug can be designed to convert to its active form by counting on its bioconversion by an enzyme expressed largely in the targeted tissue or organ.<sup>73,74</sup>

Xu *et al.* utilized the increased presence of the cathepsin B enzyme in the pancreatic cancer tissue to develop a cholesteryl hemisuccinate-1 gemcitabine prodrug that will release the gemcitabine mainly at the cancer site after contact with cathepsin B that will cleave the amide bond.<sup>75</sup>

#### 4.3. Advancements in pro-nucleosides for cancer treatment

Arising from a need to exploit the mentioned advantages of prodrugs, a great deal of research has been performed on nucleoside analog based prodrugs. Given that nucleotides and nucleosides are hydrophilic in nature, this gives rise to several limitations including restricted diffusion, limited cellular internalization and a rapid enzymatic degradation. Thus nucleoside analog based prodrugs arise from a need to improve the drug's diffusion and to protect it from metabolic degradation *via* its conjugation to a hydrophobic moiety thus giving an amphiphilic prodrug.<sup>76–78</sup> Capecitabine is the only FDA approved pro-nucleosidic drug since 1998 with an amide bond linker joining the parent drug based on fluorouracil to a chloroformate based promoity: it is used for the treatment of colonic, breast, colorectal, and stomach neoplasms. Other prodrugs are in clinical trials such as guadecitabine (SGI-110) synthesized by the conjugation of decitabine to a deoxyguanosine *via* a phosphodiester bond,<sup>79</sup> being tested in phase III trials on different cancers including acute myeloid leukemia (AML) and myelodysplastic syndrome. A selection of such promising prodrugs is presented in Table 3; these prodrugs use several types of the mentioned linker, and improve upon the parent drug by the addition of various perks.

#### 4.4. The drawbacks of the prodrug approach

Prodrugs in numerous cases are hindered at several levels, as some need specific enzymatic cleavage, chemical activation or a specific transport mechanism in order to achieve sufficient intracellular delivery. Adding to that, the presence of esterases in the serum or tumor microenvironment leads to rapid degradation of the said prodrugs before gaining entry into the cells. Additionally, despite having enhanced levels of phosphorylated nucleoside analogs released from the prodrugs inside the cell, an efficient cytotoxic concentration isn't achieved owing to the intensive catabolic processes present, such as increased 5-nucleotidase activity. Consequently, despite being an enhanced approach in comparison to traditional drugs, the prodrug approach is far from perfect and needs further innovation to reach the therapeutic level needed to elevate the medical health domain.

## 5. The nanoparticle approach

Setting a fixed definition for nanoparticles is tricky, as the size varies between different sources ranging from a few nanometers up to anything less than a micrometer. Not to mention, for some, one dimension at the nanoscale is enough while for others it should cover two or all three dimensions.

In 2011 the Commission of the European Union defined a stricter definition than was previously approved: under that definition a nano-object needs only one of its characteristic dimensions to be in the range 1–100 nm to be classed as a nanoparticle, even if its other dimensions are outside that range.<sup>88,89</sup>

This ever-evolving field of nanomedicine has progressed through four generations thus far, each improving on the previous one, starting with the first generation in the early 1970s that included liposomes, micelles and polymer nanoparticles that were made of biodegradable excipients able to passively circulate with an improved intracellular delivery and accumulate in the liver, but weren't specific to a targeted tissue and were readily eliminated by macrophages (opsonization). The second generation, two decades later utilized the physico-chemical concept of the steric repulsion to enhance upon the first generation of nanocarriers with the introduction of a new molecule, PEG (polyethylene glycol), thus taking advantage of the "Enhanced Permeability and Retention" (EPR) effect, and allowed the targeting of tumors and other inflammatory diseases. Later, the third generation of nanocarriers arrived with the decoration of the nanocarrier surface with different bio-recognition modalities providing them with additional functionalities including evasion of the immune system (stealth) and the extension of the blood circulation duration aiming to accumulate in the targeted tissue, as well as an improved targeting ability. Recently, the fourth generation provided even more advanced functionalities with stimuli-responsive nanomedicine, such as silicon nanocarriers that are able to deploy multiple waves of nanoparticles and to stimulate a signaling or biological cascade.<sup>90–93</sup>

The small size of nanoparticles is of great benefit in the medical domain, allowing them to diffuse through the endothelium, enter cells or have a premeditated ability to bind to specific cells. Such properties have ushered novel advancements in the field of nanomedicine *via* the development of novel drug delivering techniques, for instance by providing local heating (hyperthermia),<sup>94</sup> blocking vasculature to diseased tissues and tumors,<sup>95</sup> or *via* transportation of drugs.<sup>96</sup>

#### 5.1. Classification of nanoparticles

Nanoparticles can be classified into any of various types depicted in Fig. 7, depending on their size, shape, and material properties. Other classifications distinguish organic, inorganic and metal-organic excipients used to formulate (i) organic nanoparticles including liposomes, micelles, polymeric nanoparticles or dendrimers, (ii) inorganic ones encompassing quantum dots and calcium phosphate among others, and (iii) metal-organic framework nanoparticles (MOFs).



**Table 3** A list of chemotherapeutic nucleosidic analog prodrugs

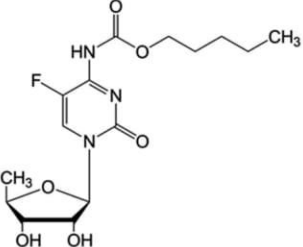
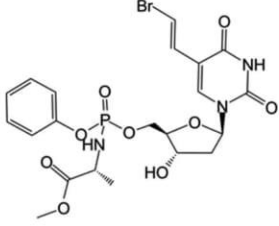
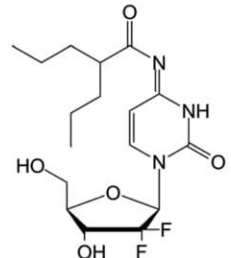
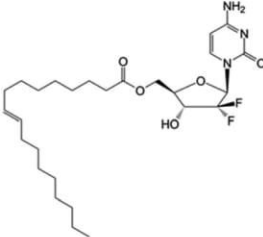
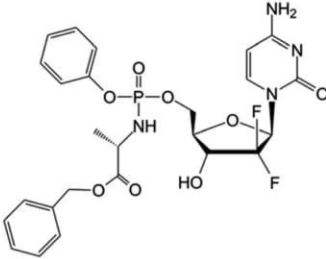
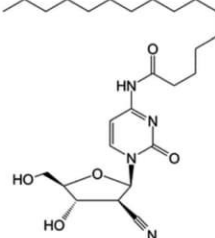
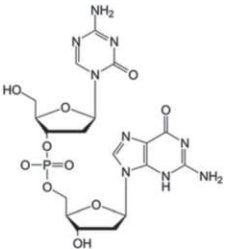
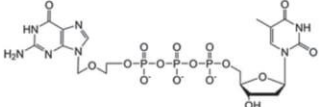
Name	Structure	Status <sup>a</sup>	Parent drug	Linker	Targeted cancer	
Capecitabine		FDA approved (1998) EMA approved (2001)	• Fluorouracil	• Amide bond	<ul style="list-style-type: none"> <li>• Colonic neoplasms</li> <li>• Breast neoplasms</li> <li>• Colorectal neoplasms</li> <li>• Stomach neoplasms</li> </ul>	36
Thymectacin		Clinical trials Phase I/II	• Brivudine	• Phosphate ester bond	• Cancers overexpressing the thymidylate synthase enzyme	80 and 81
LY2334737		Clinical trials Phase I	• Gemcitabine	• Amide bond	<ul style="list-style-type: none"> <li>• Malignant solid tumors</li> <li>• Metastatic tumors</li> </ul>	82
CP-4126		Clinical trials Phase I/II	• Gemcitabine	• Carboxyl ester bond	• Advanced adenocarcinoma of pancreas	83
Nuc-1031		Clinical trials Phase I/II/III	• Gemcitabine	• Phosphate ester bond	<ul style="list-style-type: none"> <li>• Ovarian cancer</li> <li>• Biliary tract cancer</li> <li>• Gallbladder cancer</li> <li>• Cholangiocarcinoma</li> <li>• Ampullary cancer</li> </ul>	84
Sapacitabine		Clinical trials Phase I/II/III	• Cndac (deoxycytidine analog)	• Amide bond	<ul style="list-style-type: none"> <li>• Myelodysplastic syndromes</li> <li>• Acute myeloid leukemia</li> </ul>	85





Table 3 (Contd.)

Name	Structure	Status <sup>a</sup>	Parent drug	Linker	Targeted cancer	
Guadecitabine (SGI-110)		Clinical trials Phase I/II/III	• Decitabine	• Phosphate ester bond	• Small cell lung cancer • Ovarian cancer • Hepatocellular carcinoma • Acute myeloid leukemia	79 and 86
ACV-TP-T		Preclinical	• Acyclovir	• Phosphodiester bond	• Pancreatic tumor	87

<sup>a</sup> Trial status was verified by the NIH – U.S. National Library of Medicine clinical trials database (<http://www.clinicaltrials.gov>). Approval status was verified by the European Medicines Agency (<http://www.ema.europa.eu>) and the US Food and Drug Administration (<http://www.fda.gov>).

### 5.1.1. Organic nanoparticles

**5.1.1.1. Liposomes and lipid nanocapsules.** Bangham and his coworkers are credited with the discovery of liposomes during the 1960s;<sup>97,98</sup> various studies then followed to characterize them, with alternative methods for the preparation of liposomes being discovered between 1975 and 1985. Subsequently, the study of liposomes spread to different scientific areas: biophysics (study of cell membrane properties), chemistry (energy conversion), colloid science (study of stability and thermodynamics of finite systems), biochemistry (membrane protein functions) and biology (study on cellular trafficking)

cumulating in the introduction of the first nanocarrier drug: a doxorubicin HCl liposome injection (commercial name: Doxil® (FDA approved in 1995) or Caelyx® (EMA approved in 1996)).<sup>99</sup>

Liposomes are made up of lipids with a hydrophilic tail and a hydrophobic head, creating an amphiphilic molecule that aggregates to form spherical liposomes, due to the interactions occurring upon contact with water. Liposomes have an aqueous core enclosed with a lipid bilayer.

Liposomes, *via* the modification of drug absorption, reduction of metabolism and the prolongation of the drug's half-life,

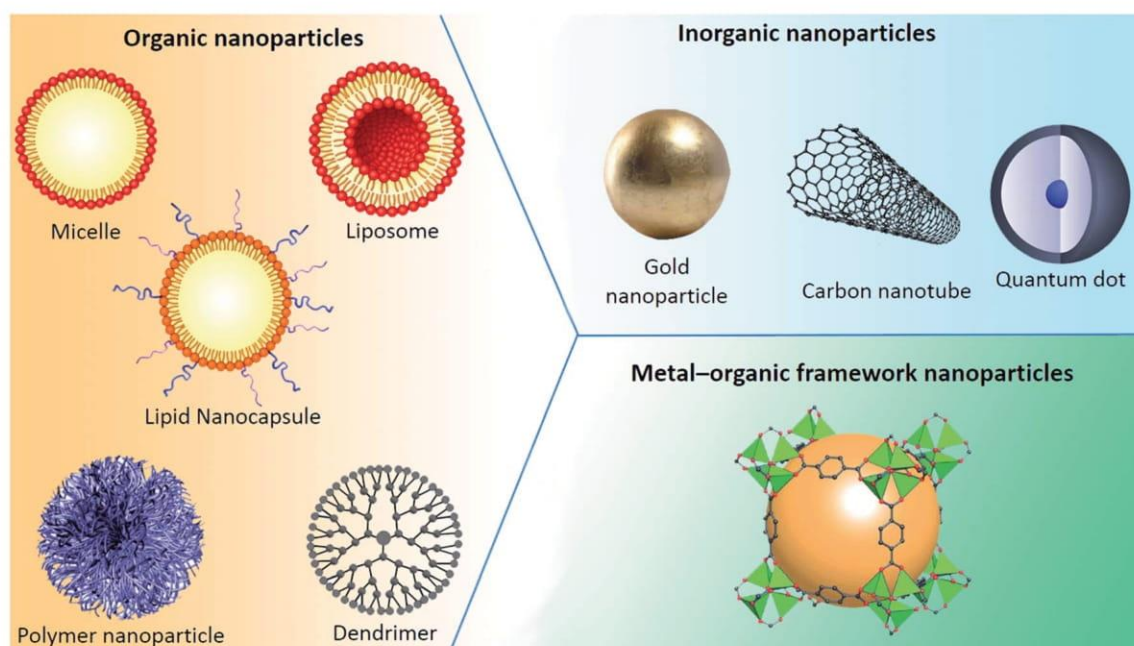


Fig. 7 Various types of nanoparticle.



are able to enhance the efficacy of conventional drugs. Upon encapsulation, the drug distribution ceases to be determined by the physico-chemical characteristics of the original drug molecule, and becomes reliant on the characteristics of the carrier. These factors, along with the ability of liposomes to solubilize both hydrophilic and hydrophobic molecules, secure liposomes as a potent drug delivery platform with application in various diseases such as cancer,<sup>100</sup> and fungal<sup>101</sup> and bacterial infections.<sup>102</sup>

When it comes to lipid nanocapsules (LNCs), Heurtault and her coworkers<sup>103</sup> are credited with the discovery of this nanocarrier. The size of LNCs ranges from 20 to 100 nm. Compared to liposomes which require an organic solvent for formulation, LNC formulation is solvent-free, producing a carrier with enhanced stability (physical stability up to 18 months). LNCs have a membrane consisting of a combination of lecithin (a phospholipid) and a PEGylated surfactant. This membrane encloses an oily core composed of medium-chain triglycerides and the formulation is founded on the phase-inversion temperature. Owing to these elements, LNCs are characterized by a hybrid structure between polymer nanocapsules and liposomes.<sup>104–107</sup>

The two drugs that have been approved by the FDA based on the encapsulation approach of nucleosidic analogs are DepoCyt<sup>TM</sup> based on the encapsulation of cytarabine (approved in 1999), and Vyxeos (cpx-351) based on a double encapsulation of cytarabine and daunorubicin (approved in 2017), and are used in the treatment of lymphomatous meningitis and acute myeloid leukemia, respectively. Both of these drugs use liposomes as the nanocarrier with varying encapsulation efficiency.<sup>108–112</sup> Several other encapsulated nucleosidic analogs for cancer treatment in different development and testing stages have been presented in Table 4.

**5.1.1.2. Polymeric nanoparticles (PnPs).** Polymers are macromolecules consisting of successive repeating units arranged in a chain-like formation that can take various shapes and can be biodegradable or not according to the use desired. Polymeric nanoparticles are being used in drug delivery, providing potential protection of the active agent, a sustained release and even an active targeting approach with a surface modification of the polymeric bone. Polyethylene glycol (PEG) may well be the most well known and frequently used synthetic polymer, owing to the properties it imparts on the nanoparticles such as “stealth”, since the densely packed hydrophilic PEG diminishes the interparticle attractive forces and causes steric repulsion to the surrounding biological components, for instance plasma proteins and antibodies: it stops phagocytosis and decreases clearance from the bloodstream or body.<sup>113–115</sup>

In his study Y. Haggag *et al.* encapsulated 5-fluorouracil (5FU) within a polymeric nanoparticle. The PnP formed had a high drug loading, a particle size of 185 nm, with a sustained drug release for 7 days. The *in vivo* results confirmed the enhanced anticancer activity of the 5FU-loaded NP. Histopathological examinations displayed the damage to tumor tissue after NP treatment. Finally, the PnP was found to be less toxic to liver and kidney tissues compared to the free 5-fluorouracil.<sup>116</sup>

**5.1.1.3. Dendrimers.** Dendrimers are characterized by a symmetric core surrounded by an inner and outer shell. At a molecular level, the dendritic branching forms globular structures. A typical dendrimer is made of three different parts, a central core made out of a single atom or an atomic group with a minimum of two identical chemical functions, repeating units forming several interior layers, and various peripheral functional groups.<sup>117</sup>

Diverse dendrimers exist, with unique biological properties, allowing them to be used as drug delivery agents for the

**Table 4** A list of encapsulated nucleosidic analogs for cancer treatment

Name	Active molecule	Status <sup>a</sup>	Nanocarrier	Targeted cancer	Encapsulation efficiency	
Vyxeos (cpx-351)	• Cytarabine • Daunorubicin	• FDA approved (2017) • EMA approved (2018) • Clinical trial phase IV	• Liposome	• Acute myeloid leukemia	• 5%	108 and 109
DepoCyt <sup>TM</sup>	• Cytarabine	• FDA approved (1999) • EMA approved (2008) • Withdrawn • Preclinical	• Liposome	• Lymphomatous meningitis	• 86.30%	110–112
Gemcitabine-loaded liposomes	• Gemcitabine	• Preclinical	• Liposome	• Anaplastic thyroid carcinoma	• 90%	156
GemC16-loaded 2N-LPs	• Gemcitabine	• Preclinical	• Liposome	• Pancreatic cancer	• 97.3% • Loading capacity (8.9%)	157
Decitabine LNCs	• Decitabine	• Preclinical	• Lipid nanocapsules	• Acute myeloid leukemia	• 88%	158

<sup>a</sup> Trial status was verified by the NIH – U.S. National Library of Medicine clinical trials database (<http://www.clinicaltrials.gov>). Approval status was verified by the European Medicines Agency (<http://www.ema.europa.eu>) and the US Food and Drug Administration (<http://www.fda.gov>).





treatment of different diseases such as HIV<sup>118,119</sup> and cancer, or as contrast agents with theranostic applications for imaging techniques such as Magnetic Resonance Imaging (MRI).<sup>120,121</sup>

Concerning the use of dendrimers as nucleoside analogue carriers, Szulc A. *et al.* have accomplished several strides. Their studies demonstrate that maltose and maltotriose modified poly(propylene imine) dendrimers (PPI dendrimers) are a potential carrier for triphosphate forms of nucleoside analogue drugs. These dendrimers have been chosen owing to their biopermeability, non-toxicity, non-immunogenicity and ability to stay in the blood circulation.<sup>122–126</sup>

Also worth mentioning is the research of M. Gorzkiewicz and coworkers, where dendrimers served as nano-carriers for fludarabine, while simultaneously improving its cellular entry and enabling both the direct and phosphorylation-independent toxicity.<sup>127</sup>

### 5.1.2. Inorganic nanoparticles

**5.1.2.1. Carbon nanotubes (CNTs).** Carbon nanotubes (CNTs) are cylindrical molecules constructed from carbon atoms forming graphene sheets rolled into a cylindrical shape that can have open or capped endings, with diameters of merely 1 nm but a length of several micrometers.<sup>128,129</sup> With such a high surface area, conjugation with different therapeutic molecules is possible upon their functionalization with specific groups able to bind the desired molecule or similarly to Qds seek a specific target on a cell or tissue.<sup>130,131</sup>

Following Zheng *et al.*'s discovery of the hybridization phenomenon of single-stranded DNA molecules and CNTs (single-walled carbon nanotubes) in 2003,<sup>132</sup> much research has been done in this field in both the theranostic and pharmaceutical domains.<sup>135,136</sup> Remarkably, Zhang P. *et al.*'s work on gemcitabine–lentinan–carbon nanotubes revealed that the combination of drug therapy and near-infrared photothermal therapy possesses great synergistic antitumor efficacy.<sup>135</sup>

**5.1.2.2. Quantum dots.** Quantum dots (Qds) are nanocrystals made from semiconducting materials ranging in diameter between 2 and 10 nm, lending them a quantum effect owing to their extremely small size. Meaning that electrons inside the dots are confined and can only occupy defined energy levels. Upon the excitation of these electrons by an external energy source, an intense response from these Qds follows.

Building upon these properties, quantum dots can be enclosed within a shell able to mimic the receptors on the cells. The quantum dots will then track down and attach to the specific receptor. Then, relying on the fluorescent nature of quantum dots the site of concern is made evident. Only a limited number of receptors are needed on the surface of the dot, and when compared to the surface area of the dot, it leaves enough space to place other things such as drugs, allowing for instance quantum dots to find and treat cancer cells. This eludes healthy cells and therefore the side effects associated with cancer treatments will decrease.<sup>136–139</sup>

Gemcitabine-Qds have been approached by several teams and showed promising results including a high drug loading capacity, reduced cytotoxicity towards normal cells and tissues, a good drug release profile, a higher cellular cytotoxicity and

more effective inhibition capacity when compared to free gemcitabine.<sup>140,141</sup>

**5.1.2.3. Gold nanoparticles.** Gold nanoparticles (GNPs) are particles with a diameter of 1 to 100 nm and have been reported as potential carriers to small drug molecules or large biomolecules, like proteins, DNA, RNA or nucleic acids. The linkage between the nucleic acids and GNPs is usually through non-covalent bonds, which are easier to break off during cellular uptake.<sup>142,143</sup>

A prominent application of using gold nanoparticles as a carrier for nucleoside analogues is revealed by S. Song and coworkers, where the gold nanoparticles are used as a vehicle to carry a purine analog called fludarabine for the treatment of hematological cancers, showing improved efficacy when compared to free fludarabine.<sup>144</sup>

**5.1.2.4. SiO<sub>2</sub> nanoparticles.** Silicon dioxide nanoparticles can be formulated to have a wide range of sizes and their surface chemistry easily modified to fit diverse applications, with mesoporous silica nanoparticles playing a great role in drug delivery and nanomedicine. Jeelani *et al.*'s work offers a comprehensive look into the different types and applications of silica nanoparticles.<sup>145</sup>

While in the field of cancer treatment, Azali and coworkers were able to formulate a SiO<sub>2</sub> nanoparticle to act as a vehicle for the nucleosidic analogue 5-fluoruracil (5-FU), the aim of their study was to compare the release of 5-FU depending on the solvent medium used to load this drug into the nanoparticle. Transmission electron microscopy (TEM) showed that these nanoparticles had a hexagonal structure. Additionally, adsorption data showed that 95.27% of 5-FU were loaded into the nanoparticles. Interestingly, in ethanol medium, the release rate percentage was lower than in deionized water medium, at 9% and 23%, respectively.<sup>146</sup>

**5.1.2.5. Iron oxide nanoparticles.** There are several phases of iron oxide crystallites exhibited as hematite ( $\alpha$ -Fe<sub>2</sub>O<sub>3</sub>), maghemite ( $\gamma$ -Fe<sub>2</sub>O<sub>3</sub>), goethite (Fe[O(OH)]) and magnetite (Fe<sub>3</sub>O<sub>4</sub>). Both hematite and magnetite are favored for biomedical applications due to their low cost and non-toxicity, including MRI contrast enhancement, detoxification of biological fluids, tissue repair, cell separation, immunoassay, hyperthermia, and drug delivery.<sup>147,148</sup>

An interesting application in the field of cancer treatment that stands out is the work of Shahabadi *et al.*: they were able to formulate a cytarabine-coated Fe<sub>3</sub>O<sub>4</sub> magnetic nanoparticle with a size of 23 nm. The *in vitro* cytotoxic activity was investigated against HL-60, KG-1, and Raji cell lines, showing a twofold efficacy increase when compared to free cytarabine. Furthermore, *in vitro* DNA binding studies were carried out, showing that DNA aggregated to the nanoparticles *via* groove binding mode.<sup>149</sup>

**5.1.3. Metal–organic framework nanoparticles (MOFs).** MOFs are composed of metal cations or clusters connected to polytopic organic linkers *via* coordination bonding. The metal ions, organic ligands, and the resultant structural motifs essentially yield an infinite number of possible combinations to form “metal–organic frameworks”.<sup>150</sup> The metals commonly used for the synthesis of MOFs include, but are not limited to,





Zn(II), Cu(II), Mg(II), Ca(II), Ln(III) (Ln = lanthanide), Al(III), Co(II), Cd(II), Zr(IV), and Ti(III). These metals can adopt a variety of coordination geometries, such as tetrahedral, trigonal bipyramidal, square pyramidal, and octahedral.<sup>151</sup> Organic ligands, such as carboxylates, amines, phosphates, and sulfonates, play important roles in the construction of MOFs.<sup>152,153</sup> MOFs have been studied for various applications, including gas storage, catalysis, drug delivery, and luminescence sensing.<sup>154</sup>

Rodriguez-Ruiz *et al.* approached the idea of a gemcitabine loaded MOF, using a monophosphorylated form of gemcitabine that was loaded into MIL-100 iron-trimesate nanoMOFs: the anticancer effect of this nanoparticle was tested on a pancreatic PANC-1 cell line. The formulated nanoparticles acted as “nanosponges”, soaking Gem-MP from its aqueous solution, with a maximal drug loading of 30 wt%, reflecting the strong interaction between the drug and MOFs. Furthermore, these MOFs were nine times more effective against the pancreatic cancer cell line when compared to free gemcitabine.<sup>155</sup>

## 5.2. Drawbacks of the nanoparticle approach

The approach of using nanoparticles such as micelles or liposomes, as a means of overcoming the shortcoming present at the levels of intracellular transport or drug activation in tumor cells, does tackle a huge hurdle faced by traditional drugs. Nevertheless, the nanoparticle approach still has its limitations, for instance the drug loading capacity of these vectors is low, as the amount of the encapsulated therapeutic molecule is feeble when considering the amount needed to reach a therapeutic effect. Moreover, excipients needed to formulate nanoparticles have a certain degree of toxicity and undesirable side effects, not to mention the large size of this vector when compared to the size of the therapeutic molecule, allowing its recognition by the immune cells as a foreign body and leading to its clearance especially by macrophages. Therefore, an approach that can combine both the prodrug and nanoparticle techniques, gaining both their advantages, can potentially be the break needed to overcome cancer resistance to nucleotide and nucleoside analogs.

## 6. Self-assembly of nucleolipid prodrugs

Molecular self-assembly is a key concept in supramolecular chemistry. The thermodynamic incompatibility between the different blocks causes a spatial organization into ordered morphologies at the nanoscale level with the production of novel structural features, as demonstrated by recent studies.<sup>159</sup> This is because assembly of molecules in such systems is directed through noncovalent interactions (*e.g.*, hydrogen bonding, metal coordination, hydrophobic forces, van der Waals forces,  $\pi$ - $\pi$  stacking, and/or electrostatic interactions) as well as electromagnetic interactions. Common examples include the formation of micelles, vesicles, liquid crystal phases, and Langmuir monolayers by surfactant molecules. Further examples of supramolecular assemblies demonstrate that a variety of different shapes and sizes can be obtained using molecular self-assembly.<sup>160</sup>

The hydrophobic forces result from an entropic phenomenon and trigger the self-assembly of hydrophobic moieties: the produced nanoparticles will thus be created owing to the collective weak interaction present, as nucleotides, nucleosides and their analogs will interact through  $\pi$ - $\pi$  stacking, hydrogen bonds, electrostatic interaction, and van der Waals forces.<sup>161</sup> Consequently, the various key factors of the self-assemblies including stability, shape, size, charge, viscosity, and surface morphology amongst others will affect their cellular internalization and diffusion, thus impacting the pharmacological activity of the new molecules.<sup>162</sup>

Therefore, building on the previous idea of the formation of a nucleoside/nucleotide based amphiphilic prodrug, an additional step can be performed *via* pushing the prodrugs with appropriate physico-chemical properties into self-assembly to form nanoparticles<sup>168</sup> (Fig. 8), consequently increasing the drug's diffusion ability as well as protecting it from enzymatic degradation and boosting its bioactivity.

Given that nucleobases, nucleosides and nucleotides have a hydrophilic nature, conjugating them to molecules having a hydrophobic nature will produce an amphiphilic molecule that is better suited for self-assembly: examples of that case are the CP-4126, capecitabine and LY2334737 prodrugs mentioned previously in Table 3, where the nucleosides have been conjugated to either a carboxylic or ester group.<sup>82</sup> Indeed, the coupling of the nucleoside and nucleotide derivatives to a fatty acid (especially unsaturated ones) seems to be the best method to achieve an amphiphilic prodrug with self-assembling potential.

Several drugs in the preclinical stage of their development are based on this approach; for instance, DOC, a self-assembling pro-nucleosidic drug, was designed by linking clofarabine to oleic acid *via* an ester bond. The obtained prodrug is able, due to the reasons mentioned above, to self-assemble into spherical nanoparticles and is being tested on breast cancer.<sup>167</sup> A selection of similar self-assembling prodrugs is presented in Table 5.

### 6.1. The PUFAylation approach

Although the term “PUFAylation” was only very recently introduced by Liming Wu *et al.*, the concept of conjugating a polyunsaturated fatty acid (PUFA) to a nucleoside leading to the spontaneous self-assembly of the created prodrug is one that has been tackled before. Certainly, this innovative strategy was established by Couvreur and colleagues, whereby squalene derivatives (a cholesterol precursor) were conjugated to nucleoside analogs in a process they termed “squalenoylation”. What is more, “PUFAylation”, while permitting this conjugate to self-assemble in water, doesn't require any excipients, an advantage it gains over traditional formulated nanoparticles, thus improving the drug tolerability in animals and demonstrating exceptional effectiveness, with an unbeatable drug loading. Moreover, this method produces prodrugs with an adequate amphiphilicity, allowing for an enhanced *in vivo* antitumor efficacy compared to the parent drug. When compared to “squalenoylation”, “PUFAylation” seems to have the edge, as the





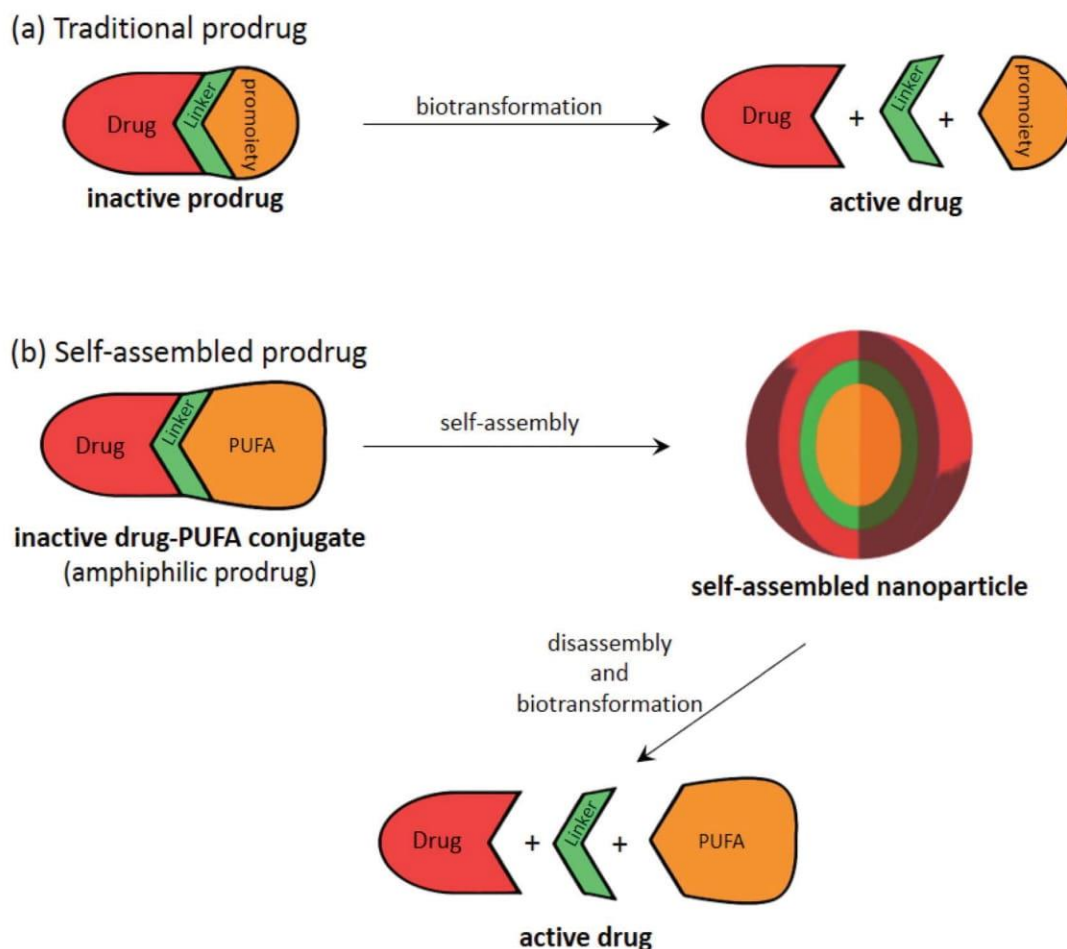


Fig. 8 Illustration showing the general process of (a) traditional prodrug biotransformation and (b) self-assembly of prodrugs, that can be applied to "PUFAs".

conversion of squalene into squalenylacetic acid is a tiresome multistep reaction, while most PUFAs are commercially accessible. Moreover, most of these "PUFAs" are essential for biological functions and are plentiful in the body meaning that they may reduce the toxicity stemming from the use of adjuvants, and finally the  $\pi$ - $\pi$  association between PUFAs will increase the stability of the self-assemblies. Based on all that, the PUFA technology is an immensely encouraging one for the manufacturing of prodrugs and their derived self-assembled nanoparticles.<sup>162,165,166,169,170</sup>

Of the several "PUFAylations" presented, the PUFAylation of the gemcitabine prodrug SQdFdC (Table 5) is a definitive example of this concept. The coupling of squalene (a cholesterol precursor) with gemcitabine leads to the spontaneous formation of nanoparticles with a diameter of 120–140 nm in an aqueous medium. The self-assemblies took the shape of an inverse hexagonal supramolecular structure, with an aqueous core that was surrounded by the gemcitabine molecules linked to the squalene moieties. This PUFAylated self-assembly has shown improved efficacy under both *in vitro* and *in vivo* conditions when compared to free gemcitabine. In *in vitro* experiments, SQdFdC exhibited higher cytotoxicity than gemcitabine

in both human and murine resistant leukemia cell lines, while in *in vivo* experiments, SQdFdC revealed notably greater anti-cancer activity than gemcitabine against both solid subcutaneously grafted tumors and aggressive metastatic leukemia. This increased efficacy of SQdFdC can be attributed to the nanoparticle shape of the self-assembling prodrug, offering protection from deamination and a specific targeting with a prodrug cleaved by cathepsin B, overexpressed in cancer cells.<sup>171–175</sup>

Mulet *et al.* also present interesting early research regarding PUFAylation, comparing the molecular structure, phase behavior, and cellular uptake differences between 3'-oleoylthymidine and other non-saturated nucleolipids, showing that the presence of lyotropic liquid crystalline phases was reliant on the number of unsaturated chains. Additionally, the complexity of the ordered systems formed, from the 1D lamellar system presented here to inverse 2D hexagonal or 3D cubic phases, would lead to different bioactive release profiles.<sup>176</sup>

Wu *et al.* have similarly shown very promising results for their LA-Gem prodrug "PUFAylated" self-assemblies (Table 5). The self-assemblies showed a high drug loading, a limited metabolism by endogenous enzymes, an improved release and intracellular uptake. Likewise, promising *in vivo* results were



Table 5 List of preclinical self-assembled nucleoside analog-based prodrugs

Name	Prodrug structure	Active drug	Fatty acid	Shape	Targeted cancer
5-FCPal		• Capecitabine	• Palmitic acid	• Lamellar sheets	• Breast cancer
LA-Gem		• Gemcitabine	• Linoleic acid	• Spherical	• Pancreatic ductal adenocarcinoma
SQdFdC		• Gemcitabine	• Squalenoyl	• Unilamellar vesicles	• Pancreatic cancer
DOC		• Clofarabine	• Oleic acid	• Spherical	• Breast cancer

obtained *versus* a pancreatic ductal adenocarcinoma (PDAC) PDX mouse model.<sup>165</sup>

Additional insights into PUFAs can be gained from the work of Maksimenko *et al.*; this research is an advancement on the previous work of Couvreur previously discussed, by taking the idea of “squalenoylation” and moving it to a more generalized “terpenoylation” concept. Several polyisoprenoyl prodrugs of gemcitabine were formulated, with different polyisoprenoyl chain lengths: the obtained nanoparticles were then tested *in vitro* on murine melanoma cell line B16F10, human pancreatic carcinoma cell line MiaPaCa-2, human lung carcinoma cell line A549 and human breast adenocarcinoma cell line MCF7. It was revealed that the anticancer efficacy of these nanoparticles was dependent on the size of the polyisoprenoyl chains: the polyisoprenoyl prodrug of gemcitabine containing three isoprene units was the most active nanoparticle on all

the cancer cell lines tested. The results obtained *in vivo* (carcinoma xenograft model in mice) were in accordance with the *in vitro* results.<sup>177</sup>

## 6.2. Critical packing parameters dictate the self-assembled nanoparticle shape

As proposed by Israelachvili and Mitchell in the mid 1970s, the architecture of self-assemblies is predicted by the molecular shape of amphiphilic phospholipids with a critical packing parameter (CPP) defined as the equation of  $CPP = V/(a_0 l_c)$ , where  $V$ ,  $l_c$  and  $a_0$  are, respectively, the volume and length of the lipophilic chain, and the cross-sectional area of the hydrophilic core of the phospholipid expressed per molecule in the aggregates.<sup>178</sup> Altering these different parameters leads to the molecule adopting a different interfacial curvature and therefore a different morphology. The values obtained by the CPP





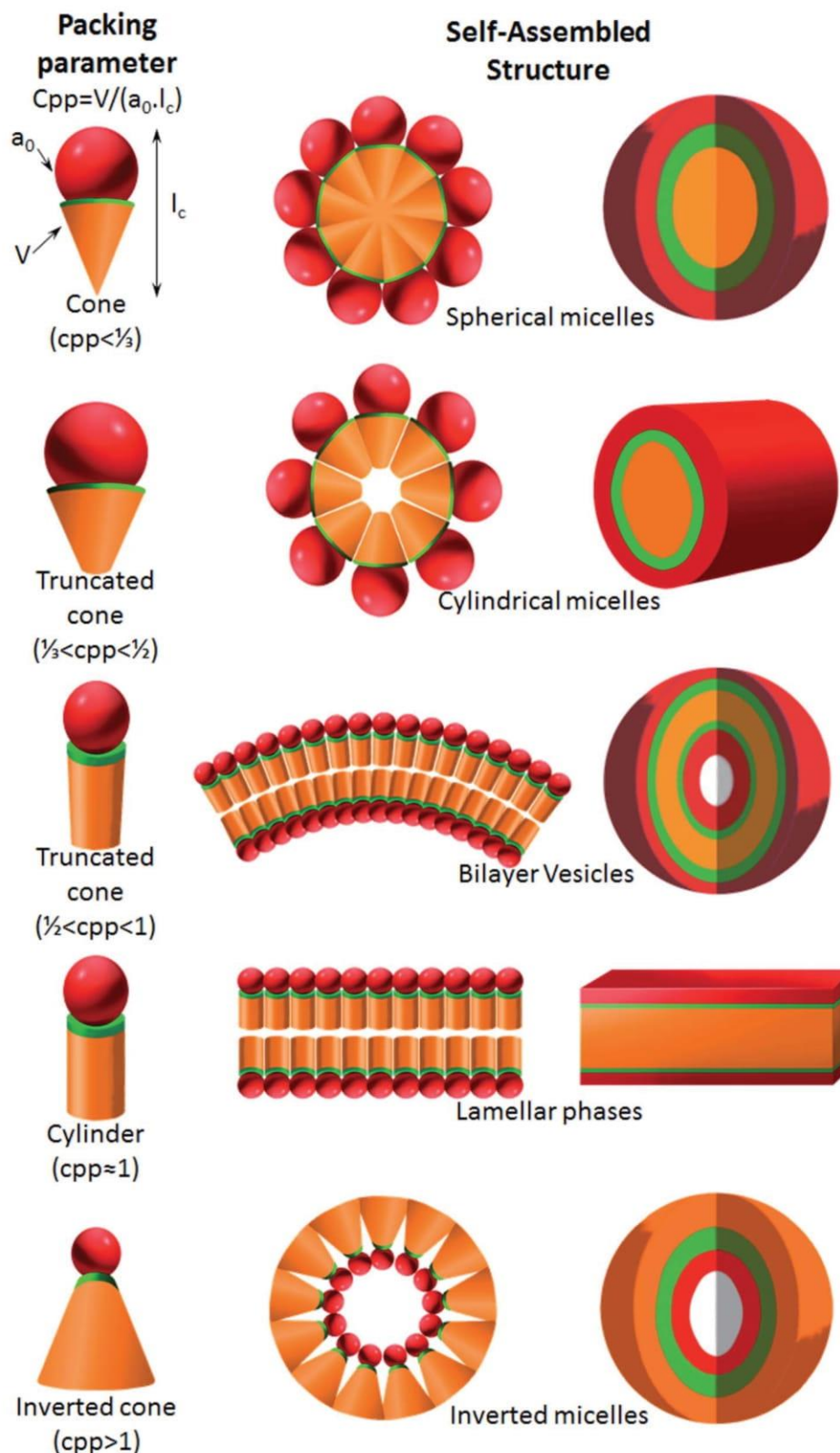


Fig. 9 Molecular shape and critical packing parameter (CPP) of amphiphilic molecules, and the self-assembly entities formed of different amphiphiles ( $v$ , the lipophilic chain volume;  $a_0$ , the cross-sectional area of the hydrophilic head group;  $l_c$ , the length of the lipophilic chain).

equation will influence the shape of the self-assemblies as shown in Fig. 9: spherical micelles, with high curvature, are formed when  $CPP \leq 1/3$ , cylinders are formed in the range  $1/3 <$

$CPP \leq 1/2$ , when  $1/2 < CPP \leq 1$ , vesicles are formed, at  $CPP \approx 1$  lamellar phases are obtained, and finally for  $CPP > 1$  inverted micelles are obtained.



## 7. Conclusion

In conclusion, nucleoside and nucleotide analogs are staple agents for the treatment of various cancers, especially hematologic malignancies, and given the limited arsenal of drugs to combat this disease, it is crucial to enhance the pre-existing drugs. Two technologies were thus approached as a means to solve this issue, the prodrug and nanoparticle strategies, and although both of them did indeed enhance the traditional parent molecule in different aspects, both of them fell short due to different drawbacks. Therefore, a combination of both approaches might be the answer. Certainly, self-assembling PUFAlated molecules are shaping up to be an impressive tool that combines the advantages of both previous approaches while disregarding their drawbacks and it warrants further investigation.

## Conflicts of interest

The authors declare no conflicts of interest. The authors declare no competing financial interest.

## Acknowledgements

Financial support by the "La Ligue contre le cancer 49" association is gratefully acknowledged.

## References

- G. M. Cooper, *The Cell: a Molecular Approach*, Sinauer Associates, an imprint of Oxford University Press, Oxford, New York, 8th edn, 2019.
- F. Bray, J. Ferlay, I. Soerjomataram, R. L. Siegel, L. A. Torre and A. Jemal, *Ca-Cancer J. Clin.*, 2018, **68**, 394–424.
- J. Ferlay, M. Colombet, I. Soerjomataram, C. Mathers, D. M. Parkin, M. Piñeros, A. Znaor and F. Bray, *Int. J. Cancer*, 2019, **144**, 1941–1953.
- C. W. Freyer, N. Gupta, M. Wetzler and E. S. Wang, *Am. J. Hematol.*, 2015, **90**, 62–72.
- N. D. Reese and G. J. Schiller, *Current Hematologic Malignancy Reports*, 2013, **8**, 141–148.
- P.-F. He, J.-D. Zhou, D.-M. Yao, J.-C. Ma, X.-M. Wen, Z.-H. Zhang, X.-Y. Lian, Z.-J. Xu, J. Qian and J. Lin, *Oncotarget*, 2017, **8**, 41498–41507.
- E. Moysan, G. Bastiat and J.-P. Benoit, *Mol. Pharm.*, 2013, **10**, 430–444.
- Q. Li, H. Yan, W. Liu, H. Zhen, Y. Yang and B. Cao, *PLoS One*, 2014, **9**(8), e104346.
- M. Bassetto and M. Slusarczyk, *Pharm. Pat. Anal.*, 2018, **7**, 277–299.
- M. Rebucci and C. Michiels, *Biochem. Pharmacol.*, 2013, **85**, 1219–1226.
- S. Mukherjee, *The Emperor of All Maladies: a Biography of Cancer*, Scribner, New York, 1st edn, 2011.
- L. Bildstein, C. Dubernet and P. Couvreur, *Adv. Drug Delivery Rev.*, 2011, **63**, 3–23.
- D. T. Bui, J. Nicolas, A. Maksimenko, D. Desmaële and P. Couvreur, *Chem. Commun.*, 2014, **50**, 5336–5338.
- C. E. Muller, *Chem. Biodiversity*, 2009, **6**, 2071–2083.
- Y. Singh, M. Palombo and P. Sinko, *Curr. Med. Chem.*, 2008, **15**, 1802–1826.
- H. Maag, *Drug Discovery Today: Technol.*, 2012, **9**, e121–e130.
- M.-H. Lin, C.-F. Hung, C.-Y. Hsu, Z.-C. Lin and J. Y. Fang, *Future Med. Chem.*, 2019, **11**, 2131–2150.
- B. Alberts, A. Johnson, J. Lewis, M. Raff, K. Roberts and P. Walter, *Molecular Biology of the Cell*, Garland Science, 4th edn, 2002.
- G. P. Moss, P. A. S. Smith and D. Tavernier, *Pure Appl. Chem.*, 1995, **67**, 1307–1375.
- R. L. P. Adams, J. T. Knowler and D. P. Leader, *The Biochemistry of the Nucleic Acids*, Chapman & Hall, London, New York, 11th edn, 1992.
- F. A. Carey and R. M. Giuliano, *Organic Chemistry*, McGraw-Hill Education, New York, NY, 10th edn, 2016.
- D. L. Nelson and M. M. Cox, *Lehninger Principles of Biochemistry*, W. H. Freeman, New York, 5th edn, 2008.
- C. Galmarini, J. Mackey and C. Dumontet, *Leukemia*, 2001, **15**, 875–890.
- C. M. Galmarini, G. Warren, M. T. Senanayake and S. V. Vinogradov, *Int. J. Pharm.*, 2010, **395**, 281–289.
- N. Degwert, E. Latuske, G. Vohwinkel, H. Stamm, M. Klokow, C. Bokemeyer, W. Fiedler and J. Wellbrock, *Eur. J. Haematol.*, 2016, **97**, 239–244.
- D. Nowak, N. L. M. Liem, M. Mossner, M. Klaumünzer, R. A. Papa, V. Nowak, J. C. Jann, T. Akagi, N. Kawamata, R. Okamoto, N. H. Thoennissen, M. Kato, M. Sanada, W.-K. Hofmann, S. Ogawa, G. M. Marshall, R. B. Lock and H. P. Koefler, *Exp. Hematol.*, 2015, **43**, 32–43.
- M. Levin, M. Stark, B. Berman and Y. G. Assaraf, *Cell Death Dis.*, 2019, **10**, 1–14.
- V. Heinemann, Y.-Z. Xu, S. Chubb, A. Sen, L. W. Hertel, G. B. Grindey and W. Plunkett, *Cancer Res.*, 1992, **52**, 533–539.
- Y. Jia and J. Xie, *Genes Dis.*, 2015, **2**, 299–306.
- M. T. de la Fuente, B. Casanova, E. Cantero, M. Hernández del Cerro, J. Garcia-Marco, A. Silva and A. Garcia-Pardo, *Biochem. Biophys. Res. Commun.*, 2003, **311**, 708–712.
- M. Mraz, K. Cerna, V. Mayerova, K. Musilova, K. Plevova, S. Pavlova, B. Tichy, M. Doubek, Y. Brychtova, J. Malcikova, J. Mayer, M. Trbusek and S. Pospisilova, *Blood*, 2012, **120**, 3883.
- T. Zenz, S. Häbe, T. Denzel, J. Mohr, D. Winkler, A. Bühler, A. Sarno, S. Groner, D. Mertens, R. Busch, M. Hallek, H. Döhner and S. Stilgenbauer, *Blood*, 2009, **114**, 2589–2597.
- I. Sturm, A. G. Bosanquet, S. Hermann, D. Güner, B. Dörken and P. T. Daniel, *Cell Death Differ.*, 2003, **10**, 477–484.
- N. Tsesmetzis, C. Paulin, S. Rudd and N. Herold, *Cancers*, 2018, **10**, 240.
- M. Venturini, *Eur. J. Cancer*, 2002, **38**, 3–9.
- N. S. Siddiqui, A. Godara, M. M. Byrne and M. W. Saif, *Expert Opin. Pharmacother.*, 2019, **20**, 399–409.





- 37 D. B. Longley, D. P. Harkin and P. G. Johnston, *Nat. Rev. Cancer*, 2003, **3**, 330–338.
- 38 T. L. Whited and D. J. Taylor, *Mol. Cell. Oncol.*, 2018, **5**, e1536844.
- 39 L. J. Scott, *Drugs*, 2016, **76**, 889–900.
- 40 C. Knies, H. Reuter, K. Hammerbacher, E. Bender, G. A. Bonaterra, R. Kinscherf and H. Rosemeyer, *Chem. Biodiversity*, 2019, e1800497.
- 41 J. Lukenbill and M. Kalaycio, *Leuk. Res.*, 2013, **37**, 986–994.
- 42 F. J. Hernandez-Ilizaliturri and M. S. Czuczman, *Clin. Med.: Ther.*, 2009, **1**.
- 43 G. I. Rodriguez, R. E. Jones, E. K. Orenberg, M. L. Stoltz and D. J. Brooks, *Clin. Cancer Res.*, 2002, **8**, 2828–2834.
- 44 R. Swords, E. Apostolidou and F. Giles, *Hematology*, 2006, **11**, 321–329.
- 45 J. E. Karp, *Acute Myelogenous Leukemia*, Springer Science & Business Media, 2009.
- 46 G. J. Peters, D. Sarkisjan, B. E. Hassouni, R. J. Honeywell, J. R. Julsing, B. Balboni, D. J. D. Klerk, S. Zekanovic, K. Smid, E. Giovannetti, Y. B. Lee and D. J. Kim, *Cancer Res.*, 2019, **79**, 1267.
- 47 H. M. Babiker, P. J. Schlegel, L. G. Hicks, A. J. Bullock, N. Burhani, E. Benaim, C. Peterson, C. Heaton and A. J. Ocean, *J. Clin. Oncol.*, 2019, **37**, 420.
- 48 R. Buettner, C.-C. Chen, B. Kumar, L. S. Chen, K. Wennerberg, R. Thompson, T. Pemovska, L. Li, V. Gandhi, G. Marcucci, V. Pullarkat and S. T. Rosen, *Blood*, 2015, **126**, 792.
- 49 A. Albert, *Nature*, 1958, **182**, 421–423.
- 50 M. A. Lesniewska-Kowiel and I. Muszalska, *Eur. J. Med. Chem.*, 2017, **129**, 53–71.
- 51 R. Mahato, W. Tai and K. Cheng, *Adv. Drug Delivery Rev.*, 2011, **63**, 659–670.
- 52 P. Ettmayer, G. L. Amidon, B. Clement and B. Testa, *J. Med. Chem.*, 2004, **47**, 2393–2404.
- 53 J. Rautio, H. Kumpulainen, T. Heimbach, R. Oliyai, D. Oh, T. Järvinen and J. Savolainen, *Nat. Rev. Drug Discovery*, 2008, **7**, 255–270.
- 54 B. M. Liederer and R. T. Borchardt, *J. Pharm. Sci.*, 2006, **95**, 1177–1195.
- 55 P. Potter and R. Wadkins, *Curr. Med. Chem.*, 2006, **13**, 1045–1054.
- 56 T. Heimbach, D.-M. Oh, L. Y. Li, N. Rodríguez-Hornedo, G. Garcia and D. Fleisher, *Int. J. Pharm.*, 2003, **261**, 81–92.
- 57 D. Petrović, K. Szeler and S. C. L. Kamerlin, *Chem. Commun.*, 2018, **54**, 3077–3089.
- 58 D. Gupta, S. V. Gupta, K.-D. Lee and G. L. Amidon, *Mol. Pharm.*, 2009, **6**, 1604–1611.
- 59 J. Soul-Lawton, E. Seaber, N. On, R. Wootton, P. Rolan and J. Posner, *Antimicrob. Agents Chemother.*, 1995, **39**, 2759–2764.
- 60 C. Y. Yang, A. H. Dantzig and C. Pidgeon, *Pharm. Res.*, 1999, **16**, 1331–1343.
- 61 S. Mahesh, K.-C. Tang and M. Raj, *Mol. J. Synth. Chem. Nat. Prod. Chem.*, 2018, **23**(10), 2615.
- 62 K. M. Huttunen and J. Rautio, *Curr. Top. Med. Chem.*, 2011, **11**, 2265–2287.
- 63 T. Heimbach, D.-M. Oh, L. Y. Li, M. Forsberg, J. Savolainen, J. Leppänen, Y. Matsunaga, G. Flynn and D. Fleisher, *Pharm. Res.*, 2003, **20**, 848–856.
- 64 A. R. Van Rompay, M. Johansson and A. Karlsson, *Pharmacol. Ther.*, 2000, **87**, 189–198.
- 65 K. Y. Hostetler, *Antiviral Res.*, 2009, **82**, A84–A98.
- 66 E. Moysan, G. Bastiat and J.-P. Benoit, *Mol. Pharm.*, 2013, **10**, 430–444.
- 67 C. Perigaud, S. Peyrottes, C. Dumontet, WO2009053654A2, 2009. <https://patents.google.com/patent/WO2009053654A2/en>.
- 68 K. Sugano, M. Kansy, P. Artursson, A. Avdeef, S. Bendels, L. Di, G. F. Ecker, B. Faller, H. Fischer, G. Gerebtzoff, H. Lennernaes and F. Senner, *Nat. Rev. Drug Discovery*, 2010, **9**, 597–614.
- 69 B. S. Vig, P. J. Lorenzi, S. Mittal, C. P. Landowski, H.-C. Shin, H. I. Mosberg, J. M. Hilfinger and G. L. Amidon, *Pharm. Res.*, 2003, **20**, 1381–1388.
- 70 K. S. Liu, O. Y. P. Hu, S. T. Ho, J. I. Tzeng, Y. W. Chen and J. J. Wang, *Br. J. Anaesth.*, 2004, **92**, 712–715.
- 71 K.-S. Liu, J.-I. Tzeng, Y.-W. Chen, K.-L. Huang, C.-H. Kuei and J.-J. Wang, *Anesth. Analg.*, 2006, **102**, 1445–1451.
- 72 K. Zuwala, A. A. A. Smith, A. Postma, C. Guerrero-Sanchez, P. Ruiz-Sanchis, J. Melchjorsen, M. Tolstrup and A. N. Zelikin, *Adv. Healthcare Mater.*, 2015, **4**, 46–50.
- 73 L.-H. Shao, S.-P. Liu, J.-X. Hou, Y.-H. Zhang, C.-W. Peng, Y.-J. Zhong, X. Liu, X.-L. Liu, Y.-P. Hong, R. A. Firestone and Y. Li, *Cancer*, 2012, **118**, 2986–2996.
- 74 Y.-J. Zhong, L.-H. Shao and Y. Li, *Internet J. Oncol.*, 2013, **42**, 373–383.
- 75 Y. Xu, J. Geng, P. An, Y. Xu, J. Huang, W. Lu, S. Liu and J. Yu, *RSC Adv.*, 2014, **5**, 6985–6992.
- 76 Q. Zhu, Y. Lu, X. He, T. Liu, H. Chen, F. Wang, D. Zheng, H. Dong and J. Ma, *Sci. Rep.*, 2017, **7**, 1–10.
- 77 D. Desai, M. Åkerfelt, N. Prabhakar, M. Toriseva, T. Näreoja, J. Zhang, M. Nees and J. Rosenholm, *Pharmaceutics*, 2018, **10**, 237.
- 78 R. Zhang, X. Qin, F. Kong, P. Chen and G. Pan, *Drug Delivery*, 2019, **26**, 328–342.
- 79 G. S. Daher-Reyes, B. M. Merchan and K. W. L. Yee, *Expert Opin. Invest. Drugs*, 2019, **28**, 835–849.
- 80 S. T. C. Neuteboom, P. L. Karjian, C. R. Boyer, M. Beryt, M. Pegram and G. M. Wahl, *Mol. Cancer Ther.*, 2002, **1**, 377–384.
- 81 U. Pradere, E. C. Garnier-Amblard, S. J. Coats, F. Amblard and R. F. Schinazi, *Chem. Rev.*, 2014, **114**, 9154–9218.
- 82 S. J. Faivre, A. J. Olszanski, K. Weigang-Köhler, H. Riess, R. B. Cohen, X. Wang, S. P. Myrand, E. R. Wickremsinhe, C. L. Horn, H. Ouyang, S. Callies, K. A. Benhadji and E. Raymond, *Invest. New Drugs*, 2015, **33**, 1206–1216.
- 83 F. E. Stuurman, E. E. Voest, A. Awada, P. O. Witteveen, T. Bergeland, P.-A. Hals, W. Rasch, J. H. M. Schellens and A. Hendlish, *Invest. New Drugs*, 2013, **31**, 959–966.
- 84 M. Slusarczyk, M. H. Lopez, J. Balzarini, M. Mason, W. G. Jiang, S. Blagden, E. Thompson, E. Ghazaly and C. McGuigan, *J. Med. Chem.*, 2014, **57**, 1531–1542.





- 85 T. M. Kadia, G. M. Borthakur, E. Jabbour, M. Y. Konopleva, F. Ravandi, C. D. DiNardo, D. Zheleva, D. Blake and J. H. Chiao, *Blood*, 2019, **134**, 3926.
- 86 G. Garcia-Manero, G. Roboz, K. Walsh, H. Kantarjian, E. Ritchie, P. Kropf, C. O'Connell, R. Tibes, S. Lunin, T. Rosenblatt, K. Yee, W. Stock, E. Griffiths, J. Mace, N. Podoltsev, J. Berdeja, E. Jabbour, J.-P. J. Issa, Y. Hao, H. N. Keer, M. Azab and M. R. Savona, *Lancet Haematology*, 2019, **6**, e317–e327.
- 87 S. Polvani, M. Calamante, V. Foresta, E. Ceni, A. Mordini, A. Quattrone, M. D'Amico, C. Luchinat, I. Bertini and A. Galli, *Gastroenterology*, 2011, **140**, 709–720.
- 88 Definition – Nanomaterials – Environment – European Commission, [https://ec.europa.eu/environment/chemicals/nanotech/faq/definition\\_en.htm](https://ec.europa.eu/environment/chemicals/nanotech/faq/definition_en.htm).
- 89 *Nat. Nanotechnol.*, 2019, **14**, 193.
- 90 J. O. Martinez, B. S. Brown, N. Quattrocchi, M. Evangelopoulos, M. Ferrari and E. Tasciotti, *Chin. Sci. Bull. Kexue Tongbao*, 2012, **57**, 3961–3971.
- 91 A. Sanchis, J.-P. Salvador and M.-P. Marco, *Colloids Surf., B*, 2019, **173**, 825–832.
- 92 Y. Diebold and M. Calonge, *Prog. Retinal Eye Res.*, 2010, **29**, 596–609.
- 93 P. Couvreur, *J. Controlled Release*, 2019, **311–312**, 319–321.
- 94 J. Chen, J. Liu, Y. Hu, Z. Tian and Y. Zhu, *Sci. Technol. Adv. Mater.*, 2019, **20**, 1043–1054.
- 95 R. S. Darweesh, N. M. Ayoub and S. Nazzal, *Int. J. Nanomed.*, 2019, **14**, 7643–7663.
- 96 L. Ruiz-Gatón, S. Espuelas, J. Huarte, E. Larrañeta, N. Martin-Arbella and J. M. Irache, *Int. J. Pharm.*, 2019, **571**, 118699.
- 97 A. D. Bangham and R. W. Horne, *J. Mol. Biol.*, 1964, **8**, 660–668.
- 98 R. W. Horne, A. D. Bangham and V. P. Whittaker, *Nature*, 1963, **200**, 1340.
- 99 V. Weissig, *Methods Mol. Biol.*, 2017, **1522**, 1–15.
- 100 G. Ricciuti, E. Finolezzi, S. Luciani, E. Ranucci, M. Federico, M. D. Nicola, I. A. L. Zecca and F. Angrilli, *Hematol. Oncol.*, 2018, **36**, 44–48.
- 101 S. Ambati, A. R. Ferarro, S. E. Kang, J. Lin, X. Lin, M. Momany, Z. A. Lewis and R. B. Meagher, *mSphere*, 2019, **4**(1), e00025-19.
- 102 N. Osborne, R. Catania, S. Stolnik-Trenkic, F. H. Falcone and K. Robinson, *Access Microbiol.*, 2019, **1**, 882.
- 103 B. Heurtault, P. Saulnier, J.-P. Benoit, J.-E. Proust, B. Pech and J. Richard, *US Pat.*, US8057823B2, 2011, <https://patents.google.com/patent/US8057823B2/en>.
- 104 B. Heurtault, P. Saulnier, B. Pech, J.-E. Proust and J.-P. Benoit, *Pharm. Res.*, 2002, **19**, 875–880.
- 105 B. Heurtault, P. Saulnier, B. Pech, J. E. Proust and J. P. Benoit, *Int. J. Pharm.*, 2002, **242**, 167–170.
- 106 B. Heurtault, P. Saulnier, B. Pech, M.-C. Venier-Julienne, J.-E. Proust, R. Phan-Tan-Luu and J.-P. Benoit, *Eur. J. Pharm. Sci.*, 2003, **18**, 55–61.
- 107 N. T. Huynh, C. Passirani, P. Saulnier and J. P. Benoit, *Int. J. Pharm.*, 2009, **379**, 201–209.
- 108 G. Howell, C. Oliai and G. Schiller, *Anticancer Res.*, 2018, **38**, 6927–6930.
- 109 J. E. Lancet, G. L. Uy, J. E. Cortes, L. F. Newell, T. L. Lin, E. K. Ritchie, R. K. Stuart, S. A. Strickland, D. Hogge, S. R. Solomon, R. M. Stone, D. L. Bixby, J. E. Kolitz, G. J. Schiller, M. J. Wieduwilt, D. H. Ryan, A. Hoering, K. Banerjee, M. Chiarella, A. C. Louie and B. C. Medeiros, *J. Clin. Oncol.*, 2018, **36**, 2684–2692.
- 110 A. Hamada, T. Kawaguchi and M. Nakano, *Clin. Pharmacokinet.*, 2002, **41**, 705–718.
- 111 B. Salehi, Z. Selamoglu, K. S. Mileski, R. Pezzani, M. Redaelli, W. C. Cho, F. Kobarfard, S. Rajabi, M. Martorell, P. Kumar, N. Martins, T. Subhra Santra and J. Sharifi-Rad, *Biomolecules*, 2019, **9**, 773.
- 112 M. C. Chamberlain, *J. Neuro-Oncol.*, 2012, **109**, 143–148.
- 113 Z. Amoozgar and Y. Yeo, *Wiley Interdiscip. Rev.: Nanomed. Nanobiotechnol.*, 2012, **4**, 219–233.
- 114 J. S. Suk, Q. Xu, N. Kim, J. Hanes and L. M. Ensign, *Adv. Drug Delivery Rev.*, 2016, **99**, 28–51.
- 115 S. Salmaso and P. Caliceti, *J. Drug Delivery*, 2013, 374252.
- 116 Y. A. Haggag, M. A. Osman, S. A. El-Gizawy, A. E. Goda, M. M. Shamloula, A. M. Faheem and P. A. McCarron, *Biomed. Pharmacother.*, 2018, **105**, 215–224.
- 117 D. A. Tomalia, *Prog. Polym. Sci.*, 2005, **30**, 294–324.
- 118 E. Vacas-Córdoba, M. Maly, F. J. De la Mata, R. Gómez, M. Pion and M. Á. Muñoz-Fernández, *Int. J. Nanomed.*, 2016, **11**, 1281–1294.
- 119 J. L. Jiménez, M. Pion, F. J. de la Mata, R. Gomez, E. Muñoz, M. Leal and M. A. Muñoz-Fernandez, *New J. Chem.*, 2012, **36**, 299–309.
- 120 E. Wiener, M. W. Brechbiel, H. Brothers, R. L. Magin, O. A. Gansow, D. A. Tomalia and P. C. Lauterbur, *Magn. Reson. Med.*, 1994, **31**, 1–8.
- 121 C. Kojima, B. Turkbey, M. Ogawa, M. Bernardo, C. A. S. Regino, L. H. Bryant, P. L. Choyke, K. Kono and H. Kobayashi, *Nanomedicine*, 2011, **7**, 1001–1008.
- 122 A. Szulc, M. Signorelli, A. Schiraldi, D. Appelhans, B. Voit, M. Bryszewska, B. Klajnert-Maculewicz and D. Fessas, *Int. J. Pharm.*, 2015, **495**, 940–947.
- 123 A. Szulc, L. Pulaski, D. Appelhans, B. Voit and B. Klajnert-Maculewicz, *Int. J. Pharm.*, 2016, **513**, 572–583.
- 124 B. Klajnert, D. Appelhans, H. Komber, N. Morgner, S. Schwarz, S. Richter, B. Brutschy, M. Ionov, A. K. Tonkikh, M. Bryszewska and B. Voit, *Chem.-Eur. J.*, 2008, **14**, 7030–7041.
- 125 A. Janaszewska, K. Mączyńska, G. Matuszko, D. Appelhans, B. Voit, B. Klajnert and M. Bryszewska, *New J. Chem.*, 2012, **36**, 428–437.
- 126 A. Janaszewska, B. Ziemba, K. Ciepluch, D. Appelhans, B. Voit, B. Klajnert and M. Bryszewska, *New J. Chem.*, 2012, **36**, 350–353.
- 127 M. Gorzkiewicz and B. Klajnert-Maculewicz, *Eur. J. Pharm. Biopharm.*, 2017, **114**, 43–56.
- 128 G. Herlem, F. Picaud, C. Girardet and O. Micheau, in *Nanocarriers for Drug Delivery*, ed. S. S. Mohapatra, S. Ranjan, N. Dasgupta, R. K. Mishra and S. Thomas, Elsevier, 2019, pp. 469–529.





- 129 M. Inagaki, F. Kang, M. Toyoda and H. Konno, in *Advanced Materials Science and Engineering of Carbon*, ed. M. Inagaki, F. Kang, M. Toyoda and H. Konno, Butterworth-Heinemann, Boston, 2014, pp. 15–40.
- 130 A. Guven, G. J. Villares, S. G. Hilsenbeck, A. Lewis, J. D. Landua, L. E. Dobrolecki, L. J. Wilson and M. T. Lewis, *Acta Biomater.*, 2017, **58**, 466–478.
- 131 A. Kazemi-Beydokhti, S. Zeinali Heris and M. R. Jaafari, *Chem. Eng. Res. Des.*, 2016, **112**, 56–63.
- 132 M. Zheng, A. Jagota, E. D. Semke, B. A. Diner, R. S. Mclean, S. R. Lustig, R. E. Richardson and N. G. Tassi, *Nat. Mater.*, 2003, **2**, 338–342.
- 133 H. Wang and A. Ceulemans, *Phys. Rev. B: Condens. Matter Mater. Phys.*, 2009, **79**, 195419.
- 134 K. Umemura, *Nanomaterials*, 2015, **5**, 321–350.
- 135 P. Zhang, W. Yi, J. Hou, S. Yoo, W. Jin and Q. Yang, *Int. J. Nanomed.*, 2018, **13**, 3069–3080.
- 136 Y. Ruan, W. Yu, F. Cheng, X. Zhang, T. Rao, Y. Xia and S. Larré, *IET Nanobiotechnol.*, 2011, **5**, 47–51.
- 137 H. Zhang, D. Yee and C. Wang, *Nanomedicine*, 2008, **3**, 83–91.
- 138 A. E. O'Connor, W. M. Gallagher and A. T. Byrne, *Photochem. Photobiol.*, 2009, **85**, 1053–1074.
- 139 M. Fang, M. Chen, L. Liu and Y. Li, *J. Biomed. Nanotechnol.*, 2017, **13**, 1–16.
- 140 S. Samimi, M. S. Ardestani and F. A. Dorkoosh, *J. Drug Delivery Sci. Technol.*, 2021, **61**, 102287.
- 141 U. Yunus, M. A. Zulfikar, M. Ajmal, M. H. Bhatti, G.-S. Chaudhry, T. S. T. Muhammad and Y. Y. Sung, *Biomed. Mater.*, 2020, **15**, 065004.
- 142 P. Ghosh, G. Han, M. De, C. K. Kim and V. M. Rotello, *Adv. Drug Delivery Rev.*, 2008, **60**, 1307–1315.
- 143 K. Pal, F. Al-suraih, R. Gonzalez-Rodriguez, S. K. Dutta, E. Wang, H. S. Kwak, T. R. Caulfield, J. L. Coffey and S. Bhattacharya, *Nanoscale*, 2017, **9**, 15622–15634.
- 144 S. Song, Y. Hao, X. Yang, P. Patra and J. Chen, *J. Nanosci. Nanotechnol.*, 2016, **16**, 2582–2586.
- 145 P. G. Jeelani, P. Mulay, R. Venkat and C. Ramalingam, *Silicon*, 2020, **12**, 1337–1354.
- 146 N. Syazaliyana Azali, N. Hidayatul Nazirah Kamarudin, A. Rasyidah Abdul Rahim, N. Syifa'a Jamal Nasir, S. Najiha Timmiati and N. Farhana Jaafar, *Mater. Today: Proc.*, 2019, **19**, 1722–1729.
- 147 P. Sangaiya and R. Jayaprakash, *J. Supercond. Novel Magn.*, 2018, **31**, 3397–3413.
- 148 L. Shen, B. Li and Y. Qiao, *Materials*, 2018, **11**, 324.
- 149 N. Shahabadi, M. Falsafi and K. Mansouri, *Colloids Surf., B*, 2016, **141**, 213–222.
- 150 H. Li, M. Eddaoudi, M. O'Keeffe and O. M. Yaghi, *Nature*, 1999, **402**, 276–279.
- 151 J. R. Long and O. M. Yaghi, *Chem. Soc. Rev.*, 2009, **38**, 1213–1214.
- 152 H. Kumagai, C. J. Kepert and M. Kurmoo, *Inorg. Chem.*, 2002, **41**, 3410–3422.
- 153 O. M. Yaghi, H. Li and T. L. Groy, *J. Am. Chem. Soc.*, 1996, **118**, 9096–9101.
- 154 D. Bradshaw, J. B. Claridge, E. J. Cussen, T. J. Prior and M. J. Rosseinsky, *Acc. Chem. Res.*, 2005, **38**, 273–282.
- 155 V. Rodriguez-Ruiz, A. Maksimenko, R. Anand, S. Monti, V. Agostoni, P. Couvreur, M. Lampropoulou, K. Yannakopoulou and R. Gref, *J. Drug Targeting*, 2015, **23**, 759–767.
- 156 M. Celano, M. G. Calvagno, S. Bulotta, D. Paolino, F. Arturi, D. Rotiroti, S. Filetti, M. Fresta and D. Russo, *BMC Cancer*, 2004, **4**, 63.
- 157 P. Li, S. Luo, L. Xiao, B. Tian, L. Wang, Z. Zhang and Y. Zeng, *Acta Pharmacol. Sin.*, 2019, **40**, 1448–1456.
- 158 T. Briot, E. Roger, N. Lautram, A. Verger, A. Clavreul and F. Lagarce, *Int. J. Nanomed.*, 2017, **12**, 8427–8442.
- 159 J. Katsaras and T. Gutberlet, *Lipid Bilayers: Structure and Interactions*, Springer-Verlag, Berlin Heidelberg, 2001.
- 160 K. Ariga, J. P. Hill, M. V. Lee, A. Vinu, R. Charvet and S. Acharya, *Sci. Technol. Adv. Mater.*, 2008, **9**, 014109.
- 161 S. Sivakova and S. J. Rowan, *Chem. Soc. Rev.*, 2005, **34**, 9–21.
- 162 E. Lepeltier, C. Bourgaux, V. Rosilio, J. H. Poupaert, F. Meneau, F. Zouhiri, S. Lepêtre-Mouelhi, D. Desmaële and P. Couvreur, *Langmuir*, 2013, **29**, 14795–14803.
- 163 X. Gong, M. J. Moghaddam, S. M. Sagnella, C. E. Conn, S. J. Danon, L. J. Waddington and C. J. Drummond, *Colloids Surf., B*, 2011, **85**, 349–359.
- 164 S. M. Sagnella, X. Gong, M. J. Moghaddam, C. E. Conn, K. Kimpton, L. J. Waddington, I. Krodkiewska and C. J. Drummond, *Nanoscale*, 2011, **3**, 919–924.
- 165 L. Wu, F. Zhang, X. Chen, J. Wan, Y. Wang, T. Li and H. Wang, *ACS Appl. Mater. Interfaces*, 2020, **12**, 3327–3340.
- 166 A. Maksimenko, J. Caron, J. Mougin, D. Desmaële and P. Couvreur, *Int. J. Pharm.*, 2015, **482**, 38–46.
- 167 D. Wang, B. Liu, Y. Ma, C. Wu, Q. Mou, R. Wang, D. Yan, C. Zhang and X. Zhu, *J. Am. Chem. Soc.*, 2017, **139**(40), 14021–14024.
- 168 D. Lombardo, M. A. Kiselev, S. Magazù and P. Calandra, *Adv. Condens. Matter Phys.*, 2015, **2015**, 1–22.
- 169 B. Xie, J. Wan, X. Chen, W. Han and H. Wang, *Mol. Cancer Ther.*, 2020, **19**, 822–834.
- 170 H. Wang, Z. Lu, L. Wang, T. Guo, J. Wu, J. Wan, L. Zhou, H. Li, Z. Li, D. Jiang, P. Song, H. Xie, L. Zhou, X. Xu and S. Zheng, *Cancer Res.*, 2017, **77**, 6963–6974.
- 171 L. Bildstein, C. Dubernet, V. Marsaud, H. Chacun, V. Nicolas, C. Gueutin, A. Sarasin, H. Bénéch, S. Lepêtre-Mouelhi, D. Desmaële and P. Couvreur, *J. Controlled Release*, 2010, **147**, 163–170.
- 172 B. Pili, C. Bourgaux, H. Amenitsch, G. Keller, S. Lepêtre-Mouelhi, D. Desmaële, P. Couvreur and M. Ollivon, *Biochim. Biophys. Acta, Biomembr.*, 2010, **1798**, 1522–1532.
- 173 V. Allain, C. Bourgaux and P. Couvreur, *Nucleic Acids Res.*, 2012, **40**, 1891–1903.
- 174 L. Bildstein, V. Marsaud, H. Chacun, S. Lepêtre-Mouelhi, D. Desmaële, P. Couvreur and C. Dubernet, *Soft Matter*, 2010, **6**, 5570–5580.
- 175 L. H. Reddy, C. Dubernet, S. L. Mouelhi, P. E. Marque, D. Desmaële and P. Couvreur, *J. Controlled Release*, 2007, **124**, 20–27.



- 176 X. Mulet, T. Kaasgaard, C. E. Conn, L. J. Waddington, D. F. Kennedy, A. Weerawardena and C. J. Drummond, *Langmuir*, 2010, **26**, 18415–18423.
- 177 A. Maksimenko, J. Mougin, S. Mura, E. Sliwinski, E. Lepeltier, C. Bourgaux, S. Lepêtre, F. Zouhiri, D. Desmaële and P. Couvreur, *Cancer Lett.*, 2013, **334**, 346–353.
- 178 J. N. Israelachvili and D. J. Mitchell, *Biochim. Biophys. Acta, Biomembr.*, 1975, **389**, 13–19.





## 4. Nanomedicines: a developing prospective for MDS and AML

Owing to the enhanced permeability and retention (EPR) phenomena that occurs in solid tumors (the mechanism by which high-molecular weight drugs, prodrugs and nanovectors accumulate in tissues, due to an increased vascularization, wide fenestrations and a reduced lymphatic drainage), there is a flood of nanomedicines focusing on taking advantage of this phenomena, with an increased buildup of nanoparticles in the tumoral microenvironment and thus enhanced efficacy<sup>162</sup>.

However, in the case of leukemias and lymphomas, cancers in which the EPR effect does not play a role, the paradigm has to be thought differently, with inventive approaches for the treatment of liquid tumors.

Nanoparticles allow for the selective transport of anticancer agents to the cancerous cells with a decreased side effect on the healthy unaffected cells, thus reducing systemic toxicity, allowing for the drug loaded nanoparticle to access tissues that were previously challenging for traditional drugs to reach, such as the bone marrow and lymph nodes. Various research efforts are embracing this advantage to develop new treatments for MDS and AML.

Indeed, a study on self-assembling alendronate-conjugated bone-targeting nanoparticles (BTNPs) showed a co-delivery of decitabine and arsenic trioxide for treating MDS. The study demonstrated an increased circulation time to 3 days, when previously these drugs needed to be administered on daily basis due to their short half-life. Additionally, when compared to the unvectorized drugs, these drug loaded nanoparticles had at least a 6.7 times increased accumulation in the bone marrow<sup>163</sup>.

Another study compared the efficacy of arsenic trisulfide to arsenic trisulfide inorganic nanoparticles on MUTZ-1 MDS cell line. They showed a 2 to 3-fold increase in inhibition (IC<sub>50</sub>), a 1.5 to 2-fold increase in apoptosis and a significant increase in cell cycle arrest, at different concentrations with a  $p < 0.01$  in all the studies, showing that the drug loaded nanoparticles were more powerful than its free one<sup>164</sup>.

A recent clinical trial is in phase I/II as a monotherapy or in combination for treatment of MDS and AML patients<sup>165</sup> on AZD 2811 nanoparticle: polylactic acid polymeric matrix with PEG stealth layer that encapsulates barasertib, a potent and selective inhibitor of aurora B kinase. This trial follows the success of the preclinical studies that showed that these nanoparticles could overcome the venetoclax resistance in TP53-mutant AML *in vitro* and *in vivo*<sup>166</sup>.

Another example of a promising nanomedicine is CPX-351 (VYXEOS™), a liposomal formulation of cytarabine and daunorubicin, which generated promising results in phase III clinical trials for

the treatment of high-risk AML. Indeed, CPX-351 significantly improved overall survival, response rates, event-free survival, in comparison with the standard regimen of cytarabine and daunorubicin. Additionally, overall survival (OS) was of 16.1 months compared to 6 months with the standard drugs (Identifier: NCT02286726)<sup>167,168</sup>.

## 5. The nanoparticle enhanced: self-assembling prodrugs

Due to the limitations of traditional drugs, the use of prodrugs to solve these issues is the next clear step. The parent drug is conjugated to another molecule that can be a targeting molecule or another drug that synergizes with it, allowing to resolve problems such as chemical instability, poor water solubility, severe toxicity or low permeability. Another approach to solve these limitations is the use of nanoparticles as drug delivery systems, with their ability to improve drug availability, to prolong systemic circulation time, to increase tumor accumulation, and to spatiotemporally control drug release<sup>169-173</sup>.

Prodrugs are molecules that are activated upon being metabolized near the targeting tissue, thus releasing the drug at the targeted site, with more specificity and reduced impact on normal tissues. Prodrugs are generally made up of three parts, with an optional fourth that is aimed to increase the targetability and specificity of the prodrug. The main therapeutic agent is the first part of the prodrug, followed by the chemical linker which binds the therapeutic agent to the rest of the prodrug, and finally a promoiety that can be a polymer, a hydrocarbon chain or another drug that synergizes with the main therapeutic agent. The goal behind prodrugs is to increase solubility in water or diffusion through the cell membrane, chemical stability, drug absorption and mainly pre-systemic metabolism. The third part of the prodrugs, the promoiety, allows the targeting of peptide transporters, antigens and enzymes that are highly present in the desired tissue<sup>171,172,174,175</sup>. A selection of prodrugs is presented in **Figure 10**. Still, prodrugs are not without faults, such as the presence of esterases in cancer microenvironment that expedites the process of their degradation, in the case of an ester bound prodrug. Subsequently, prodrugs are by no means a miracle solution and they need further innovation to achieve their full potential. A study aiming to improve paclitaxel, a well-known chemotherapeutic agent that has poor aqueous solubility and thus is formulated in Cremophor EL (CrEL) and ethanol, causing severe side effects due to these excipients. A prodrug of paclitaxel was synthesized with a DHA link, leading to a decrease in excipients needed to 15% of the original formulation, thus increasing the maximum tolerated dose by 4 folds as the toxicity decreased, with an improved antitumor activity leading this prodrug to enter clinical trials<sup>176,177</sup>.

Another study was done on doxorubicin, another famous anti-cancer agent with various side effects on healthy tissues due to a lack of specificity. They conjugated this drug to linolenic acid: the obtained prodrug had a 2-fold increase in tumor accumulation, with less side effects to healthy tissues, mainly to the heart with a 60% decrease of accumulation in that organ. Additionally, owing to the pH-sensitive nature of the linker, most of the drug was released around the tumor thus enhancing its efficacy. A continuation of this study showed that DHA allowed an increased intratumoral drug release. Thus, this prodrug was able to double the survival and halve the weight loss in leukemic mice models<sup>178,179</sup>.

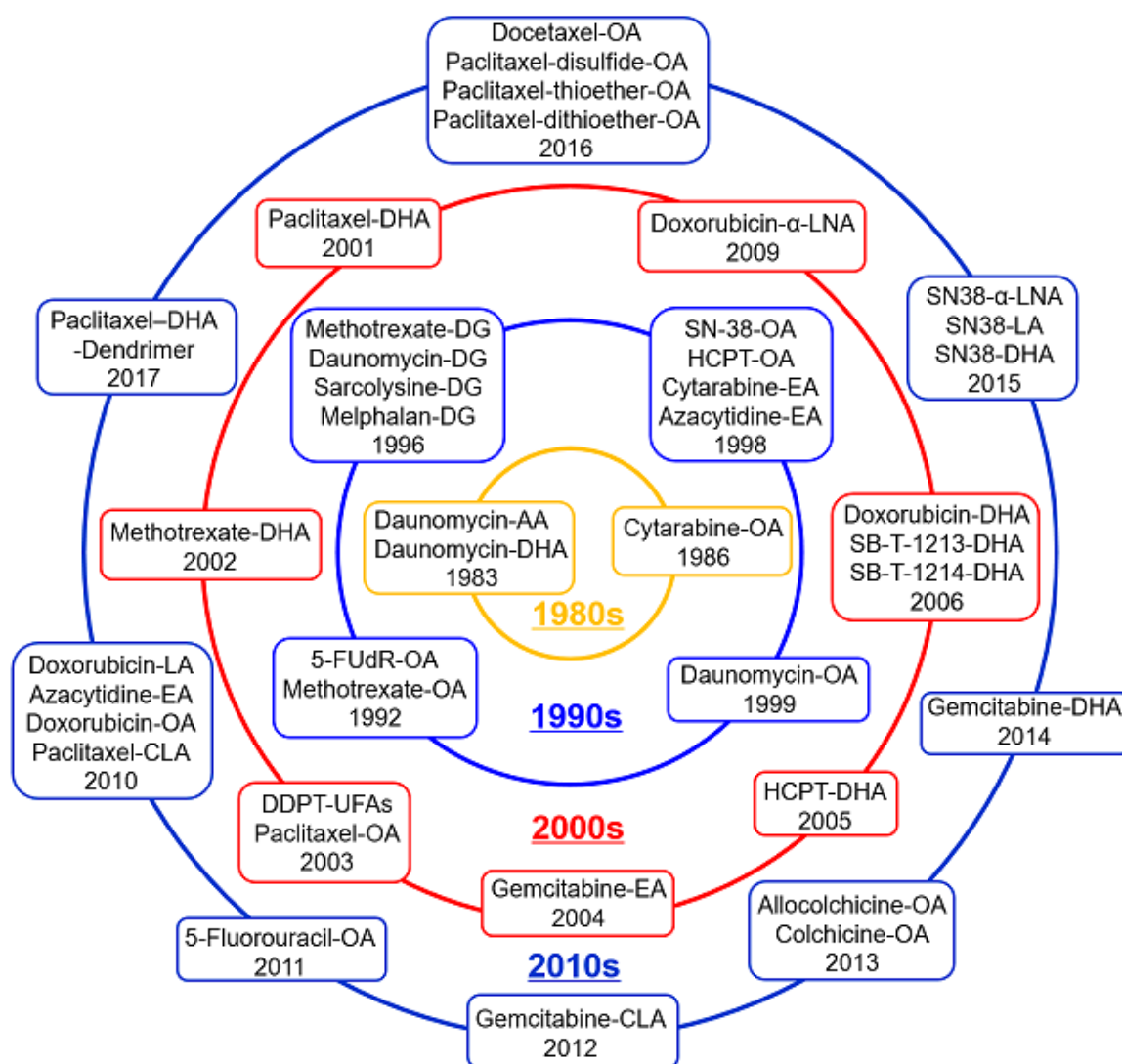


**Figure 10: The decennary progress of anti-cancer unsaturated fatty acid prodrugs.** OA: oleic acid; CLA: conjugated linoleic acid; LA: lactic acid; EA: elaidic acid; LNA: linolenic acid; AA: arachidonic acid; DG: Dioleoylglycerol. Sun et al., 2017<sup>180</sup>.

Nanomedicines are extremely small-sized objects with a diameter below the micrometer, with the ability to act as a vehicle for therapeutic molecules. The advancement in this field occurred over several generations with liposomes, micelles and polymer nanoparticles being introduced in the first generation, bringing the ability to enhanced intracellular delivery, but lacking in specificity and being highly susceptible to opsonization by macrophages and liver accumulation. The second generation was ushered by the addition of polyethylene glycol (PEG), a hydrophilic shield, allowing a passive blood circulation and an enhanced permeability and retention (EPR) effect, leading to a passive accumulation in solid cancer tumors. The stealth ability heralded the third generation of nanomedicines upon the surface decoration by a molecule of interest, such as an antibody, allowing an active targeting. The current fourth generation has even more advanced functionalities such as a drug controlled release in a specific environment in answering to local stimuli, or to signaling pathways.

There exist multiple plausible classifications for nanomedicines whether by size, shape or other characteristics. Though perhaps the most agreed upon one is by excipient nature: organic nanoparticles with for instance liposomes or polymeric micelles, inorganic nanoparticles covering quantum dots and carbon nanotubes, and finally metal-organic framework nanoparticles (MOFs)<sup>181–184</sup>.

An example of study to perfectly illustrate how nanomedicines can be probative: this study aimed at evaluating the advantages of drug encapsulation by polymeric nanoparticles. A fluorouracil polymeric nanoparticle was formulated, this 180 nm spanning vehicle allowed for a sustained agent release over the period of 7 days. Additionally, an improved anticancer effect was observed when compared to the free drug. This formulation also had reduced side effects on normal tissue after histopathological studies on the kidney and liver tissues<sup>185</sup>.

## **5.1. Self-assembly and PUFylation**

Nanomedicines are indeed capable of solving several of the difficulties faced by traditional drugs including drug transport and rapid degradation. However, being acting merely as a vehicle, it leads to several drawbacks including undesired drug release, low drug loading levels, not to mention the toxicity of the excipients used in the nanoparticle formulation. Thus, the next evolution in this field arrived by combining prodrugs and nanoparticles together in prodrug-based self-assemblies. These novel nanomedicines are capable of exploiting intermolecular forces and non-covalent interactions (such as hydrogen bonding, metal coordination, hydrophobic interactions, van der Waals forces or  $\pi$ - $\pi$  stacking) to naturally self-assemble in aqueous media into supramolecular assemblies. Accordingly, the self-assembly functionality will depend on various aspects as stability, shape, size, surface charge, viscosity, and surface morphology that

will dictate their cellular internalization, diffusion and pharmacological activity. The prodrug-based self-assemblies improved drastically the drug loading, while decreasing toxicity as the prodrugs are the only constituent of the nanoparticle with no additional excipient<sup>186-190</sup>.

The Israechvili's model presented in the 1970s allows to predict the supramolecular structure of the self-assemblies to be formed, by considering the volume and length of the fatty acid chain, and the surface area of the hydrophilic head<sup>191</sup>.

An example on this concept arises from a study where paclitaxel was conjugated to oleic acid by the means of several types of chemical bonds. It was shown that the formed prodrugs succeeded in self-assembling into nanoparticles with a high drug loading capacity (at least 55%) and, when compared to paclitaxel, these self-assemblies demonstrated improved cellular uptake, tumor buildup and pharmacokinetics<sup>192,193</sup>.

Another study described the conjugation of doxorubicin to mixed PUFAs: it showed a significantly increased drug loading with considerably improved cytotoxicity results *in vitro*, when compared to free doxorubicin or its liposome encapsulated format<sup>194</sup>.

PUFylation can be considered as a subtype of self-assembly, where the promoiety conjugated to the drug of interest is a poly-unsaturated fatty acid. It is usually done with a hydrophilic drug to produce an amphiphilic prodrug, thus improving the parent drug cellular internalization. Moreover, the PUFAs are relatively cheap easily obtained molecules, with high interaction ability due to the double bond presence lending the self-assemblies increased stability.

In that context, in a series of studies performed by Prof. Couvreur and his team, squalenic acid was conjugated with gemcitabine, resulting in 120 nm self-assembled nanoparticles with an inverse hexagonal supramolecular structure. These assemblies had enhanced biological activities in comparison to gemcitabine alone: for instance, it showed superior results to that of gemcitabine both *in vivo* and *in vitro* models of leukemia. These results were attributed to the shape of the self-assembly that was able to guard the gemcitabine from the action of deaminases thus reducing their degradation. Moreover, this self-assembly allowed an improved cell internalization, the cell membrane acting as a gemcitabine reservoir<sup>195-198</sup>.

## **5.2. Cell membrane interactions and nanoparticle entry into cells**

Upon arrival of the nanoparticles to the cellular membrane, they interact with the different components present there, allowing their entry into the cell using different pathways but mainly through endocytosis. Endocytosis will then lead the formed invagination to pinch off thus forming

vesicles that are then transported into sorting compartments. There are 5 different forms of endocytosis, and other endocytosis independent mechanisms: **Figure 11**.

The five main mechanisms of endocytosis are: phagocytosis, clathrin-mediated endocytosis, caveolin-mediated endocytosis, clathrin/caveolae-independent endocytosis, and macropinocytosis. Some debate exist that last four mechanisms are subtypes of the pinocytosis, compared to phagocytosis, that occurs in professional phagocytes, pinocytotic mechanisms may exist in several cells<sup>199</sup>.

### 5.2.1. Phagocytosis

Specialized phagocytes, belonging to the immune system ranks, are responsible for this process (dendritic cells, neutrophils, macrophages and monocytes). Fibroblasts, epithelial, and endothelial cells also exhibit this ability but in a reduced manner. This leads to a debate on whether to consider phagocytosis an endocytosis mechanism or a separate specialized mechanism.

Opsonins including antibodies and complement proteins initiate this process, as they attach to the nanoparticles, these opsonins then interact with the cellular membrane receptors. This interaction jump starts signaling pathways leading to the accumulation of actin that will form invaginations followed by phagosome formation. It has been observed that particles over the size of 200 nm are more prone to this process.

Long PEG chains are able to impart a stealth ability to nanoparticles, as these chains are able to ward off these opsonins, thus increasing the half-life of the nanoparticles. Doxil®, the first approved anti-cancer liposome, employs this technology thus enhancing the efficacy of the encapsulated doxorubicin<sup>200-203</sup>.

### 5.2.2. Clathrin-mediated endocytosis

This is usually the method by which cells obtain several of their nutrients and can be used to internalize the nanoparticles: clathrin-rich areas of the cell membrane will form an assembly unit termed the “tri-skeleton” unit that will then lead to 100 nm vesicle budding, that are then transferred to be sorted. Though, most of these vesicles end up as lysosomes, which will degrade non-resistant nanoparticles<sup>204,205</sup>.

### 5.2.3. Caveolae-dependent endocytosis

Cell signaling, regulation of membrane proteins, lipids and fatty acids are some of the chores of this process. Caveolae are flask-shaped invaginations present in cellular membranes of epithelial and non-epithelial cells. These flasks range in size between 50 to 80 nm with a lining of the caveolin protein that gives these flasks their unique shape, though caveolin will work with other

proteins to allow the final formation and budding of the forming vesicles. Conversely to clathrin-mediated endocytosis, this internalization pathway is non-lysosomal and will not damage the nanoparticles, a fortunate event for Abraxane®, a paclitaxel nanoparticle that has been observed to utilize this pathway heavily<sup>206–208</sup>.

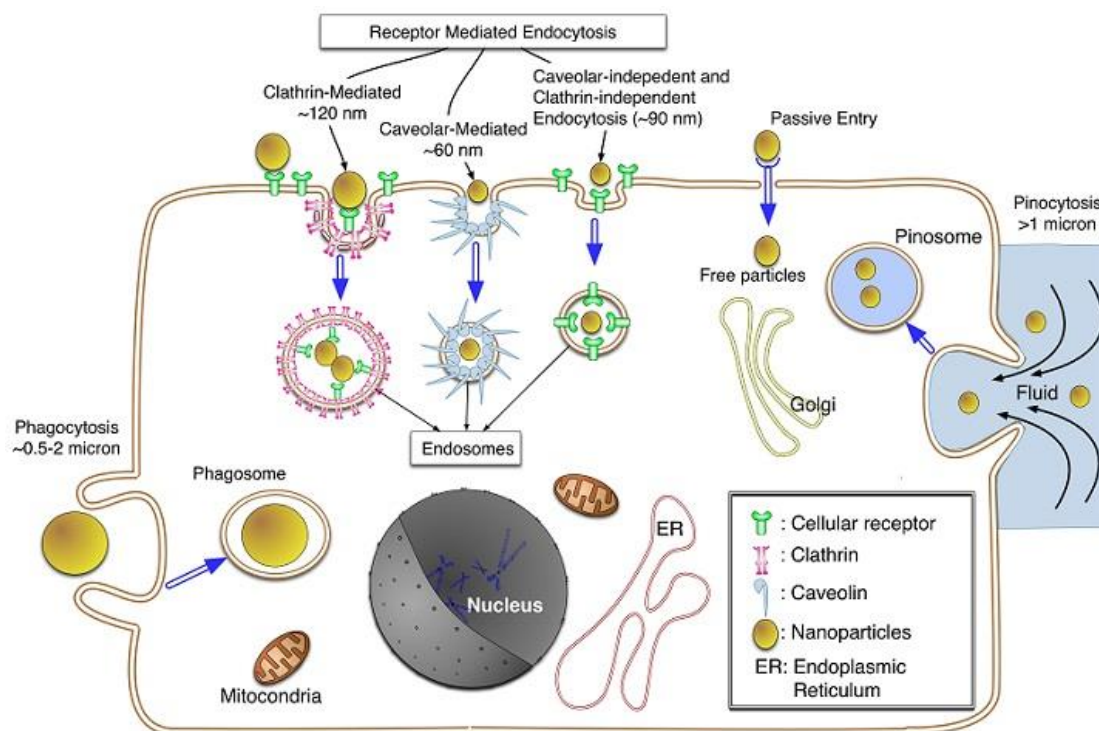


**Figure 11: Cell internalization pathways of nanoparticles<sup>209</sup>.**

#### 5.2.4. Clathrin/caveolae independent endocytosis

This pathway is active in cells that don't possess clathrin or caveolae and is used in the uptake of growth hormones and specific interleukins. The presence of some fatty acids seems essential for this uptake, allowing reasonably for hypothesizing that fatty acid based self-assembly can rely on this pathway, though it might be limited as well to the cells that are forced to bide by it<sup>210,211</sup>.

#### 5.2.5. Macropinocytosis

This process does not require pit/flask formation nor any aid from the lipid rafts. Simply, owing to the reorganization of the cytoskeleton, large membrane extensions appear from one side and then attach back to the cell membrane thus creating a large trap or vesicle that can reach 5  $\mu\text{m}$  in diameter. This process is unspecific and will uptake other molecules in the vicinity. Due to its large size, this pathway seems favorable to large nanoparticles that won't fit in the previously described processes<sup>212,213</sup>.

#### 5.2.6. Other possible pathways

It has been proposed by some researchers that other mechanisms would allow the entry of nanoparticles into cells. Indeed, a study revealed that specific quantum dots managed to pass through the RBCs membrane, via passive penetration, arguing that the zwitterionic nature of this quantum dot lead to softening of the lipid bilayer and the entry of these nanoparticles, without damaging the cell<sup>214</sup>.

Considering the points raised about MDS and its treatment, the failings and promises of azacitidine, the ripe opportunities contained within the use of omega-3 fatty acids, the review covering prodrug approach and its importance, it is possible to enhance azacitidine by turning it to a prodrug by conjugating it to fatty acid. Then taking it a step further by utilizing the self-assembly approach that was discussed from the angle of PUFAylation, to finally achieve the formulation of azacitidine that will allow to reach its full therapeutic potential.



## 6. Aims of this project

5-azacitidine, a cytidine analogue and a hypomethylating agent, is one of the main drugs being used for the treatment of myelodysplastic syndromes. However, after administration, it exhibits several limitations including restricted diffusion and cellular internalization due to its hydrophilicity, and a rapid enzymatic degradation. Our objective is to improve the cell internalization and to protect the drug from metabolic degradation via the formulation of an amphiphilic prodrug and its formulation into self-assemblies, thus gaining the advantages carried by prodrugs when compared to the parent molecule, also those of the self-assembly systems, with possibly gaining the synergistic effect to battle cancers that has been reported to be present in omega-3 fatty acids. Following the conjugation of the omega-3 fatty acid to the azacitidine, the obtained prodrug will be formulated by nanoprecipitation in self-assemblies (**Figure 12**), thus protecting the active molecule from enzymatic degradation. Additionally, this prodrug should be cleaved by cathepsin B, an enzyme overexpressed in cancerous cells, thus increasing the specificity of the drug.

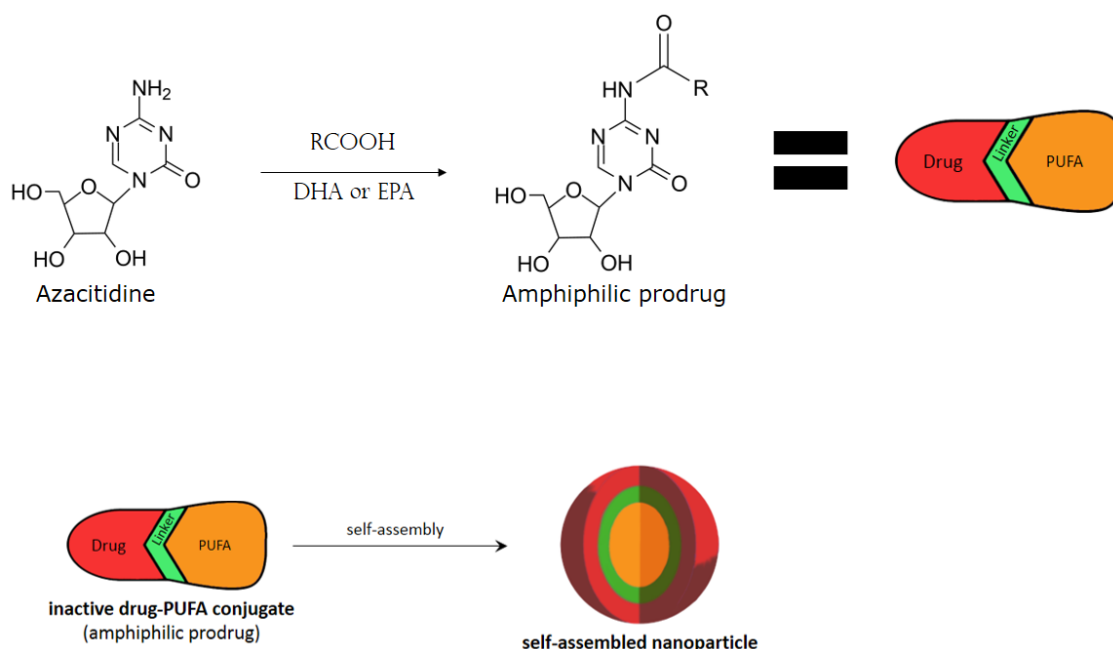


**Figure 12: Synthesis and formulation approaches for the development of an inventive platform for azacitidine administration.**

This project is divided into three sections, the first will be discussing the prodrug aspect of this project, discussing and describing the two different chemical approaches that were used to synthesize the final prodrug, followed by the chemical verification and characterization methods utilized to ensure that the correct prodrugs have been obtained. The second section will be focused on the formulation of the nanoparticles, using nanoprecipitation to achieve the self-

assembly (more accurately via subtype termed PUFAylation) of the amphiphilic prodrug, as well as the characterization of the obtained nano-objects. The last part will contain the initial biological studies performed on a human leukemia cell line (HL-60) to access the biological efficacy and cell internalization of the obtained self-assemblies.

## Chapter 2: Prodrug synthesis and self-assembly

This section aims to introduce the prodrug synthesis pathways to obtain the azacitidine –omega 3 fatty acid conjugates, using the two fatty acids presented in the state of the art section: docosahexaenoic acid (DHA) and eicosapentaenoic acid (EPA). After the successful synthesis of the prodrugs, the nanoprecipitation process was used to obtain the self-assemblies of these prodrugs and their characterization was performed.

The first year of research was focused on the optimization of a synthesis pathway that has already been used by Prof. Couvreur's team for the conjugation of nucleic acids and their derivatives to the squalene<sup>215</sup>. It is based on protecting the OH groups of azacitidine prior to conjugating the fatty acid, followed by deprotecting the OH groups of the formed conjugate to finally obtain the prodrug. Following the failure of conjugation after several optimization attempts due to the hindered reactivity of the amine group of azacitidine, several conjugating agents were tested to determine the suitable conjugation agent that would allow a successful conjugation with azacitidine.

Thus, the second year of researchs was focused on using the selected ethyl chloroformate to obtain the prodrugs, using the same protected conjugation technique previously described. Following the deprotection, the prodrug was finally obtained but numerous attempts to purify it using silica gel column chromatography were unsuccessful due to the close polarity of the final byproducts obtained.

During the last year of research, a direct conjugation method was tested and the desired prodrugs were successfully obtained and purified using a semi-preparative reversed phase high-performance liquid chromatography (RP-HPLC).

Then, the nanoprecipitation of both amphiphilic prodrugs produced the desired self-assemblies, and their physico-chemical parameters were characterized.

These steps will be described in the following chapter: the failures and the success of the organic synthesis will be first presented, to finish with an article submitted in *Pharmaceuticals*.

## 1. The three-step approach for prodrug synthesis

Nucleosides and their analogues are a staple drug that is still being used as a chemotherapeutic agent in the fight against various types of cancer, few of these drugs worth mentioning are: floxuridine cytarabine, gemcitabine and azacitidine. Although widely used, these molecules face severe limitations as a weak efficacy due to a restricted cellular internalization because of their hydrophilicity and a rapid enzymatic degradation by deaminases<sup>216–218</sup>, and severe side effects due to the absence of cancer cell selectivity.

The process of conjugating fatty acids to nucleosides and their analogues in order to combat such shortcomings is a well investigated one. Indeed, this process has been pioneered by Prof. Couvreur and his team, with the use of squalene and its derivatives that were conjugated to different nucleoside analogs in a process termed "Squalenoylation". This method was reproduced with other fatty acids mainly poly-unsaturated ones, and termed "PUFAylation"<sup>219–223</sup>.

Various nucleosides have undergone PUFAylation process to obtain prodrugs conjugated at 4-(N)-position: a linoleic acid-gemcitabine conjugate (LA-Gem) and a squalenoyl-gemcitabine (SQdFdC) are two prime examples<sup>221,222</sup>, allowing the protection of the parent drugs from the action of deaminases, increasing the lipophilicity of the conjugate to improve cell penetration, and conferring a specificity via a prodrug bond cleaved by an enzyme overexpressed in cancer cells. Yet, similar studies on azacitidine are absent, and few studies have performed the conjugation of azacitidine on the OH groups of the sugar ring, by the means of ester bonds<sup>224–226</sup>. Such approaches fail to protect azacitidine from deamination, the main reason that impacts its circulation time and decreases its biological efficacy.

Consequently, this study aims to conjugate chosen polyunsaturated fatty acids to azacitidine 4-(N)-position, to protect it from deamination and utilize the overexpression of the cathepsin-B enzyme by MDS and AML to increase its specificity to cancer cells<sup>227,228</sup>. To this end, a 3-step synthesis was adapted from P. Couvreur's team<sup>215,229</sup> (**Figure 13**).

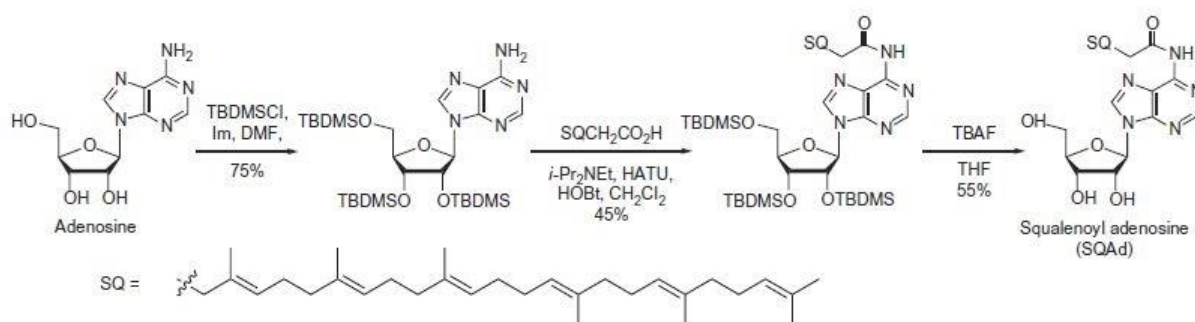


**Figure 13: Synthesis of the squalenoyl adenosine conjugate.** Adapted from Gaudin *et al.*, 2014<sup>215</sup>.

## 1.1. Overview of the 3-step synthesis process

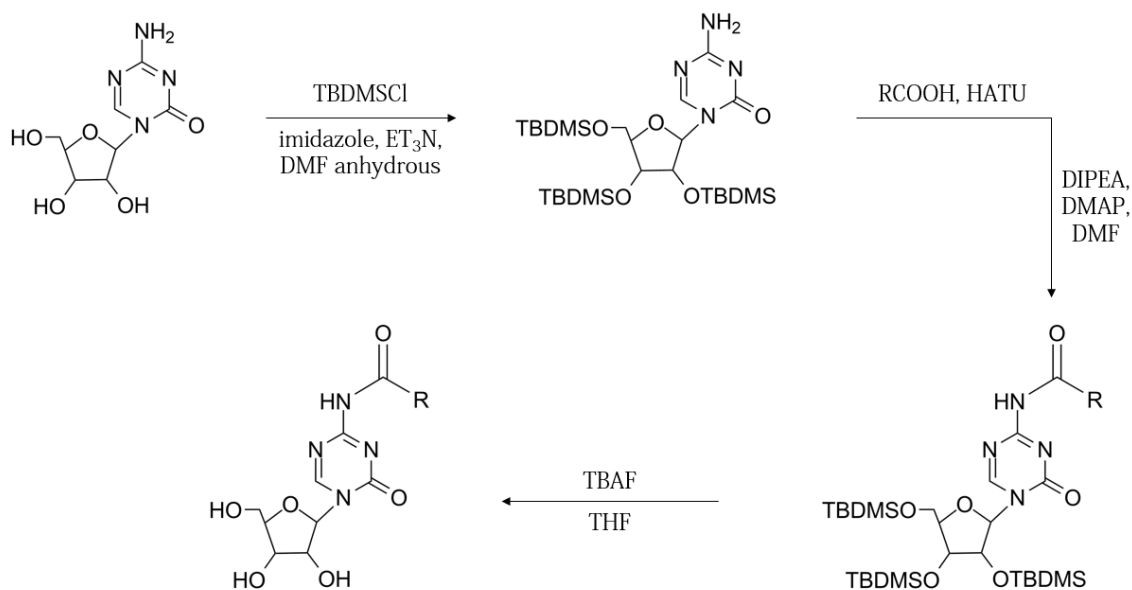


**Figure 14: The 3-step synthesis pathway for the synthesis of azacitidine-fatty acid conjugates.**

Aiming to conjugate DHA and EPA to azacitidine at its amine group (4-(N)-position), a 3-step synthesis was followed (**Figure 14**).

To start, the highly reactive alcohols groups of the sugar ring must first be protected by the action of a silylating agent, TBDMSCl (tert-Butyldimethylsilyl chloride) in this case.  $\text{Et}_3\text{N}$  (triethylamine) is used to catalyze the reaction via the deprotonation of the alcohol groups and to neutralize the acid released in the process, and imidazole used as a nucleophile that reacts with TBDMSCl to form a more reactive intermediate, that reacts with OH group readily.

Following that, an amide conjugation will allow the desired fatty acids to be linked to azacitidine, by the action of a conjugating agent called HATU (Hexafluorophosphate Azabenzotriazole Tetramethyl Uronium). This reaction was performed in the presence of DMAP (4-dimethylaminopyridine) to produce an activated ester from the fatty acids, and Hünig's base DIPEA (N, N-Diisopropylethylamine), commonly used in amide coupling, a hindered base that does not compete with the nucleophilic amine in the coupling reaction between a carboxylic acid and a nucleophilic amine.

Finally, the protection groups of the obtained silylated prodrug were removed using TBAF (tetra-n-butylammonium fluoride), a commonly utilized deprotecting agent.

As previously discussed, azacitidine is highly susceptible to hydrolysis. Therefore, all the solvents were purchased in their anhydrous form. Additionally, all the reactions were conducted in 3-necked reactors under an argon flow (**Figure 15**). The reactants were injected through the silicon septums using a glass needle, all glassware were oven dried prior to use.

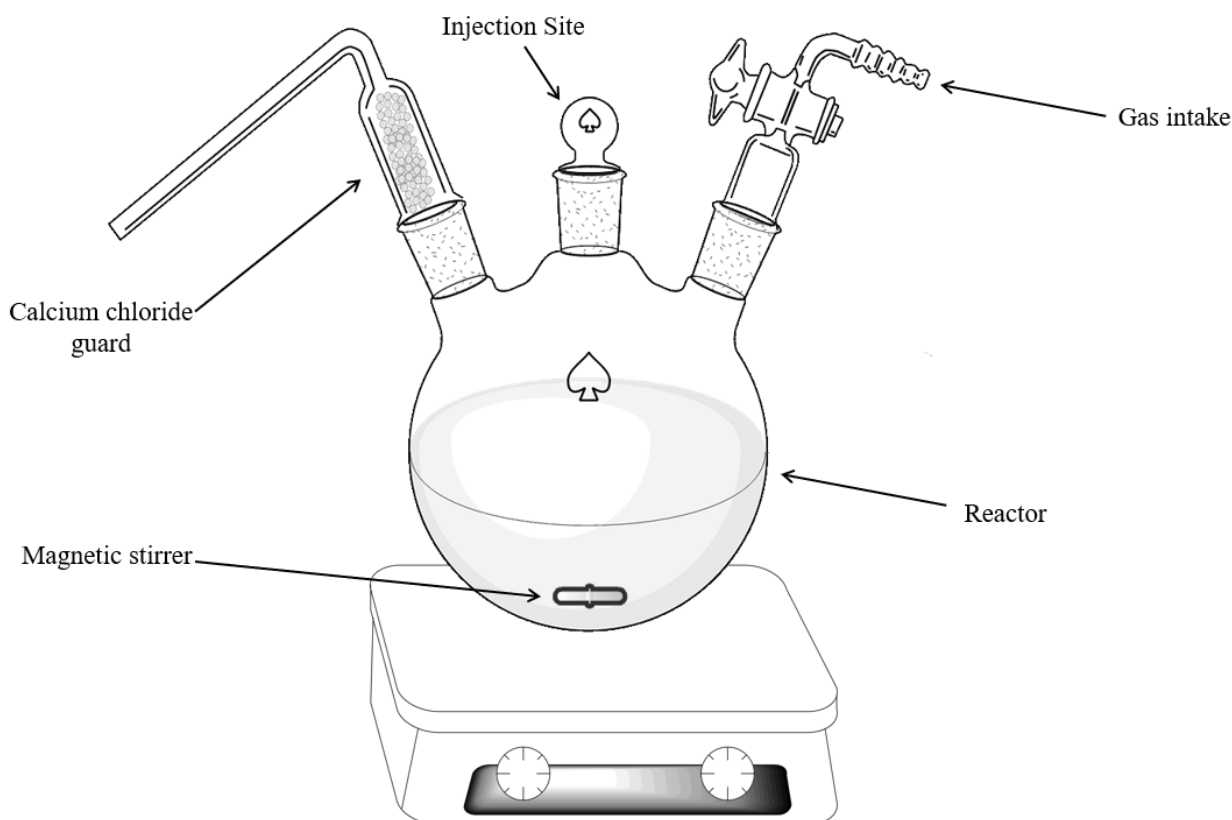


**Figure 15: Experimental setup under inert conditions** used in all reactions involving azacitidine.

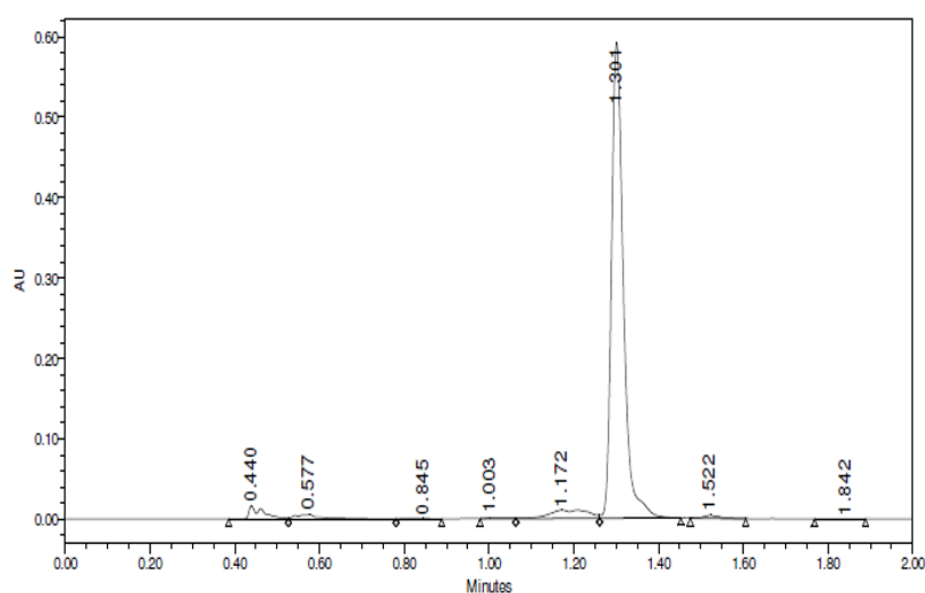
## 1.2. Protection of azacitidine

To a solution of imidazole (15 equivalents) and tert-butyldimethylsilyl chloride (TBDMSCl, 12 equivalents) in anhydrous DMF (15 mL), stirred for 30 min, 5-azacitidine (250 mg) in anhydrous DMF (20 mL) was added drop-wise, followed by the drop-wise addition of trimethylamine (5 equivalents) in anhydrous DMF (8 mL). The mixture was left to react at room temperature for 72 hours. The whole reaction was conducted under argon. The mixture was then concentrated using a rotary evaporator. The crude product was then purified by silica gel chromatography eluting with 4% methanol in dichloromethane to give pure 4-amino-1-(3,4-bis((tert-butyldimethylsilyl)oxy)-5-(((tert-butyldimethylsilyl)oxy)methyl)tetrahydrofuran-2-yl)-1,3,5-triazin-2(1H)-on (tris-O-silylated azacitidine) as a colorless oil (565mg, yield 94%, purity 90%).  $^1\text{H}$  NMR (499 MHz, DMSO- $d_6$ )  $\delta$  8.46 (s, 1H), 7.61 – 7.53 (m, 2H), 5.69 (d,  $J$  = 3.8 Hz, 1H),



4.30 (t,  $J = 4.1$  Hz, 1H), 4.14 (t,  $J = 4.5$  Hz, 1H), 3.95 (q,  $J = 4.2, 3.7$  Hz, 2H), 3.75 – 3.71 (m, 1H), 0.91 (s, 9H), 0.88 (s, 9H), 0.85 (d,  $J = 3.1$  Hz, 9H), 0.14 – 0.02 (m, 18H).

A UPLC-UV method was developed to quantify the purity of the protected azacitidine (**Figure 16**). A UPLC Acquity HClass Bio (Waters, France) was used consisting of a quaternary solvent manager, a sample manager, a photo diode array detector and a column manager was used. The system was controlled via Empower®3 software (Waters). The column used was an Acquity®UPLC BEH C18 100 x 2.1 mm, 1.7  $\mu$ m (Waters). The mobile phase was composed of a mixture of acetonitrile and methanol.



	Name	RT	Area	Height	Amount	Units
1		0.440	36745	16761		
2		0.577	22280	5537		
3		0.845	1797	473		
4		1.003	2361	908		
5		1.172	64684	10293		
6		1.301	1151289	592253		
7		1.522	9316	3534		
8		1.842	513	206		

**Column** : C18 BEH Acquity 2.1x100mm

**Isocratic** with 9:1 ACN:MeOH

**Injection Volume** : 2  $\mu$ L

**Run Time** : 2 min

**Flow Rate** : 0.6 mL/min

**$\lambda$**  : 241 nm

**Figure 16: UPLC chromatogram of protected azacitidine.**

The purified product was dissolved in acetonitrile at a concentration of 0.5 mg/mL. Prior to injection, the sample was vortexed, sonicated and filtered using a 0.22  $\mu$ m Millex-LG filter (Merck-Millipore, Germany). Flow rate was set to 0.6 mL/min and injection volume was set to 2  $\mu$ L. The product was eluted via an isocratic flow. Detection was fixed at 241 nm to detect azacitidine. After using the area under the curve to analyze the obtained chromatogram, the purity of protected azacitidine was determined at 90%: **Figure 16**.

$^1\text{H}$  NMR spectrum of the protected azacitidine was recorded in deuterated dimethyl sulfoxide (DMSO- $d_6$ ) at 400 MHz with a Bruker 500MHz AVANCE III HD spectrometer (Wissembourg, France), equilibrated at 25  $^\circ\text{C}$ , at the SFR Matrix of the University of Angers. Spectra were analyzed using the software MestReNova®. The methyl peaks of the protection groups were

detected at 0.08 ppm and 0.85-0.91 ppm, the rest of the peaks conformed to those of azacitidine: **Figure 17**.

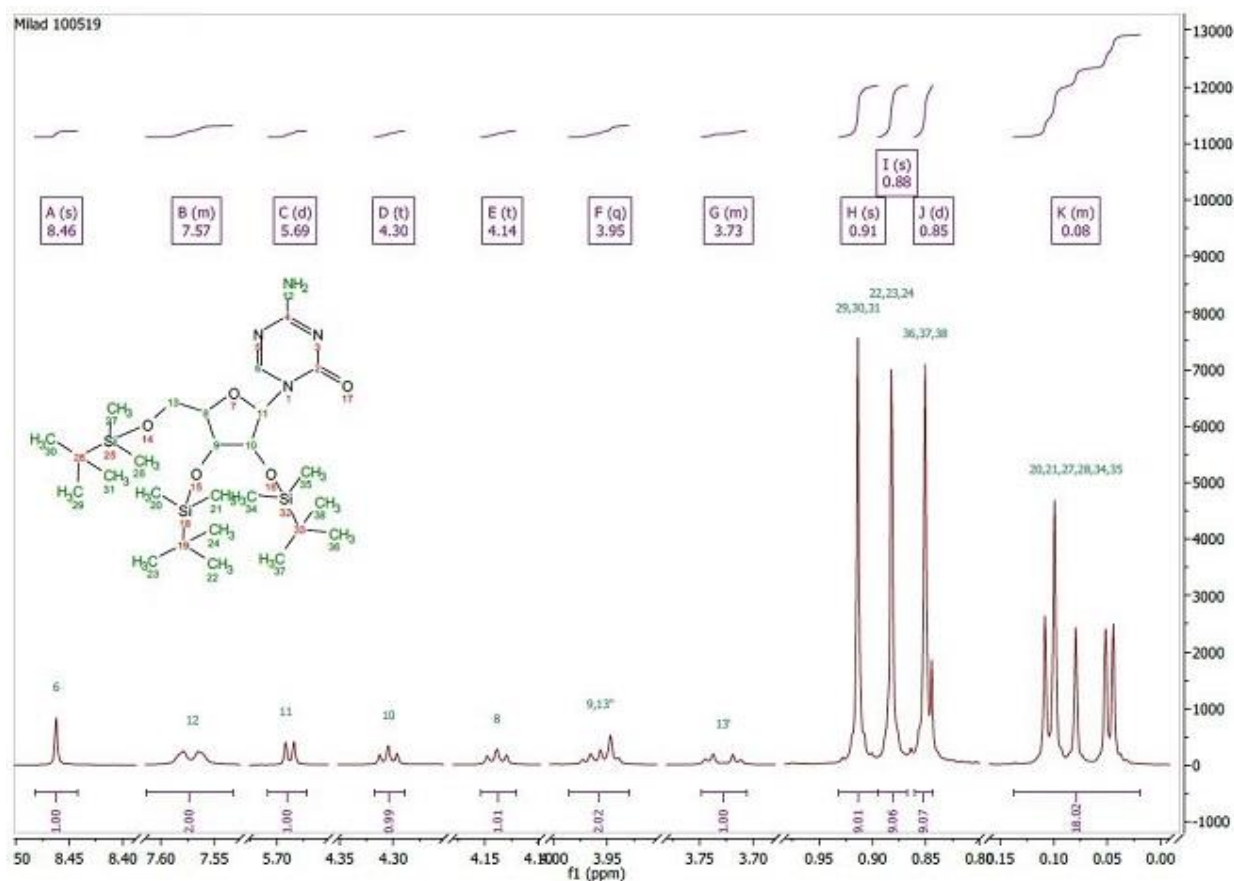


**Figure 17:**  $^1\text{H}$  NMR spectra of protected azacitidine.

Mass spectrometry was used to further verify the obtained product. Protected azacitidine was dissolved in acetonitrile+0.1% formic acid at a concentration of 50  $\mu\text{g/mL}$ . The solution was directly infused at 10  $\mu\text{L/min}$  into a Quattro Micro $^{\text{®}}$  triple quadrupole mass spectrometer (Waters). Prior to infusion, the sample was vortexed, sonicated and filtered using a 0.22  $\mu\text{m}$  Millex-LG filter (Merck-Millipore, Germany). Ionization was achieved using electrospray in positive ion mode. The mass spectrometer was operated in multiple reaction monitoring mode.

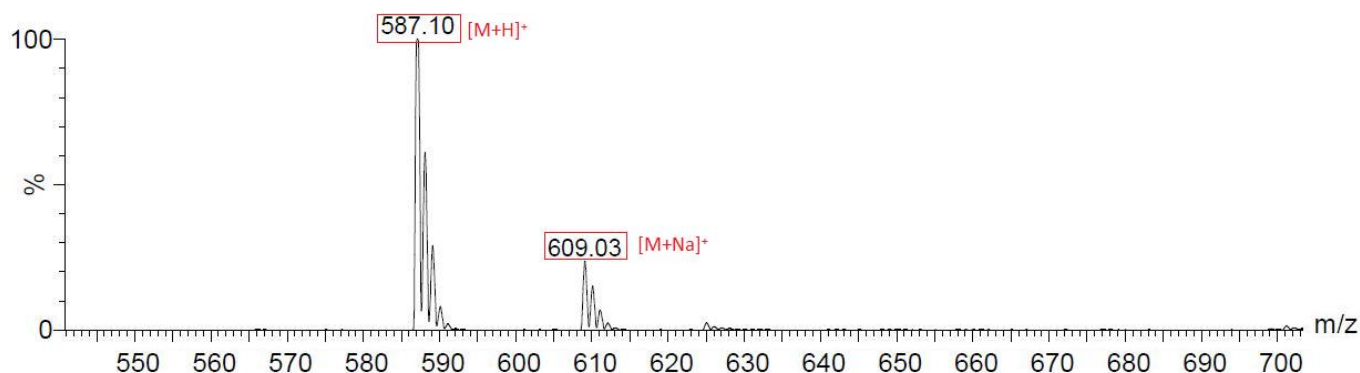


**Figure 18:** Mass spectra of the protected azacitidine.

The entire system was controlled by Masslynx® software (Waters). The molecular weights of the azacitidine and TBDMS being 244.207 g.mol<sup>-1</sup> and 150.72 g.mol<sup>-1</sup> respectively, the [M+H]<sup>+</sup> at 587.1 m/z and its sodium adduct at 609.03 m/z, confirmed the successful protection of the azacitidine (**Figure 18**).

It is noteworthy that this final reaction stated above was obtained after several attempts to optimize the experimental conditions. For instance, the initial tested conditions are presented in **Table 4**. Three OH groups (1 primary and 2 secondary alcohols) have to be protected and some hindrance was met to achieve a three-protected azacitidine molecule: initial reactions gave only the two protected azacitidine.

Reactants	Equivalent	Quantity
Azacitidine	-	200 mg
imidazole	9x	502 mg
TBDMSCl	7.5x	926 mg
ET <sub>3</sub> N	3.3x	370μl
DMF anhydrous	-	20 ml

**Table 4: Initial conditions used in the protection reaction of azacitidine.**

Different parameters were therefore changed including concentration, temperature, equivalent, base, in presence or not of different catalysts (silver nitrate or DMAP). It was found that a higher volume of solvent (2x) as well as higher equivalents of the reactants were needed. Upon using the high equivalents as described in the reaction above and conducting the reaction over 48 hours, a full protection of the three OH groups was successfully obtained with a yield ranging from 64% to 71%. In increasing the reaction time to 72 hours, it led to an optimal yield of 94%± 1.75%.

### 1.3. Conjugation of protected azacitidine to the fatty acid

To first optimize the experimental conditions, the oleic acid (OA) was used instead of docosapentaenoic acid (DPA) and eicosapentaenoic acid (EPA), due to availability and affordability in large quantities.

Initially, HATU was chosen as a conjugating agent between the protected azacitidine and the OA, owing to its high reactivity and the high yield it can give, as well as its frequent use in literature for the conjugation of nucleosides to carboxylic acid groups<sup>215,230</sup>, the reaction being carried in the presence of DIPEA and DMAP. The conjugation was done by following literature guide lines using 100 mg of protected azacitidine, 3.9 equivalents of HATU, 1.1 equivalents of oleic acid, 5 equivalents of DIPEA and 0.1 equivalents of DMAP in 10 mL of anhydrous DMF. The OA was mixed with DIPEA and DMAP for 15 minutes in order to activate the carboxylic acid function, followed by the addition of HATU that was mixed for 10 min and the final addition of the protected azacitidine. This method was unable to produce a successful conjugation. Despite changing different reaction conditions individually (including concentration, time, temperature, equivalent, reactant such as HOBt (hydroxybenzotriazole) and mixing methods), a successful conjugation using HATU as a conjugating agent was not achieved. Therefore, 2 different conjugating agents were used, the Hexafluorophosphate Benzotriazole Tetramethyl Uronium (HBTU) and the 1-Ethyl-3-(3-dimethylaminopropyl) carbodiimide (EDC) with similarly varying conditions that also were not able to perform the desired conjugation.

The failure of the conjugation was attributed to the low reactivity of this azacitidine amine group or due to the conjugating agent tested. To eliminate the first hypothesis, the 3 protected azacitidine was replaced by another control primary amine: DMAPA (dimethylaminopropylamine) (**Figure 19**). The 3 different conjugating agents were used again with the different experimental conditions describe above. Surprisingly, the conjugation was not achieved. Thus, the reactivity of the protected azacitidine was not the reason behind the failure of the conjugation, rather the conjugating agents that have been used were not suitable, despite its common use in literature.

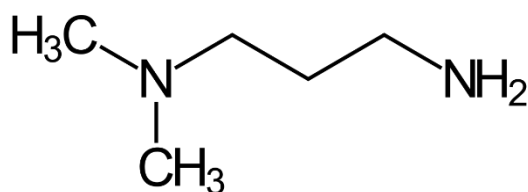


**Figure 19: Chemical structure of DMAPA.**

Therefore, ethyl chloroformate (EtCOCl) was used and was successful in conjugating the control primary amine (DMAPA) to oleic acid under the following conditions: 120 mg of DMAPA, 1 equivalent of OA, 1.2 equivalents of  $\text{Et}_3\text{N}$ , 1 equivalent of EtCOCl in 10 mL anhydrous THF and DMF (in the absence of DMF, the conjugate was not observed, for solubility reasons probably). OA and  $\text{Et}_3\text{N}$  were mixed together in THF for 15 minutes, followed by cooling down to  $-10^\circ\text{C}$  in an acetone ice bath. Then, ethyl chloroformate in THF was added drop-wise and mixed for 15 minutes. Finally, DMAPA in DMF was added to the mixture drop-wise and mixed for 10 min, before removing the acetone ice bath and allowing the mixture to reach room temperature and mixed for 72 hours under argon.

The mixture was then dried using a rotary evaporator at  $40^\circ\text{C}$ . A 1 mM solution of sodium bicarbonate was added to the mixture and the crude product was extracted using dichloromethane. The organic layer was then washed with brine, dried on magnesium sulfate ( $\text{MgSO}_4$ ), and concentrated using a rotary evaporator. The crude product was then purified using a silica gel chromatography eluting with 6% ethyl acetate in cyclohexane to give the DMAPA-OA conjugate with a final yield of 92%.

The compound obtained was confirmed using  $^1\text{H}$  NMR, the hydrogen peak belonging to the amide bond was detected at 7.73 ppm confirming the conjugation (**Figure 20**).  $^1\text{H}$  NMR (499 MHz,  $\text{DMSO}-d_6$ )  $\delta$  7.73 (t,  $J = 5.6$  Hz, 1H), 5.33 (td,  $J = 4.4, 2.1$  Hz, 2H), 3.03 (td,  $J = 7.0, 5.6$  Hz, 2H), 2.19 – 2.15 (m, 2H), 2.10 (s, 6H), 2.04 – 1.96 (m, 6H), 1.49 (dq,  $J = 14.1, 7.1$  Hz, 4H), 1.29 – 1.21 (m, 20H), 0.87 – 0.84 (m, 3H).

Following the success of the conjugation reaction using the DMAPA as a control, the same experiment was repeated using the same conditions with the protected azacitidine and the OA: 120 mg of protected azacitidine, 1 equivalents of OA, 1.2 equivalents of  $\text{Et}_3\text{N}$ , 1 equivalent of EtCOCl in 10 mL of anhydrous THF and DMF. The mixture was then dried using a rotary evaporator at  $40^\circ\text{C}$ . A 1 mM solution of sodium bicarbonate was added to the mixture and the crude product was extracted using dichloromethane.

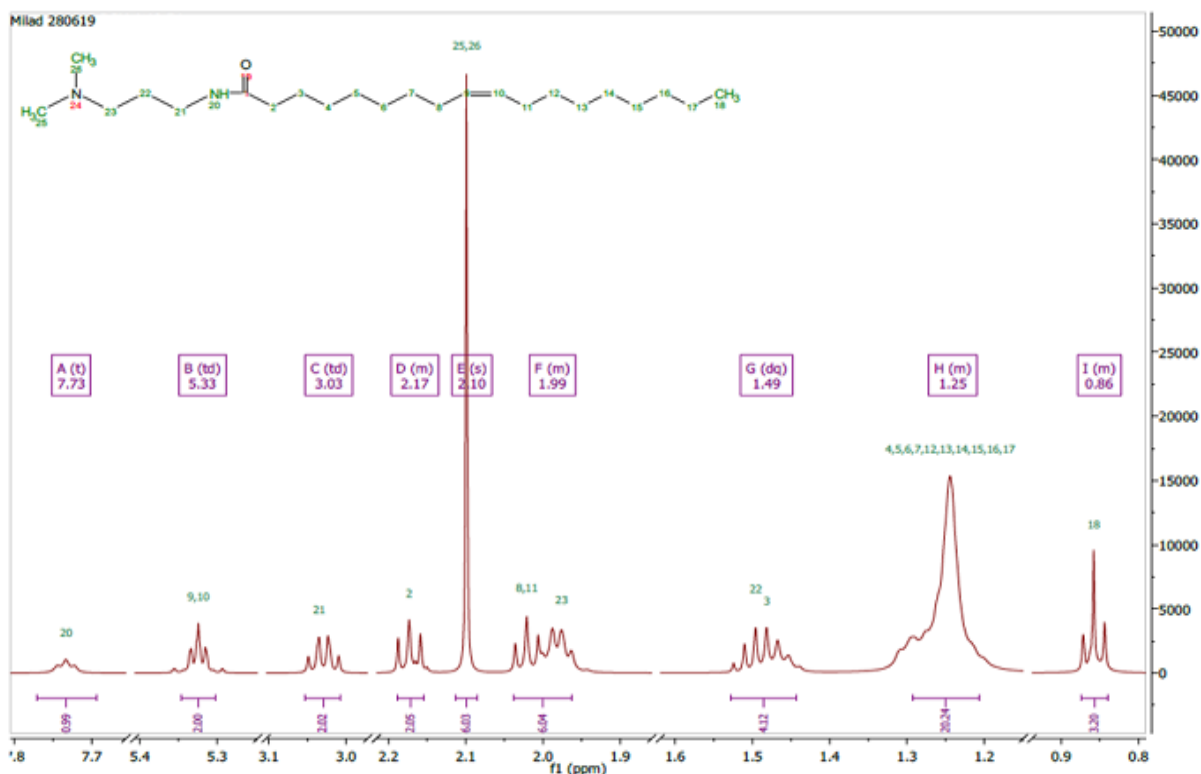


**Figure 20:  $^1\text{H}$  NMR of the DMAPA-OA conjugate.**

The organic layer was then washed with brine, dried on magnesium sulfate ( $\text{MgSO}_4$ ), then concentrated using a rotary evaporator. The crude product was then purified using a silica gel chromatography eluting with 6% ethyl acetate in cyclohexane to give the protected azacitidine-OA conjugate with a final yield of 41%. The compound obtained was confirmed using  $^1\text{H}$  NMR, the hydrogen peak belonging to the amide bond was detected at 7.57 ppm, confirming the conjugation (**Figure 21**).

$^1\text{H}$  NMR (499 MHz,  $\text{DMSO-d}_6$ )  $\delta$  8.47 (s, 1H), 7.59 – 7.56 (m, 1H), 5.76 (s, 1H), 4.31 (t,  $J = 4.1$  Hz, 1H), 4.14 (t,  $J = 4.6$  Hz, 1H), 4.04 (q,  $J = 7.1$  Hz, 2H), 3.97 – 3.94 (m, 1H), 3.76 – 3.71 (m, 1H), 1.99 (s, 3H), 1.91 (s, 3H), 1.63 (s, 2H), 1.25 (s, 20H), 1.17 (d,  $J = 7.1$  Hz, 3H), 0.92 – 0.84 (m, 27H), 0.15 – 0.03 (m, 12H).



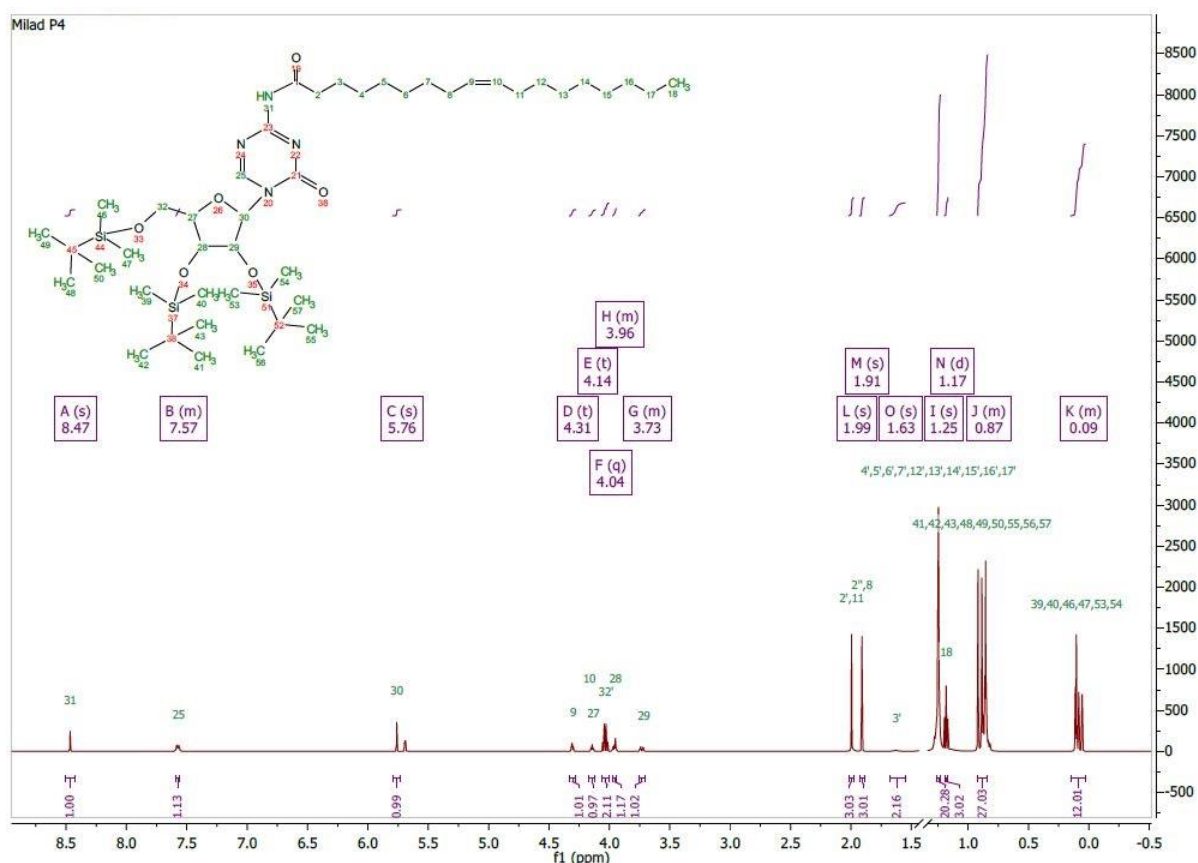


**Figure 21:  $^1\text{H}$  NMR of the protected azacitidine-OA conjugate**

Mass spectrometry was used to further confirm the obtained product. The molecular weights of the protected azacitidine and OA being  $586.99 \text{ g.mol}^{-1}$  and  $282.47 \text{ g.mol}^{-1}$  respectively, the  $[\text{M}+\text{H}]^+$  at  $851.54 \text{ m/z}$ , its sodium adduct at  $873.56 \text{ m/z}$ , and its potassium adduct at  $889.46 \text{ m/z}$  confirmed the successful conjugation of the protected azacitidine to the OA (**Figure 22**).

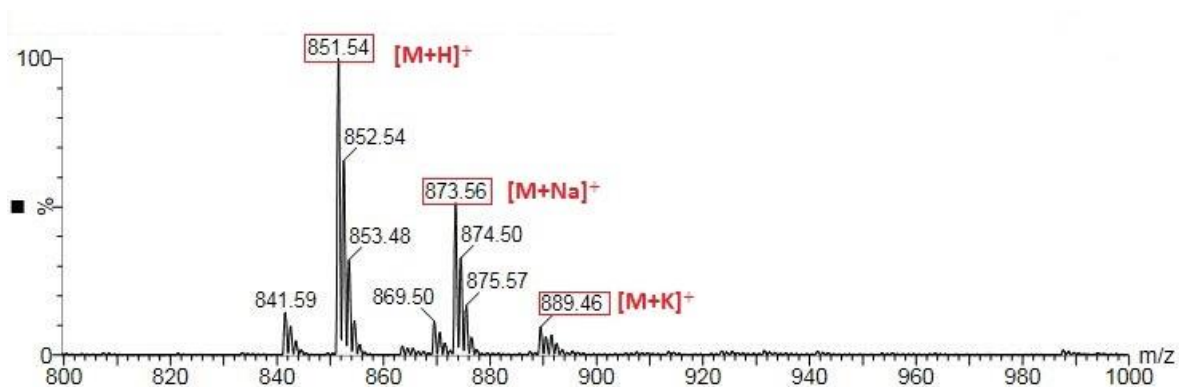


**Figure 22: Mass spectra of protected the azacitidine-OA conjugate.**

Subsequently, the successful conjugation was applied to the main fatty acids of interest, EPA and DHA. The equivalents of the reactants were doubled in order to increase the yield: 120 mg of protected azacitidine, 2 equivalents of DHA or EPA, 2.4 equivalents of  $\text{Et}_3\text{N}$ , 2.2 equivalents

of EtCOCl in 10 mL of anhydrous THF and DMF. The method of reactant addition was unchanged. The mixture was then dried using a rotary evaporator at 40°C. A 1 mM solution of sodium bicarbonate was added to the mixture and the crude product was extracted using dichloromethane. The organic layer was then washed with brine, dried on magnesium sulfate ( $\text{MgSO}_4$ ), then concentrated using a rotary evaporator. The crude product was then purified using a silica gel chromatography eluting with 6% ethyl acetate in cyclohexane to give the protected azacitidine-DHA/EPA conjugates with a final mean yield of 52%. Mass spectrometry was used to further confirm the obtained products. The molecular weights of the protected azacitidine and EPA being  $586.99 \text{ g.mol}^{-1}$  and  $302.45 \text{ g.mol}^{-1}$  respectively, the  $[\text{M}+\text{H}]^+$  at 871.50 m/z, its sodium adduct at 894.50 m/z, and its potassium adduct at 911.55 m/z confirmed the successful conjugation of the protected azacitidine to the EPA (**Figure 23**). The molecular weight of DHA being of  $328.48 \text{ g.mol}^{-1}$ , the  $[\text{M}+\text{H}]^+$  at 897.48 m/z, its sodium adduct at 920.40 m/z, and its potassium adduct at 937.49 m/z confirmed achieving the protected azacitidine covalently linked to DHA (**Figure 24**).

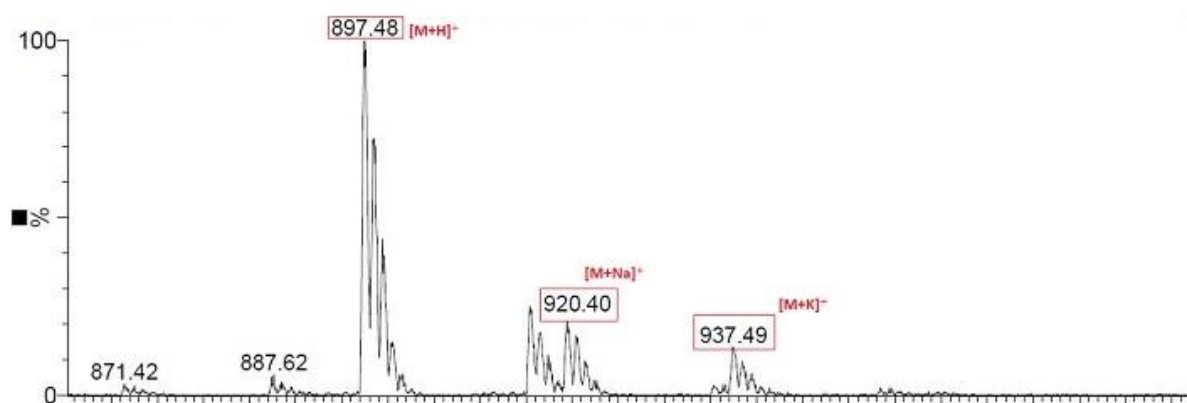


**Figure 23: Mass spectra of the protected azacitidine-EPA conjugate.**

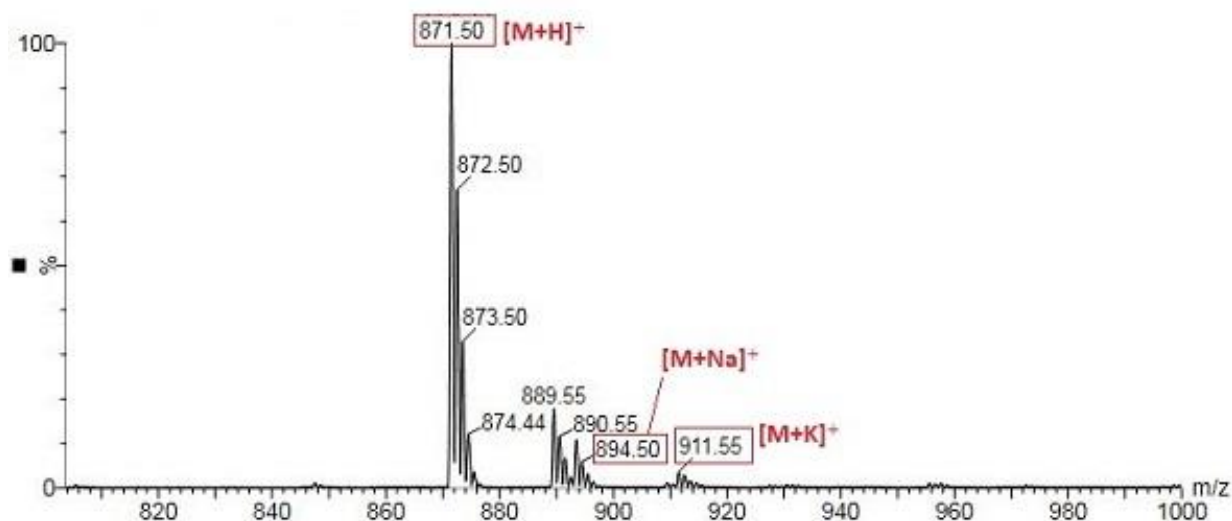


**Figure 24: Mass spectra of the protected azacitidine-DHA conjugate.**

## 1.4. Removal of the silyl protecting group

After obtaining the protected azacitidine-omega 3 fatty acid conjugates, a final step of deprotection is still needed. To reach this aim, TBAF is known to react with the protected product<sup>215,231</sup>, in using 1.1 equivalents per protecting group (3.3 in total). Prior to the reaction, THF and TBAF were mixed together and dried for 72 hours with molecular sieves (3 Å): even if both products were bought in an anhydrous state, several studies have shown that TBAF is an extremely hygroscopic molecule, that will absorb water easily, and even brand new sealed bottles showed a decent amount of water that slowed the reaction down significantly<sup>231</sup>.

The protected conjugates were mixed with the dried mixture and allowed to react for 24 hours at room temperature. The mixture was then dried using a rotary evaporator at 40°C. The crude product was analyzed by mass spectrometry and only a partial deprotection was observed. The increase of the reaction time or the amount of added TBAF did not improve the complete deprotection process.

The addition of an equal equivalents of acetic acid to this mixture after doubling the equivalents allowed for the complete deprotection to occur. Precisely, 150 mg of protected azacitidine-fatty acid conjugate was dissolved in 5 mL of THF, followed by the addition of 6 equivalents of TBAF and 6 equivalents of acetic acid, both added drop-wise. The reaction was allowed to stir for 24 hours at room temperature. The mixture was then concentrated using a rotary evaporator at 40°C and the crude product was analyzed using mass spectrometry. The deprotected conjugates were observed for the both EPA and DHA conjugates. The  $[M+H]^+$  at 529.48 m/z confirmed obtaining the desired azacitidine-EPA conjugate (**Figure 25**). The  $[M+Na]^+$  at 577.13 m/z proved the successful synthesis of the azacitidine-DHA conjugate (**Figure 26**).

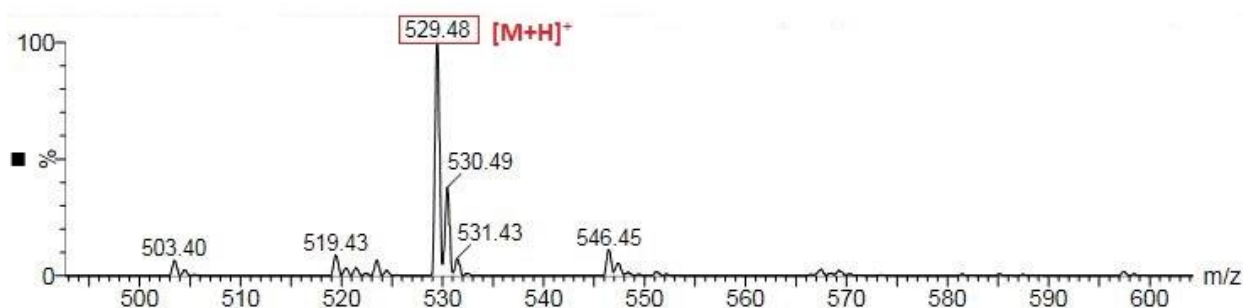


**Figure 25: Mass spectra of the azacitidine-EPA conjugate.**

After obtaining the crude products of both conjugates, the process of purification was unsuccessful both on silica gel chromatography and reversed phase high-performance liquid chromatography (RP-HPLC), while using a wide range of eluents and conditions. It could be

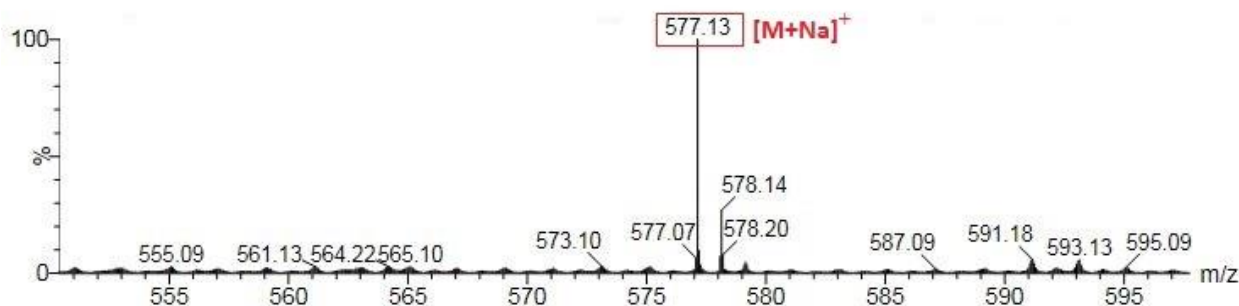


**Figure 26: Mass spectra of the azacitidine-DHA conjugate.**

explained by the extremely close polarity of the final products and the partially deprotected conjugates, which allowed them to elute together.

Therefore, a new method of conjugation was adapted using EtOCOCl as a conjugating agent without the need for protection. This method and its purification succeeded and the desired conjugates were obtained. The following section will shed the light on this process.

## **2. Azacitidine Omega-3 self-assemblies: synthesis, characterization, and potent applications for myelodysplastic syndromes.**

This section encompasses an article submitted to Pharmaceuticals, describing the alternative direct conjugation pathway used to obtain the desired prodrugs. The synthesis process will be described in details with their complete characterization to verify the obtained conjugates. Afterwards, the prodrugs were formulated into self-assemblies via nanoprecipitation, followed by the determination of some physico-chemical parameters.





Article

# Azacitidine Omega-3 self-assemblies: synthesis, characterization, and potent applications for myelodysplastic syndromes.

Milad Baroud <sup>1</sup>, Elise Lepeltier <sup>1</sup>, Sylvain Thepot <sup>2</sup>, Jérôme Béjaud <sup>1</sup>, Nolwenn Lautram <sup>1</sup>, Yolla El-Makhour <sup>3</sup>, Olivier Duval <sup>1, \*</sup>

<sup>1</sup>Translational Micro and Nanomedecines (MINT, INSERM1066 /CNRS6021), Université d'Angers, Angers, France

<sup>2</sup>University Hospital of Angers, Hematology, 49933 Angers, France

<sup>3</sup>Environmental Health Research Lab, Nabatieh, Lebanon

\* Correspondence: olivier.duval@univ-angers.fr; Tel.: +33241226604

**Abstract:** 5-Azacitidine, a cytidine analogue and a hypomethylating agent, is one of the main drugs being used for the treatment of myelodysplastic syndromes (MDS) and acute myeloid leukemia (AML). However, after administration, it exhibits several limitations including restricted diffusion and cellular internalization due to its hydrophilicity, and rapid enzymatic degradation by adenosine deaminase. The aim of this study is to improve the drug diffusion and protect it from metabolic degradation, via the synthesis of amphiphilic prodrugs and their potential self-assembly. Azacitidine was conjugated to two different omega-3 fatty acids, the eicosapentaenoic acid (EPA) and the docosahexaenoic acid (DHA). The carboxylic acid group of the omega-3 fatty acids was effectively conjugated to the amine group of the azacitidine base, giving two amphiphilic prodrugs. Nanoprecipitation of the obtained prodrugs was performed and self-assemblies were successfully obtained for both prodrugs, with a diameter of 190 nm, a polydispersity index below 0.2 and a positive zeta potential. The formation of self-assemblies was confirmed by using the pyrene as a fluorescent dye, and the critical aggregation concentration was identified. Additionally, the stability of the obtained self-assemblies was studied and after 5 days their final stable arrangement was reached.

**Keywords:** Azacitidine, Docosahexaenoic acid, Eicosapentaenoic acid, PUFAylation, myelodysplastic syndromes, nanomedicine.

**Citation:** Lastname, F.; Lastname, F.; Lastname, F. Title. *Pharmaceuticals* **2021**, *14*, x. <https://doi.org/10.3390/xxxxx>

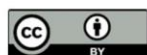
Academic Editor: Firstname Lastname

Received: date

Accepted: date

Published: date

**Publisher's Note:** MDPI stays neutral with regard to jurisdictional claims in published maps and institutional affiliations.



**Copyright:** © 2021 by the author. Submitted for possible open access publication under the terms and conditions of the Creative Commons Attribution (CC BY) license (<https://creativecommons.org/licenses/by/4.0/>).

## 1. Introduction

The myelodysplastic syndromes (MDS) are a clonal disorder of the hematopoietic stem cell characterized by evident morphological dysplasia (abnormal cells that may develop into a cancerous component), showing variable degrees of cytopenias (decreased in blood cell count), with a possibility of progressing into acute myeloid leukemia[1]. 5-azacitidine (**Figure 1**) is one of the drugs approved for the treatment of (i) higher risk MDS (advanced form of MDS)[2,3], (ii) in lower risk MDS patients following the failure of the conventional approaches[4,5], (iii) in the cases of delays for patients eligible for hematopoietic stem cell transplantation procedures in addition as post-procedure relapse prevention [6–8], and (iv) a first-line treatment for AML[9–11].

Upon the entry of this DNA hypomethylating cytidine analogue, via the action of human Equilibrative Nucleoside Transporter 1 (hENT1), azacitidine will undergo successive phosphorylation steps by the regular nucleic acid kinases, to reach its final tri-phos-

phorylated form, allowing its integration into the DNA. It acts as well on the DNA methyltransferase, causing permanent inhibition of the enzyme, leading to alteration of gene expression by decreasing the methylation levels of the cytosine, thus impacting the DNA epigenetic status and allowing the reactivation of tumor suppressor genes[12,13].

Clearly, azacitidine is a crucial weapon in the arsenal against these two diseases, coupled with a lack of other satisfying alternatives, this further stresses its significance. However, a grim prognosis awaits the patients upon the failure of azacitidine with a decreased median overall survival to 5-7.5 months[14,15]. This failure can be either a primary failure (lack of any response to azacitidine), a secondary failure (disease progressed after a first response, serum drug level is low) or a toxicity failure (azacitidine treatment was terminated due to severe side effects)[15,16]. These failures can be attributed to the chemical and pharmacological properties of this drug, as azacitidine is sensitive to water: a rapid and reversible hydrolysis producing the N-formylribosylguanylylurea, followed by its irreversible hydrolysis to ribosylguanylylurea (Figure 1)[17,18], explaining the short half-life after administration. Additionally, because of its hydrophilic nature, a poor cell internalization is observed, a common problem to most hydrophilic drugs. Finally, the presence of nucleoside deaminase in the blood further decreases the half-life of this molecule and allows its rapid degradation and elimination[18–22].

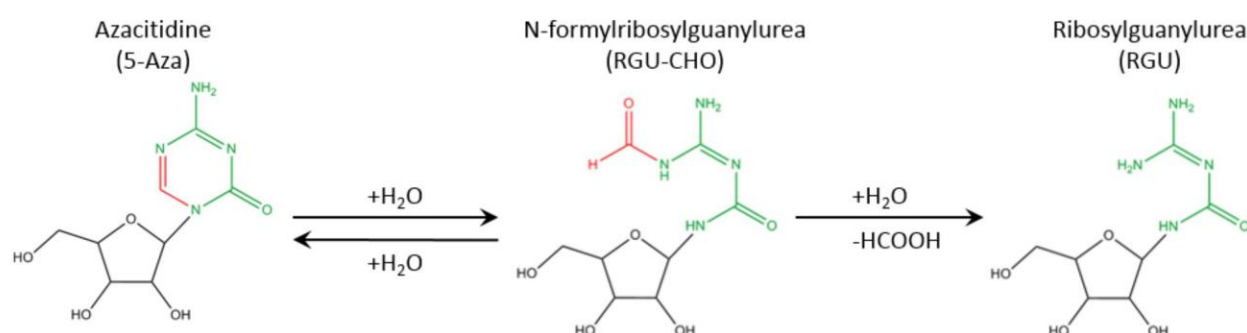


**Figure 1:** Hydrolysis of azacitidine. In the presence of water, a fast reversible hydrolysis occurs producing the N-formylribosylguanylylurea, followed by a second slow irreversible hydrolysis, producing the ribosylguanylylurea.

This study aims to counter these varied shortcomings with a dual approach: first the synthesis of an azacitidine based prodrug via its conjugation to a fatty acid at the amine group of azacitidine, second pushing the obtained prodrug towards self-assemblies. The obtained amphiphilic prodrug would have an enhanced entry into the cells owing to the similar nature of the cell lipid bilayer membrane[23,24], with a specificity to the affected cells owing to their overexpression of cathepsin-B, an enzyme that can cleave the conjugating amide bond, releasing specifically the free azacitidine [25–27]. Additionally, the prodrug based self-assemblies would be able to further protect the azacitidine from degradation by deaminases, increasing its circulation time thus reducing the required dose to achieve an equal response[12].

The choice of fatty acids to be conjugated to azacitidine was dictated by the presence of at least one double bond, thus docosahexaenoic acid (DHA) and eicosapentaenoic acid (EPA) were chosen. Indeed, the presence of double bonds on the lipophilic part is an essential asset in order to obtain spontaneously self-assemblies in water, thanks to the  $\pi$ - $\pi$  stacking interactions [28–32].

Moreover, EPA and DHA have shown a promising anticancer activity in various studies. DHA and EPA inhibited the growth of AML cell lines and induced cell death via oxidative stress pathways. Furthermore, they showed a synergistic effect after the combination of the fatty acids with cytarabine, a previously used hypomethylating agent[33]. Additional studies on DHA and EPA identified different pathways that these fatty acids utilize to impede cancer progression[34–37]. *In vivo* studies have also demonstrated that omega 3 fatty acids were able to reduce the number of abnormal progenitor cells and push them towards differentiation. The omega 3 and 6 fatty acids of the mice diet were controlled, the omega 3 ones being in a higher proportion, it led to a decrease in the number of



myeloid progenitor cells, while increasing differentiation without affecting peripheral white blood cell numbers, showing their promise in the treatment of MDS and AML[38].

The process of conjugating fatty acids to nucleosides and their analogues in order to combat such shortcomings is a well investigated one. Indeed, this process has been pioneered by Prof. Couvreur and his team, with the use of squalene and its derivatives that were conjugated to different nucleoside analogs in a process termed “Squalenoylation”. This method was reproduced with other fatty acids mainly poly-unsaturated ones, and termed “PUFAylation”[39–43].

By conjugating azacitidine to EPA and DHA two different prodrugs were obtained an azacitidine-docosahexaenoic acid conjugate (N<sup>4</sup>-azacitidine DHA, AzaDHA) and an azacitidine-eicosapentaenoic acid conjugate (N<sup>4</sup>-azacitidine EPA, AzaEPA). These conjugates have been obtained via direct conjugation in the presence of ethyl chloroformate. The nanoprecipitation of the obtained prodrugs was performed and self-assemblies were successfully obtained (**Figure 2**) for both prodrugs with a diameter of ~190 nm, a polydispersity index below 0.2 and a positive zeta potential. Self-assemblies were verified by using the pyrene as a fluorescent dye to determine the critical aggregation concentration. Furthermore, the formed self-assemblies needed 5 days to reach their final stable organization.

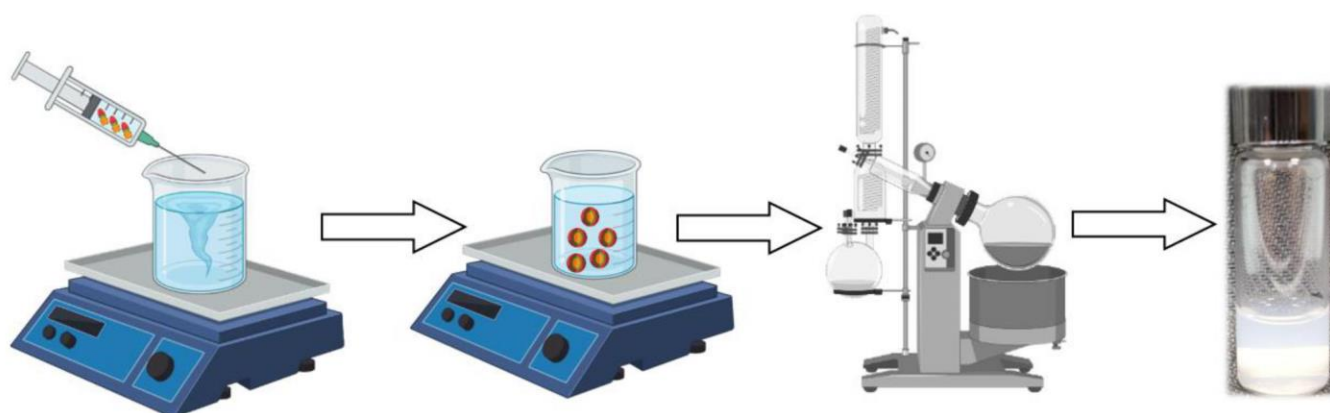


**Figure 2:** Formulation of self-assemblies via nanoprecipitation. The conjugates are dissolved in an organic solvent, here acetone, then added drop-wise to a stirring aqueous medium allowing for the spontaneous formation of self-assemblies. The organic solvent is then evaporated using a rotary evaporator, thus yielding an opalescent aqueous suspension.

## 2. Results and discussion

Nucleoside analogue derivatives that are coupled at the 4-(N)-position to various molecules exhibit enhanced metabolic stability in plasma, owing to the occupation of the deamination site, thus protecting these analogues from the irreversible hydrolytic degradation[12,32,44,45]. As a consequence of their hydrophobic nature, both DHA and EPA can act as the scaffold in the synthesis of amphiphilic prodrugs [46,47]. In this study, azacitidine was covalently

bound to either EPA or DHA, to form N<sup>4</sup>-azacitidine DHA (AzaDHA) and N<sup>4</sup>-azacitidine EPA (AzaEPA) amphiphilic prodrug conjugates through amide linkage by the action of ethyl chloroformate (**Figure 3**).

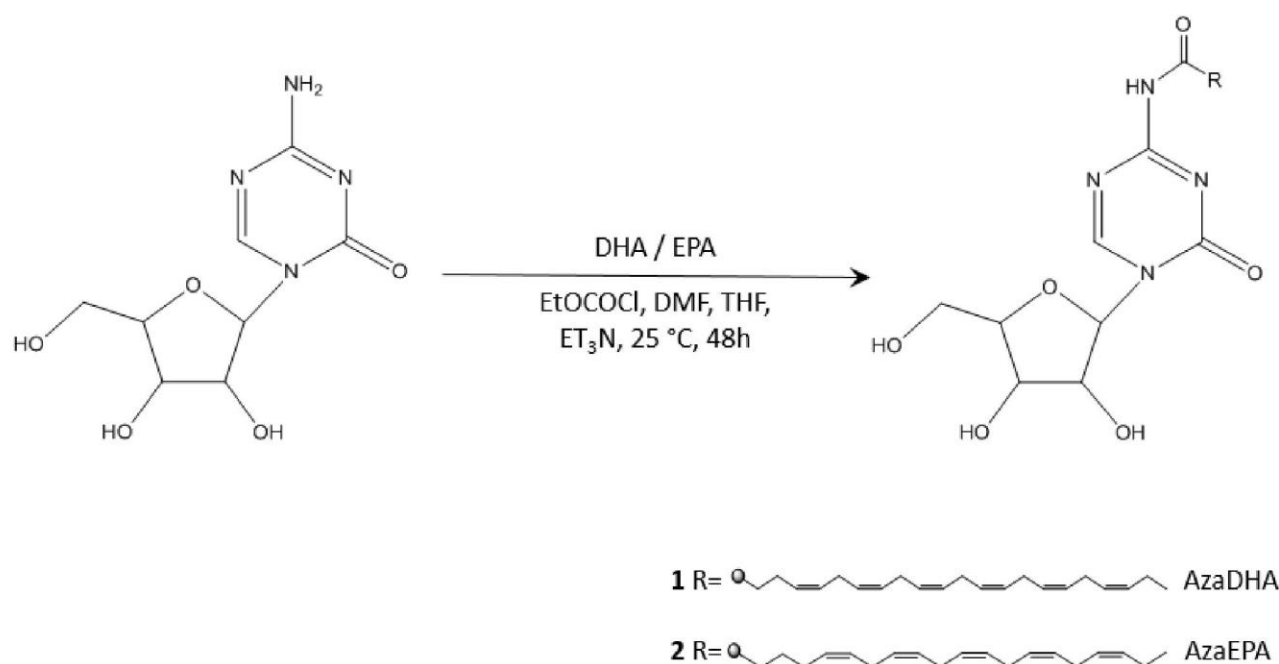


**Figure 3:** Synthesis of N<sup>4</sup>-azacitidine DHA (AzaDHA, 1) and N<sup>4</sup>-azacitidine EPA (AzaEPA, 2).

The AzaEPA and AzaDHA prodrugs were then purified via semi-preparative reversed phase high-performance liquid chromatography (RP-HPLC) with a final mean yield of ~10% and a purity of 92% for AzaEPA, AzaDHA was obtained with a mean yield of ~20% and a purity of 97%. The chemical structure of the obtained conjugates was verified by <sup>1</sup>H and <sup>13</sup>C NMR spectroscopy with characteristic chemical shifts. Mass spectrometry (**Figure S1** and **Figure S2**) confirmed these results with 528.48 and 554.21 g.mol<sup>-1</sup> obtained for AzaEPA and AzaDHA respectively. The method to determine purity is describes in **Figure S3, S4 and S5**.

The Fourier-Transform Infrared Spectroscopy (FTIR, **Figure 4**) confirmed the successful amide conjugation: the NH<sub>2</sub> stretch of azacitidine at 3391 cm<sup>-1</sup> disappeared after conjugation and was replaced with an NH stretch in both AzaEPA and AzaDHA conjugates at 3361 cm<sup>-1</sup>. Additionally, the SP<sup>2</sup> C-H stretches belonging to the fatty acid chains appeared at 3011 cm<sup>-1</sup> in both conjugates. Finally, the carboxylic group C=O stretches at 1691 cm<sup>-1</sup> and the fatty acid double bond C=C stretches appeared at 1545 cm<sup>-1</sup>. All the mentioned changes are thus an indicative of the success of the conjugation to produce the two prodrugs. Similarly, elemental analysis (**Table 1**) further confirmed the successful conjugation as the obtained elemental percentages of C, H and N atoms closely match the theoretically calculated ones.

As azacitidine is conjugated to two different polyunsaturated fatty acids, the potential process of self-assembly is termed “PUFAylation”. Though this term was recently introduced by Liming Wu et al.[45], the concept of conjugating a polyunsaturated fatty acid (PUFA) to a nucleoside, leading to the spontaneous self-assembly of the created prodrug has been tackled before. Certainly, this innovative strategy was established by Couvreur and colleagues, whereby squalene derivatives (a cholesterol precursor) were conjugated to nucleoside analogs in a process they

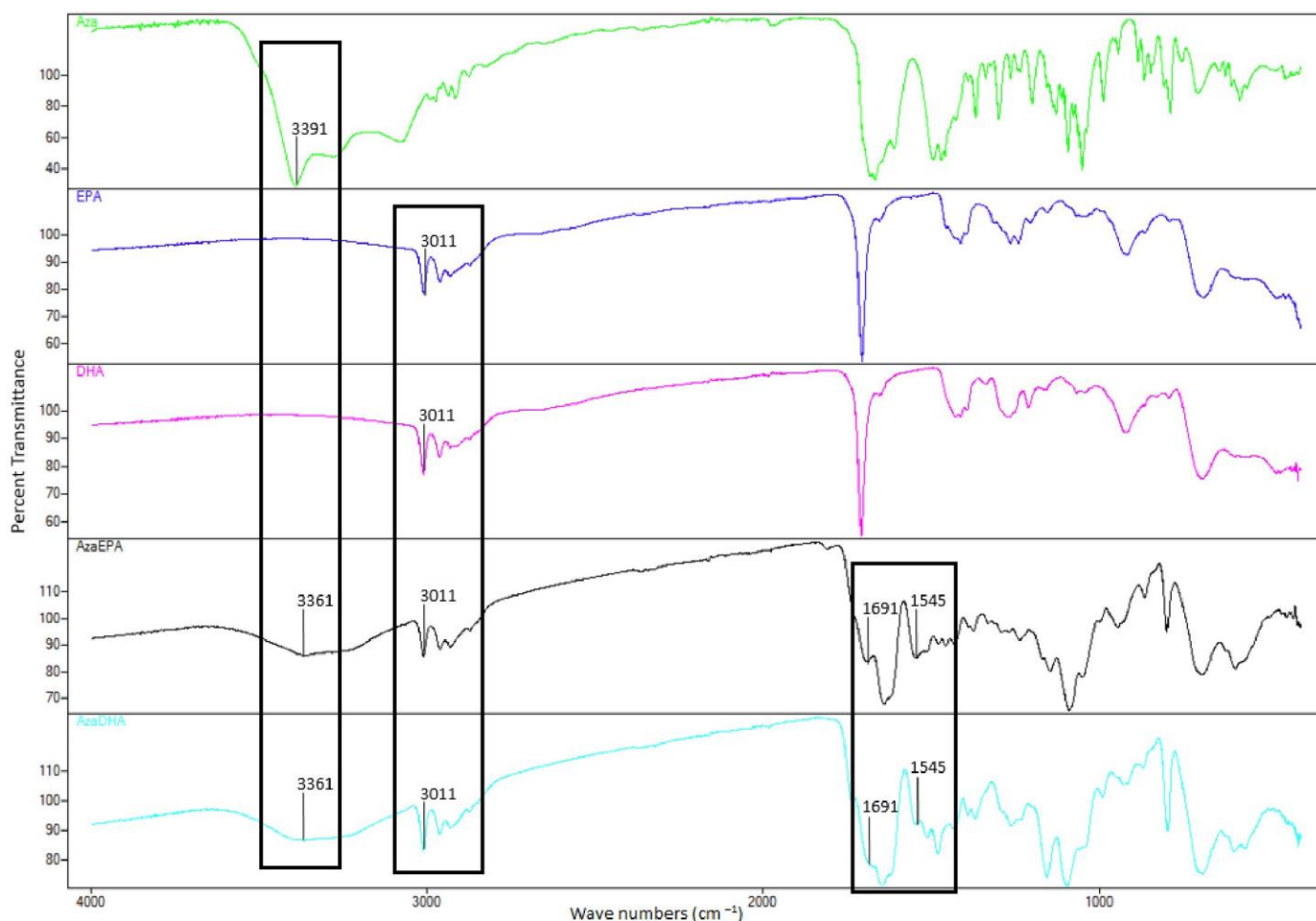


Figure 4: Fourier-Transform InfraRed spectroscopy (FTIR) curves and wave numbers of interest between (a) 4000  $\text{cm}^{-1}$  and 600  $\text{cm}^{-1}$  of azacitidine (green), EPA (purple), DHA (pink), AzaEPA (black) and AzaDHA (blue).

termed “Squalenoylation”[48]. What is more “PUFAylation” while permitting this conjugate to self-assemble in water, it does not require any additional excipient, an advantage over traditional nanomedicines such as liposomes or polymeric nanoparticles, thus improving the drug tolerability in animals and demonstrating to be exceptionally effective, with an unbeatable drug loading. Moreover, this method produces prodrugs with an adequate amphiphilicity, allowing for an enhanced *in vivo* antitumor efficacy compared to the parent drug. Moreover, most of these “PUFAs” are essential for biological functions and plentiful in the body, meaning that it may reduce toxicities stemming from the use of adjuvants, and finally the  $\pi$ - $\pi$  stacking interaction between PUFAs would increase the stability of the self-assemblies[49]. Based on all that, the PUFAs technology is an immensely encouraging one for the manufacturing of prodrugs and their derived self-assembled nanomedicines[50–53].

Table 1: Elemental analysis and elemental calculation of the obtained prodrugs.

Sample	Formula	Calculated %			Found%		
		C	H	N	C	H	N
AzaEPA	$\text{C}_{28}\text{H}_{40}\text{N}_4\text{O}_6$	63.62	7.63	10.6	61.66	7.63	9.67
AzaDHA	$\text{C}_{30}\text{H}_{42}\text{N}_4\text{O}_6$	64.96	7.63	10.1	63.2	7.71	9.31



To study the potential self-organization of the AzaEPA and AzaDHA prodrugs, the fluorescent dye pyrene method was used. Briefly, the pyrene fluorescence spectra, and specifically the emit band intensities at 372 nm and 383 nm are different if the pyrene is in a polar or apolar environment: the ratio of these intensities will be higher than 1 in a polar environment such as water and will become below 1 in a hydrophobic core. Thus, in plotting the  $I_{372}/I_{383}$  ratio in function of the prodrug concentration, if a self-assembly phenomenon occurs, a sigmoidal curve should fit the experimental points, and the CAC can be measured.

For both prodrugs, a sigmoidal curve was obtained proving the successful self-organization of the AzaEPA and AzaDHA. The CAC were determined as the first sharp decrease point[54,55] (**Figure 5**): 400  $\mu\text{M}$  for AzaEPA and 688  $\mu\text{M}$  for AzaDHA respectively.

The concentration of 2 mg/mL corresponding to 3.78 mM in AzaEPA and to 3.6 mM in AzaDHA was then chosen to study the formulation of both amphiphilic conjugates by nanoprecipitation.

The AzaEPA and AzaDHA conjugates were dissolved in acetone, then this organic phase was added drop-wise to MilliQ deionized water, leading to an aqueous suspension with a characteristic opalescence, an indicative of a suspension of nanoparticles[56]. The organic phase was then evaporated using a rotary evaporator.

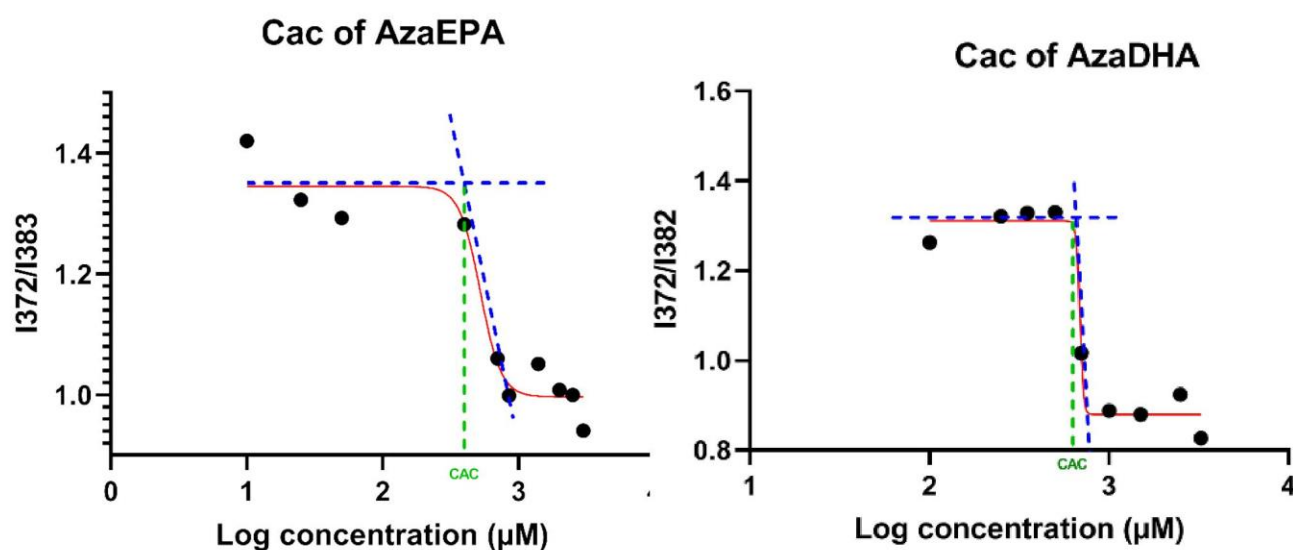


**Figure 5:** Boltzmann-type sigmoid obtained for the AzaEPA and AzaDHA suspensions in water showing the CAC value, corresponding to the first sharp decrease point.

Interestingly, diverse behaviors were observed after evaporation based on the water-to-acetone ratio at higher final concentrations ( $\geq 4\text{mg/mL}$ ). At these high concentrations, when the volume ratio of water: acetone was of 4 (v/v), visually detectable aggregates were observed in the suspension. While at a volume ratio of 5, a homogeneous suspension of nanoparticles was obtained. The influence of the experimental parameters on the obtained self-assemblies by nanoprecipitation is well-known, notably the water: organic solvent ratio and the concentration in solute. Indeed, to be in the Ouzo zone during the formulation process, in order to obtain stable nanoobjects, a highly diluted solution with a large volume of water have to be used.

The hydrodynamic diameter of these self-assembled nanoparticles was characterized by Dynamic Light Scattering (DLS) and 194.5 nm  $\pm$  0.12% for AzaEPA and 185 nm  $\pm$  0.95% for AzaDHA were obtained with a low polydispersity index  $< 0.2$  (day 5, **Table 2**). These results clearly verify that the PUFAylated azacitidine derivatives were able to form self-assembled nanoparticles devoid of the need of any excipients, with a 100% encapsulation efficacy and a drug loading of 44% for AzaDHA and 46% for AzaEPA, well improved compared to conventional nanocarriers such

as liposomes[57]. By electrophoretic mobility, a potential zeta of  $16.1 \text{ mV} \pm 8.54\%$  for AzaEPA and  $18 \text{ mV} \pm 6.74\%$  for AzaDHA were obtained after 1 day of formulation.

Additionally, the Cryo-Transmission electron microscopy (cryo-TEM) analysis was conducted to detect the morphology of the self-assemblies. The results showed that the AzaDHA and AzaEPA conjugates self-assembled into multilamellar vesicles with a mean diameter around 180 nm for AzaDHA self-assemblies, while the AzaEPA conjugate nanoparticles had a mean diameter around 190 nm (**Figure 6**).

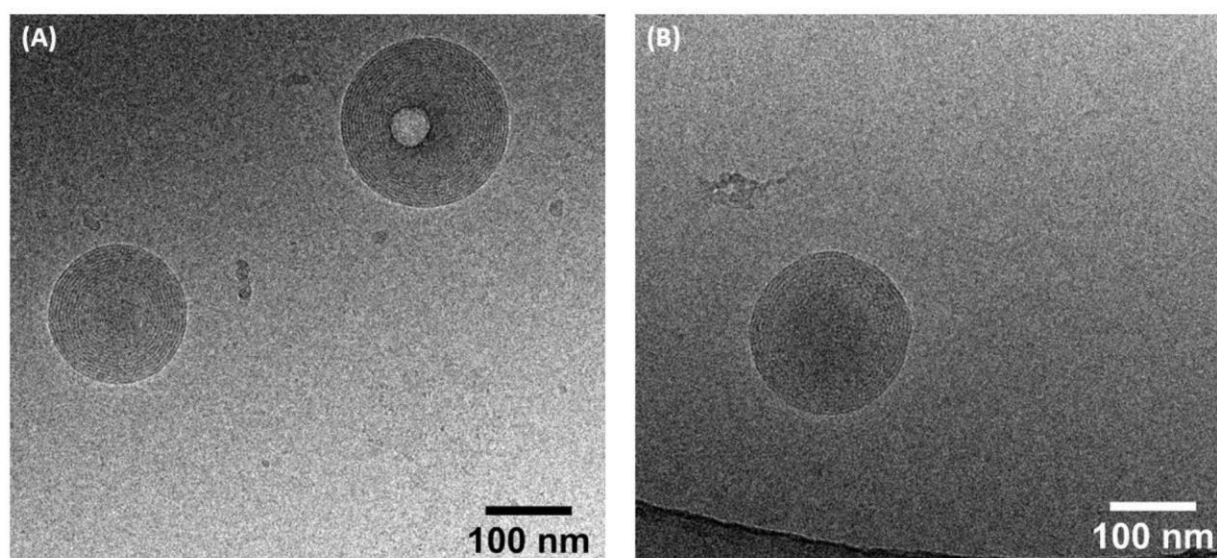


**Figure 6:** Cryo-TEM images of the formed self-assemblies: (A) AzaEPA, (B) AzaDHA.

The physico-chemical parameters stability was studied and followed by DLS and by electrophoretic mobility and interestingly, despite a PDI always below 0.2, illustrating a monodisperse suspension fluctuate zeta potential values were observed until attaining their final stable form at day 5 (**Table 2**).

This observation could be attributed by the supramolecular organization of these amphiphilic prodrugs, reaching their equilibrium after 5 days: the positive surface charge would mean that cationic amines would be in surface of the structure. Moreover, nanoassemblies have a diameter of around 200 nm, that cannot reflect a simple micelle organization (the obtained prodrugs have a length of  $17.4 \text{ \AA}$  ( $1.74 \text{ nm}$ ) for AzaDHA and  $21.2 \text{ \AA}$  ( $2.21 \text{ nm}$ ) for AzaEPA implying micelles of around 4–5 nm in diameter). Therefore, it can be hypothesized that these self-assemblies are organizing into a larger, more complex supramolecular structure. This phenomena has already been observed in similar research achieved by Lepeltier *et al.*, where squalene-based nucleolipid conjugates attained different complex supramolecular structures depending on the site of conjugation rather than forming small micelles, additionally the difference in the shape of the formed supramolecular structures led to a difference in their pharmacological activities[32,50,56]. Therefore, the obtained AzaEPA and AzaDHA nanoassemblies are forming complex molecular structures that need few days to attain their final stable structure, with a positive zeta potential that could increase the cellular internalization by facilitating a charge-based interaction with negatively charged cell membrane surface[58].

**Table 2:** Stability of AzaEPA and AzaDHA self-assemblies over 5 days, reflected by the hydrodynamic diameter, zeta potential and polydispersity index (PDI). Data is expressed as mean  $\pm$  SD%.

Sample	Days	Hydrodynamic Diameter (nm)	Zeta Potential (mV)	PDI	Attenuator
AzaEPA	1	235.8 $\pm$ 7.3%	16.1 $\pm$ 8.54%	0.121 $\pm$ 24%	7
	2	206.7 $\pm$ 1.57%	-9.89 $\pm$ 2.02%	0.169 $\pm$ 12.8%	7
	3	190.1 $\pm$ 1.37%	25.8 $\pm$ 2.33%	0.16 $\pm$ 16.6%	7
	4	190.5 $\pm$ 0.963%	25.9 $\pm$ 2.8%	0.149 $\pm$ 14.4%	7
	5	194.5 $\pm$ 0.119%	35.7 $\pm$ 7.12%	0.137 $\pm$ 22.7%	7
	6	213 $\pm$ 1.76%	33.2 $\pm$ 8.79%	0.15 $\pm$ 16.4%	7
	7	217 $\pm$ 2.89 %	35.8 $\pm$ 4.86%	0.184 $\pm$ 13%	7
AzaDHA	1	229.5 $\pm$ 0.575%	18 $\pm$ 6.74%	0.082 $\pm$ 23.9%	7
	2	232.5 $\pm$ 1.37%	21.9 $\pm$ 4.63%	0.094 $\pm$ 16.4%	7
	3	217.7 $\pm$ 0.87%	-2.63 $\pm$ 28.6%	0.075 $\pm$ 21.8%	7
	4	189.2 $\pm$ 0.242%	22.7 $\pm$ 6.68%	0.77 $\pm$ 47.2%	7
	5	185 $\pm$ 0.952%	17.8 $\pm$ 4.05%	0.055 $\pm$ 67.5%	7
	6	189.7 $\pm$ 0.777%	37.8 $\pm$ 2.97%	0.138 $\pm$ 14.3%	7
	7	182.5 $\pm$ 3.91%	33 $\pm$ 6.09%	0.155 $\pm$ 13.2%	7

To conclude, an innovative platform was set up to transport a hydrophilic and a degradation sensitive anti-cancer agent. The synthesis of two amphiphilic conjugates was successfully performed and verified via several methods including  $^1\text{H}$  and  $^{13}\text{C}$  NMR, FTIR and elemental analysis. Their self-assembly in water was successful and confirmed via using the fluorescent probe pyrene method to determine the critical aggregation concentration. The formed nanoassemblies were then characterized presenting a hydrodynamic diameter of 190 nm and a positive surface charge, needing 5 days to attain a stable configuration, owing possibly to a complex supramolecular structure, which was revealed to be multilamellar vesicles by cryo-TEM. This study highlights the importance of this method in protecting the vulnerable azacitidine drug while increasing its bioavailability and offering improved drug loading capabilities compared to traditional nanovectors. The supramolecular structure should be verified via synchrotron-based small-angle X-ray scattering. Additionally, *in vitro* studies on the HL-60 cell line (acute myeloid leukemia) will be conducted to compare the efficacy of the self-assemblies compared to the parent drug via MTT assays and internalization studies.

### 3. Materials and Methods

#### 3.1. Materials

Dimethylformamide, methanol, tetrahydrofuran, trimethylamine, ethyl chloroformate, dichloromethane, sodium dihydrogen phosphate, magnesium sulfate and acetonitrile were obtained from Fisher (France). Eicosa-pentaenoic acid and docosahexaenoic acid were obtained from Combiblocks (USA). 5-azacitidine was obtained from TCI chemicals (Japan). Deionized water was obtained from a Milli-Q plus system (Merck-Millipore, Germany). Acetone and pyrene were obtained from Sigma-Aldrich (France).

#### 3.2. Synthesis and purification

1 equivalent of either omega-3 fatty acid (5Z,8Z,11Z,14Z,17Z)-eicosa-5,8,11,14,17-pentenoic acid (Eicosa-pentaenoic acid, EPA) or (4Z,7Z,10Z,13Z,16Z,19Z)-docosa-4,7,10,13,16,19-hexaenoic acid (Docosahexaenoic acid, DHA) was mixed with 2 equivalents of trimethylamine in 3 mL of dry tetrahydrofuran (THF) for 20 min at room temperature. The flask was cooled down to -10°C using an acetone ice bath and mixed for an additional 10 min, 2 equivalents of ethyl chloroformate in 3 mL THF were then added drop-wise to the mixture and allowed to mix for 10 min. Then, 100 mg of 4-amino-1-[(2R,3R,4S,5R)-3,4-dihydroxy-5-(hydroxymethyl)oxolan-2-yl]-1,3,5-triazin-2-one (5-azacitidine) in 9 mL of dimethylformamide (DMF) were added drop-wise and allowed to mix for 10 min. The mixture was then removed from the acetone ice bath to room temperature and stirred for 48 hours. The whole procedure was conducted under argon.

The mixture was then dried on a rotary evaporator at 40°C. Aqueous 0.02M sodium dihydrogen phosphate (NaH<sub>2</sub>PO<sub>4</sub>) was added and the mixture was extracted with dichloromethane. The organic layer was then washed with brine, dried on magnesium sulfate (MgSO<sub>4</sub>), and concentrated in vacuum.

The obtained oil was then purified by semi-preparative reversed phase high-performance liquid chromatography (RP-HPLC) using a Waters (France) instrument. Purification was performed at room temperature using XBridge BEH C18 OBD Prep Column, 130 Å pore size, 5 µm particles, 30 mm X 250 mm. Eluent (A) was acetonitrile (ACN) while eluent (B) was MilliQ H<sub>2</sub>O. A gradient elution was used with a flow rate of 37 mL/min and an injection volume of 1.5 mL. Peaks were detected at a wavelength of 214 nm (amide bond) and 240 nm (azacitidine). The crude oil was solubilized in 90% (A) and 10% (B) at a concentration of 10 mg/mL. The sample was vortexed, sonicated and filtered on a 0.22 µm Millex-LG filter (Merck, Germany) previous to injection. The collected purified conjugate was then concentrated in vacuum and lyophilized to obtain a white powder (Aza-DHA: 45 mg yield 20% ± 2.1%, AzaEPA: 21 mg yield 10% ± 1.4%).

#### 3.3. <sup>1</sup>H and <sup>13</sup>C NMR

<sup>1</sup>H NMR and <sup>13</sup>C NMR spectra were recorded in deuterated dimethyl sulfoxide (DMSO-d<sub>6</sub>) at 400 MHz for the <sup>1</sup>H NMR, and at 125 MHz for the <sup>13</sup>C NMR with a Bruker 500MHz AVANCE III HD spectrometer (Wissembourg, France) equilibrated at 25 °C, at the SFR Matrix of the University of Angers. Spectra were analyzed using the software MestReNova®.

AzaEPA: <sup>1</sup>H NMR (499 MHz, DMSO-d<sub>6</sub>) δ 8.55 (s, 1H), 7.66 – 7.58 (m, 1H), 5.71 (d, J = 5.8 Hz, 1H), 5.40 – 5.28 (m, 10H), 5.17 – 5.04 (m, 1H), 4.64 – 4.49 (m, 1H), 4.42 (q, J = 5.5 Hz, 1H), 4.34 – 4.18 (m, 1H), 4.09 – 4.00 (m, 1H), 3.89 (ddt, J = 27.4, 6.0, 3.0 Hz, 1H), 3.65 (tdd, J = 11.1, 5.9, 3.2 Hz, 1H), 3.61 – 3.53 (m, 1H), 2.85 – 2.76 (m, 8H), 2.44 – 2.35 (m, 2H), 2.11 – 2.01 (m, 4H), 1.60 (ddt, J = 14.5, 10.4, 4.8 Hz, 2H), 0.92 (tt, J = 7.6, 1.9 Hz, 3H). <sup>13</sup>C NMR (125 MHz, DMSO) δ 172.11, 165.68, 157.72, 153.04, 131.55, 128.11, 128.02, 127.89, 127.70, 126.94, 90.35, 84.05, 74.07, 68.01, 59.28, 36.42, 25.97, 25.20, 20.03, 14.11.

AzaDHA: <sup>1</sup>H NMR (499 MHz, DMSO-d<sub>6</sub>) δ 8.61 (d, J = 11.4 Hz, 1H), 7.83 (s, 1H), 5.71 (d, J = 5.2 Hz, 1H), 5.42 – 5.24 (m, 12H), 4.42 (t, J = 5.3 Hz, 1H), 4.29 (q, J = 6.1, 5.7 Hz, 1H), 4.21 – 4.15 (m, 1H), 4.07 (dd, J = 5.1, 2.4 Hz,



2H), 3.73 – 3.64 (m, 2H), 3.59 – 3.54 (m, 1H), 2.81 (dq,  $J = 21.7, 6.4, 5.7$  Hz, 10H), 2.43 (d,  $J = 7.3$  Hz, 2H), 2.33 (q,  $J = 7.8, 7.2$  Hz, 2H), 2.04 (td,  $J = 7.4, 1.5$  Hz, 2H), 0.92 (td,  $J = 7.6, 1.4$  Hz, 3H).  $^{13}\text{C}$  NMR (125 MHz, DMSO)  $\delta$  172.10, 157.74, 156.47, 153.12, 131.55, 127.90, 126.94, 90.35, 88.83, 74.07, 71.94, 68.00, 36.87, 25.20, 22.14, 20.03, 14.11.

### 3.4. Elemental analysis

Elemental analyses of C and H were conducted by Thermo Scientific – Elemental analyzer FLASH 2000 in the CHNS mode at the SFR Matrix of the University of Angers.

### 3.5. Fourier-Transform InfraRed spectroscopy

Fourier-Transform InfraRed spectroscopy FTIR spectra were recorded on a ThermoFisher Scientific Nicolet iS5 FTIR, with an iD7 ATR Diamond crystal accessory, for powder analysis. The spectra were obtained applying 16 scans per spectrum after 16 background scans and were analyzed in the frequency range of 4000–600  $\text{cm}^{-1}$ .

### 3.6. Mass spectrometry

The conjugates were dissolved acetonitrile + 0.1% formic acid at a concentration of 50  $\mu\text{g/mL}$ . The solution was directly infused at 10  $\mu\text{L/min}$  into a Quattro Micro® triple quadrupole mass spectrometer (Waters). Prior to infusion, the sample was vortexed, sonicated and filtered on a 0.22  $\mu\text{m}$  Millex-LG filter (Merck-Millipore, Germany). Ionization was achieved using electrospray in positive ion mode. The mass spectrometer was operated in multiple reaction monitoring mode. The entire system was controlled by Masslynx® software (Waters).

### 3.7. Critical aggregation concentration (CAC)

The CAC of the AzaEPA and AzaDHA suspensions was determined using pyrene as a fluorescent probe. Briefly, 6  $\mu\text{L}$  of pyrene stock solution in acetone (50  $\mu\text{M}$ ) was added into tubes. Then, acetone in tubes was evaporated in dark condition. The different suspension with a concentration ranging from 10 to 3000  $\mu\text{M}$  were added into tubes and mixed overnight at 37°C. The final concentration of pyrene was 1  $\mu\text{M}$ . After 30 min of equilibration at room temperature, a fluorescence spectrophotometer (Fluoromax-4, Horiba, Japan) was used to measure the fluorescence intensities of pyrene at an excitation wavelength of 336 nm. The emission spectra were recorded in the range 350–500 nm. The slit opening for the excitation was set at 1 nm and at 3 nm for the emission. Intensity ratios of pyrene at  $I_{372}/I_{382}$  ( $I1/I3$ ) were plotted against the log of the concentration.

### 3.8. Self-assembly formulation

AzaEPA and AzaDHA self-assemblies were prepared using the nanoprecipitation process. Briefly, AzaEPA or AzaDHA was dissolved in 0.25 mL of acetone (8  $\text{mg/mL}$ ), and added drop-wise under strong mechanical stirring to 1 mL of MiliQ water. The formation of the self-assemblies occurred spontaneously. The acetone was then completely evaporated using a rotary evaporator to obtain an aqueous suspension of self-assemblies with a final concentration 2  $\text{mg/mL}$  in prodrugs.

### 3.9. Dynamic Light Scattering (DLS)

Hydrodynamic diameter (Z-average size) and size polydispersity (PDI) were determined by dynamic light scattering on a Zetasizer® Nano series DTS 1060 (Malvern Instruments S.A., UK) at a scattering angle of 173°. Three consecutive measurements were performed for each sample. A good attenuator value (7 to 9) was obtained when suspending 20  $\mu\text{L}$  of the self-assemblies in 1 mL of distilled water. The mean diameter for each preparation resulted from the average of three measurements of 60 seconds each. For zeta potential measurements, 20  $\mu\text{L}$  of the self-assemblies were dissolved in 1 mL of 1 mM NaCl before filling the measurement cell. The mean zeta

potential for each preparation resulted from the average of three measurements in automatic mode. Size, PDI and zeta-potential are expressed as mean  $\pm$  SD%.

### 3.10. Cryogenic Transmission Electron Microscopy (Cryo-TEM)

Cryo-Tem studies were accomplished with a Cryo-TEM (Tecnai<sup>TM</sup> G2 Sphera, FEI, USA), at the Microscopy Rennes Imaging Center (Biogenouest, Rennes). A drop (4  $\mu$ L) of the (4 mg/mL) sample was deposited on the surface of a carbon-coated copper grid. This grid was held under controlled humidity and temperature conditions by tweezers on a guillotine device. A filter paper was then pressed against the sample to remove the excess liquid. Afterward, the filter paper is removed, and the plunger was allowed to drop into the liquid ethane in order to vitrify the sample. The grid was then transferred to a cryo-holder. Observations were made at an accelerating voltage of 200 kV under low electron dose. Analysis was performed with the ImageJ software.

**Funding:** Financial support by “La Ligue contre le cancer 49” association is gratefully acknowledged.

**Acknowledgments:** SFR Matrix for the NMR and elemental analysis, the Microscopy Rennes Imaging Center (MRic) of the UMS Biosit.

**Conflicts of Interest** The authors declare no conflict of interest. The authors declare no competing financial interest.

## 4. References

1. Hellström-Lindberg, E.; Tobiasson, M.; Greenberg, P. Myelodysplastic Syndromes: Moving towards Personalized Management. *Haematologica* **2020**, *105*, 1765–1779, doi:10.3324/haematol.2020.248955.
2. Hong, M.; He, G. The 2016 Revision to the World Health Organization Classification of Myelodysplastic Syndromes. *J Transl Int Med* **2017**, *5*, 139–143, doi:10.1515/jtim-2017-0002.
3. Itzykson, R.; Thépot, S.; Achour, B.; Quesnel, B.; Dreyfus, F.; Turlure, P.; Taksin, A.-L.; Vey, N.; Koka, A.M.; de Botton, S.; et al. Azacytidine (AZA) in MDS (Including RAEB-t and CMML) in Patients (Pts)  $\geq$  80 Years: Results of the French ATU Program. *Blood* **2009**, *114*, 1773, doi:10.1182/blood.V114.22.1773.1773.
4. Platzbecker, U.; Kubasch, A.S.; Homer-Bouthiette, C.; Prebet, T. Current Challenges and Unmet Medical Needs in Myelodysplastic Syndromes. *Leukemia* **2021**, *35*, 2182–2198, doi:10.1038/s41375-021-01265-7.
5. Musto, P.; Maurillo, L.; Spagnoli, A.; Gozzini, A.; Rivellini, F.; Lunghi, M.; Villani, O.; Aloe-Spiriti, M.A.; Venditti, A.; Santini, V. Azacitidine for the Treatment of Lower Risk Myelodysplastic Syndromes. *Cancer* **2010**, *116*, 1485–1494, doi:10.1002/cncr.24894.
6. Waespe, N.; Akker, M.V.D.; Klaassen, R.J.; Lieberman, L.; Irwin, M.S.; Ali, S.S.; Abdelhaleem, M.; Zlateska, B.; Liebman, M.; Cada, M.; et al. Response to Treatment with Azacitidine in Children with Advanced Myelodysplastic Syndrome Prior to Hematopoietic Stem Cell Transplantation. *Haematologica* **2016**, *101*, 1508–1515, doi:10.3324/haematol.2016.145821.
7. Keruakous, A.R.; Holter-Chakrabarty, J.; Schmidt, S.A.; Khawandanah, M.O.; Selby, G.; Yuen, C. Azacitidine Maintenance Therapy Post-Allogeneic Stem Cell Transplantation in Poor-Risk Acute Myeloid Leukemia. *Hematology/Oncology and Stem Cell Therapy* **2021**, doi:10.1016/j.hemonc.2021.03.001.

8. Oshrine, B.R.; Shyr, D.; Hale, G.; Petrovic, A. Low-Dose Azacitidine for Relapse Prevention after Allogeneic Hematopoietic Cell Transplantation in Children with Myeloid Malignancies. *Pediatr Transplant* **2019**, *23*, e13423, doi:10.1111/petr.13423.
9. Carter, J.L.; Hege, K.; Yang, J.; Kalpage, H.A.; Su, Y.; Edwards, H.; Hüttemann, M.; Taub, J.W.; Ge, Y. Targeting Multiple Signaling Pathways: The New Approach to Acute Myeloid Leukemia Therapy. *Sig Transduct Target Ther* **2020**, *5*, 1–29, doi:10.1038/s41392-020-00361-x.
10. Pleyer, L.; Döhner, H.; Dombret, H.; Seymour, J.F.; Schuh, A.C.; Beach, C.; Swern, A.S.; Burgstaller, S.; Stauder, R.; Girschikofsky, M.; et al. Azacitidine for Front-Line Therapy of Patients with AML: Reproducible Efficacy Established by Direct Comparison of International Phase 3 Trial Data with Registry Data from the Austrian Azacitidine Registry of the AGMT Study Group. *Int J Mol Sci* **2017**, *18*, 415, doi:10.3390/ijms18020415.
11. Dombret, H.; Seymour, J.F.; Butrym, A.; Wierzbowska, A.; Selleslag, D.; Jang, J.H.; Kumar, R.; Cavenagh, J.; Schuh, A.C.; Candoni, A.; et al. International Phase 3 Study of Azacitidine vs Conventional Care Regimens in Older Patients with Newly Diagnosed AML with >30% Blasts. *Blood* **2015**, *126*, 291–299, doi:10.1182/blood-2015-01-621664.
12. Baroud, M.; Lepeltier, E.; Thepot, S.; El-Makhour, Y.; Duval, O. The Evolution of Nucleosidic Analogues: Self-Assembly of Prodrugs into Nanoparticles for Cancer Drug Delivery. *Nanoscale Adv.* **2021**, *3*, 2157–2179, doi:10.1039/D0NA01084G.
13. Kordella, C.; Lamprianidou, E.; Kotsianidis, I. Mechanisms of Action of Hypomethylating Agents: Endogenous Retroelements at the Epicenter. *Frontiers in Oncology* **2021**, *11*, 490, doi:10.3389/fonc.2021.650473.
14. Gil-Perez, A.; Montalban-Bravo, G. Management of Myelodysplastic Syndromes after Failure of Response to Hypomethylating Agents. *Therapeutic Advances in Hematology* **2019**, *10*, 2040620719847059, doi:10.1177/2040620719847059.
15. Prébet, T.; Thepot, S.; Gore, S.D.; Dreyfus, F.; Fenaux, P.; Vey, N. Outcome of Patients with Low-Risk Myelodysplasia after Azacitidine Treatment Failure. *Haematologica* **2013**, *98*, e18–e19, doi:10.3324/haematol.2012.071050.
16. Prébet, T.; Gore, S.D.; Esterni, B.; Gardin, C.; Itzykson, R.; Thepot, S.; Dreyfus, F.; Rauzy, O.B.; Recher, C.; Adès, L.; et al. Outcome of High-Risk Myelodysplastic Syndrome After Azacitidine Treatment Failure. *J Clin Oncol* **2011**, *29*, 3322–3327, doi:10.1200/JCO.2011.35.8135.
17. Balouzet, C.; Chanut, C.; Jobard, M.; Brandely-Piat, M.-L.; Chast, F. Stability of 25 Mg/ML Azacitidine Suspensions Kept in Fridge after Freezing. *Pharmaceutical Technology in Hospital Pharmacy* **2017**, *2*, 11–16, doi:10.1515/pthp-2016-0023.
18. Walker, S.E.; Charbonneau, L.F.; Law, S.; Earle, C. Stability of Azacitidine in Sterile Water for Injection. *Can J Hosp Pharm* **2012**, *65*, 352–359.
19. Damaraju, V.L.; Mowles, D.; Yao, S.; Ng, A.; Young, J.D.; Cass, C.E.; Tong, Z. Role of Human Nucleoside Transporters in the Uptake and Cytotoxicity of Azacitidine and Decitabine. *Nucleosides Nucleotides Nucleic Acids* **2012**, *31*, 236–255, doi:10.1080/15257770.2011.652330.
20. Fanciullino, R.; Mercier, C.; Serdjebi, C.; Berda, Y.; Fina, F.; Ouafik, L.; Lacarelle, B.; Ciccolini, J.; Costello, R. Lethal Toxicity after Administration of Azacytidine: Implication of the Cytidine Deaminase-Deficiency Syndrome. *Pharmacogenetics and Genomics* **2015**, *25*, 317–321, doi:10.1097/FPC.0000000000000139.
21. Chabner, B.A.; Drake, J.C.; Johns, D.G. Deamination of 5-Azacytidine by a Human Leukemia Cell Cytidine Deaminase. *Biochemical Pharmacology* **1973**, *22*, 2763–2765, doi:10.1016/0006-2952(73)90137-8.

22. Fanciullino, R.; Mercier, C.; Serdjabi, C.; Venton, G.; Colle, J.; Fina, F.; Ouafik, L.; Lacarelle, B.; Ciccolini, J.; Costello, R. Yin and Yang of Cytidine Deaminase Roles in Clinical Response to Azacitidine in the Elderly: A Pharmacogenetics Tale. *Pharmacogenomics* **2015**, *16*, 1907–1912, doi:10.2217/pgs.15.135.
23. Zhang, X.; Li, Y.; Hu, C.; Wu, Y.; Zhong, D.; Xu, X.; Gu, Z. Engineering Anticancer Amphipathic Peptide-Dendronized Compounds for Highly-Efficient Plasma/Organelle Membrane Perturbation and Multidrug Resistance Reversal. *ACS Appl. Mater. Interfaces* **2018**, *10*, 30952–30962, doi:10.1021/acsami.8b07917.
24. Zhang, R.; Qin, X.; Kong, F.; Chen, P.; Pan, G. Improving Cellular Uptake of Therapeutic Entities through Interaction with Components of Cell Membrane. *Drug Deliv* **2019**, *26*, 328–342, doi:10.1080/10717544.2019.1582730.
25. Zhong, Y.-J.; Shao, L.-H.; Li, Y. Cathepsin B-Cleavable Doxorubicin Prodrugs for Targeted Cancer Therapy (Review). *International Journal of Oncology* **2013**, *42*, 373–383, doi:10.3892/ijo.2012.1754.
26. Xu, Y.; Geng, J.; An, P.; Xu, Y.; Huang, J.; Lu, W.; Liu, S.; Yu, J. Cathepsin B-Sensitive Cholesteryl Hemisuccinate-Gemcitabine Prodrug Nanoparticles: Enhanced Cellular Uptake and Intracellular Drug Controlled Release. *RSC Adv.* **2014**, *5*, 6985–6992, doi:10.1039/C4RA13870H.
27. Ni, Y.; Hai, Z.; Zhang, T.; Wang, Y.; Yang, Y.; Zhang, S.; Liang, G. Cathepsin B Turning Bioluminescence “On” for Tumor Imaging. *Anal. Chem.* **2019**, *91*, 14834–14837, doi:10.1021/acs.analchem.9b04254.
28. Luo, C.; Sun, J.; Sun, B.; He, Z. Prodrug-Based Nanoparticulate Drug Delivery Strategies for Cancer Therapy. *Trends in Pharmacological Sciences* **2014**, *35*, 556–566, doi:10.1016/j.tips.2014.09.008.
29. Mura, S.; Bui, D.T.; Couvreur, P.; Nicolas, J. Lipid Prodrug Nanocarriers in Cancer Therapy. *Journal of Controlled Release* **2015**, *208*, 25–41, doi:10.1016/j.jconrel.2015.01.021.
30. Sivakova, S.; Rowan, S.J. Nucleobases as Supramolecular Motifs. *Chem. Soc. Rev.* **2005**, *34*, 9–21, doi:10.1039/B304608G.
31. Gong, X.; Moghaddam, M.J.; Sagnella, S.M.; Conn, C.E.; Danon, S.J.; Waddington, L.J.; Drummond, C.J. Lamellar Crystalline Self-Assembly Behaviour and Solid Lipid Nanoparticles of a Palmityl Prodrug Analogue of Capecitabine—A Chemotherapy Agent. *Colloids and Surfaces B: Biointerfaces* **2011**, *85*, 349–359, doi:10.1016/j.colsurfb.2011.03.007.
32. Lepeltier, E.; Bourgaux, C.; Maksimenko, A.; Meneau, F.; Rosilio, V.; Sliwinski, E.; Zouhiri, F.; Desmaële, D.; Couvreur, P. Self-Assembly of Polyisoprenoyl Gemcitabine Conjugates: Influence of Supramolecular Organization on Their Biological Activity. *Langmuir* **2014**, *30*, 6348–6357, doi:10.1021/la5007132.
33. Picou, F.; Debeissat, C.; Bourgeais, J.; Gallay, N.; Ferrié, E.; Foucault, A.; Ravalet, N.; Maciejewski, A.; Vallet, N.; Ducrocq, E.; et al. N-3 Polyunsaturated Fatty Acids Induce Acute Myeloid Leukemia Cell Death Associated with Mitochondrial Glycolytic Switch and Nrf2 Pathway Activation. *Pharmacological Research* **2018**, *136*, 45–55, doi:10.1016/j.phrs.2018.08.015.
34. Yamagami, T.; Porada, C.D.; Pardini, R.; Zanjani, E.D.; Almeida-Porada, G.D. Docosahexanoic Acid Induces Dose Dependent Cell Death in an Early Undifferentiated Subtype of Acute Myeloid Leukemia Cell Line. *Cancer Biology & Therapy* **2009**, *8*, 331–337, doi:10.4161/cbt.8.4.7334.
35. Aires, V.; Hichami, A.; Filomenko, R.; Plé, A.; Rébé, C.; Bettaieb, A.; Khan, N.A. Docosahexanoic Acid Induces Increases in  $[Ca^{2+}]_i$  via Inositol 1,4,5-Triphosphate Production and Activates Protein Kinase  $C\gamma$  and  $\delta$  via Phosphatidylserine Binding Site: Implication in Apoptosis in U937 Cells. *Mol. Pharmacol.* **2007**, *72*, 1545–1556, doi:10.1124/mol.107.039792.
36. Ceccarelli, V.; Racanicchi, S.; Martelli, M.P.; Nocentini, G.; Fettucciari, K.; Riccardi, C.; Marconi, P.; Di Nardo, P.; Grignani, F.; Binaglia, L.; et al. Eicosapentaenoic Acid Demethylates a Single CpG That Mediates Expression of



- Tumor Suppressor CCAAT/Enhancer-Binding Protein  $\delta$  in U937 Leukemia Cells. *J. Biol. Chem.* **2011**, *286*, 27092–27102, doi:10.1074/jbc.M111.253609.
37. Ceccarelli, V.; Nocentini, G.; Billi, M.; Racanicchi, S.; Riccardi, C.; Roberti, R.; Grignani, F.; Binaglia, L.; Vecchini, A. Eicosapentaenoic Acid Activates RAS/ERK/C/EBP $\beta$  Pathway through H-Ras Intron 1 CpG Island Demethylation in U937 Leukemia Cells. *PLoS ONE* **2014**, *9*, e85025, doi:10.1371/journal.pone.0085025.
38. Varney, M.E.; Hardman, W.E.; Sollars, V.E. Omega 3 Fatty Acids Reduce Myeloid Progenitor Cell Frequency in the Bone Marrow of Mice and Promote Progenitor Cell Differentiation. *Lipids Health Dis* **2009**, *8*, 9, doi:10.1186/1476-511X-8-9.
39. Desmaële, D.; Gref, R.; Couvreur, P. Squalenoylation: A Generic Platform for Nanoparticular Drug Delivery. *Journal of Controlled Release* **2012**, *161*, 609–618, doi:10.1016/j.jconrel.2011.07.038.
40. Lepeltier, E.; Bourgaux, C.; Rosilio, V.; Poupaert, J.H.; Meneau, F.; Zouhiri, F.; Lepêtre-Mouelhi, S.; Desmaële, D.; Couvreur, P. Self-Assembly of Squalene-Based Nucleolipids: Relating the Chemical Structure of the Bioconjugates to the Architecture of the Nanoparticles. *Langmuir* **2013**, *29*, 14795–14803, doi:10.1021/la403338y.
41. Maksimenko, A.; Caron, J.; Mougin, J.; Desmaële, D.; Couvreur, P. Gemcitabine-Based Therapy for Pancreatic Cancer Using the Squalenoyl Nucleoside Monophosphate Nanoassemblies. *International Journal of Pharmaceutics* **2015**, *482*, 38–46, doi:10.1016/j.ijpharm.2014.11.009.
42. Wu, L.; Zhang, F.; Chen, X.; Wan, J.; Wang, Y.; Li, T.; Wang, H. Self-Assembled Gemcitabine Prodrug Nanoparticles Show Enhanced Efficacy against Patient-Derived Pancreatic Ductal Adenocarcinoma. *ACS Appl. Mater. Interfaces* **2020**, *12*, 3327–3340, doi:10.1021/acsami.9b16209.
43. Bui, D.T.; Nicolas, J.; Maksimenko, A.; Desmaële, D.; Couvreur, P. Multifunctional Squalene-Based Prodrug Nanoparticles for Targeted Cancer Therapy. *Chem. Commun. (Camb.)* **2014**, *50*, 5336–5338, doi:10.1039/c3cc47427e.
44. Vandana, M.; Sahoo, S.K. Long Circulation and Cytotoxicity of PEGylated Gemcitabine and Its Potential for the Treatment of Pancreatic Cancer. *Biomaterials* **2010**, *31*, 9340–9356, doi:10.1016/j.biomaterials.2010.08.010.
45. Wu, L.; Zhang, F.; Chen, X.; Wan, J.; Wang, Y.; Li, T.; Wang, H. Self-Assembled Gemcitabine Prodrug Nanoparticles Show Enhanced Efficacy against Patient-Derived Pancreatic Ductal Adenocarcinoma. *ACS Appl. Mater. Interfaces* **2020**, *12*, 3327–3340, doi:10.1021/acsami.9b16209.
46. Sun, B.; Luo, C.; Cui, W.; Sun, J.; He, Z. Chemotherapy Agent-Unsaturated Fatty Acid Prodrugs and Prodrug-Nanoplatforams for Cancer Chemotherapy. *Journal of Controlled Release* **2017**, *264*, 145–159, doi:10.1016/j.jconrel.2017.08.034.
47. Naguib, Y.W.; Lansakara-P., D.; Lashinger, L.M.; Rodriguez, B.L.; Valdes, S.; Niu, M.; Aldayel, A.M.; Peng, L.; Hursting, S.D.; Cui, Z. Synthesis, Characterization, and In Vitro and In Vivo Evaluations of 4-(N)-Docosahexaenoyl 2', 2'-Difluorodeoxycytidine with Potent and Broad-Spectrum Antitumor Activity. *Neoplasia* **2016**, *18*, 33–48, doi:10.1016/j.neo.2015.11.012.
48. Desmaële, D.; Gref, R.; Couvreur, P. Squalenoylation: A Generic Platform for Nanoparticular Drug Delivery. *Journal of Controlled Release* **2012**, *161*, 609–618, doi:10.1016/j.jconrel.2011.07.038.
49. Huang, C.-W.; Mohamed, M.G.; Zhu, C.-Y.; Kuo, S.-W. Functional Supramolecular Polypeptides Involving  $\pi$ - $\pi$  Stacking and Strong Hydrogen-Bonding Interactions: A Conformation Study toward Carbon Nanotubes (CNTs) Dispersion. *Macromolecules* **2016**, *49*, 5374–5385, doi:10.1021/acs.macromol.6b01060.
50. Lepeltier, E.; Bourgaux, C.; Rosilio, V.; Poupaert, J.H.; Meneau, F.; Zouhiri, F.; Lepêtre-Mouelhi, S.; Desmaële, D.; Couvreur, P. Self-Assembly of Squalene-Based Nucleolipids: Relating the Chemical Structure of the Bioconjugates to the Architecture of the Nanoparticles. *Langmuir* **2013**, *29*, 14795–14803, doi:10.1021/la403338y.

51. Maksimenko, A.; Caron, J.; Mougin, J.; Desmaële, D.; Couvreur, P. Gemcitabine-Based Therapy for Pancreatic Cancer Using the Squalenoyl Nucleoside Monophosphate Nanoassemblies. *International Journal of Pharmaceutics* **2015**, *482*, 38–46, doi:10.1016/j.ijpharm.2014.11.009.
52. Xie, B.; Wan, J.; Chen, X.; Han, W.; Wang, H. Preclinical Evaluation of a Cabazitaxel Prodrug Using Nanoparticle Delivery for the Treatment of Taxane-Resistant Malignancies. *Mol Cancer Ther* **2020**, *19*, 822–834, doi:10.1158/1535-7163.MCT-19-0625.
53. Wang, H.; Lu, Z.; Wang, L.; Guo, T.; Wu, J.; Wan, J.; Zhou, L.; Li, H.; Li, Z.; Jiang, D.; et al. New Generation Nanomedicines Constructed from Self-Assembling Small-Molecule Prodrugs Alleviate Cancer Drug Toxicity. *Cancer Res* **2017**, *77*, 6963–6974, doi:10.1158/0008-5472.CAN-17-0984.
54. Fan, Q.; Ji, Y.; Wang, J.; Wu, L.; Li, W.; Chen, R.; Chen, Z. Self-Assembly Behaviours of Peptide–Drug Conjugates: Influence of Multiple Factors on Aggregate Morphology and Potential Self-Assembly Mechanism. *Royal Society Open Science* **2017**, *5*, 172040, doi:10.1098/rsos.172040.
55. Buettner, C.J.; Wallace, A.J.; Ok, S.; Manos, A.A.; Nicholl, M.J.; Ghosh, A.; Tweedle, M.F.; Goldberger, J.E. Balancing the Intermolecular Forces in Peptide Amphiphiles for Controlling Self-Assembly Transitions. *Org Biomol Chem* **2017**, *15*, 5220–5226, doi:10.1039/c7ob00875a.
56. Lepeltier, E.; Bourgaux, C.; Amenitsch, H.; Rosilio, V.; Lepetre-Mouelhi, S.; Zouhiri, F.; Desmaële, D.; Couvreur, P. Influence of the Nanoprecipitation Conditions on the Supramolecular Structure of Squalenoyled Nanoparticles. *European Journal of Pharmaceutics and Biopharmaceutics* **2015**, *96*, 89–95, doi:10.1016/j.ejpb.2015.07.004.
57. Panahi, Y.; Farshbaf, M.; Mohammadhosseini, M.; Mirahadi, M.; Khalilov, R.; Saghfi, S.; Akbarzadeh, A. Recent Advances on Liposomal Nanoparticles: Synthesis, Characterization and Biomedical Applications. *Artificial Cells, Nanomedicine, and Biotechnology* **2017**, *45*, 788–799, doi:10.1080/21691401.2017.1282496.
58. Gratton, S.E.A.; Ropp, P.A.; Pohlhaus, P.D.; Luft, J.C.; Madden, V.J.; Napier, M.E.; DeSimone, J.M. The Effect of Particle Design on Cellular Internalization Pathways. *PNAS* **2008**, *105*, 11613–11618, doi:10.1073/pnas.0801763105.

## Supplementary data

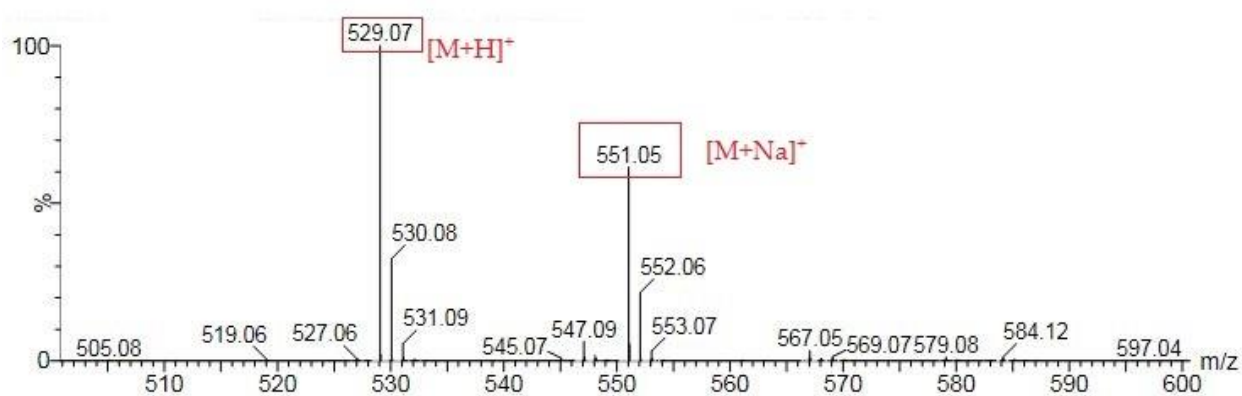


Figure S 1: Mass spectra of the azacitidine-EPA conjugate.

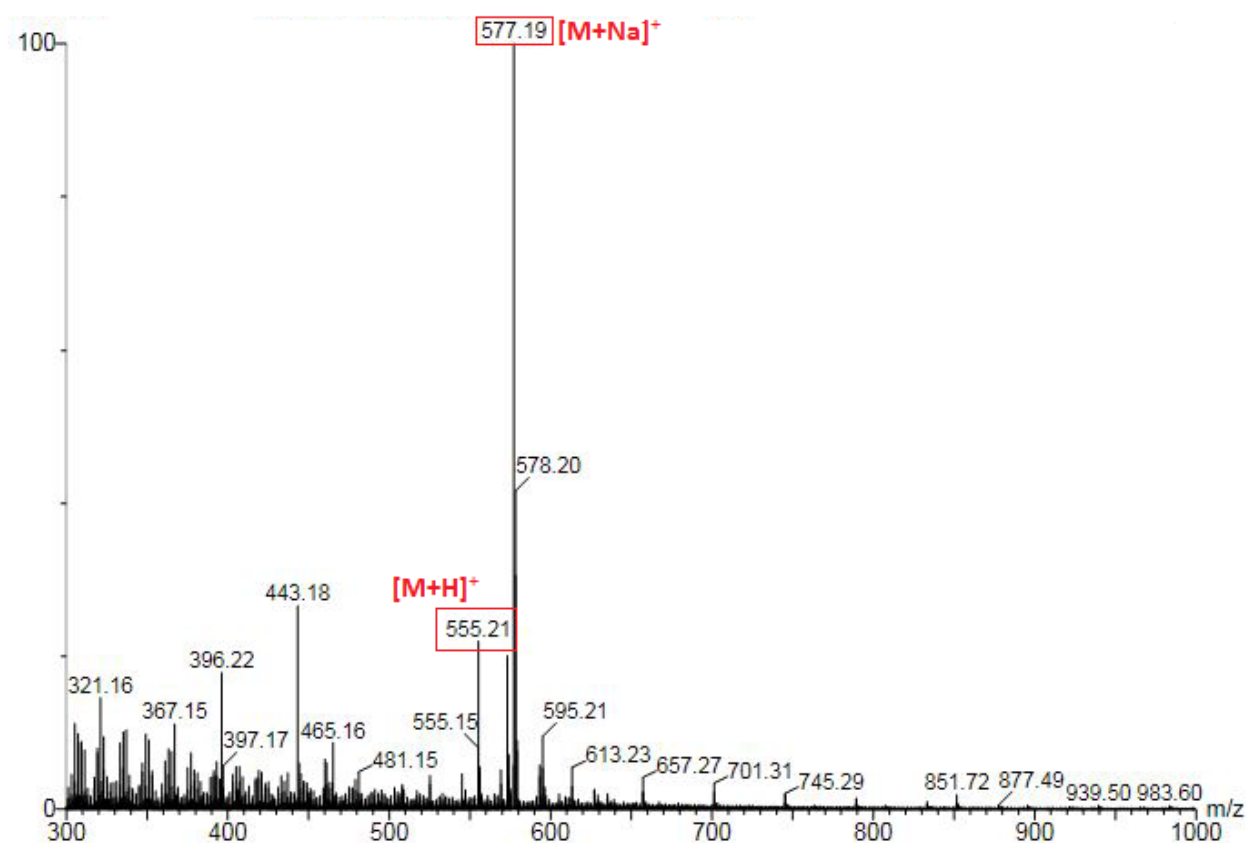
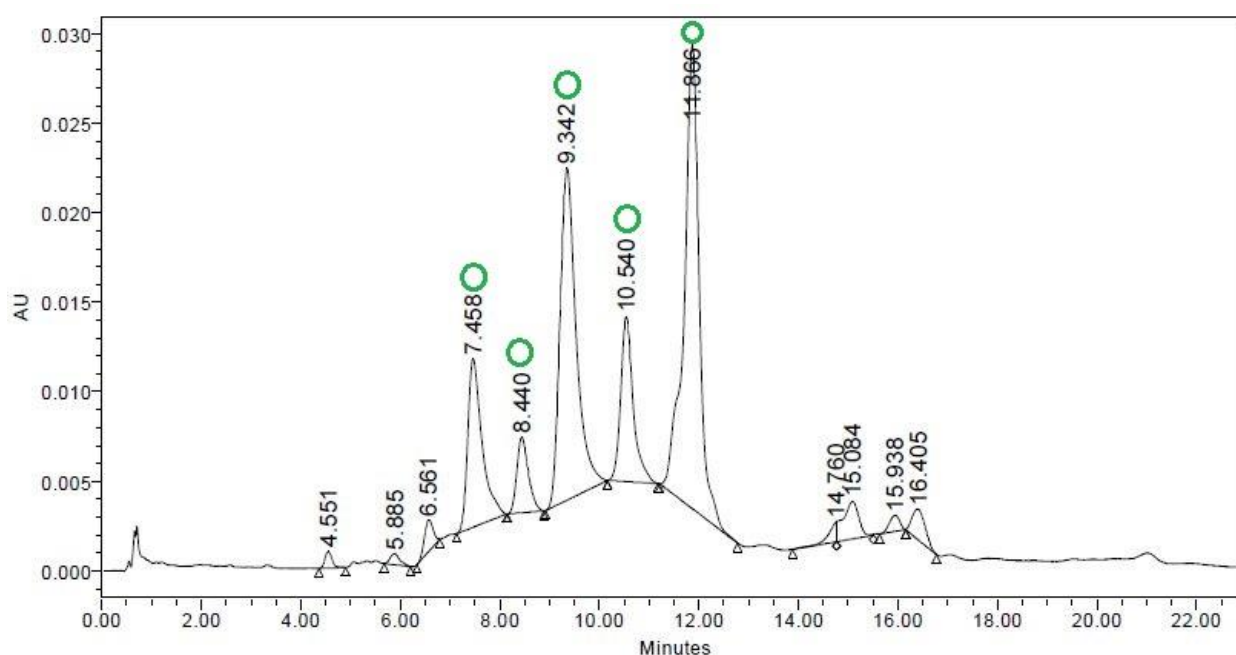


Figure S 2: Mass spectra of the azacitidine-DHA conjugate.

A UPLC-UV method was developed to evaluate the purity of the conjugates (**Figure S3**). A UPLC Acquity HClass Bio (Waters, France) consisting in a quaternary solvent manager, a sample manager, a photo diode array detector and a column manager were used. The system was controlled via Empower®3 software (Waters). The column used was an Acquity®UPLC BEH C18 50 x 2.1 mm, 1.7 µm (Waters). The mobile phase was composed of a mixture of acetonitrile and water (1:1). The purified product was dissolved in acetonitrile at a concentration of 100 µg/mL. Prior to injection, the sample was vortexed, sonicated and filtered on a 0.22 µm Millex-LG filter (Merck-Millipore, Germany). Flow rate was set to 0.2 mL/min and injection volume was set to 2 µL. The product was eluted in isocratic. Detection was fixed at 212 nm. Several peaks were observed, due to the use of an organic solvent and water, thus pushing the amphiphilic molecules to self-assemble, explaining the various retention times observed, but corresponding to the same conjugate.



**Figure S 3: Chromatogram of the azacitidine-EPA conjugate to determine its purity.** Peaks indicated by a green circle contain only AzaEPA.

The UPLC-UV method was transferred to LC-MS using Waters software to achieve a similar chromatogram (**Figure S4** and **Figure S5**). The LC-MS/MS method was developed on an Alliance® 2695 system (Waters) with a 150 × 2.0 mm, 5 µm Uptisphere C18 5ODB column (Interchim, France). The mobile phase was composed of a mixture of acetonitrile and water (1:1). The product was eluted isocratically. The purified product was dissolved in acetonitrile at a concentration of 1 mg/mL. The sample was vortexed, sonicated and filtered on a 0.22 µm Millex-



LG filter (Merck, Germany). The flow rate was 0.2 mL/min and the injection volume was set at 5  $\mu$ L. The total HPLC effluent was injected into a Quattro Micro®triple quadrupole mass spectrometer (Waters, France). Ionization was achieved using electrospray in positive ion mode in the  $m/z$  200–1500 range (full scan acquisition). An option of cone ramp was used between 20 and 60 V to optimize the acquisition. The obtained peaks from the chromatogram matched those of the UPLC: each peak was analyzed by mass spectrometry to determine the desired product. Finally the area under the curve of the UPLC chromatogram was taken into consideration to determine the purity of the products: AzaEPA purity was 92% while the purity of AzaDHA was 97%.

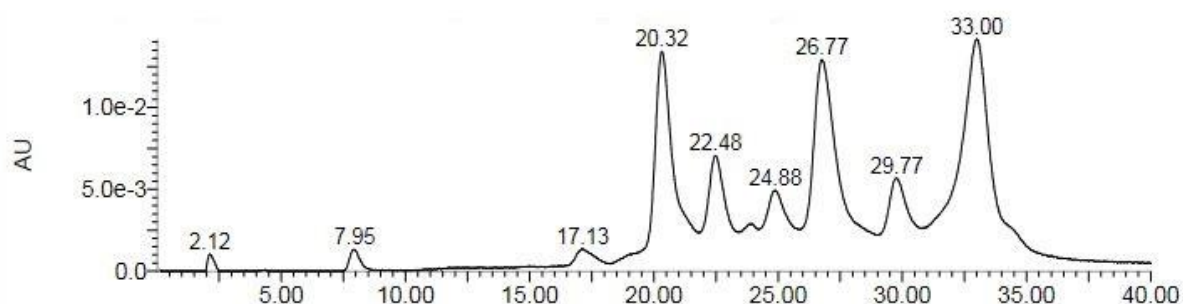


**Figure S 4: Chromatogram of the azacitidine-EPA conjugate to determine its purity.**

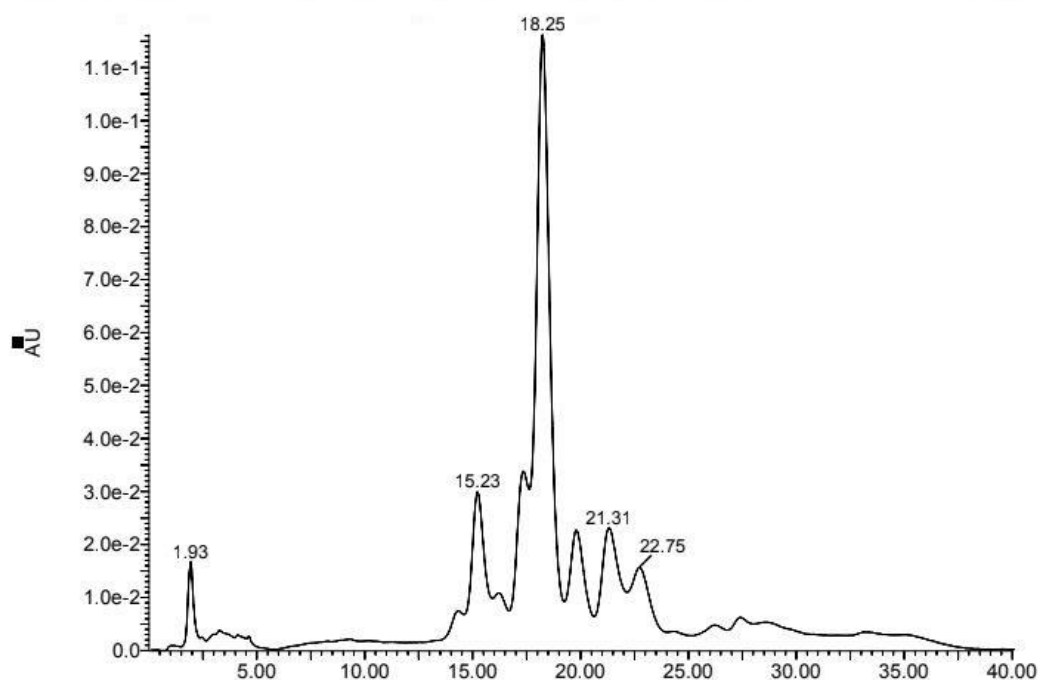


**Figure S 5: Chromatogram of the azacitidine-DHA conjugate to determine its purity.**

### 3. Nanoparticle tracking analysis

Nanoparticle tracking analysis (NTA) was carried out using the NanoSight NS300 (Malvern Instruments Ltd, UK). The suspensions were diluted in ultrapure water in order to have optimum concentration ranging between  $1 \times 10^8$  and  $1 \times 10^9$  particles per mL, to allow a conform analysis of the software to track the movement of each individual particle. Prior to each analysis, samples were filtered through a  $0.20 \mu\text{m}$  Whatman™ Anotop™ filter. Ultrapure water and suspensions were infused in the sample chamber using a syringe pump at  $40 \mu\text{L}/\text{min}$  rate. A 405 nm laser was used to illuminate the particles, and their Brownian motion was recorded using the sCMOS camera of the instrument. Subsequently, the NTA software (NTA 3.2) allowed for processing of the data. The nanoparticle concentration was obtained after correction by the dilution factor.

NTA is based on the scattered of applied light by each individual particle under Brownian motion: the diffusion constant is then obtained and used to calculate the hydrodynamic diameter number distribution via the Stokes-Einstein equation. The NTA is also able to give a concentration of particle per volume unit. The device measures the diffusion through following the random movement of each nanoparticle taken individually, achieved in using a 20x magnification microscope equipped with a camera. NTA allows for the detection of particles between 20 nm and 2000 nm of diameter. Using this technique, the concentration of observed particles can be determined as well as obtaining a distribution in number rather than in intensity (obtained by DLS). Nonetheless, this technique requires a significant dilution of the sample to be able to have a concentration ranging between  $10^8$  to  $10^9$  particles/mL to ensure that the density of these nanoparticles is not too high. As for the DLS, the NTA uses the assumption that spherical objects are studied.

The NTA analysis of the AzaEPA and AzaDHA self-assemblies revealed the presence of other populations of nanoparticles than using the DLS (**Figure 27**). Two other populations with a diameter of 116 nm and 158 nm were observed for the AzaDHA self-assemblies, whereas for the AzaEPA several others were detectable with the 108 nm, 141 nm and 178 nm populations being predominant.

Interestingly, the detected concentration of particles/mL is supplied by the analysis software, allowing for the calculation of the amount of material detected. According to these measurements and the mean diameter obtained, for both AzaDHA and AzaEPA self-assemblies, the nanoparticle population observed represents only 7% of the initial matter in suspension, raising the question of the fate of the 93% matter remaining. A hypothesis could be that the majority of the self-

assemblies would have formed micelles of around 5-10 nm in diameter, corresponding to twice the length of the molecules, undetectable by DLS or NTA. Indeed, this difficulty has already been identified in Guyon *et al.*'s work<sup>232,233</sup>: during two years, the polyarginine-ferrocifen self-assemblies were characterized as objects of 100 nm in diameter by diverse famous technics: DLS, NTA and Cryo-TEM. However, SAXS and DOSY NMR demonstrated that 99% of the matter were finally forming micelles of 5 nm in diameter. This diameter is yet a crucial parameter, which will influence the interaction with cells, the internalization pathways, the biodistribution and the final biological efficacy. Moreover, for a scale-up process, it is a critical parameter that has to be confirmed after every new batch of production: a reliable value has to be determined in order to be reproducible.

Thus, DOSY NMR (diffusion ordered spectroscopy) and SAXS should be performed to characterize AzaEPA and AzaDHA self-assemblies.

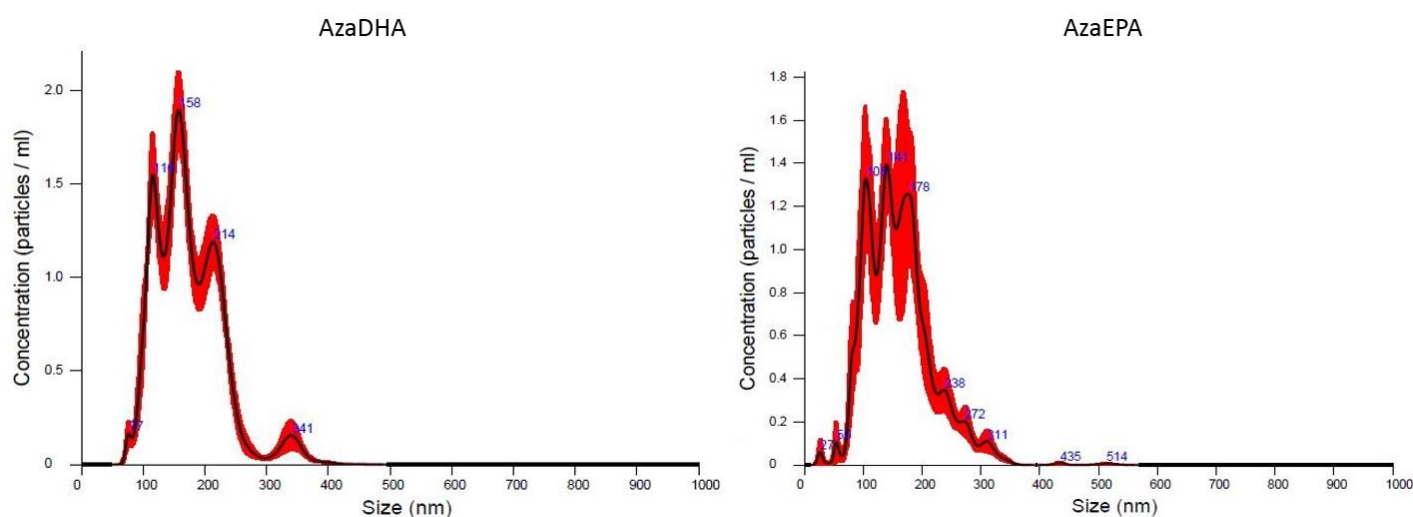


**Figure 27: Population distribution graphs of the AzaDHA and AzaEPA self-assemblies obtained by NTA.**

## 4. Conclusion

In summary, aiming to achieve the conjugation of azacitidine to the fatty acids, two approaches were executed. The first approach was initiated by the protection of the OH groups of the azacitidine sugar ring, followed by its conjugation to the fatty acids via an amide bond, lastly the protected groups were removed to attain an azacitidine-fatty acid conjugate. The second more direct approach was based on the use of a suitable conjugating agent to directly obtain the conjugate after purification.

In the protection approach, the conjugation process was hindered due to the low reactivity of the azacitidine amine group. However, ethyl chloroformate was finally successful in conjugating these azacitidine moiety to the fatty acids. The protected conjugation was followed by a deprotection step, though the final prodrug was irretrievable owing to challenges in the purification.

The direct conjugation approach succeeded with a low yield (10-20%), but with a good purity. The obtained prodrugs were verified using  $^1\text{H}$  and  $^{13}\text{C}$  NMR, FTIR, mass spectra and elemental analysis.

Then, their self-assembly in water was successful and confirmed by the fluorescent probe pyrene method to determine the critical aggregation concentration. The obtained self-assemblies were then characterized by DLS and a mean hydrodynamic diameter of 190 nm and a positive surface charge were observed. Additionally, the final stable configuration of the self-assemblies needed 5 days to be formed. Moreover, the results obtained by NTA may hint at the existence of micelles undetectable by DLS or NTA.

This study sheds the light on a drug delivery system able to protect the vulnerable azacitidine drug while increasing its bioavailability and offering improved drug loading capabilities compared to traditional nanovectors.

The multilamellar vesicle supramolecular structure observed by Cryo-TEM should be confirmed via synchrotron-based small-angle X-ray scattering. Moreover, DOSY NMR studies must be performed to confirm the existence of the hypothesized micelles.



## Chapter 3: Viability assay and internalization study

This section aims to introduce the conducted preliminary *in vitro* experiments. After obtaining the prodrug conjugates and their self-assembly, the nanoassemblies were tested *in vitro* on the HL-60 cell line (human promyelocytic cell line derived from a patient with acute myeloid leukemia).

The cytotoxicity of AzaDHA and AzaEPA self-assemblies were determined via a MTT test (Tetrazolium dye assay). Afterwards, two compatible BODIPY dyes were co-nanoprecipitated with both prodrugs, in order to perform FRET (Förster Resonance Energy Transfer). Then, the cell internalization of these self-assemblies was studied by FACS (Fluorescence-Activated Cell Sorting), after 30 min, 2 h, 4 h, 8 h and 24 h.

### 1. Materials and methods

#### 1.1. Materials

HL-60 cell line was obtained from the DSMZ German Collection of Microorganisms and Cell Cultures (Germany). Roswell Park Memorial Institute 1640 (RPMI) medium was purchased from Sigma-Aldrich (USA). Fetal bovine serum (FBS), penicillin, streptomycin and phosphate-buffered saline (PBS) were obtained from Gibco (Fisher, France). MTT (3-(4, 5- dimethylthiazol-2-yl)-2, 5-diphenyltetrazolium bromide)), phosphate buffered saline (PBS) and dimethyl sulfoxide (DMSO) were purchased from Sigma-Aldrich (USA). CholEsteryl BODIPY™ FL C12 505/511 (donor) and the CholEsteryl BODIPY™ C11 542/563 (acceptor) dyes were purchased from Thermofisher Scientific (Fisher, France). Paraformaldehyde 32% was purchased from Sigma-Aldrich (USA).

#### 1.2. Cell culture

HL-60 cells were grown in RPMI medium supplemented with 10% FBS, 1% penicillin-streptomycin (Invitrogen, Gibco), 2% Glutamax 100x, at 37°C and 5% CO<sub>2</sub>. Cells were divided to the eighth every 2-3 days, used between passage 2 and 10.

### 1.3. Self-assembly formulation

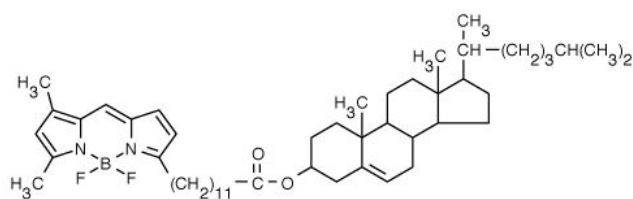
AzaEPA and AzaDHA self-assemblies were prepared using the nanoprecipitation process. Briefly, AzaEPA or AzaDHA were dissolved in 0.25 mL of acetone (8 mg/mL), and added drop-wise under strong mechanical stirring to 1 mL of MiliQ water. The formation of the self-assemblies occurred spontaneously. The acetone was then completely evaporated using a rotary evaporator to obtain an aqueous suspension of self-assemblies with a final concentration 2 mg/mL in prodrugs.

### 1.4. Self-assembly based FRET formulation

To achieve FRET, two fluorescent dyes were used: CholEsteryl BODIPY™ FL C12 505/511 (donor) and the CholEsteryl BODIPY™ C11 542/563 (acceptor), already tested by Gaudin *et al.* and established to perform FRET<sup>215</sup> (**Figure 28**).

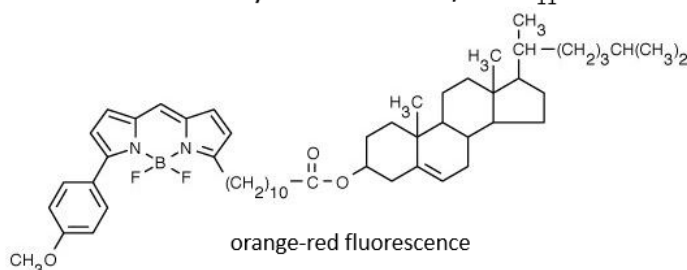
Self-assemblies based FRET were obtained using the same procedure, 0.5% w/w of the fluorescent probe CholEsteryl BODIPY® FL C12 (Invitrogen) and/or 0.5% w/w of the fluorescent probe CholEsteryl BODIPY® 542/563 C11 (Invitrogen) were dissolved in acetone (containing AzaEPA or AzaDHA prodrugs) before the drop-wise addition to the MiliQ water. The fluorescence of the self-assemblies was analyzed using a Fluoromax spectrometer (Horiba, Japan).

CholEsteryl BODIPY™ 505/511 FL C<sub>12</sub>



green fluorescence

CholEsteryl BODIPY™ 542/563 C<sub>11</sub>



orange-red fluorescence

**Figure 28: Chemical structure of CholEsteryl BODIPY™ FL C12 and CholEsteryl™ BODIPY C11.**

The following self-assemblies were obtained: AzaDHA BODIPY C12 self-assemblies (AzaDHA co-nanoprecipitated with CholEsteryl BODIPY® FL C12 at 0.5% or 1% in dye concentrations), AzaDHA BODIPY C11 self-assemblies (AzaDHA co-nanoprecipitated with CholEsteryl BODIPY® C11 at 0.5% or 1% in dye concentrations), AzaDHA BODIPY FRET self-assemblies (AzaDHA co-nanoprecipitated with both CholEsteryl BODIPY® FL C12 and CholEsteryl BODIPY® C11 at 0.5% in dye concentrations), AzaEPA BODIPY C12 self-assemblies (AzaEPA co-nanoprecipitated with CholEsteryl BODIPY® FL C12 at 0.5% or 1% in dye concentrations), AzaEPA BODIPY C11 self-assemblies (AzaEPA co-nanoprecipitated with CholEsteryl BODIPY® C11 at 0.5% or 1% in dye concentrations) and AzaEPA BODIPY FRET self-assemblies (AzaEPA co-nanoprecipitated with both CholEsteryl BODIPY® FL C12 and CholEsteryl BODIPY® C11 at 0.5% in dye concentrations).

## **1.5. MTT**

The cytotoxicity was determined with a colorimetric assay using succinate dehydrogenase activity of viable cells by the reduction of the yellow-colored tetrazolium salt, 3-(4,5-dimethylthiazol-2-yl)-2,5-diphenyl tetrazolium bromide to a purple-colored formazan crystal (MTT assay). Briefly, HL-60 cells were plated in 96-well plates at densities of 100,000 cells/well. After 24 h, cells were treated for 6, 24 and 48 h with different concentrations of self-assemblies prepared from a 2 mg/mL mother solution of self-assemblies and diluted in media. Then, cells were incubated for 4 h with the MTT solution (0.5 mg/mL in PBS). The medium was removed and 0.1 M HCl-SDS solution (100  $\mu$ L/well) was added to solubilize the formazan crystals. Samples were finally analyzed with absorbance detection at 570 nm on a plate reader (SpectraMax® M2 System, Molecular Devices, UK). The control was performed with cells cultured in medium, without any treatment. Three independent experiments were conducted with triplicate samples. The half maximal inhibitory concentration ( $IC_{50}$ ) was determined from the dose-response curve.

## **1.6. Cell internalization of FRET self-assemblies**

A total of 500,000 HL-60 cells/well was seeded in 24-wells plates. After 24 hours, they were incubated with 11.26  $\mu$ M (AzaDHA) and 16.58  $\mu$ M (AzaEPA) of FRET self-assemblies (0.5% w/w in donor/0.5% w/w in acceptor corresponding to 0.925 mol of donor and 1 mol of acceptor) diluted in culture medium for 0.5 h, 2 h, 4h, 8 h and 24 h (37°C and 5% CO<sub>2</sub>). At the end of the incubation period, cells were collected, centrifuged and washed twice with 1 mL of cold PBS, 1 mL of cold 4% paraformaldehyde was then added for 10 minutes, the cells were then washed twice with 1 mL of cold PBS and resuspended in 0.5 mL of cold PBS. The fluorescence of the cells was recorded using a Cytoflex flow cytometer (Beckman, USA). For fluorescence detection of the

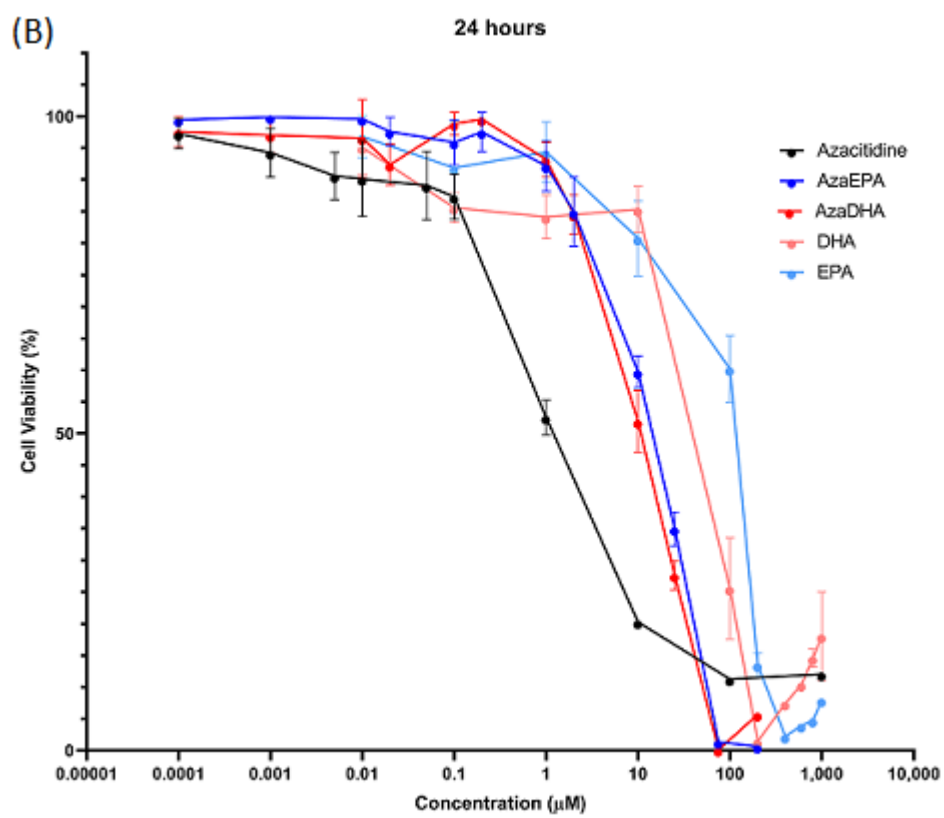
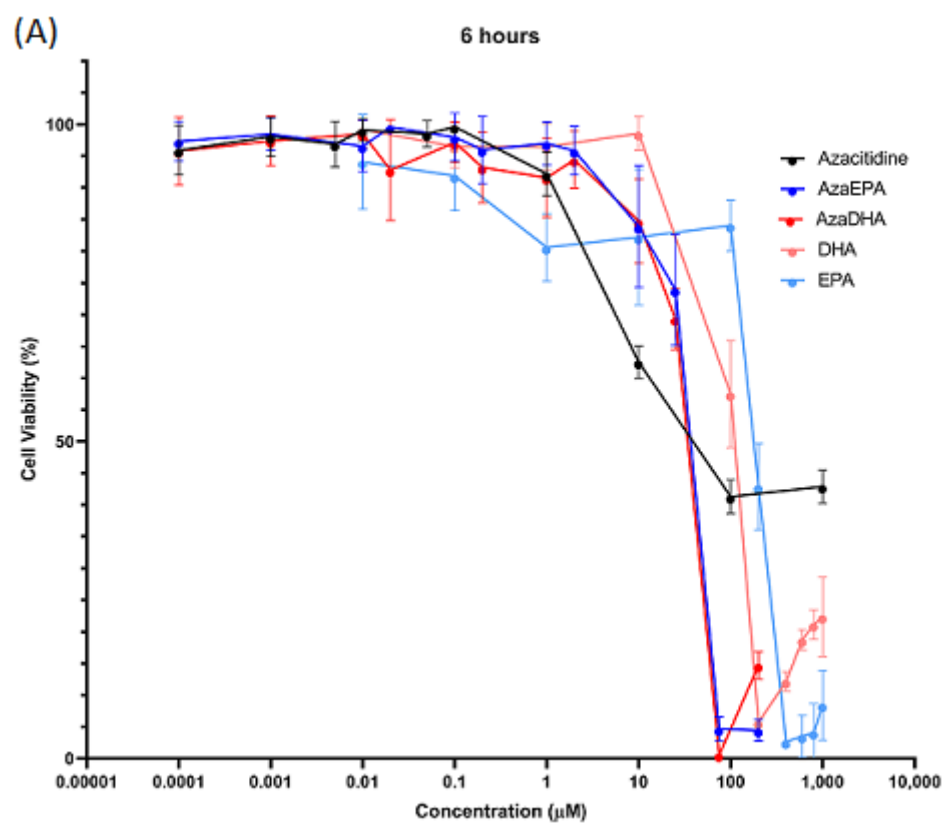
different self-assemblies, excitation was carried out using a 488 nm blue laser (corresponding to donor excitation) and emission fluorescence was measured at 562 nm (corresponding to acceptor emission). 0.5% w/w donor and 0.5% w/w acceptor self-assemblies were used as controls to evaluate the contribution of the individual dyes to the fluorescence signal. Hence, the signals obtained with each of these assemblies were added together and the difference between the sum of these signals and the one obtained with FRET self-assemblies was considered as the Förster Resonance Energy Transfer signal (FRET signal), reflecting the self-assembly integrity. 10,000 cells were studied for each measurement. The results were expressed as the median fluorescence intensity (MFI).

## 2. Results and discussion

### 2.1. Cytotoxicity studies

The cytotoxicity of the AzaDHA and AzaEPA self-assembled conjugates was determined and compared to the azacitidine and the fatty acids. A MTT assay was performed after 6, 24 and 48 hours of treatment incubation times, with various concentrations (**Figure 29**) and  $IC_{50}$  were determined (**Table 5**).

The cytotoxicities at 6, 24 and 48 hours (**Figure 29**) were reflecting the same results: a well-defined dose-response curves showing that azacitidine was the most cytotoxic of the molecules tested, followed by AzaDHA and AzaEPA, 10-folds less cytotoxic than the parent molecule. Finally, the free fatty acids appeared to have the least cytotoxic effect. Interestingly, similar to the free fatty acids where DHA had an increased cytotoxic effect compared to EPA, the cytotoxic effect of the DHA based self-assemblies was better than the EPA based ones. The half maximal inhibitory concentration (**Table 5**) further verifies these observations, as the same trend is apparent at the three time points.





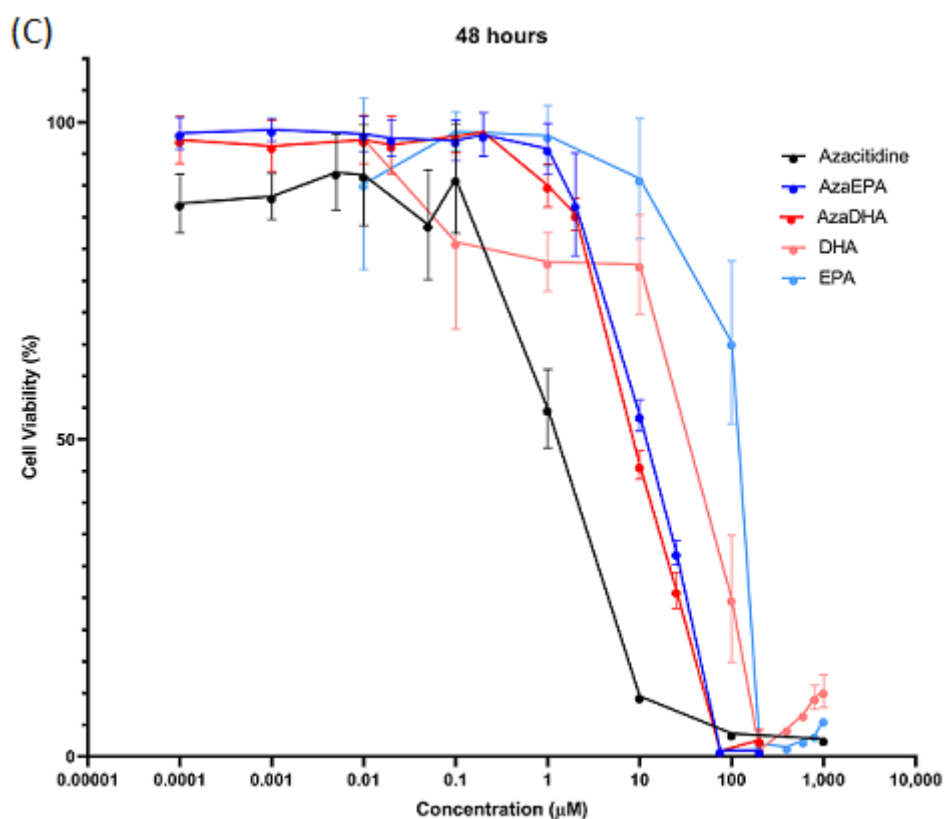


**Figure 29: Cytotoxicity studies of the self-assemblies compared to the free azacitidine and fatty acids at different time points. (A) 6 hours, (B) 24 hours, (C) 48 hours.**

<i>IC<sub>50</sub></i>	<i>Azacitidine</i>	<i>DHA</i>	<i>EPA</i>	<i>AzaDHA</i>	<i>AzaEPA</i>
<b>6 hours</b>	6.495 $\mu\text{M}$	100.2 $\mu\text{M}$	196.7 $\mu\text{M}$	27.48 $\mu\text{M}$	33.68 $\mu\text{M}$
<b>24 hours</b>	1.025 $\mu\text{M}$	92.82 $\mu\text{M}$	115.9 $\mu\text{M}$	11.26 $\mu\text{M}$	16.58 $\mu\text{M}$
<b>48 hours</b>	1.363 $\mu\text{M}$	44.51 $\mu\text{M}$	103.8 $\mu\text{M}$	10.16 $\mu\text{M}$	13.69 $\mu\text{M}$

**Table 5: The half maximal inhibitory concentration determined by a MTT assay on HL-60 cells, after treatment by azacitidine, fatty acids and self-assemblies at different time points.**

At 24 h, azacitidine showed an  $\text{IC}_{50}$  of 1.0  $\mu\text{M}$  conforming with literature values<sup>225</sup>, with the self-assembled prodrugs a  $\sim 10$  fold higher  $\text{IC}_{50}$  (11 and 16  $\mu\text{M}$  for AzaDHA and AzaEPA respectively) were obtained, while the omega-3 fatty acids  $\text{IC}_{50}$  being  $\sim 100$  folds higher (92  $\mu\text{M}$  and 116  $\mu\text{M}$  for DHA and EPA) respectively.

As expected, the cytotoxicity of the AzaEPA and AzaDHA self-assemblies was weaker than the free azacitidine, this difference in cytotoxicity is often observed for prodrugs<sup>225,234</sup>. Certainly, the azacitidine molecule must be first cleaved from the fatty acid conjugates to regain its pharmacological activity. *In vitro*, even though HL-60 cells produce cathepsin B enzyme that is

able to release azacitidine from its conjugation<sup>227,228,235</sup>, this release is slow and progressive. For a prodrug, it is known that the biological efficacy has to be determined *in vivo*, to see all its potential: the coupling nucleoside analogues with fatty acids reduced the deamination, increased the *in vivo* drug half-life, in modifying its pharmacokinetics and biodistribution<sup>221,234,236,237</sup>. Additionally, azacitidine in its clinical application is used as a hypomethylating agent, not as a cytotoxic agent, and the dose needed is less than IC<sub>50</sub>, thus these results reflect positively on the success of the studied self-assemblies. Not to mention that the need for cathepsin B to release the azacitidine will increase its specificity and decrease the toxic side effects on healthy tissues<sup>227,228</sup>.

## 2.2. Cell internalization study of the self-assemblies

The Förster resonance energy transfer (FRET) phenomena has been implemented in the field of biological studies in the late 1960s<sup>238</sup>. Considered as the ultimate molecular ruler, it found other applications such as determining the dynamics of lipid<sup>239–241</sup>.

Such applications are conceivable due to the energy transfer process, as the donor and acceptor fluorophores interact if they are at a distance of 10 nm of each other with an overlapping fluorescence spectra. After excitation with a laser at the donors excitation wavelength, the acceptor fluorophore will absorb the donor emission, leading the acceptor to emit at its specific wavelength<sup>242</sup>.

In our case utilizing the CholEsteryl BODIPY™ fluorophores allows us to take advantage of its chemical composition containing the cholesteryl lipid, allowing these fluorophores to co-nanoprecipitate alongside our prodrug to produce a fluorescently labeled self-assembly. Certainly, having these two fluorophores sharing a complementary spectra and potentially within close distance in the self-assembly structure would allow the energy transfer to occur. This was based on the work of Gaudin *et al.* where they established that these two fluorophores are able to perform FRET<sup>215</sup>. This would allow us to track the integrity of the self-assemblies.

Briefly, while using FACS, a 488 nm blue laser would excite the donor fluorophore (CholEsteryl BODIPY™ FL C12) that will emit at 511 nm, the emission energy would then be absorbed by the acceptor fluorophore (CholEsteryl BODIPY™ C11) followed by its emission at 563 nm. The acceptor emission will be detected by a 585/42 detector.

Prior to the treatment of the cells with the fluorescent self-assemblies, the concentration of the dyes needed to elicit a sufficient signal and avoid the dye photo bleaching was determined<sup>243</sup> (**Figure 30**).

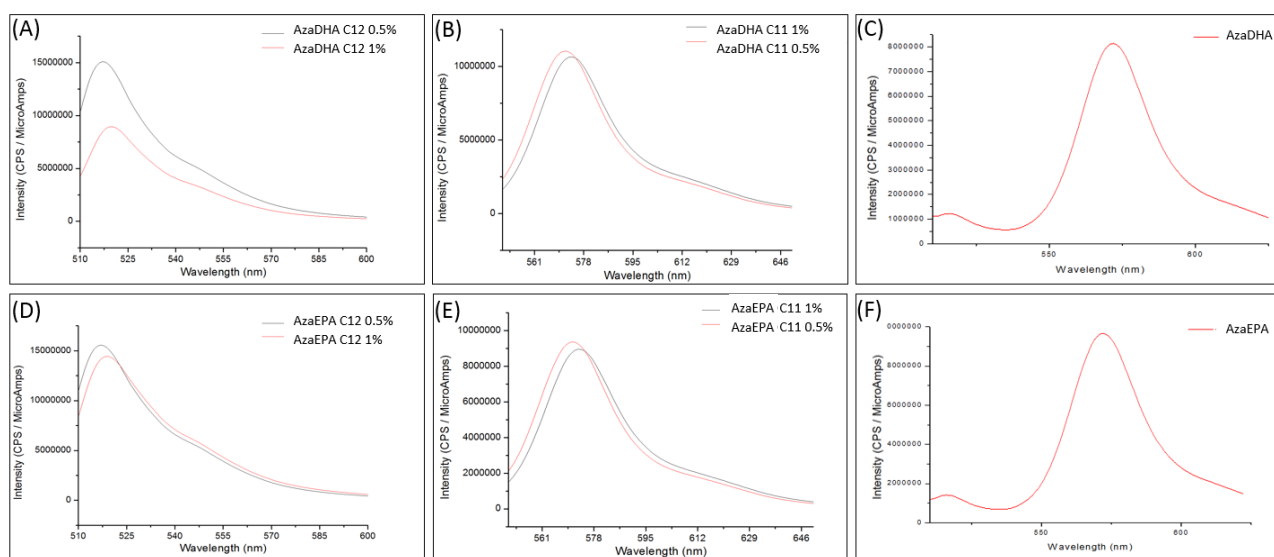


**Figure 30: Fluorescence spectra of the different BODIPY self-assemblies at 0.5% and 1% in concentration of dyes.** (A) AzaDHA BODIPY C12 self-assemblies, (B) AzaDHA BODIPY C11 self-assemblies, (C) AzaDHA BODIPY FRET self-assemblies, (D) AzaEPA BODIPY C12 self-assemblies, (E) AzaEPA BODIPY C11 self-assemblies and (F) AzaEPA BODIPY FRET self-assemblies.

For both dyes, BODIPY C11 and C12, two concentrations were used: 0.5% and 1% (w/w). In both cases, AzaEPA and AzaDHA self-assemblies, the ideal concentration was of 0.5% (w/w) in dyes. Interestingly, AzaDHA C12 with 1% in dyes had a decreased fluorescence, illustrated by an important variation of the diameter (488 nm) and zeta potential (13.4 mV) of the self-assemblies after co-nanoprecipitation with the dye (**Table 6**).

For the FRET based self-assemblies, after using a 0.5% concentration in dyes to co-nanoprecipitate self-assemblies, the FRET signal was observed after excitation of the donor (C12) with a good emission intensity from the acceptor (C11): a very slight emission of the donor was only observed.

The ratiometric FRET, the "relative" FRET efficiency, also known as the proximity ratio was calculated following the equation  $E_{rel} = \frac{I_A}{I_{D+A}}$ , where  $I_A$  and  $I_D$  are the total acceptor and donor fluorescence intensities, respectively, both following the donor excitation. In the case of FRET based AzaEPA self-assembly, a relative FRET efficiency of 0.865 is obtained, while for AzaDHA, a relative FRET efficiency of 0.867 was calculated: both  $E_{rel}$  were  $> 0.8$  meaning the FRET pair selected was appropriated.

Self-assembly	Sample	Hydrodynamic Diameter (nm)	Zeta Potential (mV)	PDI	Attenuator
AzaEPA	C11- 0.5%	215.9 ± 1.6%	26.0 ± 2.25%	0.128 ± 14.4%	7
	C11- 1%	231.4 ± 1.3%	33.5 ± 2.65%	0.098 ± 37.5%	7
	C12- 0.5%	222.1 ± 3.12%	34.2 ± 7%	0.141 ± 31.9%	7
	C12- 1%	215.8 ± 2.62%	33.9 ± 6.7%	0.176 ± 5.21%	7
	FRET	313.1 ± 24.6%	10.2 ± 2.9%	0.137 ± 38%	7
AzaDHA	C11- 0.5%	246.6 ± 2.48%	33.1 ± 5.24%	0.059 ± 24%	7
	C11- 1%	214.8 ± 0.634%	35.9 ± 4.75%	0.09 ± 25.9%	7
	C12- 0.5%	220.5 ± 153%	39.3 ± 2.94%	0.144 ± 12.4%	7
	C12- 1%	488.3 ± 2.99%	13.4 ± 3.67%	0.092 ± 66%	7
	FRET	190.5 ± 4.21%	-15.0 ± 3.66%	0.261 ± 8.98%	7

**Table 6: Physical characteristics of the fluorescent self-assemblies.** With C11 and C12 fluorescent dyes at 0.5% and 1% (w/w), and the FRET self-assemblies (0.5% of both dyes).

After this optimization of the dye concentration, the cell internalization of the fluorescent self-assemblies was performed (**Figure 30**).

For the AzaEPA FRET self-assemblies, when the mean fluorescence intensity (MFI) was looked at (**Figure 31A**), a stable value at around 2500 a.u. was observed, starting at 0.5 hours until 24 hours. However, if the number of FRET positive cells was analyzed, an increase by a factor almost 3 of AzaEPA FRET self-assembly internalization was obtained at 24 hours (**Figure 31B**). As the MFI was not varying at 24 h, it can be hypothesized that, after 24 h, the cell uptake was homogeneous, with a same mean fluorescence FRET intensity, but almost 3 times more cells were internalized by this AzaEPA self-assembly.

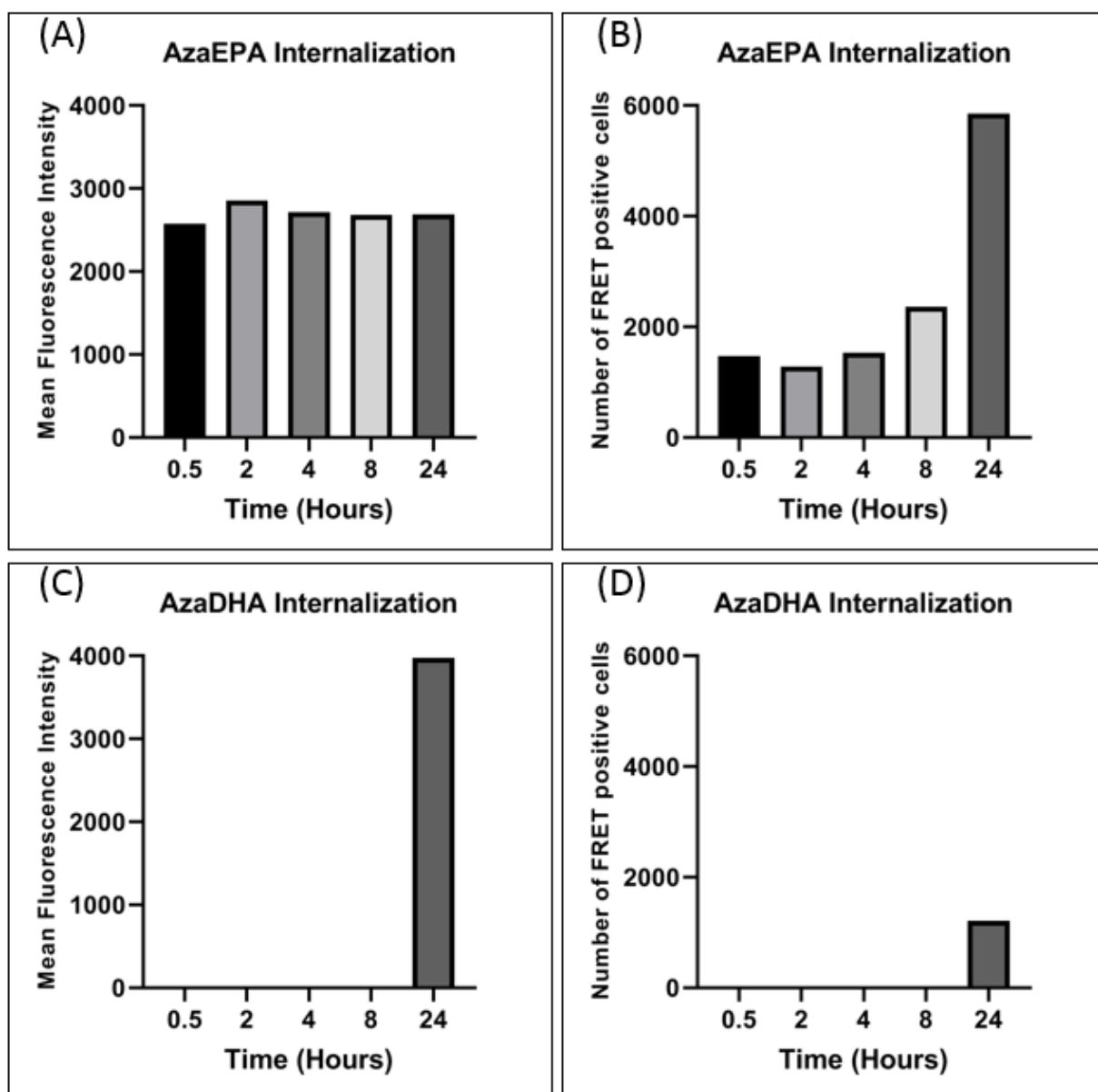


**Figure 31: Internalization of FRET AzaEPA and AzaDHA self-assemblies.** (A) MFI of FRET AzaEPA, (B) Number of cells displaying FRET upon internalization of AzaEPA, (C) MFI of FRET AzaDHA, (D) Number of cells displaying FRET upon internalization of AzaDHA.

In the case of the AzaDHA FRET self-assemblies, the internalization was really slower, with a negligible amount of cells internalizing the assemblies at 24 hours, when the internalization started.

Considering that the MTT results showed a cytotoxic effect of AzaDHA self-assemblies slightly higher than AzaEPA at 6 hours, we would have expected a better internalization (even if the cell uptake is not the only explanation of a difference in cytotoxicity). These contradictory results could be explained by the DLS measurements of these self-assemblies, as the FRET AzaDHA self-assemblies had a very different surface charge (-15 mV) from the regular positive zeta potential.



Indeed, a novel self-assembly of FRET AzaDHA must be formulated while choosing the correct amount of dyes that will not alter the nanoparticles physical characteristics.

### 3. Conclusion

In summary, the obtained formulations had a low  $IC_{50}$  comparable to that of free azacitidine, allowing them to achieve a close cytotoxicity. Indeed, the obtained prodrugs and their self-assemblies are a promising substitute to azacitidine, with a further advantage of increased specificity and decrease toxic side-effects owing to the need for cathepsin B to release the azacitidine.

Furthermore, the AzaEPA self-assemblies were internalizing swiftly starting at 0.5 hours but gradually, and were stable inside the cells for 24 hours. A longer study of the internalization is needed to determine the time point at which these self-assemblies are dissociating and confocal imaging will be performed to confirm these results. The AzaDHA self-assemblies didn't internalize efficiently due probably to the alteration of the surface charge by the co-nanoprecipitation of the dyes, and a new optimized formulation will be needed.

Finally, as azacitidine is a hypomethylating agent, the cell total DNA methylation profile must be studied via LINE-1 methylation test to determine if azacitidine retains its mode of action after being conjugated to a fatty acid. Moreover, the difference in hypomethylation degree between azacitidine itself and its self-assemblies has to be investigated.

## Discussion and perspectives

Azacitidine, a nucleosidic analogue of cytidine, has played a crucial role in the treatment of MDS and AML<sup>244-246</sup>. Indeed, advanced cases of MDS, categorized as higher-risk MDS, rely on azacitidine as one of the few options available in their arsenal against this blood disorder<sup>53,247</sup>. Additionally, it has shown great merit in the cases of delays for hematopoietic stem cell transplantation eligible patients, as well as in post-procedure relapse prevention<sup>248-250</sup>. Though not commonly used for lower-risk MDS patients, azacitidine is still a treatment option after the failure of regular approaches for this group<sup>89,251</sup>. Owing to its DNA hypomethylating activity, this molecule is capable of reactivating the tumor suppressor genes<sup>252,253</sup>. The lack of substitutes further stresses its importance.

However, azacitidine suffers from low serum drug levels and high toxicity levels<sup>91,254</sup>, leaving the patients facing a poor prognosis<sup>254,255</sup>. It is explained by its hydrophilic nature, leading to poor cell internalization<sup>101,102</sup>, coupled its degradation by nucleoside deaminases<sup>102-106</sup>, resulting to a short half-life.

This project aimed to counter these limitations on two levels. The first was to protect the labile amine group of azacitidine via its conjugation to a polyunsaturated fatty acid, thus increasing the drugs half-life. The second level was to use the amphiphilic nature of the obtained prodrug and to formulate self-assemblies. This approach additionally lends other advantages, as the newly obtained amphiphilic prodrug should enhance the entry into the cells<sup>256,257</sup>, not to mention an increased specificity stemming from the unique cleavability of the formed amide bond by cathepsin B enzyme, overexpressed in MDS and cancer cells<sup>258-260</sup>.

This approach of conjugating a nucleoside to a polyunsaturated fatty acid is termed "PUFAylation", a generalized approach of the well-known "Squalenoylation" concept developed by Prof. Couvreur and his team<sup>261</sup>. Another boon of this approach over traditional nanomedicines such as liposomes or polymeric nanoparticles, is the ability of this conjugate to self-assemble in water without the requirement for additional excipient, thus improving drug loading and tolerability in animals<sup>262-265</sup>.

Two omega-3 fatty acids were chosen for the conjugation: docosahexaenoic acid (DHA) and eicosapentaenoic acid (EPA). Owing to the presence of double bonds, prodrugs based on these fatty acids are able to spontaneously self-assemblies in water, by the virtue of the  $\pi$ - $\pi$  stacking interactions, increasing the stability of the self-assemblies<sup>186-190,266</sup>.

Additionally, these omega-3 fatty acid display anti-AML activity, promoting cell death via oxidative stress pathways. Besides, when used in combination with other nucleosides such as cytarabine, a synergistic effect was observed<sup>139</sup>.

Two PUFAylated prodrugs were successfully obtained via direct conjugation in the presence of ethyl chloroformate: an azacitidine-docosahexaenoic acid conjugate (N<sup>4</sup>-azacitidine DHA, called AzaDHA) and an azacitidine-eicosapentaenoic acid conjugate (N<sup>4</sup>-azacitidine EPA, called AzaEPA). The nanoprecipitation of these prodrugs was performed and self-assemblies were successfully achieved. The critical aggregation concentration obtained by the pyrene method was 400 mM for AzaEPA and 688 mM for AzaDHA, confirming the formation of self-assemblies. A diameter of ~190 nm was observed in both prodrug self-assemblies, with a polydispersity index below 0.2 and a positive zeta potential. 5 days were needed to reach their final stable organization. The self-assemblies presented a low IC<sub>50</sub> comparable to that of free azacitidine, with a homogeneous internalization observed at 24 h for the AzaEPA FRET self-assemblies, performed on a human acute myeloid leukemia cell line (HL-60).

## 1. Prodrug synthesis

Addressing the prodrug synthesis, two approaches were implemented to achieve the conjugation of azacitidine to the selected fatty acids. The first approach focused on the need to protect the OH groups of the azacitidine sugar ring, followed by its conjugation to the fatty acids via an amide bond. The protected groups will have then to be removed and the crude product purified in order to achieve the final desired azacitidine-fatty acid conjugate. The second approach was a more direct one, focusing on the use of a suitable conjugating agent to directly obtain the conjugate after purification.

The protection approach was directly adapted from Prof. Couvreur's work on the conjugation of nucleotides/nucleosides and their analogues to squalenic acid<sup>215,229</sup>. The protection of the OH groups was driven by the need to avoid unwanted secondary byproducts stemming from the ester linkage of the fatty acids to azacitidine, leading to a decreased yield. Though the conjugation was hindered by the low reactivity azacitidine amine group, ethyl chloroformate was finally successful in conjugating these azacitidine moiety to the fatty acids. The protected conjugation was followed by a deprotection step, though the final prodrug was irrecoverable due to challenges in the purification.

This approach holds a lot of merit and is definitely a successful one, with various examples in literature from Gaudin *et al.* on conjugating adenosine to squalenoyl<sup>215</sup>, to the work of Lepeltier

*et al.* as well as Bildstein *et al.* on the conjugation of gemcitabine to squalene<sup>190,229</sup>. This synthesis method would aid in boosting the low yields observed with direct conjugations. However, azacitidine did not conjugate as readily as gemcitabine, owing to the presence of an additional nitrogen when compared to gemcitabine in the nucleobase ring of the molecule. The additional nitrogen led to a decreased reactivity of the adjacent NH<sub>2</sub> group, leading to the failure of several conjugating agents, except the ethyl chloroformate that was successful. The obtained protected prodrug was deprotected using TBAF in the presence of acetic acid, yet purification was unsuccessful.

Clearly this approach can be improved: though the protection of the OH groups was effective with a yield of 94%, the step of conjugation had a rather low yield that may be improved by using related conjugating agents that could push the yield further such as isobutyl, isopropyl and isopropenyl chloroformate<sup>267-269</sup>. Concerning the purification of the deprotected prodrug, given that the partially deprotected prodrugs shared a close polarity with the fully deprotected ones, traditional silica gel chromatography might be hindered. Using semi-preparative reversed phase high-performance liquid chromatography (RP-HPLC) might be the answer, with the implementation of another chemistry of column that would allow a better interaction with the azacitidine nucleobase ring to increase retention time and allow purification of the amphiphilic conjugate: the BEH Z-HILIC columns could be the key.

The direct conjugation approach, though having a lower yield (10-20%), was more cost effective with the need for less reactants than the protected conjugation approach, and less purification steps between the different stages. This type of conjugations has been implemented in the work of Wu *et al.* for the conjugation of gemcitabine to linoleic acid<sup>222</sup>, but a huge limitation faces this approach: the scale-up of this procedure in order to produce larger amounts of product needed for future studies and *in vivo* tests will be difficult in considering the low yield. The use of other conjugating agents to increase the yield will be met by the same problem: the weak azacitidine reactivity observed. This has been tested by substituting ethyl chloroformate with isopropyl chloroformate: this led to a decrease in yield as it favored the creation of ester linkage rather than an amide one. Moreover, the last difficulty to be solved in order to envisage a potential scale-up is the purification step. Indeed, the purification procedure of amphiphilic molecules is always problematic and asks for time before an optimization of the experimental parameters: column nature, eluent, flow rate and gradient method. In our case, the purification was performed using a reversed phase high-performance liquid chromatography (RP-HPLC): the cost of this process is high, owing to the need of large quantities of HPLC-grade eluents and only

small amounts of the crude product can be purified per run. Therefore, a silica gel method could be developed to allow purification of larger amounts of products

## 2. Self-assembly formulation

The obtained prodrugs were able to achieve self-assembly upon nanoprecipitation, giving nanoassemblies with a mean diameter around 190 nm, a positive zeta potential and a PDI < 0.2, characterized by dynamic light scattering and electrophoretic mobility. Additionally, the critical aggregation concentration obtained by the pyrene method<sup>270,271</sup> further verified the formation of the self-assemblies. Interestingly, the positive zeta potential may increase the cellular internalization due to charge-based interactions with negatively charged cell membrane surface<sup>272</sup>. Considering that the prodrug length is around 17.4 Å (1.74 nm) for AzaDHA and 21.2 Å (2.21 nm) for AzaEPA, if micelles were formed, a diameter of 4-5 nm would be observed. Therefore, it can be theorized that these self-assemblies are organizing into a larger, more complex supramolecular structure, where the amphiphilic prodrugs use non-covalent forces that push the self-assembly towards forming these larger structures. These forces include Van der Waals interactions, hydrogen bonding, hydrophobic effect and  $\pi$ - $\pi$  stacking interaction. As these noncovalent forces are reversible, external stimuli such as temperature, pH and electromagnetic waves are able to induce a change in the morphology, structure and the function of the supramolecular self-assembly<sup>273-275</sup>. Undeniably, Lepeltier *et al.*'s work has led to similar observations, where different supramolecular structures were observed with the squalene-based nucleolipid conjugates, rather than forming micelles<sup>262,276</sup>.

By Cryo-TEM, a multilamellar vesicle supramolecular structure could clearly be observed for both prodrug self-assemblies. The formation of these multilamellar vesicles evidently demonstrates that obtained prodrugs exhibit a critical packing parameter  $CPP \approx 1$ , based on the model proposed by Israelachvili and Mitchell. Indeed, CPP is defined as  $CPP = V/(a_0 \cdot l_c)$ , where  $V$ ,  $l_c$  and  $a_0$  are respectively, the volume and length of the lipophilic chain, and the cross-section area of the hydrophilic head of the amphiphilic molecule. Therefore, the large volume of the lipid chain that leads to obtaining a CPP value of 1 and thus the formation of the observed lamellar structure, can be attributed to the fatty acid conformation in space arising from the multiple double-bonds present in them (**Figure 32**).



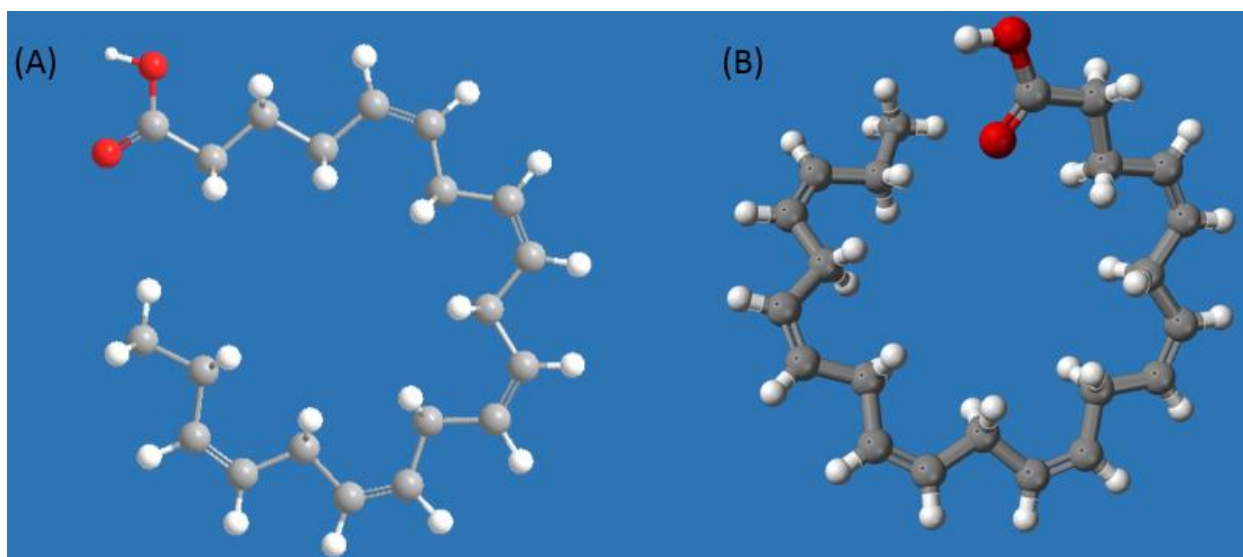


**Figure 32: Chemical structure of omega-3 fatty acids.** EPA (A) and DHA (B)

Certainly, both EPA and DHA conjugates have demonstrated in studies their affinity to form multilamellar vesicles. A recent study by Shao *et al.* has shown that monoglycerides-DHA/EPA self-assemble into multilamellar vesicles that would be a promising vector for the delivery of therapeutic agents<sup>277</sup>. Similarly, De Santis *et al.* while aiming to study the effect of omega-3 fatty acids on the fluidity of biological membranes, has proved that these two fatty acids can self-assemble via film hydration into multilamellar vesicles<sup>278</sup>. Additionally, several studies have also shown that DHA and EPA based nanoparticles have also achieved a multilamellar vesicle supramolecular structure<sup>279–281</sup>.

Moreover, owing to formed multilamellar phases, azacitidine will be inaccessible to the deaminases. This protection of the azacitidine between the formed bilayers will lead to an increased half-life coupled to diminished elimination<sup>103,106</sup>. This would additionally allow for a gradual release of azacitidine<sup>282</sup>.

Indeed, the obtained supramolecular structure could be further verified using synchrotron-based small-angle X-ray scattering (SAXS), where equally spaced Bragg's peaks should be obtained. Furthermore, this technique would allow us to obtain the width of the formed bilayers (*d*-space) as well as the distance between bilayers (intrabilayer distance)<sup>283</sup>.

However, several interrogations can be formulated. Indeed, the nanoparticle tracking analysis (NTA) performed for both prodrug self-assemblies suggested several populations of nano-objects. Moreover, according to the concentration of nanoparticles/mL given by the NTA ( $1.29\text{e}^8 \pm 4.03\text{e}^6$  particles/mL), the observed self-assemblies would account for only a small fraction ( $\sim 7\%$ ) of the matter in suspension.

Interestingly, DLS and electronic microscopy are the main two methods used to characterize self-assemblies, used in respectively 48% and 14% of the studies with only 8% of nanoparticles characterized by other complementary methods<sup>284</sup>. However, analysis by DLS is mainly focused on “big” objects in the suspension albeit such objects represent less than 1% of the initial matter used. Indeed, the work of Guyon *et al.* further sheds a light on these limitations, as the formed polyarginine-ferrocifen self-assemblies detected by DLS with a diameter around 120 nm account for less than 1% of the initial matter in the suspension. This observation was demonstrated by SAXS and other complementary methods such as NMR diffusometry, finally micelles with a diameter around 5 nm were characterized, invisible by DLS or NTA <sup>233</sup>.

Therefore, regarding the AzaDHA and AzaEPA self-assemblies, the DLS must only be regarded as an initial and handy analytical method. In order to establish if these self-assemblies are forming simple micelles that could not be detected by DLS, more advanced characterization methods should be used. By Cryo-TEM, it is clear that micelles are mainly present (**Figure 33**).

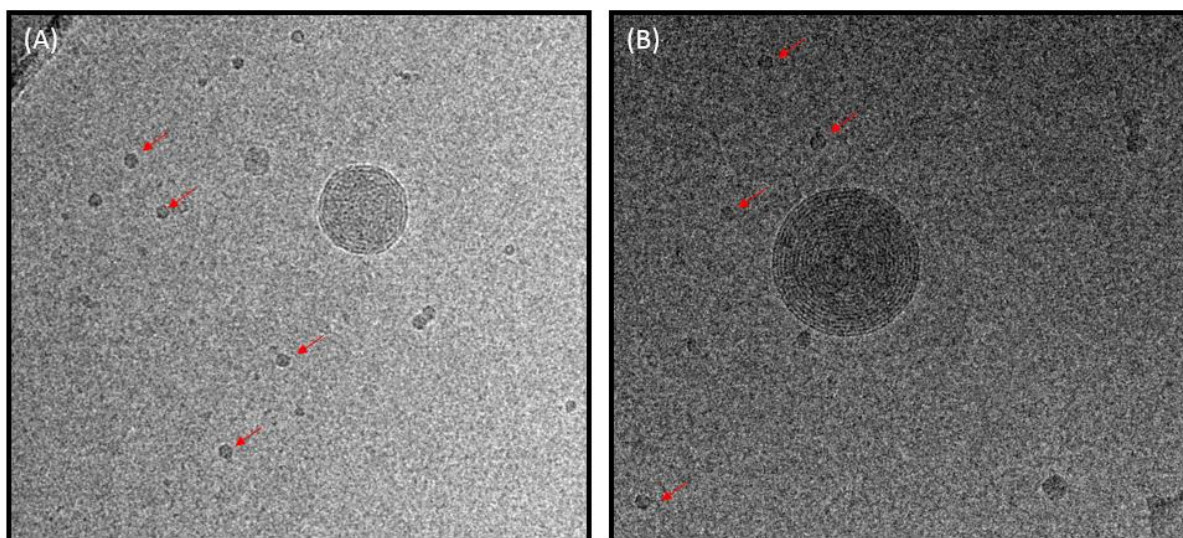


**Figure 33: Cryo-TEM images of AzaDHA (A) and AzaEPA (B) self-assemblies showing the presence micelles.**

Certainly, synchrotron-based small-angle X-ray scattering (SAXS) is needed to verify the supramolecular structure and the real diameter of the nano-objects. It should also be coupled with other techniques such as multiangle light scattering (*MALS*), quantification and NTA after successive filtration through gradual pore sizes and NMR diffusometry (DOSY) to obtain a reliable characterization<sup>285–288</sup>.

### 3. Evaluation of the biological effects

Early *in vitro* studies on the HL-60 cell line with both self-assemblies showed that they possess an anti-cancerous effect that is comparable to that of free azacitidine, though being slightly higher, a phenomenon classically observed during *in vitro* testing of prodrugs, and rectified *in vivo*<sup>225,234</sup>.

Additionally, preliminary cell internalization tests performed with self-assembly based FRET and analyzed by FACS, showed that the AzaEPA self-assemblies had a slow and gradual entry into the leukemia cells with a good stability inside the cells, as no decrease of fluorescence was observed over 24 hours.

The internalization studies were chosen to be performed using two fluorescent dyes: the CholEsteryl BODIPY™ FL C12 505/511 (donor) and the CholEsteryl™ BODIPY C11 542/563 (acceptor), already tested by Gaudin *et al.* and established to perform FRET<sup>215</sup>.

The Förster resonance energy transfer (FRET) phenomena has been used for several years in imaging and more recently has been introduced to flow cytometry. Various applications exist for FRET such as determining the dynamics of lipid membranes and protein folding, as well as the distance at the scale of molecular interactions<sup>239–241</sup>. These applications are possible due to the energy transfer process, as the donor and acceptor fluorophores are able to interact if they are within 10 nm of each other, as after excitation with a suitable source, the acceptor will absorb the donor emission (that can't be then detected ) as its excitation source, and the acceptor emission will be then detected<sup>242</sup>.

The advantage of using a FRET dual dye system of this nature is its chemical composition containing the cholesteryl lipid, allowing the dyes to assemble alongside our prodrug to produce a fluorescently labeled self-assembly. Additionally, having two dyes with complementary spectra and potentially close enough in the self-assembly structure will allow the energy transfer to occur. Thus, the integrity of the self-assembly structure can be followed and the time point at which the self-assemblies dissociate can be detected via losing the signal of the acceptor emission and in detecting the emission of the donor. This phenomenon holds an additional advantage over the traditional use of a single dye to track internalization. Indeed, we don't track directly the nanoparticle itself but only the fluorophore and various errors may occur at that point, such as tracking the dye that has been released or leaked from the nanoparticle, leading to false results. Not to mention the possibility of dye quenching as demonstrated by the work of Prof S. Lavielle's team, proving that the absence of fluorescence might be due to the self-quenching of the probe due to the local

intensity of the fluorescence signal and the local concentration of the fluorescent probe used<sup>243</sup>. Such problems could be directly avoided using two dyes that can produce a FRET signal.

Certainly, the preliminary *in vitro* results are promising and warrant further investigation as various more aspects still need to be studied. Most importantly, the stability of the self-assemblies in biological media at 37°C should be determined to mimic the conditions of the self-assembly during *in vitro* studies. This will allow for a better understanding of the fate of the self-assemblies as well as a more accurate analysis of the obtained results.

The covered internalization studies should be repeated with a new AzaDHA formulation holding the same physico-chemical characteristics of the self-assembly pre-dye addition. The time points of 48 hours and 72 hours should be obtained to have a better understanding of the self-assembly intracellular dissociation. Furthermore, confocal microscopy studies based on the obtained fluorescent self-assemblies are needed to verify the results obtained by FACS. The cell internalization mechanisms could be as well determined, by the use of specific inhibitors such as chlorpromazine to identify clathrin-mediated endocytosis pathways through blocking the formation of membrane invaginations<sup>289</sup>. The fate of the self-assemblies could be thus identified: a caveolae-mediated endocytosis does not lead to pH and enzyme degradations, as observed in endosomes and lysosomes<sup>272</sup>.

Additionally, apoptosis studies using annexin V/ propidium iodide as well as cell cycle arrest studies should be conducted by FACS to determine the cell death mechanism that is occurring upon treatment with the prodrug self-assemblies and if it differs from azacitidine one, while comparing effectiveness.

To then assess whether cells after treatment are able to regain their previous functionality and continue with their differentiation, differentiation studies, both morphological and via Mgg coloration should be conducted. Not to mention that as the azacitidine drug is used in its hypomethylating capacity, the methylation levels of the DNA must be evaluated by methylation quantification studies (LINE global methylation studies).

Finally, as previously described, *in vitro* testing is insufficient to paint a correct picture when working with prodrug self-assemblies. Thus *in vivo* studies will be conducted on a patient derived xenograft murine AML model, in collaboration with "Pathologie et virologie moléculaire de l'Institut Universitaire d'Hématologie" laboratory INSERM 944/ CNRS UMR 7212 (Université Paris Diderot). The studies will focus on the survival after treatment, as well as on the phenotypic and genotypic changes that are occurring in the AML cells after

treatment, coupled to the cell methylation levels of treated and non-treated groups. The stability of the self-assemblies in the plasma will have to be first determined, then the choice of suitable near infra-red fluorochromes to be tracked *in vivo*, in order to determine the biodistribution of the nanoparticles and verify their increased specificity/decreased toxicity.



## References

- (1) Bennett, J. M.; Catovsky, D.; Daniel, M. T.; Flandrin, G.; Galton, D. a. G.; Gralnick, H. R.; Sultan, C. Proposals for the Classification of the Myelodysplastic Syndromes. *British Journal of Haematology* **1982**, *51* (2), 189–199. <https://doi.org/10.1111/j.1365-2141.1982.tb02771.x>.
- (2) Hellström-Lindberg, E. Myelodysplastic Syndromes: An Historical Perspective. *Hematology* **2008**, *2008* (1), 42–42. <https://doi.org/10.1182/asheducation-2008.1.42>.
- (3) Neukirchen, J.; Schoonen, W. M.; Strupp, C.; Gattermann, N.; Aul, C.; Haas, R.; Germing, U. Incidence and Prevalence of Myelodysplastic Syndromes: Data from the Düsseldorf MDS-Registry. *Leukemia Research* **2011**, *35* (12), 1591–1596. <https://doi.org/10.1016/j.leukres.2011.06.001>.
- (4) Hellström-Lindberg, E.; Tobiasson, M.; Greenberg, P. Myelodysplastic Syndromes: Moving towards Personalized Management. *Haematologica* **2020**, *105* (7), 1765–1779. <https://doi.org/10.3324/haematol.2020.248955>.
- (5) Browse the Tables and Figures - SEER Cancer Statistics Review (CSR) 1975-2016 [https://seer.cancer.gov/archive/csr/1975\\_2016/browse\\_csr.php?sectionSEL=13&pageSEL=sect\\_13\\_table.13](https://seer.cancer.gov/archive/csr/1975_2016/browse_csr.php?sectionSEL=13&pageSEL=sect_13_table.13) (accessed 2021 -08 -29).
- (6) Cancer today <http://gco.iarc.fr/today/home> (accessed 2021 -08 -29).
- (7) Vardiman, J. W.; Harris, N. L.; Brunning, R. D. The World Health Organization (WHO) Classification of the Myeloid Neoplasms. *Blood* **2002**, *100* (7), 2292–2302. <https://doi.org/10.1182/blood-2002-04-1199>.
- (8) Vardiman, J. W.; Thiele, J.; Arber, D. A.; Brunning, R. D.; Borowitz, M. J.; Porwit, A.; Harris, N. L.; Le Beau, M. M.; Hellström-Lindberg, E.; Tefferi, A.; Bloomfield, C. D. The 2008 Revision of the World Health Organization (WHO) Classification of Myeloid Neoplasms and Acute Leukemia: Rationale and Important Changes. *Blood* **2009**, *114* (5), 937–951. <https://doi.org/10.1182/blood-2009-03-209262>.
- (9) Arber, D. A.; Orazi, A.; Hasserjian, R.; Thiele, J.; Borowitz, M. J.; Le Beau, M. M.; Bloomfield, C. D.; Cazzola, M.; Vardiman, J. W. The 2016 Revision to the World Health Organization Classification of Myeloid Neoplasms and Acute Leukemia. *Blood* **2016**, *127* (20), 2391–2405. <https://doi.org/10.1182/blood-2016-03-643544>.
- (10) Visconte, V.; Tabarrok, A.; Zhang, L.; Parker, Y.; Hasrouni, E.; Mahfouz, R.; Isono, K.; Koseki, H.; Sekeres, M. A.; Sauntharajah, Y.; Barnard, J.; Lindner, D.; Rogers, H. J.; Tiu, R. V. Splicing Factor 3b Subunit 1 (Sf3b1) Haploinsufficient Mice Display Features of Low Risk Myelodysplastic Syndromes with Ring Sideroblasts. *Journal of Hematology & Oncology* **2014**, *7* (1), 89. <https://doi.org/10.1186/s13045-014-0089-x>.
- (11) Shekhar, R.; Srinivasan, V. K.; Pai, S. How I Investigate Dysgranulopoiesis. *International Journal of Laboratory Hematology* **2021**, *43* (4), 538–546. <https://doi.org/10.1111/ijlh.13607>.
- (12) Gordon, S. W.; Krystal, G. W. Auer Rods <https://www.nejm.org/doi/10.1056/NEJMicm1612344> (accessed 2021 -10 -11). <https://doi.org/10.1056/NEJMicm1612344>.
- (13) Zini, G. CHAPTER 16 - Abnormalities in Leukocyte Morphology and Number. In *Blood and Bone Marrow Pathology (Second Edition)*; Porwit, A., McCullough, J., Erber, W. N., Eds.; Churchill Livingstone: Edinburgh, 2011; pp 247–261. <https://doi.org/10.1016/B978-0-7020-3147-2.00016-X>.
- (14) Ogawa, S. Genetics of MDS. *Blood* **2019**, *133* (10), 1049–1059. <https://doi.org/10.1182/blood-2018-10-844621>.
- (15) Will, B.; Vogler, T. O.; Narayanagari, S.; Bartholdy, B.; Todorova, T. I.; da Silva Ferreira, M.; Chen, J.; Yu, Y.; Mayer, J.; Barreyro, L.; Carvajal, L.; Ben Neriah, D.; Roth, M.; van Oers, J.; Schaetzlein, S.; McMahon, C.; Edelmann, W.; Verma, A.; Steidl, U. Minimal PU.1

- Reduction Induces a Preleukemic State and Promotes Development of Acute Myeloid Leukemia. *Nat Med* **2015**, 21 (10), 1172–1181. <https://doi.org/10.1038/nm.3936>.
- (16) Thol, F.; Kade, S.; Schlarmann, C.; Löffeld, P.; Morgan, M.; Krauter, J.; Wlodarski, M. W.; Kölking, B.; Wichmann, M.; Görlich, K.; Göhring, G.; Bug, G.; Ottmann, O.; Niemeyer, C. M.; Hofmann, W.-K.; Schlegelberger, B.; Ganser, A.; Heuser, M. Frequency and Prognostic Impact of Mutations in SRSF2, U2AF1, and ZRSR2 in Patients with Myelodysplastic Syndromes. *Blood* **2012**, 119 (15), 3578–3584. <https://doi.org/10.1182/blood-2011-12-399337>.
  - (17) Corces-Zimmerman, M. R.; Majeti, R. Pre-Leukemic Evolution of Hematopoietic Stem Cells – the Importance of Early Mutations in Leukemogenesis. *Leukemia* **2014**, 28 (12), 2276–2282. <https://doi.org/10.1038/leu.2014.211>.
  - (18) Salama, M. E.; Hoffman, R. Chapter 55 - Progress in the Classification of Hematopoietic and Lymphoid Neoplasms: Clinical Implications. In *Hematology (Seventh Edition)*; Hoffman, R., Benz, E. J., Silberstein, L. E., Heslop, H. E., Weitz, J. I., Anastasi, J., Salama, M. E., Abutalib, S. A., Eds.; Elsevier, 2018; pp 763–773. <https://doi.org/10.1016/B978-0-323-35762-3.00055-X>.
  - (19) DiNardo, C. D.; Garcia-Manero, G.; Pierce, S.; Nazha, A.; Bueso-Ramos, C.; Jabbour, E.; Ravandi, F.; Cortes, J.; Kantarjian, H. Interactions and Relevance of Blast Percentage and Treatment Strategy among Younger and Older Patients with Acute Myeloid Leukemia (AML) and Myelodysplastic Syndrome (MDS). *Am J Hematol* **2016**, 91 (2), 227–232. <https://doi.org/10.1002/ajh.24252>.
  - (20) Hassarjian, R. P.; Campigotto, F.; Klepeis, V.; Fu, B.; Wang, S. A.; Bueso-Ramos, C.; Cascio, M. J.; Rogers, H. J.; Hsi, E. D.; Soderquist, C.; Bagg, A.; Yan, J.; Ochs, R.; Orazi, A.; Moore, F.; Mahmoud, A.; George, T. I.; Foucar, K.; Odem, J.; Booth, C.; Morice, W.; DeAngelo, D. J.; Steensma, D.; Stone, R. M.; Neuberg, D.; Arber, D. A. De Novo Acute Myeloid Leukemia with 20–29% Blasts Is Less Aggressive than Acute Myeloid Leukemia with ≥30% Blasts in Older Adults: A Bone Marrow Pathology Group Study. *American Journal of Hematology* **2014**, 89 (11), E193–E199. <https://doi.org/10.1002/ajh.23808>.
  - (21) Greenberg, P. L.; Stone, R. M.; Al-Kali, A.; Barta, S. K.; Bejar, R.; Bennett, J. M.; Carraway, H.; Castro, C. M. D.; Deeg, H. J.; DeZern, A. E.; Fathi, A. T.; Frankfurt, O.; Gaensler, K.; Garcia-Manero, G.; Griffiths, E. A.; Head, D.; Horsfall, R.; Johnson, R. A.; Juckett, M.; Klimek, V. M.; Komrokji, R.; Kujawski, L. A.; Maness, L. J.; O'Donnell, M. R.; Pollyea, D. A.; Shami, P. J.; Stein, B. L.; Walker, A. R.; Westervelt, P.; Zeidan, A.; Shead, D. A.; Smith, C. Myelodysplastic Syndromes, Version 2.2017, NCCN Clinical Practice Guidelines in Oncology. *Journal of the National Comprehensive Cancer Network* **2017**, 15 (1), 60–87. <https://doi.org/10.6004/jnccn.2017.0007>.
  - (22) Bains, A.; Luthra, R.; Medeiros, L. J.; Zuo, Z. FLT3 and NPM1 Mutations in Myelodysplastic Syndromes: Frequency and Potential Value for Predicting Progression to Acute Myeloid Leukemia. *American Journal of Clinical Pathology* **2011**, 135 (1), 62–69. <https://doi.org/10.1309/AJCPEI9XU8PYBCIO>.
  - (23) Caponetti, G. C.; Bagg, A. Mutations in Myelodysplastic Syndromes: Core Abnormalities and CHIPping Away at the Edges. *International Journal of Laboratory Hematology* **2020**, 42 (6), 671–684. <https://doi.org/10.1111/ijlh.13284>.
  - (24) Lorand-Metze, I.; Niero-Melo, L.; Buzzini, R.; Bernardo, W. M. Part 2: Myelodysplastic Syndromes – Classification Systems. *Hematol Transfus Cell Ther* **2018**, 40 (3), 262–266. <https://doi.org/10.1016/j.htct.2018.05.005>.
  - (25) Della Porta, M. G.; Tuechler, H.; Malcovati, L.; Schanz, J.; Sanz, G.; Garcia-Manero, G.; Solé, F.; Bennett, J. M.; Bowen, D.; Fenaux, P.; Dreyfus, F.; Kantarjian, H.; Kuendgen, A.; Levis, A.; Cermak, J.; Fonatsch, C.; Le Beau, M. M.; Slovak, M. L.; Krieger, O.; Luebbert, M.; Maciejewski, J.; Magalhaes, S. M. M.; Miyazaki, Y.; Pfeilstöcker, M.; Sekeres, M. A.; Sperr, W. R.; Stauder, R.; Tauro, S.; Valent, P.; Vallespi, T.; van de Loosdrecht, A. A.; Germing, U.; Haase, D.; Greenberg, P. L.; Cazzola, M. Validation of WHO Classification-

- Based Prognostic Scoring System (WPSS) for Myelodysplastic Syndromes and Comparison with the Revised International Prognostic Scoring System (IPSS-R). A Study of the International Working Group for Prognosis in Myelodysplasia (IWG-PM). *Leukemia* **2015**, 29 (7), 1502–1513. <https://doi.org/10.1038/leu.2015.55>.
- (26) Komrokji, R.; Ramadan, H.; Ali, N. A.; Corrales-Yepez, M.; Zhang, L.; Padron, E.; Lancet, J.; List, A. Validation of the Lower-Risk MD Anderson Prognostic Scoring System for Patients With Myelodysplastic Syndrome. *Clinical Lymphoma, Myeloma and Leukemia* **2015**, 15, S60–S63. <https://doi.org/10.1016/j.clml.2015.03.011>.
- (27) Komrokji, R. S.; Corrales-Yepez, M.; Al Ali, N.; Kharfan-Dabaja, M.; Padron, E.; Fields, T.; Lancet, J. E.; List, A. F. Validation of the MD Anderson Prognostic Risk Model for Patients with Myelodysplastic Syndrome. *Cancer* **2012**, 118 (10), 2659–2664. <https://doi.org/10.1002/cncr.26567>.
- (28) Jonas, B. A.; Greenberg, P. L. MDS Prognostic Scoring Systems – Past, Present, and Future. *Best Pract Res Clin Haematol* **2015**, 28 (1), 3–13. <https://doi.org/10.1016/j.beha.2014.11.001>.
- (29) Malcovati, L.; Germing, U.; Kuendgen, A.; Della Porta, M. G.; Pascutto, C.; Invernizzi, R.; Giagounidis, A.; Hildebrandt, B.; Bernasconi, P.; Knipp, S.; Strupp, C.; Lazzarino, M.; Aul, C.; Cazzola, M. Time-Dependent Prognostic Scoring System for Predicting Survival and Leukemic Evolution in Myelodysplastic Syndromes. *JCO* **2007**, 25 (23), 3503–3510. <https://doi.org/10.1200/JCO.2006.08.5696>.
- (30) Itzykson, R.; Thépot, S.; Quesnel, B.; Dreyfus, F.; Beyne-Rauzy, O.; Turlure, P.; Vey, N.; Recher, C.; Dartigeas, C.; Legros, L.; Delaunay, J.; Salanoubat, C.; Visanica, S.; Stamatoullas, A.; Isnard, F.; Marfaing-Koka, A.; de Botton, S.; Chelghoum, Y.; Taksin, A.-L.; Plantier, I.; Ame, S.; Boehrer, S.; Gardin, C.; Beach, C. L.; Adès, L.; Fenaux, P. Prognostic Factors for Response and Overall Survival in 282 Patients with Higher-Risk Myelodysplastic Syndromes Treated with Azacitidine. *Blood* **2011**, 117 (2), 403–411. <https://doi.org/10.1182/blood-2010-06-289280>.
- (31) Greenberg, P. L.; Tuechler, H.; Schanz, J.; Sanz, G.; Garcia-Manero, G.; Solé, F.; Bennett, J. M.; Bowen, D.; Fenaux, P.; Dreyfus, F.; Kantarjian, H.; Kuendgen, A.; Levis, A.; Malcovati, L.; Cazzola, M.; Cermak, J.; Fonatsch, C.; Le Beau, M. M.; Slovak, M. L.; Krieger, O.; Luebbert, M.; Maciejewski, J.; Magalhaes, S. M. M.; Miyazaki, Y.; Pfeilstöcker, M.; Sekeres, M.; Sperr, W. R.; Stauder, R.; Tauro, S.; Valent, P.; Vallespi, T.; van de Loosdrecht, A. A.; Germing, U.; Haase, D. Revised International Prognostic Scoring System for Myelodysplastic Syndromes. *Blood* **2012**, 120 (12), 2454–2465. <https://doi.org/10.1182/blood-2012-03-420489>.
- (32) Woll, P. S.; Kjällquist, U.; Chowdhury, O.; Doolittle, H.; Wedge, D. C.; Thongjuea, S.; Erlandsson, R.; Ngara, M.; Anderson, K.; Deng, Q.; Mead, A. J.; Stenson, L.; Giustacchini, A.; Duarte, S.; Giannoulatou, E.; Taylor, S.; Karimi, M.; Scharenberg, C.; Mortera-Blanco, T.; Macaulay, I. C.; Clark, S.-A.; Dybedal, I.; Josefsen, D.; Fenaux, P.; Hokland, P.; Holm, M. S.; Cazzola, M.; Malcovati, L.; Tauro, S.; Bowen, D.; Boultonwood, J.; Pellagatti, A.; Pimanda, J. E.; Unnikrishnan, A.; Vyas, P.; Göhring, G.; Schlegelberger, B.; Tobiasson, M.; Kvalheim, G.; Constantinescu, S. N.; Nerlov, C.; Nilsson, L.; Campbell, P. J.; Sandberg, R.; Papaemmanuil, E.; Hellström-Lindberg, E.; Linnarsson, S.; Jacobsen, S. E. W. Myelodysplastic Syndromes Are Propagated by Rare and Distinct Human Cancer Stem Cells In Vivo. *Cancer Cell* **2014**, 25 (6), 794–808. <https://doi.org/10.1016/j.ccr.2014.03.036>.
- (33) Will, B.; Zhou, L.; Vogler, T. O.; Ben-Neriah, S.; Schinke, C.; Tamari, R.; Yu, Y.; Bhagat, T. D.; Bhattacharyya, S.; Barreyro, L.; Heuck, C.; Mo, Y.; Parekh, S.; McMahon, C.; Pellagatti, A.; Boultonwood, J.; Montagna, C.; Silverman, L.; Maciejewski, J.; Greally, J. M.; Ye, B. H.; List, A. F.; Steidl, C.; Steidl, U.; Verma, A. Stem and Progenitor Cells in Myelodysplastic Syndromes Show Aberrant Stage-Specific Expansion and Harbor Genetic and Epigenetic Alterations. *Blood* **2012**, 120 (10), 2076–2086. <https://doi.org/10.1182/blood-2011-12-399683>.

- (34) Shastri, A.; Will, B.; Steidl, U.; Verma, A. Stem and Progenitor Cell Alterations in Myelodysplastic Syndromes. *Blood* **2017**, *129* (12), 1586–1594. <https://doi.org/10.1182/blood-2016-10-696062>.
- (35) Giagounidis, A. Current Treatment Algorithm for the Management of Lower-Risk MDS. *Hematology Am Soc Hematol Educ Program* **2017**, *2017* (1), 453–459.
- (36) Guidelines Detail <https://www.nccn.org/guidelines/guidelines-detail> (accessed 2021 -06 -18).
- (37) Platzbecker, U. Treatment of MDS. *Blood* **2019**, *133* (10), 1096–1107. <https://doi.org/10.1182/blood-2018-10-844696>.
- (38) Germing, U.; Schroeder, T.; Kaivers, J.; Kündgen, A.; Kobbe, G.; Gattermann, N. Novel Therapies in Low- and High-Risk Myelodysplastic Syndrome. *Expert Review of Hematology* **2019**, *12* (10), 893–908. <https://doi.org/10.1080/17474086.2019.1647778>.
- (39) Malcovati, L.; Hellström-Lindberg, E.; Bowen, D.; Adès, L.; Cermak, J.; del Cañizo, C.; Della Porta, M. G.; Fenaux, P.; Gattermann, N.; Germing, U.; Jansen, J. H.; Mittelman, M.; Mufti, G.; Platzbecker, U.; Sanz, G. F.; Selleslag, D.; Skov-Holm, M.; Stauder, R.; Symeonidis, A.; van de Loosdrecht, A. A.; de Witte, T.; Cazzola, M. Diagnosis and Treatment of Primary Myelodysplastic Syndromes in Adults: Recommendations from the European LeukemiaNet. *Blood* **2013**, *122* (17), 2943–2964. <https://doi.org/10.1182/blood-2013-03-492884>.
- (40) Fenaux, P.; Platzbecker, U.; Ades, L. How We Manage Adults with Myelodysplastic Syndrome. *British Journal of Haematology* **2020**, *189* (6), 1016–1027. <https://doi.org/10.1111/bjh.16206>.
- (41) Steensma, D. P. Myelodysplastic Syndromes Current Treatment Algorithm 2018. *Blood Cancer Journal* **2018**, *8* (5), 1–7. <https://doi.org/10.1038/s41408-018-0085-4>.
- (42) Platzbecker, U.; Germing, U.; Götze, K. S.; Kiewe, P.; Mayer, K.; Chromik, J.; Radsak, M.; Wolff, T.; Zhang, X.; Laadem, A.; Sherman, M. L.; Attie, K. M.; Giagounidis, A. Luspatercept for the Treatment of Anaemia in Patients with Lower-Risk Myelodysplastic Syndromes (PACE-MDS): A Multicentre, Open-Label Phase 2 Dose-Finding Study with Long-Term Extension Study. *The Lancet Oncology* **2017**, *18* (10), 1338–1347. [https://doi.org/10.1016/S1470-2045\(17\)30615-0](https://doi.org/10.1016/S1470-2045(17)30615-0).
- (43) Fenaux, P.; Kiladjian, J. J.; Platzbecker, U. Luspatercept for the Treatment of Anemia in Myelodysplastic Syndromes and Primary Myelofibrosis. *Blood* **2019**, *133* (8), 790–794. <https://doi.org/10.1182/blood-2018-11-876888>.
- (44) Fenaux, P.; Platzbecker, U.; Mufti, G. J.; Garcia-Manero, G.; Buckstein, R.; Santini, V.; Díez-Campelo, M.; Finelli, C.; Cazzola, M.; Ilhan, O.; Sekeres, M. A.; Falantes, J. F.; Arrizabalaga, B.; Salvi, F.; Giai, V.; Vyas, P.; Bowen, D.; Selleslag, D.; DeZern, A. E.; Jurcic, J. G.; Germing, U.; Götze, K. S.; Quesnel, B.; Beyne-Rauzy, O.; Cluzeau, T.; Voso, M.-T.; Mazure, D.; Vellenga, E.; Greenberg, P. L.; Hellström-Lindberg, E.; Zeidan, A. M.; Adès, L.; Verma, A.; Savona, M. R.; Laadem, A.; Benzohra, A.; Zhang, J.; Rampersad, A.; Dunshee, D. R.; Linde, P. G.; Sherman, M. L.; Komrokji, R. S.; List, A. F. Luspatercept in Patients with Lower-Risk Myelodysplastic Syndromes. *New England Journal of Medicine* **2020**, *382* (2), 140–151. <https://doi.org/10.1056/NEJMoa1908892>.
- (45) Leader, A.; Hofstetter, L.; Spectre, G. Challenges and Advances in Managing Thrombocytopenic Cancer Patients. *JCM* **2021**, *10* (6), 1169. <https://doi.org/10.3390/jcm10061169>.
- (46) Ghanima, W.; Cooper, N.; Rodeghiero, F.; Godeau, B.; Bussel, J. B. Thrombopoietin Receptor Agonists: Ten Years Later. *Haematologica* **2019**, *104* (6), 1112–1123. <https://doi.org/10.3324/haematol.2018.212845>.
- (47) Goldman, L.; Schafer, A. I.; ClinicalKey. *Goldman-Cecil Medicine*; 2020.
- (48) Angelucci, E.; Li, J.; Greenberg, P. L.; Depei, W.; Hou, M.; Montañó Figueroa, E.; Rodríguez, G.; Dong, X.; Ghosh, J.; Bornstein, O.; Garcia-Manero, G. Safety and Efficacy, Including Event-Free Survival, of Deferasirox Versus Placebo in Iron-Overloaded Patients with Low-

- and Int-1-Risk Myelodysplastic Syndromes (MDS): Outcomes from the Randomized, Double-Blind Telesio Study. *Blood* **2018**, 132 (Supplement 1), 234. <https://doi.org/10.1182/blood-2018-99-111134>.
- (49) Lodé, L.; Ménard, A.; Flet, L.; Richebourg, S.; Loirat, M.; Eveillard, M.; Le Bris, Y.; Godon, C.; Theisen, O.; Gagez, A.-L.; Cartron, G.; Commes-Maerten, T.; Villemagne, B.; Luyckx, O.; Godmer, P.; Pellat-Deceunynck, C.; Soussi, T.; Béné, M. C.; Delaunay, J.; Peterlin, P. Emergence and Evolution of TP53 Mutations Are Key Features of Disease Progression in Myelodysplastic Patients with Lower-Risk Del(5q) Treated with Lenalidomide. *Haematologica* **2018**, 103 (4), e143–e146. <https://doi.org/10.3324/haematol.2017.181404>.
- (50) Fink, E. C.; Ebert, B. L. The Novel Mechanism of Lenalidomide Activity. *Blood* **2015**, 126 (21), 2366–2369. <https://doi.org/10.1182/blood-2015-07-567958>.
- (51) Fenaux, P.; Giagounidis, A.; Selleslag, D.; Beyne-Rauzy, O.; Mufti, G.; Mittelman, M.; Muus, P.; te Boekhorst, P.; Sanz, G.; del Cañizo, C.; Guerci-Bresler, A.; Nilsson, L.; Platzbecker, U.; Lübbert, M.; Quesnel, B.; Cazzola, M.; Ganser, A.; Bowen, D.; Schlegelberger, B.; Aul, C.; Knight, R.; Francis, J.; Fu, T.; Hellström-Lindberg, E.; for the MDS-004 Lenalidomide del5q Study Group. A Randomized Phase 3 Study of Lenalidomide versus Placebo in RBC Transfusion-Dependent Patients with Low-/Intermediate-1-Risk Myelodysplastic Syndromes with Del5q. *Blood* **2011**, 118 (14), 3765–3776. <https://doi.org/10.1182/blood-2011-01-330126>.
- (52) Santini, V.; Almeida, A.; Giagounidis, A.; Gröpper, S.; Jonasova, A.; Vey, N.; Mufti, G. J.; Buckstein, R.; Mittelman, M.; Platzbecker, U.; Shpilberg, O.; Ram, R.; del Cañizo, C.; Gattermann, N.; Ozawa, K.; Risueño, A.; MacBeth, K. J.; Zhong, J.; Séguin, F.; Hoenekopp, A.; Beach, C. I.; Fenaux, P. Randomized Phase III Study of Lenalidomide Versus Placebo in RBC Transfusion-Dependent Patients With Lower-Risk Non-Del(5q) Myelodysplastic Syndromes and Ineligible for or Refractory to Erythropoiesis-Stimulating Agents. *JCO* **2016**, 34 (25), 2988–2996. <https://doi.org/10.1200/JCO.2015.66.0118>.
- (53) Itzykson, R.; Thépot, S.; Achour, B.; Quesnel, B.; Dreyfus, F.; Turlure, P.; Taksin, A.-L.; Vey, N.; Koka, A. M.; de Botton, S.; Wattel, E.; Isnard, F.; Plantier, I.; Dartigeas, C.; Zerhouni, C.; Gardin, C.; Ades, L.; Beyne-Rauzy, O.; Fenaux, P. Azacytidine (AZA) in MDS (Including RAEB-t and CMML) in Patients (Pts) ≥ 80 Years: Results of the French ATU Program. *Blood* **2009**, 114 (22), 1773. <https://doi.org/10.1182/blood.V114.22.1773.1773>.
- (54) Thepot, S.; Itzykson, R.; Seegers, V.; Raffoux, E.; Quesnel, B.; Chait, Y.; Sorin, L.; Dreyfus, F.; Cluzeau, T.; Delaunay, J.; Sanhes, L.; Eclache, V.; Dartigeas, C.; Turlure, P.; Harel, S.; Salanoubat, C.; Kiladjian, J.-J.; Fenaux, P.; Adès, L. Treatment of Progression of Philadelphia-Negative Myeloproliferative Neoplasms to Myelodysplastic Syndrome or Acute Myeloid Leukemia by Azacytidine: A Report on 54 Cases on the Behalf of the Groupe Francophone Des Myelodysplasies (GFM). *Blood* **2010**, 116 (19), 3735–3742. <https://doi.org/10.1182/blood-2010-03-274811>.
- (55) Fenaux, P.; Mufti, G. J.; Hellstrom-Lindberg, E.; Santini, V.; Finelli, C.; Giagounidis, A.; Schoch, R.; Gattermann, N.; Sanz, G.; List, A.; Gore, S. D.; Seymour, J. F.; Bennett, J. M.; Byrd, J.; Backstrom, J.; Zimmerman, L.; McKenzie, D.; Beach, C. L.; Silverman, L. R. Efficacy of Azacytidine Compared with That of Conventional Care Regimens in the Treatment of Higher-Risk Myelodysplastic Syndromes: A Randomised, Open-Label, Phase III Study. *The Lancet Oncology* **2009**, 10 (3), 223–232. [https://doi.org/10.1016/S1470-2045\(09\)70003-8](https://doi.org/10.1016/S1470-2045(09)70003-8).
- (56) Itzykson, R.; Kosmider, O.; Renneville, A.; Morabito, M.; Preudhomme, C.; Berthon, C.; Adès, L.; Fenaux, P.; Platzbecker, U.; Gagey, O.; Rameau, P.; Meurice, G.; Oréar, C.; Delhommeau, F.; Bernard, O. A.; Fontenay, M.; Vainchenker, W.; Droin, N.; Solary, E. Clonal Architecture of Chronic Myelomonocytic Leukemias. *Blood* **2013**, 121 (12), 2186–2198. <https://doi.org/10.1182/blood-2012-06-440347>.



- (57) Derissen, E. J. B.; Beijnen, J. H.; Schellens, J. H. M. Concise Drug Review: Azacitidine and Decitabine. *The Oncologist* **2013**, *18* (5), 619–624. <https://doi.org/10.1634/theoncologist.2012-0465>.
- (58) Lee, B.-H.; Kang, K.-W.; Jeon, M. J.; Yu, E. S.; Kim, D. S.; Choi, H.; Lee, S. R.; Sung, H. J.; Kim, B. S.; Choi, C. W.; Park, Y. Comparison between 5-Day Decitabine and 7-Day Azacitidine for Lower-Risk Myelodysplastic Syndromes with Poor Prognostic Features: A Retrospective Multicentre Cohort Study. *Sci Rep* **2020**, *10* (1), 39. <https://doi.org/10.1038/s41598-019-56642-1>.
- (59) Bhatt, V. R.; Steensma, D. P. Hematopoietic Cell Transplantation for Myelodysplastic Syndromes. *JOP* **2016**, *12* (9), 786–792. <https://doi.org/10.1200/JOP.2016.015214>.
- (60) Gerds, A. T.; Ahn, K. W.; Hu, Z.-H.; Abdel-Azim, H.; Akpek, G.; Aljurf, M.; Ballen, K. K.; Beitinjaneh, A.; Bacher, U.; Cahn, J.-Y.; Chhabra, S.; Cutler, C.; Daly, A.; DeFilipp, Z.; Gale, R. P.; Gergis, U.; Grunwald, M. R.; Hale, G. A.; Hamilton, B. K.; Jagasia, M.; Kamble, R. T.; Kindwall-Keller, T.; Nishihori, T.; Olsson, R. F.; Ramanathan, M.; Saad, A. A.; Solh, M.; Ustun, C.; Valcárcel, D.; Warlick, E.; Wirk, B. M.; Kalaycio, M.; Alyea, E.; Popat, U.; Sobecks, R.; Saber, W. Outcomes after Umbilical Cord Blood Transplantation for Myelodysplastic Syndromes. *Biol Blood Marrow Transplant* **2017**, *23* (6), 971–979. <https://doi.org/10.1016/j.bbmt.2017.03.014>.
- (61) de Witte, T.; Bowen, D.; Robin, M.; Malcovati, L.; Niederwieser, D.; Yakoub-Agha, I.; Mufti, G. J.; Fenaux, P.; Sanz, G.; Martino, R.; Alessandrino, E. P.; Onida, F.; Symeonidis, A.; Passweg, J.; Kobbe, G.; Ganser, A.; Platzbecker, U.; Finke, J.; van Gelder, M.; van de Loosdrecht, A. A.; Ljungman, P.; Stauder, R.; Volin, L.; Deeg, H. J.; Cutler, C.; Saber, W.; Champlin, R.; Giral, S.; Anasetti, C.; Kröger, N. Allogeneic Hematopoietic Stem Cell Transplantation for MDS and CMML: Recommendations from an International Expert Panel. *Blood* **2017**, *129* (13), 1753–1762. <https://doi.org/10.1182/blood-2016-06-724500>.
- (62) Grunwald, M. R.; Zhang, M.-J.; Elmariah, H.; Johnson, M. H.; St. Martin, A.; Bashey, A.; Bolanos-Meade, J.; Bredeson, C.; Copelan, E. A.; George, B.; Gupta, V.; Kanakry, C. G.; Mehta, R. S.; Battiwalla, M.; Mussetti, A.; Nakamura, R.; Nishihori, T.; Saber, W.; Solh, M.; Tomlinson, B. K.; Weisdorf, D. J.; Eapen, M. Allogeneic Transplantation for Myelodysplastic Syndrome in Adults over 50 Years Old Using Reduced Intensity/Non-Myeloablative Conditioning: Haploidentical Relative Versus Matched Unrelated Donor. *Blood* **2019**, *134* (Supplement\_1), 3323–3323. <https://doi.org/10.1182/blood-2019-125865>.
- (63) Sorrow, M. L.; Storb, R. F.; Sandmaier, B. M.; Maziarz, R. T.; Pulsipher, M. A.; Maris, M. B.; Bhatia, S.; Ostronoff, F.; Deeg, H. J.; Syrjala, K. L.; Estey, E.; Maloney, D. G.; Appelbaum, F. R.; Martin, P. J.; Storer, B. E. Comorbidity-Age Index: A Clinical Measure of Biologic Age Before Allogeneic Hematopoietic Cell Transplantation. *J Clin Oncol* **2014**, *32* (29), 3249–3256. <https://doi.org/10.1200/JCO.2013.53.8157>.
- (64) Roberts, L.; Salit, R. B.; Longo, L.; Xue, E.; Summers, C.; Delaney, C.; Dahlberg, A.; Milano, F. Cord Blood Transplantation Is an Effective Treatment Option in Patients with Myelodysplastic and Myeloproliferative Syndromes. *Blood* **2019**, *134* (Supplement\_1), 2048–2048. <https://doi.org/10.1182/blood-2019-126216>.
- (65) Guillaume, T.; Thépot, S.; Peterlin, P.; Ceballos, P.; Bourgeois, A. L.; Garnier, A.; Orvain, C.; Giltat, A.; François, S.; Bris, Y. L.; Fronteau, C.; Planche, L.; Chevallier, P. Prophylactic or Preemptive Low-Dose Azacitidine and Donor Lymphocyte Infusion to Prevent Disease Relapse Following Allogeneic Transplantation in Patients with High-Risk Acute Myelogenous Leukemia or Myelodysplastic Syndrome. *Transplantation and Cellular Therapy, Official Publication of the American Society for Transplantation and Cellular Therapy* **2021**, *27* (10), 839.e1–839.e6. <https://doi.org/10.1016/j.jtct.2021.06.029>.
- (66) Oran, B.; de Lima, M.; Garcia-Manero, G.; Thall, P. F.; Lin, R.; Popat, U.; Alousi, A. M.; Hosing, C.; Giral, S.; Rondon, G.; Woodworth, G.; Champlin, R. E. A Phase 3 Randomized Study of 5-Azacitidine Maintenance vs Observation after Transplant in High-Risk AML and

- MDS Patients. *Blood Adv* **2020**, 4 (21), 5580–5588. <https://doi.org/10.1182/bloodadvances.2020002544>.
- (67) Garcia-Manero, G.; Roboz, G.; Walsh, K.; Kantarjian, H.; Ritchie, E.; Kropf, P.; O'Connell, C.; Tibes, R.; Lunin, S.; Rosenblat, T.; Yee, K.; Stock, W.; Griffiths, E.; Mace, J.; Podoltsev, N.; Berdeja, J.; Jabbour, E.; Issa, J.-P. J.; Hao, Y.; Keer, H. N.; Azab, M.; Savona, M. R. Guadecitabine (SGI-110) in Patients with Intermediate or High-Risk Myelodysplastic Syndromes: Phase 2 Results from a Multicentre, Open-Label, Randomised, Phase 1/2 Trial. *The Lancet Haematology* **2019**, 6 (6), e317–e327. [https://doi.org/10.1016/S2352-3026\(19\)30029-8](https://doi.org/10.1016/S2352-3026(19)30029-8).
- (68) Komrokji, R.; Garcia-Manero, G.; Ades, L.; Prebet, T.; Steensma, D. P.; Jurcic, J. G.; Sekeres, M. A.; Berdeja, J.; Savona, M. R.; Beyne-Rauzy, O.; Stamatoullas, A.; DeZern, A. E.; Delaunay, J.; Borthakur, G.; Rifkin, R.; Boyd, T. E.; Laadem, A.; Vo, B.; Zhang, J.; Puccio-Pick, M.; Attie, K. M.; Fenaux, P.; List, A. F. Sotatercept with Long-Term Extension for the Treatment of Anaemia in Patients with Lower-Risk Myelodysplastic Syndromes: A Phase 2, Dose-Ranging Trial. *The Lancet. Haematology* **2018**, 5 (2), e63–e72. [https://doi.org/10.1016/S2352-3026\(18\)30002-4](https://doi.org/10.1016/S2352-3026(18)30002-4).
- (69) Henry, D. Oral Roxadustat Demonstrates Efficacy in Anemia Secondary to Lower-Risk Myelodysplastic Syndrome Irrespective of Ring Sideroblasts and Baseline Erythropoietin Levels; ASH, 2020.
- (70) Steensma, D. P.; Fenaux, P.; Van Eygen, K.; Raza, A.; Santini, V.; Germing, U.; Font, P.; Diez-Campelo, M.; Thepot, S.; Vellenga, E.; Patnaik, M. M.; Jang, J. H.; Varsos, H.; Bussolari, J.; Rose, E.; Sherman, L.; Sun, L.; Wan, Y.; Dougherty, S.; Huang, F.; Feller, F.; Rizo, A.; Platzbecker, U. Imetelstat Achieves Meaningful and Durable Transfusion Independence in High Transfusion-Burden Patients With Lower-Risk Myelodysplastic Syndromes in a Phase II Study. *J Clin Oncol* **2021**, 39 (1), 48–56. <https://doi.org/10.1200/JCO.20.01895>.
- (71) Garcia-Manero, G.; Santini, V.; Almeida, A.; Platzbecker, U.; Jonasova, A.; Silverman, L. R.; Falantes, J.; Reda, G.; Buccisano, F.; Fenaux, P.; Buckstein, R.; Diez Campelo, M.; Larsen, S.; Valcarcel, D.; Vyas, P.; Giai, V.; Olíva, E. N.; Shortt, J.; Niederwieser, D.; Mittelman, M.; Fianchi, L.; La Torre, I.; Zhong, J.; Laille, E.; Lopes de Menezes, D.; Skikne, B.; Beach, C. L.; Giagounidis, A. Phase III, Randomized, Placebo-Controlled Trial of CC-486 (Oral Azacitidine) in Patients With Lower-Risk Myelodysplastic Syndromes. *JCO* **2021**, 39 (13), 1426–1436. <https://doi.org/10.1200/JCO.20.02619>.
- (72) Sébert, M.; Renneville, A.; Bally, C.; Peterlin, P.; Beyne-Rauzy, O.; Legros, L.; Gourin, M.-P.; Sanhes, L.; Wattel, E.; Gyan, E.; Park, S.; Stamatoullas, A.; Banos, A.; Laribi, K.; Jueliger, S.; Bevan, L.; Chermat, F.; Sapena, R.; Nibourel, O.; Chaffaut, C.; Chevret, S.; Preudhomme, C.; Adès, L.; Fenaux, P. A Phase II Study of Guadecitabine in Higher-Risk Myelodysplastic Syndrome and Low Blast Count Acute Myeloid Leukemia after Azacitidine Failure. *Haematologica* **2019**, 104 (8), 1565–1571. <https://doi.org/10.3324/haematol.2018.207118>.
- (73) Savona, M.; McCloskey, J.; Griffiths, E.; Yee, K.; Al-Kali, A.; Zeidan, A.; Deeg, H.; Patel, P.; Sabloff, M.; Keating, M.-M.; Dao, K.-H.; Zhu, N.; Gabrail, N.; Fazal, S.; Maly, J.; Odenike, O.; Kantarjian, H.; Dezern, A.; O'Connell, C.; Garcia-Manero, G. Clinical Efficacy and Safety of Oral Decitabine/Cedazuridine in 133 Patients with Myelodysplastic Syndromes (MDS) and Chronic Myelomonocytic Leukemia (CMML). *Blood* **2020**, 136, 37–38. <https://doi.org/10.1182/blood-2020-133855>.
- (74) Sekeres, M. Efficacy and Safety of Pevonedistat Plus Azacitidine Vs Azacitidine Alone in Higher-Risk Myelodysplastic Syndromes (MDS) from Study P-2001 (NCT02610777); ASH, 2020.
- (75) Richard-Carpentier, G.; DeZern, A. E.; Takahashi, K.; Konopleva, M. Y.; Loghavi, S.; Masarova, L.; Alvarado, Y.; Ravandi, F.; Montalban Bravo, G.; Naqvi, K.; Sasaki, K.; Delumpa, R.; Kwari, M.; Sekeres, M. A.; Nazha, A.; Roboz, G. J.; Kantarjian, H. M.; Garcia-

- Manero, G.; DiNardo, C. D. Preliminary Results from the Phase II Study of the IDH2-Inhibitor Enasidenib in Patients with High-Risk IDH2-Mutated Myelodysplastic Syndromes (MDS). *Blood* **2019**, *134* (Supplement\_1), 678–678. <https://doi.org/10.1182/blood-2019-130501>.
- (76) Stein, E. M.; Fathi, A. T.; DiNardo, C. D.; Pollyea, D. A.; Roboz, G. J.; Collins, R.; Sekeres, M. A.; Stone, R. M.; Attar, E. C.; Frattini, M. G.; Tosolini, A.; Xu, Q.; See, W. L.; MacBeth, K. J.; Botton, S. de; Tallman, M. S.; Kantarjian, H. M. Enasidenib in Patients with Mutant IDH2 Myelodysplastic Syndromes: A Phase 1 Subgroup Analysis of the Multicentre, AG221-C-001 Trial. *The Lancet Haematology* **2020**, *7* (4), e309–e319. [https://doi.org/10.1016/S2352-3026\(19\)30284-4](https://doi.org/10.1016/S2352-3026(19)30284-4).
- (77) Cortes, J. E.; Wang, E. S.; Watts, J. M.; Lee, S.; Baer, M. R.; Dao, K.-H.; Dinner, S.; Yang, J.; Donnellan, W. B.; Schwarzer, A. P.; Recher, C.; Kelly, P.; Sweeney, J.; Brevard, J.; Henrick, P.; Forsyth, S.; Guichard, S.; Mohamed, H.; Wei, A. H. Olutasidenib (FT-2102) Induces Rapid Remissions in Patients with IDH1-Mutant Myelodysplastic Syndrome: Results of Phase 1/2 Single Agent Treatment and Combination with Azacitidine. *Blood* **2019**, *134* (Supplement\_1), 674–674. <https://doi.org/10.1182/blood-2019-124360>.
- (78) Zeidan, A. M.; Pollyea, D. A.; Garcia, J. S.; Brunner, A.; Roncolato, F.; Borate, U.; Odenike, O.; Bajel, A. R.; Watson, A. M.; Götze, K.; Nolte, F.; Tan, P. T.; Hong, W.-J.; Dunbar, M.; Zhou, Y.; Gressick, L.; Ainsworth, W.; Harb, J.; Salem, A. H.; Hayslip, J.; Swords, R.; Garcia-Manero, G. A Phase 1b Study Evaluating the Safety and Efficacy of Venetoclax As Monotherapy or in Combination with Azacitidine for the Treatment of Relapsed/Refractory Myelodysplastic Syndrome. *Blood* **2019**, *134* (Supplement\_1), 565–565. <https://doi.org/10.1182/blood-2019-124994>.
- (79) Wei, A. H.; Garcia, J. S.; Borate, U.; Fong, C. Y.; Baer, M. R.; Nolte, F.; Peterlin, P.; Jurcic, J. G.; Garcia-Manero, G.; Hong, W.-J.; Platzbecker, U.; Odenike, O.; Dunbar, M.; Zhou, Y.; Harb, J.; Tanwani, P.; Wolff, J. E.; Jacoby, M. A Phase 1b Study Evaluating the Safety and Efficacy of Venetoclax in Combination with Azacitidine in Treatment-Naïve Patients with Higher-Risk Myelodysplastic Syndrome. *Blood* **2019**, *134* (Supplement\_1), 568–568. <https://doi.org/10.1182/blood-2019-124437>.
- (80) Zeidan, A. M.; Cavenagh, J.; Voso, M. T.; Taussig, D.; Tormo, M.; Boss, I.; Copeland, W. B.; Gray, V. E.; Previtali, A.; O'Connor, T.; Rose, S.; Beach, C.; Silverman, L. R. Efficacy and Safety of Azacitidine (AZA) in Combination with the Anti-PD-L1 Durvalumab (Durva) for the Front-Line Treatment of Older Patients (Pts) with Acute Myeloid Leukemia (AML) Who Are Unfit for Intensive Chemotherapy (IC) and Pts with Higher-Risk Myelodysplastic Syndromes (HR-MDS): Results from a Large, International, Randomized Phase 2 Study. *Blood* **2019**, *134* (Supplement\_1), 829–829. <https://doi.org/10.1182/blood-2019-122896>.
- (81) Gerds, A. T.; Scott, B. L.; Greenberg, P. L.; Khaled, S. K.; Lin, T. L.; Pollyea, D. A.; Verma, A.; Dail, M.; Green, C.; Ma, C.; Medeiros, B. C.; Phuong, P.; Wenger, M.; Yan, M.; Donnellan, W. B. PD-L1 Blockade with Atezolizumab in Higher-Risk Myelodysplastic Syndrome: An Initial Safety and Efficacy Analysis. *Blood* **2018**, *132* (Supplement 1), 466–466. <https://doi.org/10.1182/blood-2018-99-118577>.
- (82) Garcia-Manero, G.; Sasaki, K.; Montalban-Bravo, G.; Daver, N. G.; Jabbour, E. J.; Alvarado, Y.; DiNardo, C. D.; Ravandi, F.; Borthakur, G.; Bose, P.; Pemmaraju, N.; Naqvi, K.; Cortes, J. E.; Kadia, T. M.; Konopleva, M. Y.; Colla, S.; Yang, H.; Rausch, C. R.; Gasior, Y.; Bueso-Ramos, C. E.; Kanagal-Shamanna, R.; Patel, K. P.; Kantarjian, H. M. A Phase II Study of Nivolumab or Ipilimumab with or without Azacitidine for Patients with Myelodysplastic Syndrome (MDS). *Blood* **2018**, *132* (Supplement 1), 465–465. <https://doi.org/10.1182/blood-2018-99-119424>.
- (83) Brunner, A. Efficacy and Safety of Sabatolimab (MBG453) in Combination with Hypomethylating Agents (HMAs) in Patients with Acute Myeloid Leukemia (AML) and High-Risk Myelodysplastic Syndrome (HR-MDS): Updated Results from a Phase 1b Study; ASH, 2020.

- (84) Navada, S. C.; Garcia-Manero, G.; Atallah, E. L.; Rajeh, M. N.; Shammo, J. M.; Griffiths, E. A.; Khaled, S. K.; Dakhil, S. R.; Young, D. E.; Odchimar-Reissig, R.; Adesanya, A. R.; Zbyszewski, P. S.; Woodman, R. C.; Fenaux, P.; Silverman, L. R. Phase II Study of Oral Rigosertib Combined with Azacitidine (AZA) As First Line Therapy in Patients (Pts) with Higher-Risk Myelodysplastic Syndromes (HR-MDS). *Blood* **2019**, *134* (Supplement\_1), 566–566. <https://doi.org/10.1182/blood-2019-131676>.
- (85) Cortes, J. E.; Douglas Smith, B.; Wang, E. S.; Merchant, A.; Oehler, V. G.; Arellano, M.; DeAngelo, D. J.; Pollyea, D. A.; Sekeres, M. A.; Robak, T.; Ma, W. W.; Zeremski, M.; Naveed Shaik, M.; Douglas Laird, A.; O'Connell, A.; Chan, G.; Schroeder, M. A. Glasdegib in Combination with Cytarabine and Daunorubicin in Patients with AML or High-risk MDS: Phase 2 Study Results. *Am J Hematol* **2018**, *93* (11), 1301–1310. <https://doi.org/10.1002/ajh.25238>.
- (86) Cluzeau, T.; Sebert, M.; Rahmé, R.; Cuzzubbo, S.; Walter-petrich, A.; Lehmann che, J.; Peterlin, P.; Beve, B.; Attalah, H.; Chermat, F.; Miekoutima, E.; Beyne-Rauzy, O.; Recher, C.; Stamatoullas, A.; Willems, L.; Raffoux, E.; Berthon, C.; Quesnel, B.; Carpentier, A.; Sallman, D. A.; Chevret, S.; Ades, L.; Fenaux, P. APR-246 Combined with Azacitidine (AZA) in TP53 Mutated Myelodysplastic Syndrome (MDS) and Acute Myeloid Leukemia (AML). a Phase 2 Study By the Groupe Francophone Des Myélodysplasies (GFM). *Blood* **2019**, *134* (Supplement\_1), 677–677. <https://doi.org/10.1182/blood-2019-125579>.
- (87) Sallman, D. A.; DeZern, A. E.; Garcia-Manero, G.; Steensma, D. P.; Roboz, G. J.; Sekeres, M. A.; Cluzeau, T.; Sweet, K. L.; McLemore, A.; McGraw, K. L.; Puskas, J.; Zhang, L.; Yao, J.; Mo, Q.; Nardelli, L.; Al Ali, N. H.; Padron, E.; Korbel, G.; Attar, E. C.; Kantarjian, H. M.; Lancet, J. E.; Fenaux, P.; List, A. F.; Komrokji, R. S. Eprenetapopt (APR-246) and Azacitidine in TP53-Mutant Myelodysplastic Syndromes. *JCO* **2021**, *39* (14), 1584–1594. <https://doi.org/10.1200/JCO.20.02341>.
- (88) Sallman, D. A.; Asch, A. S.; Al Malki, M. M.; Lee, D. J.; Donnellan, W. B.; Marcucci, G.; Kambhampati, S.; Daver, N. G.; Garcia-Manero, G.; Komrokji, R. S.; Van Elk, J.; Lin, M.; Volkmer, J.-P.; Takimoto, C. H.; Chao, M.; Vyas, P. The First-in-Class Anti-CD47 Antibody Magrolimab (5F9) in Combination with Azacitidine Is Effective in MDS and AML Patients: Ongoing Phase 1b Results. *Blood* **2019**, *134* (Supplement\_1), 569–569. <https://doi.org/10.1182/blood-2019-126271>.
- (89) Platzbecker, U.; Kubasch, A. S.; Homer-Bouthiette, C.; Prebet, T. Current Challenges and Unmet Medical Needs in Myelodysplastic Syndromes. *Leukemia* **2021**, *35* (8), 2182–2198. <https://doi.org/10.1038/s41375-021-01265-7>.
- (90) Navada, S. C.; Silverman, L. R. Safety and Efficacy of Azacitidine in Elderly Patients with Intermediate to High-Risk Myelodysplastic Syndromes. *Ther Adv Hematol* **2017**, *8* (1), 21–27. <https://doi.org/10.1177/2040620716674677>.
- (91) Prébet, T.; Gore, S. D.; Esterni, B.; Gardin, C.; Itzykson, R.; Thepot, S.; Dreyfus, F.; Rauzy, O. B.; Recher, C.; Adès, L.; Quesnel, B.; Beach, C. L.; Fenaux, P.; Vey, N. Outcome of High-Risk Myelodysplastic Syndrome After Azacitidine Treatment Failure. *J Clin Oncol* **2011**, *29* (24), 3322–3327. <https://doi.org/10.1200/JCO.2011.35.8135>.
- (92) Wei, A. H.; Döhner, H.; Pocock, C.; Montesinos, P.; Afanasyev, B.; Dombret, H.; Ravandi, F.; Sayar, H.; Jang, J.-H.; Porkka, K.; Selleslag, D.; Sandhu, I.; Turgut, M.; Giai, V.; Ofran, Y.; Kizil Çakar, M.; Botelho de Sousa, A.; Rybka, J.; Frairia, C.; Borin, L.; Beltrami, G.; Čermák, J.; Ossenkoppele, G. J.; La Torre, I.; Skikne, B.; Kumar, K.; Dong, Q.; Beach, C. L.; Roboz, G. J. Oral Azacitidine Maintenance Therapy for Acute Myeloid Leukemia in First Remission. *New England Journal of Medicine* **2020**, *383* (26), 2526–2537. <https://doi.org/10.1056/NEJMoa2004444>.
- (93) Sorm, F.; Vesely, J. THE ACTIVITY OF A NEW ANTIMETABOLITE, 5-AZACYTIDINE, AGAINST LYMPHOID LEUKAEMIA IN AK MICE. *Neoplasma* **1964**, *11*, 123–130.
- (94) Lu, L.-J. W.; Randerath, K. Mechanism of 5-Azacytidine-Induced Transfer RNA Cytosine-5-Methyltransferase Deficiency. *Cancer Res* **1980**, *40* (8 Part 1), 2701–2705.

- (95) Lee, T. T.; Karon, M. R. Inhibition of Protein Synthesis in 5-Azacytidine-Treated HeLa Cells. *Biochemical Pharmacology* **1976**, 25 (15), 1737–1742. [https://doi.org/10.1016/0006-2952\(76\)90407-X](https://doi.org/10.1016/0006-2952(76)90407-X).
- (96) Schaefer, M.; Hagemann, S.; Hanna, K.; Lyko, F. Azacytidine Inhibits RNA Methylation at DNMT2 Target Sites in Human Cancer Cell Lines. *Cancer Res* **2009**, 69 (20), 8127–8132. <https://doi.org/10.1158/0008-5472.CAN-09-0458>.
- (97) Wu, L.; Shi, W.; Li, X.; Chang, C.; Xu, F.; He, Q.; Wu, D.; Su, J.; Zhou, L.; Song, L.; Xiao, C.; Zhang, Z. High Expression of the Human Equilibrative Nucleoside Transporter 1 Gene Predicts a Good Response to Decitabine in Patients with Myelodysplastic Syndrome. *Journal of Translational Medicine* **2016**, 14 (1), 66. <https://doi.org/10.1186/s12967-016-0817-9>.
- (98) Stresemann, C.; Lyko, F. Modes of Action of the DNA Methyltransferase Inhibitors Azacytidine and Decitabine. *International Journal of Cancer* **2008**, 123 (1), 8–13. <https://doi.org/10.1002/ijc.23607>.
- (99) Quesnel, B.; Guillermin, G.; Vereecque, R.; Wattel, E.; Preudhomme, C.; Bauters, F.; Vanrumbeke, M.; Fenaux, P. Methylation of the P15INK4b Gene in Myelodysplastic Syndromes Is Frequent and Acquired During Disease Progression. *Blood* **1998**, 91 (8), 2985–2990. [https://doi.org/10.1182/blood.V91.8.2985.2985\\_2985\\_2990](https://doi.org/10.1182/blood.V91.8.2985.2985_2985_2990).
- (100) Gowher, H.; Jeltsch, A. Mammalian DNA Methyltransferases: New Discoveries and Open Questions. *Biochem Soc Trans* **2018**, 46 (5), 1191–1202. <https://doi.org/10.1042/BST20170574>.
- (101) Balouzet, C.; Chanut, C.; Jobard, M.; Brandely-Piat, M.-L.; Chast, F. Stability of 25 Mg/ML Azacytidine Suspensions Kept in Fridge after Freezing. *Pharmaceutical Technology in Hospital Pharmacy* **2017**, 2 (1), 11–16. <https://doi.org/10.1515/ptph-2016-0023>.
- (102) Walker, S. E.; Charbonneau, L. F.; Law, S.; Earle, C. Stability of Azacytidine in Sterile Water for Injection. *Can J Hosp Pharm* **2012**, 65 (5), 352–359.
- (103) Damaraju, V. L.; Mowles, D.; Yao, S.; Ng, A.; Young, J. D.; Cass, C. E.; Tong, Z. Role of Human Nucleoside Transporters in the Uptake and Cytotoxicity of Azacytidine and Decitabine. *Nucleosides Nucleotides Nucleic Acids* **2012**, 31 (3), 236–255. <https://doi.org/10.1080/15257770.2011.652330>.
- (104) Fanciullino, R.; Mercier, C.; Serdjebi, C.; Berda, Y.; Fina, F.; Ouafik, L.; Lacarelle, B.; Ciccolini, J.; Costello, R. Lethal Toxicity after Administration of Azacytidine: Implication of the Cytidine Deaminase-Deficiency Syndrome. *Pharmacogenetics and Genomics* **2015**, 25 (6), 317–321. <https://doi.org/10.1097/FPC.0000000000000139>.
- (105) Chabner, B. A.; Drake, J. C.; Johns, D. G. Deamination of 5-Azacytidine by a Human Leukemia Cell Cytidine Deaminase. *Biochemical Pharmacology* **1973**, 22 (21), 2763–2765. [https://doi.org/10.1016/0006-2952\(73\)90137-8](https://doi.org/10.1016/0006-2952(73)90137-8).
- (106) Fanciullino, R.; Mercier, C.; Serdjebi, C.; Venton, G.; Colle, J.; Fina, F.; Ouafik, L.; Lacarelle, B.; Ciccolini, J.; Costello, R. Yin and Yang of Cytidine Deaminase Roles in Clinical Response to Azacytidine in the Elderly: A Pharmacogenetics Tale. *Pharmacogenomics* **2015**, 16 (17), 1907–1912. <https://doi.org/10.2217/pgs.15.135>.
- (107) DiNardo, C. D.; Jonas, B. A.; Pullarkat, V.; Thirman, M. J.; Garcia, J. S.; Wei, A. H.; Konopleva, M.; Döhner, H.; Letai, A.; Fenaux, P.; Koller, E.; Havelange, V.; Leber, B.; Esteve, J.; Wang, J.; Pejsa, V.; Hájek, R.; Porkka, K.; Illés, A.; Lavie, D.; Lemoli, R. M.; Yamamoto, K.; Yoon, S.-S.; Jang, J.-H.; Yeh, S.-P.; Turgut, M.; Hong, W.-J.; Zhou, Y.; Potluri, J.; Pratz, K. W. Azacytidine and Venetoclax in Previously Untreated Acute Myeloid Leukemia. *New England Journal of Medicine* **2020**, 383 (7), 617–629. <https://doi.org/10.1056/NEJMoa2012971>.
- (108) Jin, S.; Cojocari, D.; Purkal, J. J.; Popovic, R.; Talaty, N. N.; Xiao, Y.; Solomon, L. R.; Boghaert, E. R.; Levenson, J. D.; Phillips, D. C. 5-Azacytidine Induces NOXA to Prime AML Cells for Venetoclax-Mediated Apoptosis. *Clin Cancer Res* **2020**, 26 (13), 3371–3383. <https://doi.org/10.1158/1078-0432.CCR-19-1900>.



- (109) Pollyea, D. A.; Stevens, B. M.; Jones, C. L.; Winters, A.; Pei, S.; Minhajuddin, M.; D'Alessandro, A.; Culp-Hill, R.; Riemondy, K. A.; Gillen, A. E.; Hesselberth, J. R.; Abbott, D.; Schatz, D.; Gutman, J. A.; Purev, E.; Smith, C.; Jordan, C. T. Venetoclax with Azacitidine Disrupts Energy Metabolism and Targets Leukemia Stem Cells in Acute Myeloid Leukemia Patients. *Nat Med* **2018**, *24* (12), 1859–1866. <https://doi.org/10.1038/s41591-018-0233-1>.
- (110) Onec, B.; Okutan, H.; Albayrak, M.; Can, E. S.; Aslan, V.; Koluman, B. U.; Kosemehmetoglu, O. S.; Albayrak, A. Combination Therapy with Azacitidine, Etoposide, and Cytarabine in the Treatment of Elderly Acute Myeloid Leukemia Patients: A Single Center Experience. *J Cancer Res Ther* **2018**, *14* (5), 1105–1111. <https://doi.org/10.4103/0973-1482.187369>.
- (111) Gottfried, E. L. Lipids of Human Leukocytes: Relation to Cell Type. *Journal of Lipid Research* **1967**, *8* (4), 321–327. [https://doi.org/10.1016/S0022-2275\(20\)39561-4](https://doi.org/10.1016/S0022-2275(20)39561-4).
- (112) Pabst, T.; Kortz, L.; Fiedler, G. M.; Ceglarek, U.; Idle, J. R.; Beyoğlu, D. The Plasma Lipidome in Acute Myeloid Leukemia at Diagnosis in Relation to Clinical Disease Features. *BBA Clinical* **2017**, *7*, 105–114. <https://doi.org/10.1016/j.bbacli.2017.03.002>.
- (113) Glatz, J. F. C.; Luiken, J. J. F. P.; Bonen, A. Membrane Fatty Acid Transporters as Regulators of Lipid Metabolism: Implications for Metabolic Disease. *Physiological Reviews* **2010**, *90* (1), 367–417. <https://doi.org/10.1152/physrev.00003.2009>.
- (114) Chen, M.; Huang, J. The Expanded Role of Fatty Acid Metabolism in Cancer: New Aspects and Targets. *Precis Clin Med* **2019**, *2* (3), 183–191. <https://doi.org/10.1093/pcmedi/pbz017>.
- (115) Kuhajda, F. P.; Jenner, K.; Wood, F. D.; Hennigar, R. A.; Jacobs, L. B.; Dick, J. D.; Pasternack, G. R. Fatty Acid Synthesis: A Potential Selective Target for Antineoplastic Therapy. *Proc Natl Acad Sci U S A* **1994**, *91* (14), 6379–6383.
- (116) Galluzzi, L.; Vitale, I.; Aaronson, S. A.; Abrams, J. M.; Adam, D.; Agostinis, P.; Alnemri, E. S.; Altucci, L.; Amelio, I.; Andrews, D. W.; Annicchiarico-Petruzzelli, M.; Antonov, A. V.; Arama, E.; Baehrecke, E. H.; Barlev, N. A.; Bazan, N. G.; Bernassola, F.; Bertrand, M. J. M.; Bianchi, K.; Blagosklonny, M. V.; Blomgren, K.; Borner, C.; Boya, P.; Brenner, C.; Campanella, M.; Candi, E.; Carmona-Gutierrez, D.; Cecconi, F.; Chan, F. K.-M.; Chandel, N. S.; Cheng, E. H.; Chipuk, J. E.; Cidlowski, J. A.; Ciechanover, A.; Cohen, G. M.; Conrad, M.; Cubillos-Ruiz, J. R.; Czabotar, P. E.; D'Angiolella, V.; Dawson, T. M.; Dawson, V. L.; De Laurenzi, V.; De Maria, R.; Debatin, K.-M.; DeBerardinis, R. J.; Deshmukh, M.; Di Daniele, N.; Di Virgilio, F.; Dixit, V. M.; Dixon, S. J.; Duckett, C. S.; Dynlacht, B. D.; El-Deiry, W. S.; Elrod, J. W.; Fimia, G. M.; Fulda, S.; García-Sáez, A. J.; Garg, A. D.; Garrido, C.; Gavathiotis, E.; Golstein, P.; Gottlieb, E.; Green, D. R.; Greene, L. A.; Gronemeyer, H.; Gross, A.; Hajnoczky, G.; Hardwick, J. M.; Harris, I. S.; Hengartner, M. O.; Hetz, C.; Ichijo, H.; Jäättelä, M.; Joseph, B.; Jost, P. J.; Juin, P. P.; Kaiser, W. J.; Karin, M.; Kaufmann, T.; Kepp, O.; Kimchi, A.; Kitsis, R. N.; Klionsky, D. J.; Knight, R. A.; Kumar, S.; Lee, S. W.; Lemasters, J. J.; Levine, B.; Linkermann, A.; Lipton, S. A.; Lockshin, R. A.; López-Otín, C.; Lowe, S. W.; Luedde, T.; Lugli, E.; MacFarlane, M.; Madeo, F.; Malewicz, M.; Malorni, W.; Manic, G.; Marine, J.-C.; Martin, S. J.; Martinou, J.-C.; Medema, J. P.; Mehlen, P.; Meier, P.; Melino, S.; Miao, E. A.; Molkentin, J. D.; Moll, U. M.; Muñoz-Pinedo, C.; Nagata, S.; Nuñez, G.; Oberst, A.; Oren, M.; Overholtzer, M.; Pagano, M.; Panaretakis, T.; Pasparakis, M.; Penninger, J. M.; Pereira, D. M.; Pervaiz, S.; Peter, M. E.; Piacentini, M.; Pinton, P.; Prehn, J. H. M.; Puthalakath, H.; Rabinovich, G. A.; Rehm, M.; Rizzuto, R.; Rodrigues, C. M. P.; Rubinsztein, D. C.; Rudel, T.; Ryan, K. M.; Sayan, E.; Scorrano, L.; Shao, F.; Shi, Y.; Silke, J.; Simon, H.-U.; Sistigu, A.; Stockwell, B. R.; Strasser, A.; Szabadkai, G.; Tait, S. W. G.; Tang, D.; Tavernarakis, N.; Thorburn, A.; Tsujimoto, Y.; Turk, B.; Vanden Berghe, T.; Vandenabeele, P.; Vander Heiden, M. G.; Villunger, A.; Virgin, H. W.; Vousden, K. H.; Vucic, D.; Wagner, E. F.; Walczak, H.; Wallach, D.; Wang, Y.; Wells, J. A.; Wood, W.; Yuan, J.; Zakeri, Z.; Zhivotovsky, B.; Zitvogel, L.; Melino, G.; Kroemer, G. Molecular Mechanisms

- of Cell Death: Recommendations of the Nomenclature Committee on Cell Death 2018. *Cell Death Differ* **2018**, 25 (3), 486–541. <https://doi.org/10.1038/s41418-017-0012-4>.
- (117) Dixon, S. J.; Lemberg, K. M.; Lamprecht, M. R.; Skouta, R.; Zaitsev, E. M.; Gleason, C. E.; Patel, D. N.; Bauer, A. J.; Cantley, A. M.; Yang, W. S.; Morrison, B.; Stockwell, B. R. Ferroptosis: An Iron-Dependent Form of Non-Apoptotic Cell Death. *Cell* **2012**, 149 (5), 1060–1072. <https://doi.org/10.1016/j.cell.2012.03.042>.
- (118) Wang, D.; DuBois, R. N. Eicosanoids and Cancer. *Nat Rev Cancer* **2010**, 10 (3), 181–193. <https://doi.org/10.1038/nrc2809>.
- (119) Rysman, E.; Brusselmans, K.; Scheys, K.; Timmermans, L.; Derua, R.; Munck, S.; Veldhoven, P. P. V.; Waltregny, D.; Daniëls, V. W.; Machiels, J.; Vanderhoydonc, F.; Smans, K.; Waelkens, E.; Verhoeven, G.; Swinnen, J. V. De Novo Lipogenesis Protects Cancer Cells from Free Radicals and Chemotherapeutics by Promoting Membrane Lipid Saturation. *Cancer Res* **2010**, 70 (20), 8117–8126. <https://doi.org/10.1158/0008-5472.CAN-09-3871>.
- (120) Doll, S.; Proneth, B.; Tyurina, Y. Y.; Panzilius, E.; Kobayashi, S.; Ingold, I.; Irmeler, M.; Beckers, J.; Aichler, M.; Walch, A.; Prokisch, H.; Trümbach, D.; Mao, G.; Qu, F.; Bayir, H.; Füllekrug, J.; Scheel, C.; Wurst, W.; Schick, J. A.; Kagan, V. E.; Angeli, J. P. F.; Conrad, M. AcsL4 Dictates Ferroptosis Sensitivity by Shaping Cellular Lipid Composition. *Nat Chem Biol* **2017**, 13 (1), 91–98. <https://doi.org/10.1038/nchembio.2239>.
- (121) Masaldan, S.; Bush, A. I.; Devos, D.; Rolland, A. S.; Moreau, C. Striking While the Iron Is Hot: Iron Metabolism and Ferroptosis in Neurodegeneration. *Free Radical Biology and Medicine* **2019**, 133, 221–233. <https://doi.org/10.1016/j.freeradbiomed.2018.09.033>.
- (122) Sun, X.; Ou, Z.; Xie, M.; Kang, R.; Fan, Y.; Niu, X.; Wang, H.; Cao, L.; Tang, D. HSPB1 as a Novel Regulator of Ferroptotic Cancer Cell Death. *Oncogene* **2015**, 34 (45), 5617–5625. <https://doi.org/10.1038/onc.2015.32>.
- (123) Chen, H.; Zheng, C.; Zhang, Y.; Chang, Y.-Z.; Qian, Z.-M.; Shen, X. Heat Shock Protein 27 Downregulates the Transferrin Receptor 1-Mediated Iron Uptake. *The International Journal of Biochemistry & Cell Biology* **2006**, 38 (8), 1402–1416. <https://doi.org/10.1016/j.biocel.2006.02.006>.
- (124) Moosmayer, D.; Hilpmann, A.; Hoffmann, J.; Schnirch, L.; Zimmermann, K.; Badock, V.; Furst, L.; Eaton, J. K.; Viswanathan, V. S.; Schreiber, S. L.; Gradl, S.; Hillig, R. C. Crystal Structures of the Selenoprotein Glutathione Peroxidase 4 in Its Apo Form and in Complex with the Covalently Bound Inhibitor ML162. *Acta Crystallogr D Struct Biol* **2021**, 77 (Pt 2), 237–248. <https://doi.org/10.1107/S2059798320016125>.
- (125) Yang, W. S.; SriRamaratnam, R.; Welsch, M. E.; Shimada, K.; Skouta, R.; Viswanathan, V. S.; Cheah, J. H.; Clemons, P. A.; Shamji, A. F.; Clish, C. B.; Brown, L. M.; Girotti, A. W.; Cornish, V. W.; Schreiber, S. L.; Stockwell, B. R. Regulation of Ferroptotic Cancer Cell Death by GPX4. *Cell* **2014**, 156 (0), 317–331. <https://doi.org/10.1016/j.cell.2013.12.010>.
- (126) Sui, X.; Zhang, R.; Liu, S.; Duan, T.; Zhai, L.; Zhang, M.; Han, X.; Xiang, Y.; Huang, X.; Lin, H.; Xie, T. RSL3 Drives Ferroptosis Through GPX4 Inactivation and ROS Production in Colorectal Cancer. *Front Pharmacol* **2018**, 9, 1371. <https://doi.org/10.3389/fphar.2018.01371>.
- (127) Lu, B.; Chen, X.; Ying, M.; He, Q.; Cao, J.; Yang, B. The Role of Ferroptosis in Cancer Development and Treatment Response. *Front. Pharmacol.* **2018**. <https://doi.org/10.3389/fphar.2017.00992>.
- (128) Yu, Y.; Xie, Y.; Cao, L.; Yang, L.; Yang, M.; Lotze, M. T.; Zeh, H. J.; Kang, R.; Tang, D. The Ferroptosis Inducer Erastin Enhances Sensitivity of Acute Myeloid Leukemia Cells to Chemotherapeutic Agents. *Mol Cell Oncol* **2015**, 2 (4), e1054549. <https://doi.org/10.1080/23723556.2015.1054549>.
- (129) Grignano, E.; Birsén, R.; Chapuis, N.; Bouscary, D. From Iron Chelation to Overload as a Therapeutic Strategy to Induce Ferroptosis in Leukemic Cells. *Front Oncol* **2020**, 10, 586530. <https://doi.org/10.3389/fonc.2020.586530>.

- (130) Lv, Q.; Niu, H.; Yue, L.; Liu, J.; Yang, L.; Liu, C.; Jiang, H.; Dong, S.; Shao, Z.; Xing, L.; Wang, H. Abnormal Ferroptosis in Myelodysplastic Syndrome. *Front Oncol* **2020**, *10*, 1656. <https://doi.org/10.3389/fonc.2020.01656>.
- (131) Gerken, H.; Liu, J.; Sun, Z. *Recent Advances in Microalgal Biotechnology*; 2012.
- (132) Germain, E.; Chajès, V.; Cognault, S.; Lhuillery, C.; Bougnoux, P. Enhancement of Doxorubicin Cytotoxicity by Polyunsaturated Fatty Acids in the Human Breast Tumor Cell Line MBA-MB-231: Relationship to Lipid Peroxidation. *International Journal of Cancer* **1998**, *75* (4), 578–583. [https://doi.org/10.1002/\(SICI\)1097-0215\(19980209\)75:4<578::AID-IJC14>3.0.CO;2-5](https://doi.org/10.1002/(SICI)1097-0215(19980209)75:4<578::AID-IJC14>3.0.CO;2-5).
- (133) Colas, S.; Paon, L.; Denis, F.; Prat, M.; Louisot, P.; Hoinard, C.; Floch, O. L.; Ogilvie, G.; Bougnoux, P. Enhanced Radiosensitivity of Rat Autochthonous Mammary Tumors by Dietary Docosahexaenoic Acid. *International Journal of Cancer* **2004**, *109* (3), 449–454. <https://doi.org/10.1002/ijc.11725>.
- (134) Vibet, S.; Goupille, C.; Bougnoux, P.; Steghens, J.-P.; Goré, J.; Mahéo, K. Sensitization by Docosahexaenoic Acid (DHA) of Breast Cancer Cells to Anthracyclines through Loss of Glutathione Peroxidase (GPx1) Response. *Free Radical Biology and Medicine* **2008**, *44* (7), 1483–1491. <https://doi.org/10.1016/j.freeradbiomed.2008.01.009>.
- (135) Kang, K. S.; Wang, P.; Yamabe, N.; Fukui, M.; Jay, T.; Zhu, B. T. Docosahexaenoic Acid Induces Apoptosis in MCF-7 Cells In Vitro and In Vivo via Reactive Oxygen Species Formation and Caspase 8 Activation. *PLOS ONE* **2010**, *5* (4), e10296. <https://doi.org/10.1371/journal.pone.0010296>.
- (136) Zhu, S.; Feng, N.; Lin, G.; Tong, Y.; Jiang, X.; Yang, Q.; Wang, S.; Chen, W.; He, Z.; Chen, Y. Q. Metabolic Shift Induced by  $\omega$ -3 PUFAs and Rapamycin Lead to Cancer Cell Death. *CPB* **2018**, *48* (6), 2318–2336. <https://doi.org/10.1159/000492648>.
- (137) Ou, W.; Mulik, R. S.; Anwar, A.; McDonald, J. G.; He, X.; Corbin, I. R. Low-Density Lipoprotein Docosahexaenoic Acid Nanoparticles Induce Ferroptotic Cell Death in Hepatocellular Carcinoma. *Free Radical Biology and Medicine* **2017**, *112*, 597–607. <https://doi.org/10.1016/j.freeradbiomed.2017.09.002>.
- (138) Signori, C.; El-Bayoumy, K.; Russo, J.; Thompson, H. J.; Richie, J. P.; Hartman, T. J.; Manni, A. Chemoprevention of Breast Cancer by Fish Oil in Preclinical Models: Trials and Tribulations. *Cancer Res* **2011**, *71* (19), 6091–6096. <https://doi.org/10.1158/0008-5472.CAN-11-0977>.
- (139) Picou, F.; Debeissat, C.; Bourgeois, J.; Gallay, N.; Ferrière, E.; Foucault, A.; Ravalet, N.; Maciejewski, A.; Vallet, N.; Ducrocq, E.; Haddaoui, L.; Domenech, J.; Héroult, O.; Gyan, E. N-3 Polyunsaturated Fatty Acids Induce Acute Myeloid Leukemia Cell Death Associated with Mitochondrial Glycolytic Switch and Nrf2 Pathway Activation. *Pharmacological Research* **2018**, *136*, 45–55. <https://doi.org/10.1016/j.phrs.2018.08.015>.
- (140) Yamagami, T.; Porada, C. D.; Pardini, R.; Zanjani, E. D.; Almeida-Porada, G. D. Docosahexanoic Acid Induces Dose Dependent Cell Death in an Early Undifferentiated Subtype of Acute Myeloid Leukemia Cell Line. *Cancer Biology & Therapy* **2009**, *8* (4), 331–337. <https://doi.org/10.4161/cbt.8.4.7334>.
- (141) Aires, V.; Hichami, A.; Filomenko, R.; Plé, A.; Rébé, C.; Bettaieb, A.; Khan, N. A. Docosahexaenoic Acid Induces Increases in  $[Ca^{2+}]_i$  via Inositol 1,4,5-Triphosphate Production and Activates Protein Kinase C $\gamma$  and  $\delta$  via Phosphatidylserine Binding Site: Implication in Apoptosis in U937 Cells. *Mol Pharmacol* **2007**, *72* (6), 1545–1556. <https://doi.org/10.1124/mol.107.039792>.
- (142) Ceccarelli, V.; Racanicchi, S.; Martelli, M. P.; Nocentini, G.; Fettucciari, K.; Riccardi, C.; Marconi, P.; Di Nardo, P.; Grignani, F.; Binaglia, L.; Vecchini, A. Eicosapentaenoic Acid Demethylates a Single CpG That Mediates Expression of Tumor Suppressor CCAAT/Enhancer-Binding Protein  $\delta$  in U937 Leukemia Cells. *J. Biol. Chem.* **2011**, *286* (31), 27092–27102. <https://doi.org/10.1074/jbc.M111.253609>.

- (143) Ceccarelli, V.; Nocentini, G.; Billi, M.; Racanicchi, S.; Riccardi, C.; Roberti, R.; Grignani, F.; Binaglia, L.; Vecchini, A. Eicosapentaenoic Acid Activates RAS/ERK/C/EBP $\beta$  Pathway through H-Ras Intron 1 CpG Island Demethylation in U937 Leukemia Cells. *PLoS ONE* **2014**, 9 (1), e85025. <https://doi.org/10.1371/journal.pone.0085025>.
- (144) Varney, M. E.; Hardman, W. E.; Sollars, V. E. Omega 3 Fatty Acids Reduce Myeloid Progenitor Cell Frequency in the Bone Marrow of Mice and Promote Progenitor Cell Differentiation. *Lipids Health Dis* **2009**, 8 (1), 9. <https://doi.org/10.1186/1476-511X-8-9>.
- (145) Schley, P. D.; Brindley, D. N.; Field, C. J. (N-3) PUFA Alter Raft Lipid Composition and Decrease Epidermal Growth Factor Receptor Levels in Lipid Rafts of Human Breast Cancer Cells. *The Journal of Nutrition* **2007**, 137 (3), 548–553. <https://doi.org/10.1093/jn/137.3.548>.
- (146) Corsetto, P. A.; Montorfano, G.; Zava, S.; Jovenitti, I. E.; Cremona, A.; Berra, B.; Rizzo, A. M. Effects of N-3 PUFAs on Breast Cancer Cells through Their Incorporation in Plasma Membrane. *Lipids in Health and Disease* **2011**, 10 (1), 73. <https://doi.org/10.1186/1476-511X-10-73>.
- (147) Corsetto, P. A.; Cremona, A.; Montorfano, G.; Jovenitti, I. E.; Orsini, F.; Arosio, P.; Rizzo, A. M. Chemical–Physical Changes in Cell Membrane Microdomains of Breast Cancer Cells After Omega-3 PUFA Incorporation. *Cell Biochem Biophys* **2012**, 64 (1), 45–59. <https://doi.org/10.1007/s12013-012-9365-y>.
- (148) Zhang, H.; Zhou, L.; Shi, W.; Song, N.; Yu, K.; Gu, Y. A Mechanism Underlying the Effects of Polyunsaturated Fatty Acids on Breast Cancer. *International Journal of Molecular Medicine* **2012**, 30 (3), 487–494. <https://doi.org/10.3892/ijmm.2012.1022>.
- (149) Dimri, M.; Bommi, P. V.; Sahasrabudhe, A. A.; Khandekar, J. D.; Dimri, G. P. Dietary Omega-3 Polyunsaturated Fatty Acids Suppress Expression of EZH2 in Breast Cancer Cells. *Carcinogenesis* **2010**, 31 (3), 489–495. <https://doi.org/10.1093/carcin/bgp305>.
- (150) Tsujita-Kyutoku, M.; Yuri, T.; Danbara, N.; Senzaki, H.; Kiyozuka, Y.; Uehara, N.; Takada, H.; Hada, T.; Miyazawa, T.; Ogawa, Y.; Tsubura, A. Conjugated Docosahexaenoic Acid Suppresses KPL-1 Human Breast Cancer Cell Growth in Vitro and in Vivo: Potential Mechanisms of Action. *Breast Cancer Research* **2004**, 6 (4), R291. <https://doi.org/10.1186/bcr789>.
- (151) Menendez, J. A.; Vellon, L.; Colomer, R.; Lupu, R. Oleic Acid, the Main Monounsaturated Fatty Acid of Olive Oil, Suppresses Her-2/Neu (ErbB-2) Expression and Synergistically Enhances the Growth Inhibitory Effects of Trastuzumab (Herceptin<sup>TM</sup>) in Breast Cancer Cells with Her-2/Neu Oncogene Amplification. *Annals of Oncology* **2005**, 16 (3), 359–371. <https://doi.org/10.1093/annonc/mdi090>.
- (152) Menendez, J. A.; Lupu, R.; Colomer, R. Exogenous Supplementation with  $\omega$ -3 Polyunsaturated Fatty Acid Docosahexaenoic Acid (DHA; 22:6n-3) Synergistically Enhances Taxane Cytotoxicity and Downregulates Her-2/Neu (c-ErbB-2) Oncogene Expression in Human Breast Cancer Cells. *European Journal of Cancer Prevention* **2005**, 14 (3), 263–270.
- (153) Menendez, J. A.; Roperio, S.; Lupu, R.; Colomer, R. Dietary Fatty Acids Regulate the Activation Status of Her-2/Neu (c-ErbB-2) Oncogene in Breast Cancer Cells. *Annals of Oncology* **2004**, 15 (11), 1719–1721. <https://doi.org/10.1093/annonc/mdh442>.
- (154) Menendez, J. A.; Roperio, S.; Lupu, R.; Colomer, R.  $\omega$ -6 Polyunsaturated Fatty Acid  $\gamma$ -Linolenic Acid (18:3n-6) Enhances Docetaxel (Taxotere) Cytotoxicity in Human Breast Carcinoma Cells: Relationship to Lipid Peroxidation and HER-2/Neu Expression. *Oncology Reports* **2004**, 11 (6), 1241–1252. <https://doi.org/10.3892/or.11.6.1241>.
- (155) Menendez, J. A.; Colomer, R.; Lupu, R.  $\omega$ -6 Polyunsaturated Fatty Acid  $\gamma$ -Linolenic Acid (18:3n-6) Is a Selective Estrogen-Response Modulator in Human Breast Cancer Cells:  $\gamma$ -Linolenic Acid Antagonizes Estrogen Receptor-Dependent Transcriptional Activity, Transcriptionally Represses Estrogen Receptor Expression and Synergistically Enhances

- Tamoxifen and ICI 182,780 (Faslodex) Efficacy in Human Breast Cancer Cells. *International Journal of Cancer* **2004**, 109 (6), 949–954. <https://doi.org/10.1002/ijc.20096>.
- (156) Menéndez, J. A.; Vázquez-Martín, A.; Ropero, S.; Colomer, R.; Lupu, R.; Trueta, J. HER2 (ErbB-2)-Targeted Effects of the  $\omega$ -3 Polyunsaturated Fatty Acid  $\alpha$ -Linolenic Acid (ALA; 18:3n-3) in Breast Cancer Cells: The «fat Features» of the «Mediterranean Diet» as an «anti-HER2 Cocktail». *Clin Transl Oncol* **2006**, 8 (11), 812–820. <https://doi.org/10.1007/s12094-006-0137-2>.
- (157) Menéndez, J. A.; Barbacid, M. del M.; Montero, S.; Sevilla, E.; Escrich, E.; Solanas, M.; Cortés-Funes, H.; Colomer, R. Effects of Gamma-Linolenic Acid and Oleic Acid on Paclitaxel Cytotoxicity in Human Breast Cancer Cells. *European Journal of Cancer* **2001**, 37 (3), 402–413. [https://doi.org/10.1016/S0959-8049\(00\)00408-1](https://doi.org/10.1016/S0959-8049(00)00408-1).
- (158) Menéndez, J. A.; Ropero, S.; Barbacid, M. del M.; Montero, S.; Solanas, M.; Escrich, E.; Cortés-Funes, H.; Colomer, R. Synergistic Interaction Between Vinorelbine and Gamma-Linolenic Acid in Breast Cancer Cells. *Breast Cancer Res Treat* **2002**, 72 (3), 203–219. <https://doi.org/10.1023/A:1014968415759>.
- (159) Zou, Z.; Bellenger, S.; Massey, K. A.; Nicolaou, A.; Geissler, A.; Bidu, C.; Bonnotte, B.; Pierre, A.-S.; Minville-Walz, M.; Rialland, M.; Seubert, J.; Kang, J. X.; Lagrost, L.; Narce, M.; Bellenger, J. Inhibition of the HER2 Pathway by N-3 Polyunsaturated Fatty Acids Prevents Breast Cancer in Fat-1 Transgenic Mice. *Journal of Lipid Research* **2013**, 54 (12), 3453–3463. <https://doi.org/10.1194/jlr.M042754>.
- (160) Sauer, L. A.; Dauchy, R. T.; Blask, D. E.; Krause, J. A.; Davidson, L. K.; Dauchy, E. M. Eicosapentaenoic Acid Suppresses Cell Proliferation in MCF-7 Human Breast Cancer Xenografts in Nude Rats via a Pertussis Toxin-Sensitive Signal Transduction Pathway. *The Journal of Nutrition* **2005**, 135 (9), 2124–2129. <https://doi.org/10.1093/jn/135.9.2124>.
- (161) Cao, W.; Ma, Z.; Rasenick, M. M.; Yeh, S.; Yu, J. N-3 Poly-Unsaturated Fatty Acids Shift Estrogen Signaling to Inhibit Human Breast Cancer Cell Growth. *PLOS ONE* **2012**, 7 (12), e52838. <https://doi.org/10.1371/journal.pone.0052838>.
- (162) Kalyane, D.; Raval, N.; Maheshwari, R.; Tambe, V.; Kalia, K.; Tekade, R. K. Employment of Enhanced Permeability and Retention Effect (EPR): Nanoparticle-Based Precision Tools for Targeting of Therapeutic and Diagnostic Agent in Cancer. *Materials Science and Engineering: C* **2019**, 98, 1252–1276. <https://doi.org/10.1016/j.msec.2019.01.066>.
- (163) Wu, X.; Hu, Z.; Nizzero, S.; Zhang, G.; Ramirez, M. R.; Shi, C.; Zhou, J.; Ferrari, M.; Shen, H. Bone-Targeting Nanoparticle to Co-Deliver Decitabine and Arsenic Trioxide for Effective Therapy of Myelodysplastic Syndrome with Low Systemic Toxicity. *J Control Release* **2017**, 268, 92–101. <https://doi.org/10.1016/j.jconrel.2017.10.012>.
- (164) Shao, Z.-Y.; Tang, M.; Chen, B.-A.; Xia, G.-H.; Zhang, L.; Zhu, H.-G. [Experimental study of effect of As<sub>2</sub>S<sub>3</sub> nanoparticles on human MDS cell line (MUTZ-1)]. *Zhonghua Xue Ye Xue Za Zhi* **2009**, 30 (1), 29–32.
- (165) Donnellan, W. B.; Atallah, E. L.; Asch, A. S.; Patel, M. R.; Yang, J.; Eghtedar, A.; Borthakur, G. M.; Charlton, J.; MacDonald, A.; Korzeniowska, A.; Sainsbury, E.; Strickland, D. K.; Jones, S.; Overend, P.; Adelman, C. A.; Fabbri, G.; Travers, J.; Smith, S.; Pease, J. E.; Cosaert, J. A Phase I/II Study of AZD2811 Nanoparticles (NP) As Monotherapy or in Combination in Treatment-Naïve or Relapsed/Refractory AML/MDS Patients Not Eligible for Intensive Induction Therapy. *Blood* **2019**, 134 (Supplement\_1), 3919. <https://doi.org/10.1182/blood-2019-130635>.
- (166) Brown, F. C.; Urosevic, J.; Polanska, U.; Cosaert, J.; Pease, J. E.; Pomilio, G.; Litalien, V.; Travers, J.; Wei, A. H. Targeting Aurora Kinase B with AZD2811 Enhances Venetoclax Activity in TP53-Mutant AML. *Blood* **2019**, 134, 3930. <https://doi.org/10.1182/blood-2019-129564>.
- (167) Lancet, J. E.; Uy, G. L.; Cortes, J. E.; Newell, L. F.; Lin, T. L.; Ritchie, E. K.; Stuart, R. K.; Strickland, S. A.; Hogge, D.; Solomon, S. R.; Stone, R. M.; Bixby, D. L.; Kolitz, J. E.; Schiller, G. J.; Wieduwilt, M. J.; Ryan, D. H.; Hoering, A.; Banerjee, K.; Chiarella, M.; Louie,



- A. C.; Medeiros, B. C. CPX-351 (Cytarabine and Daunorubicin) Liposome for Injection Versus Conventional Cytarabine Plus Daunorubicin in Older Patients With Newly Diagnosed Secondary Acute Myeloid Leukemia. *JCO* **2018**, 36 (26), 2684–2692. <https://doi.org/10.1200/JCO.2017.77.6112>.
- (168) Chiche, E.; Rahmé, R.; Bertoli, S.; Dumas, P.-Y.; Micol, J.-B.; Hicheri, Y.; Pasquier, F.; Peterlin, P.; Chevallier, P.; Thomas, X.; Loschi, M.; Genthon, A.; Legrand, O.; Mohty, M.; Raffoux, E.; Auberger, P.; Caulier, A.; Joris, M.; Bonmati, C.; Roth-Guepin, G.; Lejeune, C.; Pigneux, A.; Vey, N.; Recher, C.; Ades, L.; Cluzeau, T. Real-Life Experience with CPX-351 and Impact on the Outcome of High-Risk AML Patients: A Multicentric French Cohort. *Blood Advances* **2021**, 5 (1), 176–184. <https://doi.org/10.1182/bloodadvances.2020003159>.
- (169) Bildstein, L.; Dubernet, C.; Couvreur, P. Prodrug-Based Intracellular Delivery of Anticancer Agents. *Advanced Drug Delivery Reviews* **2011**, 63 (1–2), 3–23. <https://doi.org/10.1016/j.addr.2010.12.005>.
- (170) Bui, D. T.; Nicolas, J.; Maksimenko, A.; Desmaële, D.; Couvreur, P. Multifunctional Squalene-Based Prodrug Nanoparticles for Targeted Cancer Therapy. *Chem. Commun. (Camb.)* **2014**, 50 (40), 5336–5338. <https://doi.org/10.1039/c3cc47427e>.
- (171) Muller, C. E. Prodrug Approaches for Enhancing the Bioavailability of Drugs with Low Solubility. *C&B* **2009**, 6 (11), 2071–2083. <https://doi.org/10.1002/cbdv.200900114>.
- (172) Singh, Y.; Palombo, M.; Sinko, P. Recent Trends in Targeted Anticancer Prodrug and Conjugate Design. *CMC* **2008**, 15 (18), 1802–1826. <https://doi.org/10.2174/092986708785132997>.
- (173) Maag, H. Overcoming Poor Permeability – the Role of Prodrugs for Oral Drug Delivery. *Drug Discovery Today: Technologies* **2012**, 9 (2), e121–e130. <https://doi.org/10.1016/j.ddtec.2012.04.002>.
- (174) Lesniewska-Kowiel, M. A.; Muszalska, I. Strategies in the Designing of Prodrugs, Taking into Account the Antiviral and Anticancer Compounds. *European Journal of Medicinal Chemistry* **2017**, 129, 53–71. <https://doi.org/10.1016/j.ejmech.2017.02.011>.
- (175) Mahato, R.; Tai, W.; Cheng, K. Prodrugs for Improving Tumor Targetability and Efficiency. *Advanced Drug Delivery Reviews* **2011**, 63 (8), 659–670. <https://doi.org/10.1016/j.addr.2011.02.002>.
- (176) Bradley, M. O.; Swindell, C. S.; Anthony, F. H.; Witman, P. A.; Devanesan, P.; Webb, N. L.; Baker, S. D.; Wolff, A. C.; Donehower, R. C. Tumor Targeting by Conjugation of DHA to Paclitaxel. *Journal of Controlled Release* **2001**, 74 (1), 233–236. [https://doi.org/10.1016/S0168-3659\(01\)00321-2](https://doi.org/10.1016/S0168-3659(01)00321-2).
- (177) Bradley, M. O.; Webb, N. L.; Anthony, F. H.; Devanesan, P.; Witman, P. A.; Hemamalini, S.; Chander, M. C.; Baker, S. D.; He, L.; Horwitz, S. B.; Swindell, C. S. Tumor Targeting by Covalent Conjugation of a Natural Fatty Acid to Paclitaxel. *Clin Cancer Res* **2001**, 7 (10), 3229–3238.
- (178) Huan, M.-L.; Zhou, S.-Y.; Teng, Z.-H.; Zhang, B.; Liu, X.-Y.; Wang, J.-P.; Mei, Q.-B. Conjugation with Alpha-Linolenic Acid Improves Cancer Cell Uptake and Cytotoxicity of Doxorubicin. *Bioorg Med Chem Lett* **2009**, 19 (9), 2579–2584. <https://doi.org/10.1016/j.bmcl.2009.03.016>.
- (179) HUAN, M.; CUI, H.; TENG, Z.; ZHANG, B.; WANG, J.; LIU, X.; XIA, H.; ZHOU, S.; MEI, Q. In Vivo Anti-Tumor Activity of a New Doxorubicin Conjugate via  $\alpha$ -Linolenic Acid. *Bioscience, Biotechnology, and Biochemistry* **2012**, 76 (8), 1577–1579. <https://doi.org/10.1271/bbb.120256>.
- (180) Sun, B.; Luo, C.; Cui, W.; Sun, J.; He, Z. Chemotherapy Agent-Unsaturated Fatty Acid Prodrugs and Prodrug-Nanoplatforms for Cancer Chemotherapy. *Journal of Controlled Release* **2017**, 264, 145–159. <https://doi.org/10.1016/j.jconrel.2017.08.034>.

- (181) Martinez, J. O.; Brown, B. S.; Quattrocchi, N.; Evangelopoulos, M.; Ferrari, M.; Tasciotti, E. Multifunctional to Multistage Delivery Systems: The Evolution of Nanoparticles for Biomedical Applications. *Chin Sci Bull* **2012**, 57 (31), 3961–3971.
- (182) Sanchis, A.; Salvador, J.-P.; Marco, M.-P. Light-Induced Mechanisms for Nanocarrier's Cargo Release. *Colloids and Surfaces B: Biointerfaces* **2019**, 173, 825–832. <https://doi.org/10.1016/j.colsurfb.2018.10.056>.
- (183) Diebold, Y.; Calonge, M. Applications of Nanoparticles in Ophthalmology. *Progress in Retinal and Eye Research* **2010**, 29 (6), 596–609. <https://doi.org/10.1016/j.preteyeres.2010.08.002>.
- (184) Couvreur, P. Nanomedicine: From Where Are We Coming and Where Are We Going? *Journal of Controlled Release* **2019**, 311–312, 319–321. <https://doi.org/10.1016/j.jconrel.2019.10.020>.
- (185) Haggag, Y. A.; Osman, M. A.; El-Gizawy, S. A.; Goda, A. E.; Shamloula, M. M.; Faheem, A. M.; McCarron, P. A. Polymeric Nano-Encapsulation of 5-Fluorouracil Enhances Anti-Cancer Activity and Ameliorates Side Effects in Solid Ehrlich Carcinoma-Bearing Mice. *Biomedicine & Pharmacotherapy* **2018**, 105, 215–224. <https://doi.org/10.1016/j.biopha.2018.05.124>.
- (186) Luo, C.; Sun, J.; Sun, B.; He, Z. Prodrug-Based Nanoparticulate Drug Delivery Strategies for Cancer Therapy. *Trends in Pharmacological Sciences* **2014**, 35 (11), 556–566. <https://doi.org/10.1016/j.tips.2014.09.008>.
- (187) Mura, S.; Bui, D. T.; Couvreur, P.; Nicolas, J. Lipid Prodrug Nanocarriers in Cancer Therapy. *Journal of Controlled Release* **2015**, 208, 25–41. <https://doi.org/10.1016/j.jconrel.2015.01.021>.
- (188) Sivakova, S.; Rowan, S. J. Nucleobases as Supramolecular Motifs. *Chem. Soc. Rev.* **2005**, 34 (1), 9–21. <https://doi.org/10.1039/B304608G>.
- (189) Gong, X.; Moghaddam, M. J.; Sagnella, S. M.; Conn, C. E.; Danon, S. J.; Waddington, L. J.; Drummond, C. J. Lamellar Crystalline Self-Assembly Behaviour and Solid Lipid Nanoparticles of a Palmityl Prodrug Analogue of Capecitabine—A Chemotherapy Agent. *Colloids and Surfaces B: Biointerfaces* **2011**, 85 (2), 349–359. <https://doi.org/10.1016/j.colsurfb.2011.03.007>.
- (190) Lepeltier, E.; Bourgaux, C.; Maksimenko, A.; Meneau, F.; Rosilio, V.; Sliwinski, E.; Zouhiri, F.; Desmaële, D.; Couvreur, P. Self-Assembly of Polyisoprenoyl Gemcitabine Conjugates: Influence of Supramolecular Organization on Their Biological Activity. *Langmuir* **2014**, 30 (22), 6348–6357. <https://doi.org/10.1021/la5007132>.
- (191) Israelachvili, J. N.; Mitchell, D. J. A Model for the Packing of Lipids in Bilayer Membranes. *Biochimica et Biophysica Acta (BBA) - Biomembranes* **1975**, 389 (1), 13–19. [https://doi.org/10.1016/0005-2736\(75\)90381-8](https://doi.org/10.1016/0005-2736(75)90381-8).
- (192) Luo, C.; Sun, J.; Liu, D.; Sun, B.; Miao, L.; Musetti, S.; Li, J.; Han, X.; Du, Y.; Li, L.; Huang, L.; He, Z. Self-Assembled Redox Dual-Responsive Prodrug-Nanosystem Formed by Single Thioether-Bridged Paclitaxel-Fatty Acid Conjugate for Cancer Chemotherapy. *Nano Lett.* **2016**, 16 (9), 5401–5408. <https://doi.org/10.1021/acs.nanolett.6b01632>.
- (193) Luo, C.; Sun, J.; Sun, B.; Liu, D.; Miao, L.; Goodwin, T. J.; Huang, L.; He, Z. Facile Fabrication of Tumor Redox-Sensitive Nanoassemblies of Small-Molecule Oleate Prodrug as Potent Chemotherapeutic Nanomedicine. *Small* **2016**, 12 (46), 6353–6362. <https://doi.org/10.1002/smll.201601597>.
- (194) Wang, Y.; Fan, P.; Zhu, L.; Zhuang, W.; Jiang, L.; Zhang, H.; Huang, H. Enhanced in Vitro Antitumor Efficacy of a Polyunsaturated Fatty Acid-Conjugated PH-Responsive Self-Assembled Ion-Pairing Liposome-Encapsulated Prodrug. *Nanotechnology* **2020**, 31 (15), 155101. <https://doi.org/10.1088/1361-6528/ab62d1>.
- (195) Allain, V.; Bourgaux, C.; Couvreur, P. Self-Assembled Nucleolipids: From Supramolecular Structure to Soft Nucleic Acid and Drug Delivery Devices. *Nucleic Acids Research* **2012**, 40 (5), 1891–1903. <https://doi.org/10.1093/nar/gkr681>.

- (196) Bildstein, L.; Pili, B.; Marsaud, V.; Wack, S.; Meneau, F.; Lepêtre-Mouelhi, S.; Desmaële, D.; Bourgaux, C.; Couvreur, P.; Dubernet, C. Interaction of an Amphiphilic Squalenoyl Prodrug of Gemcitabine with Cellular Membranes. *Eur J Pharm Biopharm* **2011**, 79 (3), 612–620. <https://doi.org/10.1016/j.ejpb.2011.07.003>.
- (197) Pili, B.; Bourgaux, C.; Amenitsch, H.; Keller, G.; Lepêtre-Mouelhi, S.; Desmaële, D.; Couvreur, P.; Ollivon, M. Interaction of a New Anticancer Prodrug, Gemcitabine-Squalene, with a Model Membrane: Coupled DSC and XRD Study. *Biochim Biophys Acta* **2010**, 1798 (8), 1522–1532. <https://doi.org/10.1016/j.bbamem.2010.04.011>.
- (198) Reddy, L. H.; Dubernet, C.; Mouelhi, S. L.; Marque, P. E.; Desmaële, D.; Couvreur, P. A New Nanomedicine of Gemcitabine Displays Enhanced Anticancer Activity in Sensitive and Resistant Leukemia Types. *J Control Release* **2007**, 124 (1–2), 20–27. <https://doi.org/10.1016/j.jconrel.2007.08.018>.
- (199) Behzadi, S.; Serpooshan, V.; Tao, W.; Hamaly, M. A.; Alkawareek, M. Y.; Dreaden, E. C.; Brown, D.; Alkilany, A. M.; Farokhzad, O. C.; Mahmoudi, M. Cellular Uptake of Nanoparticles: Journey Inside the Cell. *Chem Soc Rev* **2017**, 46 (14), 4218–4244. <https://doi.org/10.1039/c6cs00636a>.
- (200) Swanson, J. A. Shaping Cups into Phagosomes and Macropinosomes. *Nat Rev Mol Cell Biol* **2008**, 9 (8), 639–649. <https://doi.org/10.1038/nrm2447>.
- (201) Aderem, A.; Underhill, D. M. Mechanisms of Phagocytosis in Macrophages. *Annu. Rev. Immunol.* **1999**, 17 (1), 593–623. <https://doi.org/10.1146/annurev.immunol.17.1.593>.
- (202) Hillaireau, H.; Couvreur, P. Nanocarriers' Entry into the Cell: Relevance to Drug Delivery. *Cell. Mol. Life Sci.* **2009**, 66 (17), 2873–2896. <https://doi.org/10.1007/s00018-009-0053-z>.
- (203) Barenholz, Y. (Chezy). Doxil® — The First FDA-Approved Nano-Drug: Lessons Learned. *Journal of Controlled Release* **2012**, 160 (2), 117–134. <https://doi.org/10.1016/j.jconrel.2012.03.020>.
- (204) Conner, S. D.; Schmid, S. L. Regulated Portals of Entry into the Cell. *Nature* **2003**, 422 (6927), 37–44. <https://doi.org/10.1038/nature01451>.
- (205) Ehrlich, M.; Boll, W.; Oijen, A. van; Hariharan, R.; Chandran, K.; Nibert, M. L.; Kirchhausen, T. Endocytosis by Random Initiation and Stabilization of Clathrin-Coated Pits. *Cell* **2004**, 118 (5), 591–605. <https://doi.org/10.1016/j.cell.2004.08.017>.
- (206) Pelkmans, L.; Helenius, A. Endocytosis Via Caveolae. *Traffic* **2002**, 3 (5), 311–320. <https://doi.org/10.1034/j.1600-0854.2002.30501.x>.
- (207) Sahay, G.; Alakhova, D. Y.; Kabanov, A. V. Endocytosis of Nanomedicines. *J Control Release* **2010**, 145 (3), 182–195. <https://doi.org/10.1016/j.jconrel.2010.01.036>.
- (208) Rothberg, K. G.; Heuser, J. E.; Donzell, W. C.; Ying, Y.-S.; Glenney, J. R.; Anderson, R. G. W. Caveolin, a Protein Component of Caveolae Membrane Coats. *Cell* **1992**, 68 (4), 673–682. [https://doi.org/10.1016/0092-8674\(92\)90143-Z](https://doi.org/10.1016/0092-8674(92)90143-Z).
- (209) My Gallery - Ports of entry of nanoparticles into cells <http://eacademic.ju.edu.jo/A.Alkilany/My%20Gallery/Forms/DispForm.aspx?ID=5> (accessed 2021 -10 -11).
- (210) Damm, E.-M.; Pelkmans, L.; Kartenbeck, J.; Mezzacasa, A.; Kurzchalia, T.; Helenius, A. Clathrin- and Caveolin-1-Independent Endocytosis. *J Cell Biol* **2005**, 168 (3), 477–488. <https://doi.org/10.1083/jcb.200407113>.
- (211) Kirkham, M.; Fujita, A.; Chadda, R.; Nixon, S. J.; Kurzchalia, T. V.; Sharma, D. K.; Pagano, R. E.; Hancock, J. F.; Mayor, S.; Parton, R. G. Ultrastructural Identification of Uncoated Caveolin-Independent Early Endocytic Vehicles. *J Cell Biol* **2005**, 168 (3), 465–476. <https://doi.org/10.1083/jcb.200407078>.
- (212) Kuhn, D. A.; Vanhecke, D.; Michen, B.; Blank, F.; Gehr, P.; Petri-Fink, A.; Rothen-Rutishauser, B. Different Endocytotic Uptake Mechanisms for Nanoparticles in Epithelial Cells and Macrophages. *Beilstein J Nanotechnol* **2014**, 5, 1625–1636. <https://doi.org/10.3762/bjnano.5.174>.

- (213) Lim, J. P.; Gleeson, P. A. Macropinocytosis: An Endocytic Pathway for Internalising Large Gulps. *Immunology & Cell Biology* **2011**, 89 (8), 836–843. <https://doi.org/10.1038/icb.2011.20>.
- (214) Wang, T.; Bai, J.; Jiang, X.; Nienhaus, G. U. Cellular Uptake of Nanoparticles by Membrane Penetration: A Study Combining Confocal Microscopy with FTIR Spectroelectrochemistry. *ACS Nano* **2012**, 6 (2), 1251–1259. <https://doi.org/10.1021/nn203892h>.
- (215) Gaudin, A.; Yemisci, M.; Eroglu, H.; Lepetre-Mouelhi, S.; Turkoglu, O. F.; Dönmez-Demir, B.; Caban, S.; Sargon, M. F.; Garcia-Argote, S.; Pieters, G.; Loreau, O.; Rousseau, B.; Tagit, O.; Hildebrandt, N.; Le Dantec, Y.; Mougin, J.; Valetti, S.; Chacun, H.; Nicolas, V.; Desmaële, D.; Andrieux, K.; Capan, Y.; Dalkara, T.; Couvreur, P. Squalenoyl Adenosine Nanoparticles Provide Neuroprotection after Stroke and Spinal Cord Injury. *Nature Nanotech* **2014**, 9 (12), 1054–1062. <https://doi.org/10.1038/nnano.2014.274>.
- (216) Baroud, M.; Lepeltier, E.; Thepot, S.; El-Makhour, Y.; Duval, O. The Evolution of Nucleosidic Analogues: Self-Assembly of Prodrugs into Nanoparticles for Cancer Drug Delivery. *Nanoscale Adv.* **2021**, 3 (8), 2157–2179. <https://doi.org/10.1039/D0NA01084G>.
- (217) Hajdo, L.; Szulc, A. B.; Klajnert, B.; Bryszewska, M. Metabolic Limitations of the Use of Nucleoside Analogs in Cancer Therapy May Be Overcome by Application of Nanoparticles as Drug Carriers: A Review. *Drug Development Research* **2010**, 71 (7), 383–394. <https://doi.org/10.1002/ddr.20390>.
- (218) Jordheim, L. P.; Durantel, D.; Zoulim, F.; Dumontet, C. Advances in the Development of Nucleoside and Nucleotide Analogues for Cancer and Viral Diseases. *Nature Reviews Drug Discovery* **2013**, 12 (6), 447–464. <https://doi.org/10.1038/nrd4010>.
- (219) Desmaële, D.; Gref, R.; Couvreur, P. Squalenoylation: A Generic Platform for Nanoparticulate Drug Delivery. *Journal of Controlled Release* **2012**, 161 (2), 609–618. <https://doi.org/10.1016/j.jconrel.2011.07.038>.
- (220) Lepeltier, E.; Bourgaux, C.; Rosilio, V.; Poupaert, J. H.; Meneau, F.; Zouhiri, F.; Lepêtre-Mouelhi, S.; Desmaële, D.; Couvreur, P. Self-Assembly of Squalene-Based Nucleolipids: Relating the Chemical Structure of the Bioconjugates to the Architecture of the Nanoparticles. *Langmuir* **2013**, 29 (48), 14795–14803. <https://doi.org/10.1021/la403338y>.
- (221) Maksimenko, A.; Caron, J.; Mougin, J.; Desmaële, D.; Couvreur, P. Gemcitabine-Based Therapy for Pancreatic Cancer Using the Squalenoyl Nucleoside Monophosphate Nanoassemblies. *International Journal of Pharmaceutics* **2015**, 482 (1–2), 38–46. <https://doi.org/10.1016/j.ijpharm.2014.11.009>.
- (222) Wu, L.; Zhang, F.; Chen, X.; Wan, J.; Wang, Y.; Li, T.; Wang, H. Self-Assembled Gemcitabine Prodrug Nanoparticles Show Enhanced Efficacy against Patient-Derived Pancreatic Ductal Adenocarcinoma. *ACS Appl. Mater. Interfaces* **2020**, 12 (3), 3327–3340. <https://doi.org/10.1021/acsami.9b16209>.
- (223) Bui, D. T.; Nicolas, J.; Maksimenko, A.; Desmaële, D.; Couvreur, P. Multifunctional Squalene-Based Prodrug Nanoparticles for Targeted Cancer Therapy. *Chem. Commun. (Camb.)* **2014**, 50 (40), 5336–5338. <https://doi.org/10.1039/c3cc47427e>.
- (224) Xu, F.; Zhang, M.; Wu, Q.; Lin, X. Novel L-Amino Acid Ester Prodrugs of Azacitidine: Design, Enzymatic Synthesis and the Investigation of Release Behavior. *Journal of Molecular Catalysis B: Enzymatic* **2014**, 105, 49–57. <https://doi.org/10.1016/j.molcatb.2014.03.018>.
- (225) Brueckner, B.; Rius, M.; Markelova, M. R.; Fichtner, I.; Hals, P.-A.; Sandvold, M. L.; Lyko, F. Delivery of 5-Azacytidine to Human Cancer Cells by Elaidic Acid Esterification Increases Therapeutic Drug Efficacy. *Molecular Cancer Therapeutics* **2010**, 9 (5), 1256–1264. <https://doi.org/10.1158/1535-7163.MCT-09-1202>.
- (226) Silverman, L.; Holland, J. Azacytidine Analogues and Uses Thereof. US8158605B2, April 17, 2012.

- (227) Zhong, Y.-J.; Shao, L.-H.; Li, Y. Cathepsin B-Cleavable Doxorubicin Prodrugs for Targeted Cancer Therapy (Review). *International Journal of Oncology* **2013**, 42 (2), 373–383. <https://doi.org/10.3892/ijo.2012.1754>.
- (228) Xu, Y.; Geng, J.; An, P.; Xu, Y.; Huang, J.; Lu, W.; Liu, S.; Yu, J. Cathepsin B-Sensitive Cholesteryl Hemisuccinate–Gemcitabine Prodrug Nanoparticles: Enhanced Cellular Uptake and Intracellular Drug Controlled Release. *RSC Adv.* **2014**, 5 (9), 6985–6992. <https://doi.org/10.1039/C4RA13870H>.
- (229) Bildstein, L.; Dubernet, C.; Marsaud, V.; Chacun, H.; Nicolas, V.; Gueutin, C.; Sarasin, A.; Bénech, H.; Lepêtre-Mouelhi, S.; Desmaële, D.; Couvreur, P. Transmembrane Diffusion of Gemcitabine by a Nanoparticulate Squalenoyl Prodrug: An Original Drug Delivery Pathway. *Journal of Controlled Release* **2010**, 147 (2), 163–170. <https://doi.org/10.1016/j.jconrel.2010.07.120>.
- (230) Caron, J.; Maksimenko, A.; Mougin, J.; Couvreur, P.; Desmaële, D. Combined Antitumoral Therapy with Nanoassemblies of Bolaform Polyisoprenoyl Paclitaxel/Gemcitabine Prodrugs. *Polym. Chem.* **2014**, 5 (5), 1662–1673. <https://doi.org/10.1039/C3PY01177A>.
- (231) Higashibayashi, S.; Shinko, K.; Ishizu, T.; Hashimoto, K.; Shirahama, H.; Nakata, M. Selective Deprotection of T-Butyldiphenylsilyl Ethers in the Presence of t-Butyldimethylsilyl Ethers by Tetrabutylammonium Fluoride, Acetic Acid, and Water. *Synlett* **2000**, No. 9, 1306–1308.
- (232) Guyon, L.; Lepeltier, E.; Passirani, C. Self-Assembly of Peptide-Based Nanostructures: Synthesis and Biological Activity. *Nano Research* **2018**, 11 (5), 2315–2335. <https://doi.org/10.1007/s12274-017-1892-9>.
- (233) Guyon, L.; Lepeltier, E.; Gimel, J.-C.; Calvignac, B.; Franconi, F.; Lautram, N.; Dupont, A.; Bourgaux, C.; Pigeon, P.; Saulnier, P.; Jaouen, G.; Passirani, C. Importance of Combining Advanced Particle Size Analysis Techniques To Characterize Cell-Penetrating Peptide–Ferrocifen Self-Assemblies. *J. Phys. Chem. Lett.* **2019**, 10 (21), 6613–6620. <https://doi.org/10.1021/acs.jpcllett.9b01493>.
- (234) Lepeltier, E.; Bourgaux, C.; Maksimenko, A.; Meneau, F.; Rosilio, V.; Sliwinski, E.; Zouhiri, F.; Desmaële, D.; Couvreur, P. Self-Assembly of Polyisoprenoyl Gemcitabine Conjugates: Influence of Supramolecular Organization on Their Biological Activity. *Langmuir* **2014**, 30 (22), 6348–6357. <https://doi.org/10.1021/la5007132>.
- (235) Mihalik, R.; Imre, G.; Petak, I.; Szende, B.; Kopper, L. Cathepsin B-Independent Abrogation of Cell Death by CA-074-OMe Upstream of Lysosomal Breakdown. *Cell Death Differ* **2004**, 11 (12), 1357–1360. <https://doi.org/10.1038/sj.cdd.4401493>.
- (236) Fanciullino, R.; Mercier, C.; Serdjebi, C.; Berda, Y.; Fina, F.; Ouafik, L.; Lacarelle, B.; Ciccolini, J.; Costello, R. Lethal Toxicity after Administration of Azacytidine: Implication of the Cytidine Deaminase-Deficiency Syndrome. *Pharmacogenetics and Genomics* **2015**, 25 (6), 317–321. <https://doi.org/10.1097/FPC.0000000000000139>.
- (237) Chabner, B. A.; Drake, J. C.; Johns, D. G. Deamination of 5-Azacytidine by a Human Leukemia Cell Cytidine Deaminase. *Biochemical Pharmacology* **1973**, 22 (21), 2763–2765. [https://doi.org/10.1016/0006-2952\(73\)90137-8](https://doi.org/10.1016/0006-2952(73)90137-8).
- (238) Deal, J.; Pleshinger, D. J.; Johnson, S. C.; Leavesley, S. J.; Rich, T. C. Milestones in the Development and Implementation of FRET-Based Sensors of Intracellular Signals: A Biological Perspective of the History of FRET. *Cellular Signalling* **2020**, 75, 109769. <https://doi.org/10.1016/j.cellsig.2020.109769>.
- (239) Sahoo, H. Förster Resonance Energy Transfer – A Spectroscopic Nanoruler: Principle and Applications. *Journal of Photochemistry and Photobiology C: Photochemistry Reviews* **2011**, 12 (1), 20–30. <https://doi.org/10.1016/j.jphotochemrev.2011.05.001>.
- (240) Gravier, J.; Sancey, L.; Hirsjärvi, S.; Rustique, E.; Passirani, C.; Benoît, J.-P.; Coll, J.-L.; Texier, I. FRET Imaging Approaches for in Vitro and in Vivo Characterization of Synthetic



- Lipid Nanoparticles. *Mol. Pharmaceutics* **2014**, *11* (9), 3133–3144. <https://doi.org/10.1021/mp500329z>.
- (241) Fruhwirth, G. O.; Fernandes, L. P.; Weitsman, G.; Patel, G.; Kelleher, M.; Lawler, K.; Brock, A.; Poland, S. P.; Matthews, D. R.; Kéri, G.; Barber, P. R.; Vojnovic, B.; Ameer-Beg, S. M.; Coolen, A. C. C.; Fraternali, F.; Ng, T. How Förster Resonance Energy Transfer Imaging Improves the Understanding of Protein Interaction Networks in Cancer Biology. *ChemPhysChem* **2011**, *12* (3), 442–461. <https://doi.org/10.1002/cphc.201000866>.
- (242) Chen, H.; Puhl, H. L.; Koushik, S. V.; Vogel, S. S.; Ikeda, S. R. Measurement of FRET Efficiency and Ratio of Donor to Acceptor Concentration in Living Cells. *Biophysical Journal* **2006**, *91* (5), L39–L41. <https://doi.org/10.1529/biophysj.106.088773>.
- (243) Swiecicki, J.-M.; Thiebaut, F.; Di Pisa, M.; Gourdin -Bertin, S.; Tailhades, J.; Mansuy, C.; Burlina, F.; Chwetzoff, S.; Trugnan, G.; Chassaing, G.; Lavielle, S. How to Unveil Self-Quenched Fluorophores and Subsequently Map the Subcellular Distribution of Exogenous Peptides. *Sci Rep* **2016**, *6*, 20237. <https://doi.org/10.1038/srep20237>.
- (244) Carter, J. L.; Hege, K.; Yang, J.; Kalpage, H. A.; Su, Y.; Edwards, H.; Hüttemann, M.; Taub, J. W.; Ge, Y. Targeting Multiple Signaling Pathways: The New Approach to Acute Myeloid Leukemia Therapy. *Sig Transduct Target Ther* **2020**, *5* (1), 1–29. <https://doi.org/10.1038/s41392-020-00361-x>.
- (245) Pleyer, L.; Döhner, H.; Dombret, H.; Seymour, J. F.; Schuh, A. C.; Beach, C.; Swern, A. S.; Burgstaller, S.; Stauder, R.; Girschikofsky, M.; Sill, H.; Schlick, K.; Thaler, J.; Halter, B.; Machherndl Spandl, S.; Zebisch, A.; Pichler, A.; Pfeilstöcker, M.; Autzinger, E. M.; Lang, A.; Geissler, K.; Voskova, D.; Sperr, W. R.; Hojas, S.; Rogulj, I. M.; Andel, J.; Greil, R. Azacitidine for Front-Line Therapy of Patients with AML: Reproducible Efficacy Established by Direct Comparison of International Phase 3 Trial Data with Registry Data from the Austrian Azacitidine Registry of the AGMT Study Group. *Int J Mol Sci* **2017**, *18* (2), 415. <https://doi.org/10.3390/ijms18020415>.
- (246) Dombret, H.; Seymour, J. F.; Butrym, A.; Wierzbowska, A.; Selleslag, D.; Jang, J. H.; Kumar, R.; Cavenagh, J.; Schuh, A. C.; Candoni, A.; Récher, C.; Sandhu, I.; Bernal del Castillo, T.; Al-Ali, H. K.; Martinelli, G.; Falantes, J.; Noppeney, R.; Stone, R. M.; Minden, M. D.; McIntyre, H.; Songer, S.; Lucy, L. M.; Beach, C. L.; Döhner, H. International Phase 3 Study of Azacitidine vs Conventional Care Regimens in Older Patients with Newly Diagnosed AML with >30% Blasts. *Blood* **2015**, *126* (3), 291–299. <https://doi.org/10.1182/blood-2015-01-621664>.
- (247) Hong, M.; He, G. The 2016 Revision to the World Health Organization Classification of Myelodysplastic Syndromes. *J Transl Int Med* **2017**, *5* (3), 139–143. <https://doi.org/10.1515/jtim-2017-0002>.
- (248) Waespe, N.; Akker, M. V. D.; Klaassen, R. J.; Lieberman, L.; Irwin, M. S.; Ali, S. S.; Abdelhaleem, M.; Zlateska, B.; Liebman, M.; Cada, M.; Schechter, T.; Dror, Y. Response to Treatment with Azacitidine in Children with Advanced Myelodysplastic Syndrome Prior to Hematopoietic Stem Cell Transplantation. *Haematologica* **2016**, *101* (12), 1508–1515. <https://doi.org/10.3324/haematol.2016.145821>.
- (249) Keruakous, A. R.; Holter-Chakrabarty, J.; Schmidt, S. A.; Khawandanah, M. O.; Selby, G.; Yuen, C. Azacitidine Maintenance Therapy Post-Allogeneic Stem Cell Transplantation in Poor-Risk Acute Myeloid Leukemia. *Hematology/Oncology and Stem Cell Therapy* **2021**. <https://doi.org/10.1016/j.hemonc.2021.03.001>.
- (250) Oshrine, B. R.; Shyr, D.; Hale, G.; Petrovic, A. Low-Dose Azacitidine for Relapse Prevention after Allogeneic Hematopoietic Cell Transplantation in Children with Myeloid Malignancies. *Pediatr Transplant* **2019**, *23* (4), e13423. <https://doi.org/10.1111/petr.13423>.
- (251) Musto, P.; Maurillo, L.; Spagnoli, A.; Gozzini, A.; Rivellini, F.; Lunghi, M.; Villani, O.; Aloe-Spiriti, M. A.; Venditti, A.; Santini, V. Azacitidine for the Treatment of Lower Risk

- Myelodysplastic Syndromes. *Cancer* **2010**, *116* (6), 1485–1494. <https://doi.org/10.1002/cncr.24894>.
- (252) Baroud, M.; Lepeltier, E.; Thepot, S.; El-Makhour, Y.; Duval, O. The Evolution of Nucleosidic Analogues: Self-Assembly of Prodrugs into Nanoparticles for Cancer Drug Delivery. *Nanoscale Adv.* **2021**, *3* (8), 2157–2179. <https://doi.org/10.1039/D0NA01084G>.
- (253) Kordella, C.; Lamprianidou, E.; Kotsianidis, I. Mechanisms of Action of Hypomethylating Agents: Endogenous Retroelements at the Epicenter. *Frontiers in Oncology* **2021**, *11*, 490. <https://doi.org/10.3389/fonc.2021.650473>.
- (254) Prébet, T.; Thepot, S.; Gore, S. D.; Dreyfus, F.; Fenaux, P.; Vey, N. Outcome of Patients with Low-Risk Myelodysplasia after Azacitidine Treatment Failure. *Haematologica* **2013**, *98* (2), e18–e19. <https://doi.org/10.3324/haematol.2012.071050>.
- (255) Gil-Perez, A.; Montalban-Bravo, G. Management of Myelodysplastic Syndromes after Failure of Response to Hypomethylating Agents. *Therapeutic Advances in Hematology* **2019**, *10*, 2040620719847059. <https://doi.org/10.1177/2040620719847059>.
- (256) Zhang, X.; Li, Y.; Hu, C.; Wu, Y.; Zhong, D.; Xu, X.; Gu, Z. Engineering Anticancer Amphipathic Peptide-Dendronized Compounds for Highly-Efficient Plasma/Organelle Membrane Perturbation and Multidrug Resistance Reversal. *ACS Appl. Mater. Interfaces* **2018**, *10* (37), 30952–30962. <https://doi.org/10.1021/acsami.8b07917>.
- (257) Zhang, R.; Qin, X.; Kong, F.; Chen, P.; Pan, G. Improving Cellular Uptake of Therapeutic Entities through Interaction with Components of Cell Membrane. *Drug Deliv* **2019**, *26* (1), 328–342. <https://doi.org/10.1080/10717544.2019.1582730>.
- (258) Zhong, Y.-J.; Shao, L.-H.; Li, Y. Cathepsin B-Cleavable Doxorubicin Prodrugs for Targeted Cancer Therapy (Review). *International Journal of Oncology* **2013**, *42* (2), 373–383. <https://doi.org/10.3892/ijo.2012.1754>.
- (259) Xu, Y.; Geng, J.; An, P.; Xu, Y.; Huang, J.; Lu, W.; Liu, S.; Yu, J. Cathepsin B-Sensitive Cholesteryl Hemisuccinate–Gemcitabine Prodrug Nanoparticles: Enhanced Cellular Uptake and Intracellular Drug Controlled Release. *RSC Adv.* **2014**, *5* (9), 6985–6992. <https://doi.org/10.1039/C4RA13870H>.
- (260) Ni, Y.; Hai, Z.; Zhang, T.; Wang, Y.; Yang, Y.; Zhang, S.; Liang, G. Cathepsin B Turning Bioluminescence “On” for Tumor Imaging. *Anal. Chem.* **2019**, *91* (23), 14834–14837. <https://doi.org/10.1021/acs.analchem.9b04254>.
- (261) Desmaële, D.; Gref, R.; Couvreur, P. Squalenoylation: A Generic Platform for Nanoparticular Drug Delivery. *Journal of Controlled Release* **2012**, *161* (2), 609–618. <https://doi.org/10.1016/j.jconrel.2011.07.038>.
- (262) Lepeltier, E.; Bourgaux, C.; Rosilio, V.; Poupert, J. H.; Meneau, F.; Zouhiri, F.; Lepêtre-Mouelhi, S.; Desmaële, D.; Couvreur, P. Self-Assembly of Squalene-Based Nucleolipids: Relating the Chemical Structure of the Bioconjugates to the Architecture of the Nanoparticles. *Langmuir* **2013**, *29* (48), 14795–14803. <https://doi.org/10.1021/la403338y>.
- (263) Maksimenko, A.; Caron, J.; Mougin, J.; Desmaële, D.; Couvreur, P. Gemcitabine-Based Therapy for Pancreatic Cancer Using the Squalenoyl Nucleoside Monophosphate Nanoassemblies. *International Journal of Pharmaceutics* **2015**, *482* (1–2), 38–46. <https://doi.org/10.1016/j.ijpharm.2014.11.009>.
- (264) Xie, B.; Wan, J.; Chen, X.; Han, W.; Wang, H. Preclinical Evaluation of a Cabazitaxel Prodrug Using Nanoparticle Delivery for the Treatment of Taxane-Resistant Malignancies. *Mol Cancer Ther* **2020**, *19* (3), 822–834. <https://doi.org/10.1158/1535-7163.MCT-19-0625>.
- (265) Wang, H.; Lu, Z.; Wang, L.; Guo, T.; Wu, J.; Wan, J.; Zhou, L.; Li, H.; Li, Z.; Jiang, D.; Song, P.; Xie, H.; Zhou, L.; Xu, X.; Zheng, S. New Generation Nanomedicines Constructed from Self-Assembling Small-Molecule Prodrugs Alleviate Cancer Drug Toxicity. *Cancer Res* **2017**, *77* (24), 6963–6974. <https://doi.org/10.1158/0008-5472.CAN-17-0984>.

- (266) Huang, C.-W.; Mohamed, M. G.; Zhu, C.-Y.; Kuo, S.-W. Functional Supramolecular Polypeptides Involving  $\pi$ - $\pi$  Stacking and Strong Hydrogen-Bonding Interactions: A Conformation Study toward Carbon Nanotubes (CNTs) Dispersion. *Macromolecules* **2016**, 49 (15), 5374–5385. <https://doi.org/10.1021/acs.macromol.6b01060>.
- (267) Gallop, M.; Peng, G.; Woiwode, T.; Cundy, K. Gemcitabine Prodrugs, Pharmaceutical Compositions and Uses Thereof. US20040142857A1, July 22, 2004.
- (268) Pradere, U.; Garnier-Amblard, E. C.; Coats, S. J.; Amblard, F.; Schinazi, R. F. Synthesis of Nucleoside Phosphate and Phosphonate Prodrugs. *Chem. Rev.* **2014**, 114 (18), 9154–9218. <https://doi.org/10.1021/cr5002035>.
- (269) Groot, F. M. H. de; Broxterman, H. J.; Adams, H. P. H. M.; Vliet, A. van; Tesser, G. I.; Elderkamp, Y. W.; Schraa, A. J.; Kok, R. J.; Molema, G.; Pinedo, H. M.; Scheeren, H. W. Design, Synthesis, and Biological Evaluation of a Dual Tumor-Specific Motive Containing Integrin-Targeted Plasmin-Cleavable Doxorubicin Prodrug 1 This Work Was Partly Supported by the Spinoza Award (to H. M. P.). 1. *Mol Cancer Ther* **2002**, 1 (11), 901–911.
- (270) Fan, Q.; Ji, Y.; Wang, J.; Wu, L.; Li, W.; Chen, R.; Chen, Z. Self-Assembly Behaviours of Peptide–Drug Conjugates: Influence of Multiple Factors on Aggregate Morphology and Potential Self-Assembly Mechanism. *Royal Society Open Science* 5 (4), 172040. <https://doi.org/10.1098/rsos.172040>.
- (271) Buettner, C. J.; Wallace, A. J.; Ok, S.; Manos, A. A.; Nicholl, M. J.; Ghosh, A.; Tweedle, M. F.; Goldberger, J. E. Balancing the Intermolecular Forces in Peptide Amphiphiles for Controlling Self-Assembly Transitions. *Org Biomol Chem* **2017**, 15 (24), 5220–5226. <https://doi.org/10.1039/c7ob00875a>.
- (272) Gratton, S. E. A.; Ropp, P. A.; Pohlhaus, P. D.; Luft, J. C.; Madden, V. J.; Napier, M. E.; DeSimone, J. M. The Effect of Particle Design on Cellular Internalization Pathways. *PNAS* **2008**, 105 (33), 11613–11618. <https://doi.org/10.1073/pnas.0801763105>.
- (273) Wang, Y.; Xu, H.; Zhang, X. Tuning the Amphiphilicity of Building Blocks: Controlled Self-Assembly and Disassembly for Functional Supramolecular Materials. **2009**. <https://doi.org/10.1002/ADMA.200803276>.
- (274) Lombardo, D.; Kiselev, M. A.; Magazù, S.; Calandra, P. Amphiphiles Self-Assembly: Basic Concepts and Future Perspectives of Supramolecular Approaches. *Advances in Condensed Matter Physics* **2015**, 2015, 1–22. <https://doi.org/10.1155/2015/151683>.
- (275) Dubtsov, A. V.; Pasechnik, S. V.; Shmeliova, D. V.; Kralj, S.; Repnik, R. Controlled Nanoparticle Targeting and Nanoparticle-Driven Nematic Structural Transition. *Advances in Condensed Matter Physics* **2015**, 2015, e803480. <https://doi.org/10.1155/2015/803480>.
- (276) Lepeltier, E.; Bourgaux, C.; Amenitsch, H.; Rosilio, V.; Lepetre-Mouelhi, S.; Zouhiri, F.; Desmaële, D.; Couvreur, P. Influence of the Nanoprecipitation Conditions on the Supramolecular Structure of Squalenoyled Nanoparticles. *European Journal of Pharmaceutics and Biopharmaceutics* **2015**, 96, 89–95. <https://doi.org/10.1016/j.ejpb.2015.07.004>.
- (277) Shao, X.; Bor, G.; Al-Hosayni, S.; Salentinig, S.; Yaghmur, A. Structural Characterization of Self-Assemblies of New Omega-3 Lipids: Docosahexaenoic Acid and Docosapentaenoic Acid Monoglycerides. *Phys. Chem. Chem. Phys.* **2018**, 20 (37), 23928–23941. <https://doi.org/10.1039/C8CP04256J>.
- (278) De Santis, A.; Varela, Y.; Sot, J.; D'Errico, G.; Goñi, F. M.; Alonso, A. Omega-3 Polyunsaturated Fatty Acids Do Not Fluidify Bilayers in the Liquid-Crystalline State. *Sci Rep* **2018**, 8 (1), 16240. <https://doi.org/10.1038/s41598-018-34264-3>.
- (279) Sahari, M. A.; Moghimi, H. R.; Hadian, Z.; Barzegar, M.; Mohammadi, A. Improved Physical Stability of Docosahexaenoic Acid and Eicosapentaenoic Acid Encapsulated Using Nanoliposome Containing  $\alpha$ -Tocopherol. *International Journal of Food Science & Technology* **2016**, 51 (5), 1075–1086. <https://doi.org/10.1111/ijfs.13068>.

- (280) Namani, T.; Ishikawa, T.; Morigaki, K.; Walde, P. Vesicles from Docosahexaenoic Acid. *Colloids and Surfaces B: Biointerfaces* **2007**, *54* (1), 118–123. <https://doi.org/10.1016/j.colsurfb.2006.05.022>.
- (281) Stillwell, W.; Ehringer, W.; Jenski, L. J. Docosahexaenoic Acid Increases Permeability of Lipid Vesicles and Tumor Cells. *Lipids* **1993**, *28* (2), 103–108. <https://doi.org/10.1007/BF02535772>.
- (282) Agnihotri, S. A.; Soppimath, K. S.; Betageri, G. V. Controlled Release Application of Multilamellar Vesicles: A Novel Drug Delivery Approach. *Drug Delivery* **2010**, *17* (2), 92–101. <https://doi.org/10.3109/10717540903509027>.
- (283) Sherratt, S. C. R.; Juliano, R. A.; Copland, C.; Bhatt, D. L.; Libby, P.; Mason, R. P. EPA and DHA Containing Phospholipids Have Contrasting Effects on Membrane Structure. *J Lipid Res* **2021**, *62*, 100106. <https://doi.org/10.1016/j.jlr.2021.100106>.
- (284) D’Mello, S. R.; Cruz, C. N.; Chen, M.-L.; Kapoor, M.; Lee, S. L.; Tyner, K. M. The Evolving Landscape of Drug Products Containing Nanomaterials in the United States. *Nat Nanotechnol* **2017**, *12* (6), 523–529. <https://doi.org/10.1038/nnano.2017.67>.
- (285) Skou, S.; Gillilan, R. E.; Ando, N. Synchrotron-Based Small-Angle X-Ray Scattering (SAXS) of Proteins in Solution. *Nat Protoc* **2014**, *9* (7), 1727–1739. <https://doi.org/10.1038/nprot.2014.116>.
- (286) Maguire, C. M.; Rösslein, M.; Wick, P.; Prina-Mello, A. Characterisation of Particles in Solution – a Perspective on Light Scattering and Comparative Technologies. *Science and Technology of Advanced Materials* **2018**, *19* (1), 732–745. <https://doi.org/10.1080/14686996.2018.1517587>.
- (287) Varenne, F.; Makky, A.; Gaucher-Delmas, M.; Violleau, F.; Vauthier, C. Multimodal Dispersion of Nanoparticles: A Comprehensive Evaluation of Size Distribution with 9 Size Measurement Methods. *Pharm Res* **2016**, *33* (5), 1220–1234. <https://doi.org/10.1007/s11095-016-1867-7>.
- (288) Mehn, D.; Caputo, F.; Rösslein, M.; Calzolari, L.; Saint-Antonin, F.; Courant, T.; Wick, P.; Gilliland, D. Larger or More? Nanoparticle Characterisation Methods for Recognition of Dimers. *RSC Adv.* **2017**, *7* (44), 27747–27754. <https://doi.org/10.1039/C7RA02432K>.
- (289) Vercauteren, D.; Vandenbroucke, R. E.; Jones, A. T.; Rejman, J.; Demeester, J.; De Smedt, S. C.; Sanders, N. N.; Braeckmans, K. The Use of Inhibitors to Study Endocytic Pathways of Gene Carriers: Optimization and Pitfalls. *Mol Ther* **2010**, *18* (3), 561–569. <https://doi.org/10.1038/mt.2009.281>.

# ENGAGEMENT DE NON PLAGIAT

Je, soussigné(e) **Milad Baroud**  
déclare être pleinement conscient(e) que le plagiat de documents ou d'une  
partie d'un document publiée sur toutes formes de support, y compris l'internet,  
constitue une violation des droits d'auteur ainsi qu'une fraude caractérisée.  
En conséquence, je m'engage à citer toutes les sources que j'ai utilisées  
pour écrire ce rapport ou mémoire.

signé par l'étudiant(e) le 09 / 11 / 2021

**Cet engagement de non plagiat doit être signé et joint  
à tous les rapports, dossiers, mémoires.**

Présidence de l'université  
40 rue de rennes – BP 73532  
49035 Angers cedex  
Tél. 02 41 96 23 23 | Fax 02 41 96 23 00





**Titre :** Auto-assemblages de prodrogues d'azacitidine: une stratégie d'intérêt pour le traitement des syndromes myélodysplasiques et des leucémies aiguës.

**Mots clés :** azacitidine, prodrogue, auto-assemblage, cathepsine B, syndromes myélodysplasiques, PUFAylation

**Résumé :** La 5-Azacitidine, analogue de la cytidine et agent hypométhylant, est l'une des molécules principales utilisées pour le traitement des syndromes myélodysplasiques et des leucémies aiguës. Cependant, après administration, cette molécule présente une faible efficacité thérapeutique : internalisation cellulaire limitée à cause de son caractère hydrophile et dégradation enzymatique rapide par l'adénosine déaminase. L'objectif de ce projet est ainsi d'améliorer l'activité de la molécule et de la protéger de la dégradation enzymatique via le développement d'une prodrogue amphiphile capable potentiellement de s'auto-assembler. L'azacitidine a été donc conjuguée à deux acides gras différents, dérivés de l'oméga 3: l'acide eicosapentaénoïque (EPA)

et l'acide docosahexaénoïque (DHA). Le groupement acide carboxylique de l'acide gras a été couplé covalamment au groupement amine de l'azacitidine, donnant ainsi une prodrogue amphiphile. Ensuite, la nanopréciipitation des prodrogues a été réalisée et des auto-assemblages ont été obtenus pour les deux molécules avec un diamètre de l'ordre de 200 nm, un indice de polydispersité inférieur à 0.2 et un potentiel zêta positif. Les deux types d'auto-assemblages avaient une IC<sub>50</sub> proche de l'azacitidine sur la lignée cellulaire HL-60, une lignée cellulaire de leucémie humaine. Les auto-assemblages d'AzaEPA ont également montré une internalisation cellulaire lente et progressive dans cette même lignée. Ainsi, cette stratégie permettra la protection de l'azacitidine tout en améliorant sa spécificité et sa biodisponibilité.

**Title:** Self-assemblies of azacitidine prodrugs: a promising strategy of treatment for myelodysplastic syndromes and acute myeloid leukemia

**Keywords:** azacitidine, prodrug, self-assembly, cathepsin B, myelodysplastic syndromes, PUFAylation

**Abstract:** 5-Azacitidine, a cytidine analogue and a hypomethylating agent, is one of the main drugs being used for the treatment of myelodysplastic syndromes and of acute myeloid leukemia. However, after administration, it exhibits several limitations including restricted cancer cell internalization due to its hydrophilicity, and a rapid enzymatic degradation by adenosine deaminase. The aim of this project was to improve the cancer cell internalization and protect it from metabolic degradation via the synthesis of an amphiphilic prodrug and their potential self-assembly. The azacitidine was conjugated to two different omega-3 fatty acids, the eicosapentaenoic acid (EPA)

and the docosahexaenoic acid (DHA). The carboxylic acid group of the omega-3 fatty acids was covalently conjugated to the amine group of azacitidine, yielding an amphiphilic prodrug. Next, the nanoprecipitation of the obtained prodrugs was performed and self-assemblies were successfully obtained for both prodrugs with a diameter of around 200 nm, a polydispersity index below 0.2 and a positive zeta potential. Both self-assemblies had an IC<sub>50</sub> close to azacitidine on a human leukemia cell line HL-60. Moreover, AzaEPA self-assemblies showed a slow and gradual cell internalization. This strategy would allow protection while increasing azacitidine specificity and bioavailability.